

Issue 2

2015 | Volume 11

The Journal on Advanced Studies in Theoretical and Experimental Physics,
including Related Themes from Mathematics

PROGRESS IN PHYSICS



“All scientists shall have the right to present their scientific research results, in whole or in part, at relevant scientific conferences, and to publish the same in printed scientific journals, electronic archives, and any other media.” — Declaration of Academic Freedom, Article 8

ISSN 1555-5534

PROGRESS IN PHYSICS

A quarterly issue scientific journal, registered with the Library of Congress (DC, USA). This journal is peer reviewed and included in the abstracting and indexing coverage of: Mathematical Reviews and MathSciNet (AMS, USA), DOAJ of Lund University (Sweden), Zentralblatt MATH (Germany), Scientific Commons of the University of St. Gallen (Switzerland), Open-J-Gate (India), Referativnyi Zhurnal VINITI (Russia), etc.

Electronic version of this journal:
<http://www.ptep-online.com>

Advisory Board

Dmitri Rabounski,
Editor-in-Chief, Founder
Florentin Smarandache,
Associate Editor, Founder
Larissa Borissova,
Associate Editor, Founder

Editorial Board

Pierre Millette
millette@ptep-online.com
Andreas Ries
ries@ptep-online.com
Gunn Quznetsov
quznetsov@ptep-online.com
Felix Scholkmann
scholkmann@ptep-online.com
Ebenezer Chifu
chifu@ptep-online.com

Postal Address

Department of Mathematics and Science,
University of New Mexico,
705 Gurley Ave., Gallup, NM 87301, USA

Copyright © Progress in Physics, 2015

All rights reserved. The authors of the articles do hereby grant *Progress in Physics* non-exclusive, worldwide, royalty-free license to publish and distribute the articles in accordance with the Budapest Open Initiative: this means that electronic copying, distribution and printing of both full-size version of the journal and the individual papers published therein for non-commercial, academic or individual use can be made by any user without permission or charge. The authors of the articles published in *Progress in Physics* retain their rights to use this journal as a whole or any part of it in any other publications and in any way they see fit. Any part of *Progress in Physics* howsoever used in other publications must include an appropriate citation of this journal.

This journal is powered by L^AT_EX

A variety of books can be downloaded free from the Digital Library of Science:
<http://www.gallup.unm.edu/~smarandache>

ISSN: 1555-5534 (print)
ISSN: 1555-5615 (online)

Standard Address Number: 297-5092
Printed in the United States of America

April 2015

Vol. 11, Issue 2

CONTENTS

Rabounski D., Borissova L., Ries A., Millette P., Chifu E., Quznetsov G. Celebrating the 60th Anniversary of Florentin Smarandache (<i>Editorial Message</i>)	109
Zhang T. X. A Physical Model of Pulsars as Gravitational Shielding and Oscillating Neutron Stars	110
Daywitt W. C. The Structured Proton and the Structureless Electron as Viewed in the Planck Vacuum Theory	117
Robitaille P.-M., Crothers S. J. “The Theory of Heat Radiation” Revisited: A Commentary on the Validity of Kirchhoff’s Law of Thermal Emission and Max Planck’s Claim of Universality	120
Müller H. Scaling of Body Masses and Orbital Periods in the Solar System	133
Rabounski D., Borissova L. In Memoriam of Joseph C. Hafele (1933–2014) (<i>Editorial Message</i>)	136
Scholkmann F. Solar-Time or Sidereal-Time Dependent? The Diurnal Variation in the Anisotropy of Diffusion Patterns Observed by J. Dai (2014, Nat. Sci.) (<i>Letters to Progress in Physics</i>)	137
McCulloch M. E. Energy from Swastika-Shaped Rotors	139
Khalaf A. M., Gaballah N., Elgabry M. F., Ghanim H. A. Nuclear Phase Transition from Spherical to Axially Symmetric Deformed Shapes Using Interacting Boson Model	141
Ogiba F. Planck’s Radiation Law: Thermal Excitations of Vacuum Induced Fluctuations	146
Tosto S. Diffusion Equations, Quantum Fields and Fundamental Interactions	149
Müller Scaling of Moon Masses and Orbital Periods in the Systems of Saturn, Jupiter and Uranus	165
Scott D. E. Birkeland Currents: A Force-Free Field-Aligned Model	167
Suhendro I. An Eidetic Reflex and Moment of Breakthrough in Time and Scientific Creation: 10 Years of Progress in Physics, 100 Years of General Relativity, and the Zelmanov Cosmological Group (<i>Letters to Progress in Physics</i>)	180
Ries A. Qualitative Prediction of Isotope Abundances with the Bipolar Model of Oscillations in a Chain System	183
Dumitru S. Addenda to My Paper “New Possible Physical Evidence of the Homogeneous Electromagnetic Vector Potential for Quantum Theory. Idea of a Test Based on a G. P. Thomson-like Arrangement” (<i>Letters to Progress in Physics</i>)	187
Daywitt W. C. The de Broglie Relations Derived from the Electron and Proton Coupling to the Planck Vacuum State	189

Information for Authors and Subscribers

Progress in Physics has been created for publications on advanced studies in theoretical and experimental physics, including related themes from mathematics and astronomy. All submitted papers should be professional, in good English, containing a brief review of a problem and obtained results.

All submissions should be designed in \LaTeX format using *Progress in Physics* template. This template can be downloaded from *Progress in Physics* home page <http://www.ptep-online.com>. Abstract and the necessary information about author(s) should be included into the papers. To submit a paper, mail the file(s) to the Editor-in-Chief.

All submitted papers should be as brief as possible. Short articles are preferable. Large papers can also be considered in exceptional cases. Letters related to the publications in the journal or to the events among the science community can be applied to the section *Letters to Progress in Physics*.

All that has been accepted for the online issue of *Progress in Physics* is printed in the paper version of the journal. To order printed issues, contact the Editors.

This journal is non-commercial, academic edition. It is printed from private donations. (Look for the current author fee in the online version of the journal.)

EDITORIAL MESSAGE**Celebrating the 60th Anniversary of Florentin Smarandache**

December 10, 2014, marked the 60th anniversary of Florentin Smarandache's birth. Through great personal sacrifice, our friend and colleague became one of the co-founders, and Executive Editor of our journal *Progress in Physics*. He is a mathematician of international renown, and a Professor in the Department of Mathematics and Science at the University of New Mexico, where he was Department Chair for many years. His detailed biography was previously published one year ago, in our journal.*

We, the colleagues and friends who have been privileged to know Florentin closely, wish him a happy life for many decades to come, good health, prosperity, and enthusiasm for his further research.

Dmitri Rabounski, Larissa Borissova, Andreas Ries,
Pierre Millette, Ebenezer Chifu, Gunn Quznetsov



Prof. Florentin Smarandache,
Executive Editor of *Progress in Physics*

*Rabounski D. Florentin Smarandache: A Celebration. *Progress in Physics*, 2014, issue 1, 25–27.

A Physical Model of Pulsars as Gravitational Shielding and Oscillating Neutron Stars

T. X. Zhang

Department of Physics, Alabama A & M University, Normal, Alabama 35762. E-mail: tianxi.zhang@aamu.edu

Pulsars are thought to be fast rotating neutron stars, synchronously emitting periodic Dirac-delta-shape radio-frequency pulses and Lorentzian-shape oscillating X-rays. The acceleration of charged particles along the magnetic field lines of neutron stars above the magnetic poles that deviate from the rotating axis initiates coherent beams of radio emissions, which are viewed as pulses of radiation whenever the magnetic poles sweep the viewers. However, the conventional lighthouse model of pulsars is only conceptual. The mechanism through which particles are accelerated to produce coherent beams is still not fully understood. The process for periodically oscillating X-rays to emit from hot spots at the inner edge of accretion disks remains a mystery. In addition, a lack of reflecting X-rays of the pulsar by the Crab Nebula in the OFF phase does not support the lighthouse model as expected. In this study, we develop a physical model of pulsars to quantitatively interpret the emission characteristics of pulsars, in accordance with the author's well-developed five-dimensional fully covariant Kaluza-Klein gravitational shielding theory and the physics of thermal and accelerating charged particle radiation. The results obtained from this study indicate that, with the significant gravitational shielding by scalar field, a neutron star nonlinearly oscillates and produces synchronous periodically Dirac-delta-shape radio-frequency pulses (emitted by the oscillating or accelerating charged particles) as well as periodically Lorentzian-shape oscillating X-rays (as the thermal radiation of neutron stars whose temperature varies due to the oscillation). This physical model of pulsars broadens our understanding of neutron stars and develops an innovative mechanism to model the emissions of pulsars.

1 Introduction

Neutron stars are extremely compact objects, resulting from supernova explosions of dying massive stars with 8 to 20 solar masses. The theoretical prediction for the existence of neutron stars in nature was proposed eight decades ago [1]. But the observational discovery of these compact objects was only done in the middle of the 1960s from the measurement of an unusual Dirac-delta-shape pulse-like radio emission from the Crab Nebula [2,3] first observed by Chinese astronomers in 1054. The mass and radius of neutron stars are mostly around 1.4 solar masses and 10 to 20 km, respectively. The recent measurement for the Shapiro delay of light from a binary millisecond pulsar has discovered a neutron star with a mass of about two solar masses [4]; and other measurements have found the radii of some neutron stars to be less than 10 km [5–7]. The mass-radius relation of these unusual neutron stars has been modeled recently by [8].

The conventional interpretation for the observed Dirac-delta-shape pulse-like radio emission was based on the lighthouse model of pulsars as fast rotating neutron stars [9–12]. Figure 1 sketches a diagram for the lighthouse model of pulsars. Charged particles that are accelerated along the magnetic field lines above the magnetic poles produce or give off coherent beams of radio emissions, through mechanisms which are, however, not yet entirely understood. These beams are viewed as pulsing radio-frequency radiation

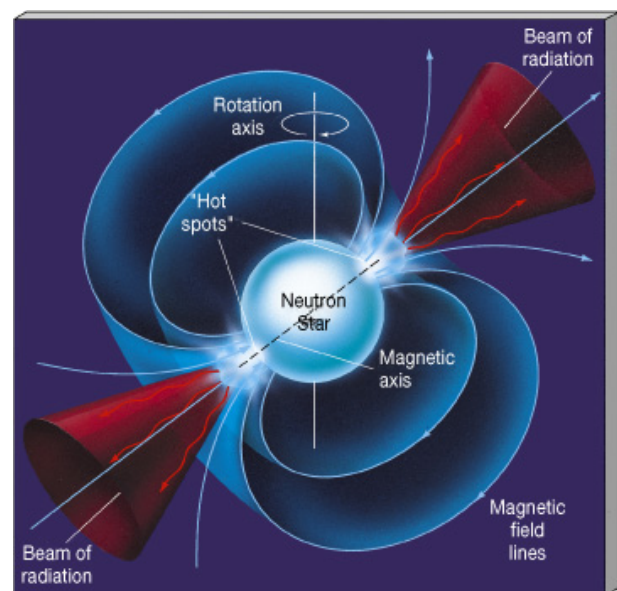


Fig. 1: A sketched diagram for the lighthouse model of pulsars as fast rotating neutron stars (Credit: www.pas.rochester.edu/afrank/A105). Charged particles, accelerated by the magnetism of the neutron star, flow along the magnetic field lines, producing radio radiation that beams outward.



Fig. 2: A flashlight beam through the air (Credit: www.youtube.com/watch?v=ggr5YQYqD0I). One can see the beam, even if it does not point to the viewer, because the air reflects the beam of the flashlight.

when the magnetic poles sweep the viewers. Twenty years after the discovery of neutron stars, quasi-periodic oscillations (QPOs) of X-rays were observed first from white dwarfs and then from neutron stars [13–14]. The recent observations of pulsar PSR B0943+10 by combining the X-ray telescope XMM-Newton and the radio telescope LOFAR have shown that this pulsar synchronously emits periodic Dirac-delta-shape pulses of radio-frequency radiation and Lorentzian shape oscillating X-rays [15]. At present, pulsar quasi-periodically oscillating X-rays are believed to come from inner edges of the accretion disks of white dwarfs, neutron stars, and black holes, but the physical cause still remains unsolved and a detailed consistent theory of how these fascinating stars work remains elusive.

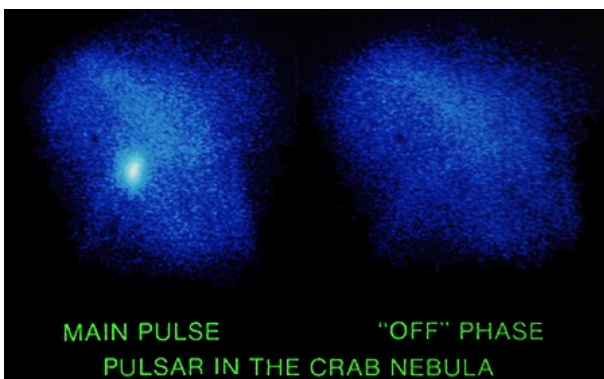


Fig. 3: X-ray images of the Crab Nebula. The left panel is the case when the pulsar turns on and the right panel is the case when the pulsar turns off. When the beam of X-rays points away, why we cannot see the radiation beam formed by the nebula reflection (Einstein Observatory image, Smithsonian Institution Photo No. 80-16234).

It is well known or experienced that a beam of flashlight is visible from the side because part of the light is scattered by the tiny particles like dust in the air (Figure 2). A beam of radio waves can bend or change the direction of propagation due to ionospheric reflections and refractions. However, the similar case does not happen for the beam of emissions (including radio waves through gamma rays) from the pulsar in the Crab Nebula. In visible light, the Crab Nebula consists largely of filaments with ionized gases of temperature $\sim 10 - 100$ times higher than ionosphere and density $\sim 1 - 1000$ times lower than ionosphere. The Crab Nebula, though behaving unlike the air or ionosphere, should be able to reflect or scatter the beams of radio waves or X-rays from the pulsar. But the observations have not shown such events occurring when the pulsar is in the OFF phase (see the right image of Figure 3). Figure 3 shows the X-ray images of the Crab Nebula taken by the Einstein Observatory when the pulsar is in the ON (the left panel) and OFF (the right panel) phases. According to the lighthouse model, the ON phase of the pulsar refers to the beam of radiation pointing to the Earth or the viewer; while the OFF phase refers to the beam of radiation pointing to other directions. The X-ray image of the entire Crab Nebula in the ON phase is significantly brighter than that in the OFF phase, especially the region above the lighting pulsar. This indicates that the Crab Nebula does reflect/scatter some X-rays of the pulsar when the pulsar is ON. However, there is not any reflection/scattering happened and perceived when the beam points to other directions through the Nebula in the OFF phase. This fact strongly implies that our conventional lighthouse model may not work. The lack of reflecting/scattering X-rays of the pulsar by the Crab Nebula in the OFF phase does not support the lighthouse model as expected. In the OFF phase, the pulsar is more likely to turn the radiation off entirely rather than just to direct the radiation away from the Earth or the viewer. In addition, the lighthouse model may not be able to theoretically form, except for when the deviation of the rotating axis from the magnetic poles is negligible, a stable accretion disk and jets, which were clearly seen in the X-ray images recently captured by the Chandra Observatory. It is also hard to explain why some pulsars are gamma rays only [16,17].

Recently, the author has developed a new mechanism for supernova explosion caused by gravitational field shielding [18], in accordance with his five-dimensional (5D) fully covariant Kaluza-Klein theory with a scalar field [8,19,20]. According to the gravitational field shielding theory, a supernova explosion takes place when its core collapses to a critical density where the gravitational field suddenly disappears or is shielded by the strong scalar field. At this moment, the extremely large pressure of matter immediately stops the core from collapsing and then the core quickly expands to powerfully push the mantle part of the supernova moving radially outward as a supernova explosion. As the core expands, the gravity resumes. After the mantle explodes out of the super-

nova, the core is left as a neutron star and starts to oscillate about its equilibrium of gravity and pressure. Rather than the rotation, acoustic wave and neutrino driven mechanisms of supernova explosions, this new mechanism is driven by the extreme pressure of the core when the gravitational field is suddenly weakened by the strong scalar field.

In this paper, we develop a physical model of pulsars, through which we propose an alternative explanation for neutron stars to emit the Dirac-delta-shape pulse-like radio frequency radiation and the Lorentzian shape oscillating X-rays, in terms of the 5D gravitational field shielding theory and the self-gravitating oscillations of neutron stars. We will also discuss how the frequency of emissions depends on the mass of the neutron star, the initial conditions, the equation of state, and the frozen magnetic field. In contrast to the conceptual lighthouse model, this physical oscillating model is based on the simple physics of thermal and accelerating charged particle radiation and the 5D gravity, and predicts power-time profiles of pulsars that are highly consistent with the measurements and observations.

2 Emissions of oscillating neutron stars

As described above, a neutron star starts to oscillate about its equilibrium of gravity and pressure once the mantle is exploded out of the supernova. The oscillation of the neutron star oscillates or accelerates inside particles. At the surface or in the crust, the acceleration of particles can be simply given by the following equation of motion,

$$a(t) \equiv \frac{d^2 R(t)}{dt^2} = -g(R) - \frac{1}{\rho(R)} \frac{dP(\rho)}{dR}, \quad (1)$$

where $a(t)$ is the acceleration of the particle; $R(t)$ is the radial distance of the particle or simply the radius of the neutron star; $\rho(R)$ is the density of neutron star; $P(\rho)$ is the pressure of neutron star, which in this study is given by the Skyrme model for the Equation of State (EOS) of neutron stars [21,22],

$$P = 5.32 \times 10^9 \rho^{5/3} + 1.632 \times 10^{-5} \rho^{8/3} - 1.381 \times 10^5 \rho^2, \quad (2)$$

in the cgs unit system; and $g(R)$ is the gravitational field or acceleration, which in this study is determined according to the five-dimensional fully covariant Kaluza-Klein gravitational shielding theory with a scalar field that the author previously developed [18],

$$g = \frac{c^2}{2\phi^2} \left(\frac{d\phi}{dr} + \phi \frac{dv}{dr} \right) e^{-\lambda}, \quad (3)$$

in the Einstein frame. Here the scalar field ϕ , the metric 00- and 11-components e^ν and e^λ were solved as ([19] and references therein)

$$\phi^2 = -\alpha^2 \psi^4 + (1 + \alpha^2) \psi^{-2}, \quad (4)$$

$$e^\nu = \psi^2 \phi^{-2}, \quad (5)$$

$$e^\lambda = \left(1 - \frac{B^2}{r^2} \right)^2 \psi^{-2}, \quad (6)$$

in the Jordan frame, where ψ , B , and α are given by

$$\psi = \left(\frac{r-B}{r+B} \right)^{1/\sqrt{3}}, \quad (7)$$

$$B = \frac{GM}{\sqrt{3(1+\alpha^2)}c^2}, \quad (8)$$

$$\alpha = \frac{Q}{2\sqrt{GM}}. \quad (9)$$

This solution does not have an unknown parameter and reduces to the Schwarzschild solution in the Einstein frame when fields are weak and matter that generates the fields is neutral [8,18,23]. The weak field tests of general relativity are also the tests of this 5D gravity. In the case of strong fields, especially charged, the 5D gravity gives new effects such as the space polarization [24,25], electric redshift [19], gravitational field shielding or spacetime flattening [18], gravitationless black hole [23], and so on. The new effects are results of the strong scalar field, which significantly reduces the local gravity or, in other words, decreases the equivalent gravitational constant [20].

Figure 4a plots the radial distance as a function of time that is obtained from numerically solving (1). The result indicates that the neutron star nonlinear periodically oscillates, non-uniformly with quick stop and bounce by the pressure force when the gravity loses its dominance. It is in a dynamic equilibrium state rather than a static one. According to the gravitational shielding model [18], a supernova explosion takes place, due to the extremely large pressure pushing outward, when its core collapses to a critical density, at which the gravitational field suddenly disappears or is shed by the strong scalar field. Once a supernova or a dying star has exploded its mantle, the core as a stellar remnant forms a neutron star, located at the center of the supernova progenitor, with a relative large initial radius where the gravity is resumed. Then, the formed neutron star starts to gravitationally compress from its initial state. As it squeezes, the scalar field increases and reduces the gravitational field or flattens the spacetime again. To about the critical density, the gravitational field is disappeared or shed again by the strong scalar field. At this moment, the extensive pressure immediately stops the neutron star from the further collapse and extremely drives the neutron star to rapidly expand. Particles are extremely accelerated by the extensive pressure when the gravitational field is shed. After the neutron star is sufficiently expanded, the gravity resumes because the scalar field is weakened. When the gravity becomes dominant, the neutron star collapses again. This periodic switching of the dominance between the gravity and the pressure force leads to a nonlinear oscillation of the neutron star. Here in Figure 4 as an example we have chosen the mass of the neutron star to be about 1.5

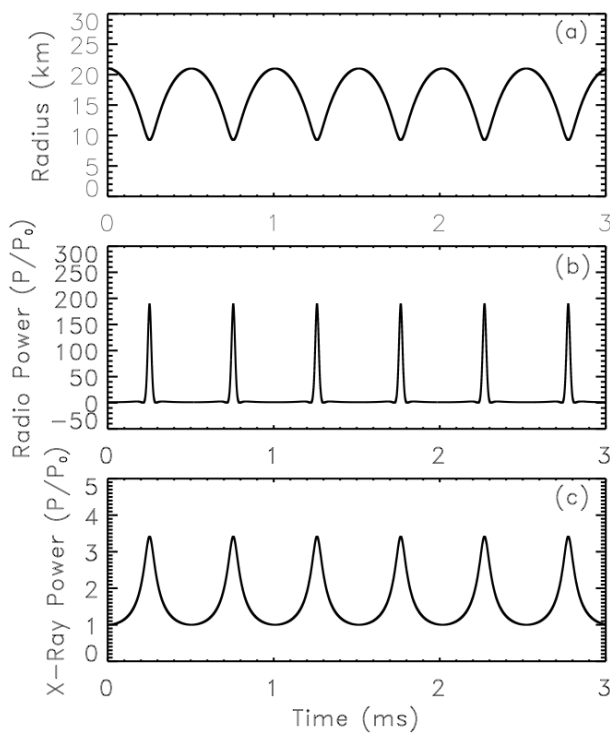


Fig. 4: Oscillation of a neutron star with 1.5 solar masses versus synchronous emissions of the Dirac Delta shape radio pulses and the Lorentzian shape X-ray oscillations. The radial distance (a), the power of radio emission (b), and the power of X-ray emission (c) are plotted as functions of time. The initial conditions for the radial distance and velocity of oscillation are chosen to be $R_0 = 22$ km and $v_0 = 0$.

solar masses; and the initial radial distance and velocity to be about $R_0 = 22$ km and $v_0 = 0$, respectively.

The accelerating particles, if electrically charged, generate radio emissions. According to the Larmor equation [26], the power of radio emissions generated by the accelerating charged particle is proportional to the square of the magnitude of the acceleration,

$$P_r(t) = \frac{q^2 a^2(t)}{6\pi\epsilon_0 c^3} \propto a^2(t), \quad (10)$$

where q is the particle charge; ϵ_0 is the dielectric constant in the free space; and c is the speed of light in free space. Figure 4b plots the power of radio emissions normalized to the power at the initial state, in terms of the Larmor equation (10) and the acceleration (1). The result indicates that the radio emissions by the nonlinearly oscillating neutron star are periodically pulse-like radiation with the Dirac delta shape, which is consistent with the general observations of pulsars. A neutron star could be possibly charged as a consequence of holding some certain amount of net protons or nuclei. The fraction and effect of protons in neutron stars have been considered for years [27,28]. To explain the observations of Geminga,

a model of a dense neutron star with localized protons was proposed [29,30]. In [28], the maximum amount of charge in a compact star can be $\sim \sqrt{GM}$, which is $\sim 2.5 \times 10^{20}$ C for a neutron star with 1.5 solar masses.

On the other hand, a hot neutron star can emit thermal or blackbody radiation in the frequency range of X-rays. For instance, according to Wien's law, the frequency of blackbody radiation at the maximum or at the peak of the power by a hot body with surface temperature of 100 million Kelvins is about 10^{19} Hz, which is in the frequency range of X-rays. The total power of X-rays emitted by a hot neutron star can be given by

$$P_X(t) = 4\pi R^2(t) \sigma T^4(t) \propto R^{-\delta}(t), \quad (11)$$

where σ is the Stefan-Boltzmann constant. Here we have also considered that the surface temperature of the neutron star varies as the neutron star oscillates, or in other words, the temperature is a function of the radius or density. Figure 4c plots the power of X-rays normalized to the initial power, in terms of the blackbody radiation or (11). Here we have chosen the index $\delta = 3/2$, which corresponds to $T \propto R^{-(\delta+2)/4} = R^{-7/8}$. Choosing a larger δ does not alter the shape of the radiation, but can lead to a more significant oscillation of X-ray emissions, because the variation of temperature responding to the oscillation of neutron star increases with the index δ . The result shown in Figure 1c indicates that the X-rays emitted by the nonlinearly oscillating neutron star are synchronous periodically oscillating blackbody radiation with the Lorentzian shape, which is also consistent with the general observations of pulsars.

A neutron star may have a temperature as high as thousand billion degrees (10^{12} K) at the moment of its birth by an explosion of a supernova and then quickly cools down to a hundred million degrees (10^8 K) because of its strong radiation and neutrino emissions [31]. Therefore, for an early-aged neutron star, if the temperature is above 10^{10} K, the dominant thermal or blackbody radiation can be gamma rays. In other words, a younger pulsar as a hotter neutron star can emit gamma-rays mainly, which may explain the gamma ray only pulsars recently measured by NASA's Fermi Gamma Ray Telescope [32,33].

The frequency of the pulses shown in Figure 4 is about 2000 Hz (with a period of about 0.5 milliseconds), which depends on (1) the mass of the neutron star, (2) the initial kinetic and potential energy of the neutron star (or initial conditions of R_0 and v_0), and (3) the applied EOS. In general, at the same initial conditions with the same applied EOS, the pulse frequency is higher if the mass of the neutron star is greater because a larger mass, and thus larger gravity, collapses the neutron star quicker. Figures 5 and 6 show, respectively, the radial distance and the radio emission power for oscillating neutron stars with four different masses under the same initial conditions and the same applied EOS. It is seen that the frequency decreases with decreasing neutron star mass. For a

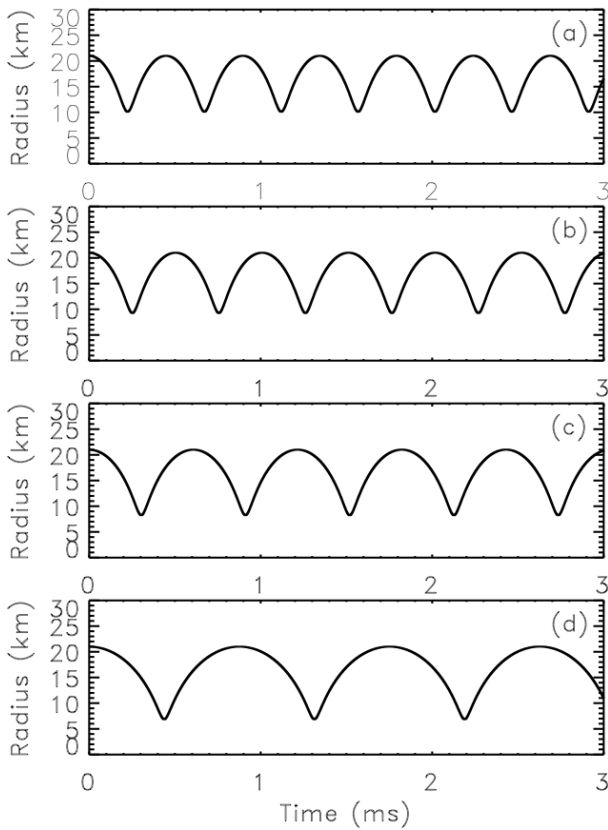


Fig. 5: Oscillations of neutron stars. The radial distance is plotted as a function of time for neutron stars with mass equal to 2, 1.5, 1, and 0.5 solar masses, respectively, from (a) through (d). The initial conditions and applied EOS are the same as in Figure 4.

neutron star with mass four times smaller, the pulse frequency will be twice lower. The oscillation model of pulsars also gives very precise intervals between pulses as shown in Figures 3 to 5. Different pulsars can have quite different periods of pulses because they have different masses and start their oscillations from different initial states. Given a neutron star, the periodic switch between gravity and pressure dominant forces does not vary the period or frequency of oscillation.

3 Discussions and conclusions

For neutron stars with the same mass and the same applied EOS, the frequency of pulses is lower if the initial R_0 or v_0 is greater, because it takes a longer time to make one oscillation not only due to the longer course for the oscillation but also due to the weaker initial gravity. For neutron stars with the same mass and at the same initial state of motion, the frequency is greater if the density dependence of the pressure determined by the EOS is harder, because the pressure gradient push is greater and thus the oscillation is faster. On the other hand, the oscillation of the neutron star compresses and relaxes the frozen magnetic field of the neutron star as well as varies the particle radial speed of motion. The mag-

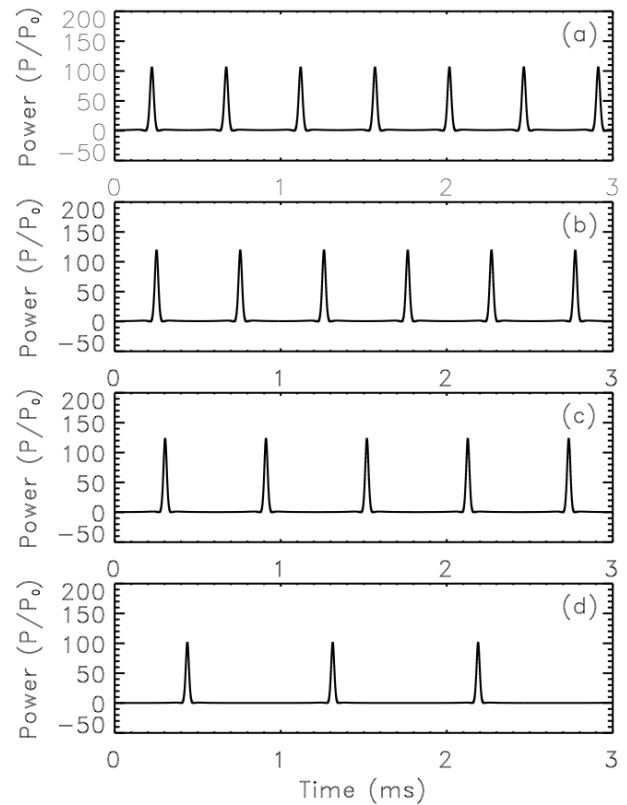


Fig. 6: Radio emissions of oscillating neutron stars. The power of radio emissions for neutron stars with mass equal to 2, 1.5, 1, and 0.5 solar masses, respectively, from (a) through (d). The initial conditions and applied EOS are the same as in Figure 5. The powers for all cases are normalized.

netic pressure and speed gradients also play some role in resisting the oscillations and thus decreasing the frequency of the oscillations, but not changing the emission characteristics. Therefore, oscillation periods of neutron stars can be in a wide range [34,35], when all these effects are considered. Details on these effects will be studied next.

The oscillation of a neutron star will be damped and thus slowed down due to the loss of energy or mass. Neutron stars can speed up their oscillations when they accrete more energy or mass than they lose. They may also twitch or glitch their pulses when their states of matter suddenly change [36,37]. Very hot neutron stars (e.g. 10^{10} K) may emit oscillating gamma rays [38,39]. Sufficiently cooled down neutron stars (e.g. 10^6 K) can emit oscillating ultraviolet radiation [40]. All the temperature-related emissions are periodically oscillating with the Lorentzian shape. Only the acceleration-related radio frequency emissions are pulse-like with the Dirac delta shape. Since electrons have much smaller inertia than nuclei, the pressure gradient buoyant forces accelerate them in different strengths with time lag. Therefore, the radio emissions from electrons and nuclei in the neutral crust of an oscillating neutron star are not completely destructed. Net ra-

radio emissions from the electrons and nuclei in the neutral crust of a neutron star can be generated by the self-gravitating oscillating neutron star. Due to the time lag, each primary pulse, which is produced by electrons, may follow a secondary pulse, which is produced by nuclei.

The sudden disappearance of gravitational field due to the shielding by the strong scalar field is significant for the radio emissions of neutron stars to be pulses with the Dirac delta shape. Under the Newtonian and Einsteinian gravitational theories, the gravitational oscillations of neutron stars may also produce the observed Dirac delta shape radio emissions, but need the neutron star to be over compressed in order for the pressure gradient push to dominate the non-shielding strong gravity. On the other hand, it should be noted that (1) and (2) are valid only for non-relativistic motion. According to the calculation done in Figure 1, we can see that the maximum speed of the oscillation is less than about one third of the light speed in vacuum. In this case, we have a relativistic factor $\gamma < 1.1$, which means that the relativistic effect is not significant and thus negligible. The shape of radio emissions depends on the acceleration of charged particles and the shape of X-ray emissions depends on the surface temperature or radius of the neutron star. This physical model quantitatively explains the emission characteristics of pulsars.

The energy dissipation deficiently decreases the neutron star's total energy, mass, amplitude of oscillation, EOS (or the bounce of the neutron star), magnetic field strength, and thus slightly changes or reduces both the power and frequency of pulses. The small energy dissipation or loss due to radiation (or damping) can only weakly slow down the pulses. The measured polarizations of pulsars can be considered as the causes of particles flowing, electromagnetic activities, and unevenly distributed surface temperatures. This paper has only addressed the radio emission of charged particles that are accelerated due to the oscillation of the neutron star. If we also consider the radio emission of charged particles that are accelerated due to particle flowing and electromagnetic activities, the pulse profiles should be polarized with multiple components [41–43] and complicated pulse profiles. The Dirac-delta shape and Lorentzian shape are only the main characteristics (i.e. periodicities) of radio pulses and X-ray emissions. The emissions of pulsars are gravitation-powered with effects of rotation, accretion, and/or magnetism, respectively. The gravitational (or oscillatory) energy dissipation provides the power for the pulsar-nebula system. The radio emissions are coherent with high brightness temperature because charged particles are coherently accelerated along with the oscillation of neutron stars. The X-ray emission of a pulsar is thermal but with the temperature varying in a range rather than a single temperature. To obtain the energy spectra of X-rays, we must integrate the flux of emission over a temperature range. The result of integration should be non-thermal as measured. All these aspects will be explored in details in future.

As a summary, we have developed a physical model of pulsars to quantitatively interpret the emission characteristics of pulsars, in accordance with the five-dimensional fully covariant Kaluza-Klein gravitational shielding theory and the physics of thermal and accelerating charged particle radiation. With the significant gravitational shielding by the strong scalar field, a neutron star nonlinearly oscillates and produces synchronous periodically Dirac-delta-shape pulse-like radio-frequency radiation as well as periodically Lorentzian shape oscillating X-rays. The oscillating or accelerating charged particles produce the Dirac-delta-shape pulse-like radio frequency radiation, while the thermal/blackbody radiation of neutron stars that oscillate and thus vary the temperature produces the Lorentzian shape X-rays. This physical model of pulsars as gravitational shielding and oscillating neutron stars broadens our understanding of neutron stars and develops an innovative mechanism to disclose the mystery of pulsars.

Acknowledgements

This work was supported by NASA EPSCoR, AAMU Title III, and Natural Science Foundation of China. The author also acknowledges B. J. Zhang for his numerical assistance.

Submitted on December 20, 2014 / Accepted on January 8, 2015

References

1. Baade W., Zwicky F. Remarks on supernovae and cosmic rays. *Physical Review*, 1934, v. 46, 76–77.
2. Hewish A., Okoye S. E. Evidence for an unusual source of high radio brightness temperature in the Crab Nebula. *Nature*, 1965, v. 207, 59–60.
3. Hewish A., Bell S. J., Pilkington J. D. H., Scott P. F., Collings R. A. Observation of a rapidly pulsating radio source. *Nature*, 1968, v. 217, 709–713.
4. Demorest P. B., Pennucci T., Ransom S. M., Roberts M. S. E., Hessels J. W. T. A two-solar-mass neutron star measured using Shapiro delay. *Nature*, 2010, v. 467, 1081–1083.
5. Guillot S., Rutledge R. E., Brown E. F. Neutron star radius measurement with the quiescent low-mass X-ray binary U24 in NGC 6397. *Astrophysical Journal*, 2011, v. 732, id. 88.
6. Güver T., Wroblewski P., Camarota L., Özel F. The mass and radius of the neutron star in 4U 1820-30. *Astrophysical Journal*, 2010, v. 719, 1807–1812.
7. Güver T., Özel P., Cabrera-Lavers A. The distance, mass, and radius of the Neutron Star in 4U 1608-52. *Astrophysical Journal*, 2010, v. 712, 964–973.
8. Zhang B. J., Zhang, T. X., Guggila P., Dokhanian M. Neutron star mass-radius relation with gravitational field shielding by a scalar field. *Research in Astronomy and Astrophysics*, 2013, v. 13, 571–578.
9. Pacini F. Energy emission from a neutron star. *Nature*, 1967, v. 216, 567–568.
10. Gold T. Rotating Neutron Stars as the Origin of the Pulsating Radio Sources. *Nature*, 1968, v. 218, 731–732.
11. Goldreich P., Julian W. H. Pulsar electrodynamics. *Astrophysical Journal*, 1969, v. 157, 869–880.
12. Lyne A. G., Graham-Smith F. *Pulsar Astronomy*. Cambridge Univ. Press, Cambridge, 2012.

13. van der Klis M., Jansen F., van Paradijs, Lewin, W.H.G., van der Heuve, E.P.J. Intensity-dependent quasi-periodic oscillations in the X-ray flux of GX5 – 1. *Nature*, 1985, v. 316, 225–230.
14. Middleditch J., Priedhorsky W.C. Discovery of rapid quasi-periodic oscillations in Scorpius X-1. *Astrophysical Journal*, 1986, v. 306, 230–237.
15. Hermsen W. *et al.* Synchronous X-ray and radio mode switches: A rapid global transformation of the pulsar magnetosphere. *Science*, 2013, v. 339, 436–439.
16. Abdo A. *et al.* A population of gamma-ray millisecond pulsars seen with the Fermi Large Area Telescope. *Science*, 2009, v. 325, 848–852.
17. Abdo A. *et al.* The First Fermi Large Area Telescope catalog of gamma-ray pulsars. *Astrophysical Journal Supplement*, 2010, v. 187, 460–494.
18. Zhang T. X. Gravitational field shielding and supernova explosions. *Astrophysical Journal Letters*, 2010, v. 725, L117–L121.
19. Zhang T. X. Electric redshift and quasars. *Astrophysical Journal Letters*, 2006, v. 636, L61–L64.
20. Zhang B. J., Zhang T. X., Guggilla P., Dokhanian M. Gravitational field shielding by scalar field and type II superconductors. *Progress in Physics*, 2013, v. 9 (1), 69–73.
21. Skyrme T. H. R. The effective nuclear potential *Nuclear Physics*, 1959, v. 9, 615–634.
22. Cameron A. G. W. Neutron star models. *Astrophysical Journal*, 1959, v. 130, 884–894.
23. Zhang T. X. Gravitationless black hole. *Astrophysics and Space Science*, 2011, v. 334, 311–316.
24. Nodvik J. S. Suppression of singularities by the g^{55} field with mass and classical vacuum polarization in a classical Kaluza-Klein theory. *Physical Review Letters*, 1985, v. 55, L2519–L2522.
25. Dragilev V. M. Vacuum polarization of a scalar field in anisotropic multidimensional cosmology. *Theoretical Mathematics in Physics*, 1990, v. 84, 887–893.
26. Jackson J. D. *Classical Electrodynamics*, 3rd Edition. John Wiley and Sons, 1999, p. 665.
27. Whinnett A. W., Torres D. F. Charged scalar-tensor boson stars: Equilibrium, stability, and evolution. *Physical Review D*, 1999, v. 60, id. 104050.
28. Ray S., Espindola A. L., Malheiro M., Lemos J. P. S., Zanchin V. T. Electrically charged compact stars and formation of charged black holes. *Physical Review D*, 2003, v. 68, id. 084004.
29. Kutschera M., Wojcik W. Proton impurity in the neutron matter: A nuclear polaron problem. *Physical Review C*, 1993, v. 47, 1077–1085.
30. Baiko D. A., Haensel P. Cooling neutron stars with localized protons. *Astronomy and Astrophysics*, 2000, v. 356, 171–174.
31. Yakovlev D. G., Gnedin O. Y., Kaminker A. D., Levenfish K. P., Potekhin A. Y. Neutron star cooling: Theoretical aspects and observational constraints. *Advances in Space Research*, 2004, v. 33, 523–530.
32. Atkinson N. Molecules in gamma-ray bursts detected. *Universe Today*, 2009, January 6.
33. Caraveo P. A. Gamma-ray pulsar revolution. *Annual Review of Astronomy and Astrophysics*, 2014, v. 52, 211–250.
34. Tsuruta S., Wright J. P. Oscillation periods of neutron stars. *Nature*, 1965, v. 206, 1137–1138.
35. Glass E. N., Lindblom L. The radial oscillations of neutron stars. *Astrophysical Journal Supplement*, 1983, v. 53, 93–103.
36. Anderson P. W., Itoh N. Pulsar glitches and restlessness as a hard superfluidity phenomenon. *Nature*, 1975, v. 256, 25–27.
37. Shemar S. L., Lyne A. G. Observations of pulsar glitches. *Monthly Notices of the Royal Astronomical Society*, 1996, v. 282, 677–690.
38. Harding A. K. Pulsar gamma-rays - Spectra, luminosities, and efficiencies. *Astrophysical Journal*, 1981, v. 245, 267–273.
39. Romani R. W., Yadigaroglu I. A. Gamma-ray pulsars: Emission zones and viewing geometries. *Astrophysical Journal*, 1995, v. 438, 314–321.
40. Romani R. W., Kargaltsev O., Pavlov G. G. The Vela pulsar in the ultraviolet. *Astrophysical Journal*, 2005, v. 627, 383–389.
41. Lyne A. G., Smith F. G. Linear polarization in pulsating radio sources. *Nature*, 1968, v. 218, 124–126.
42. Han J. L., Demorest P. B., van Straten W., Lyne A. G. Polarization observations of 100 pulsars at 774 MHz by the Green Bank Telescope. *Astrophysical Journal Supplement*, 2009, v. 181, 557–571.
43. Yan W. M. *et al.* Polarization observations of 20 millisecond pulsars. *Monthly Notices of the Royal Astronomical Society*, 2011, v. 414, 2087–2100.

The Structured Proton and the Structureless Electron as Viewed in the Planck Vacuum Theory

William C. Daywitt

National Institute for Standards and Technology (retired), Boulder, Colorado. E-mail: wcdawitt@me.com

This paper argues that the proton possesses structure because the positive proton charge attracts the negative-energy vacuum toward the massive proton core, exposing a small spherical portion of that vacuum to free-space perturbations. Calculations indicate that the apparent charge spread of the proton is due to this structure.

1 Introduction

The proton and electron are Dirac particles in the sense that they both possess a Compton radius and they both obey the Dirac equation, but the positive and negative charge of the proton and electron make their characteristics radically different. For example, the proton is smaller and more massive than the electron because of this charge difference [1]. It is shown below that this difference also accounts for the proton structure and its apparent charge spread. The structure is the result of the perturbed Planck vacuum (PV) state [2] in the vicinity of the massive proton core.

In its rest frame the proton core (e_*, m_p) exerts the following two-term coupling force [3] [4]

$$F_p(r) = \frac{(e_*)(-e_*)}{r^2} + \frac{m_p c^2}{r} = -F_s \left(\frac{r_p^2}{r^2} - \frac{r_p}{r} \right) \quad (1)$$

on the PV negative-energy continuum, where the proton Compton radius $r_p (= e_*^2/m_p c^2)$ is the radius at which the force vanishes. The mass of the proton is m_p and the bare charge e_* is massless. The radius r begins at the proton core and ends on any particular Planck-particle charge ($-e_*$) at a radius r within the PV. The strong force

$$F_s \equiv \left| \frac{(e_*)(-e_*)}{r_p^2} \right| = \frac{m_p c^2}{r_p} \quad (2)$$

is the magnitude of the two forces in the first sum of (1) where the sum vanishes. The (e_*) in (1) and (2) belongs to the free-space proton and the ($-e_*$) to the separate Planck particles of the PV, where the first and second ratios in (1) and (2) are vacuum polarization and curvature forces respectively. It follows that the strong force is a proton/PV force (rather than a free-space/free-space force). The Planck particle mass m_* and Compton radius r_* are equal to the Planck Mass and Planck Length [5, p. 1234]. (The three Compton relations $r_e m_e c^2 = r_p m_p c^2 = r_* m_* c^2 = e_*^2$ and $c\hbar = e_*^2$ are used throughout the preceding and the following calculations.)

The massive electron core ($-e_*, m_e$) exerts the coupling force

$$F_e(r) = \frac{(-e_*)(-e_*)}{r^2} - \frac{m_e c^2}{r} = F_w \left(\frac{r_e^2}{r^2} - \frac{r_e}{r} \right) \quad (3)$$

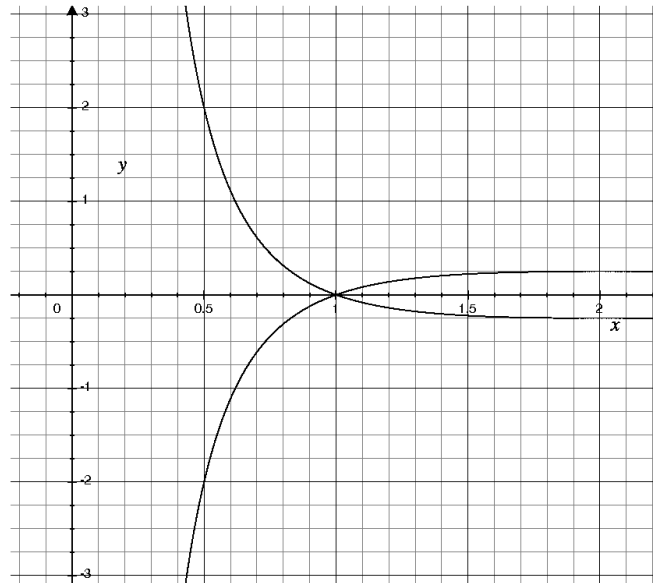


Fig. 1: Graphs of the normalized coupling forces $F_p(r)/F_s$ with $r_p = 1$ (negative to the left), and $F_e(r)/F_w$ with $r_e = 1$ (positive to the left). ($r_e/r_p = 1836$)

on the vacuum state and leads to the Compton radius $r_e (= e_*^2/m_e c^2)$, where the first ($-e_*$) in (3) belongs to the electron. The weak force

$$F_w \equiv \frac{(-e_*)(-e_*)}{r_e^2} = \frac{m_e c^2}{r_e} \quad (4)$$

is the magnitude of the two forces in the first sum of (3) where the sum vanishes. Again, the first and second ratios in (3) and (4) are vacuum polarization and curvature forces respectively. Thus the weak force, like the strong force, is an electron/PV force.

It is important to note that, for $r < r_p \ll r_e$, $F_p(r)$ and $F_e(r)$ are negative and positive respectively (Figure 1). That is, the proton and electron cores attract and repel respectively the Planck particles ($-e_*, m_*$) within the PV. This is the phenomenon that gives the proton structure, while denying structure to the electron.

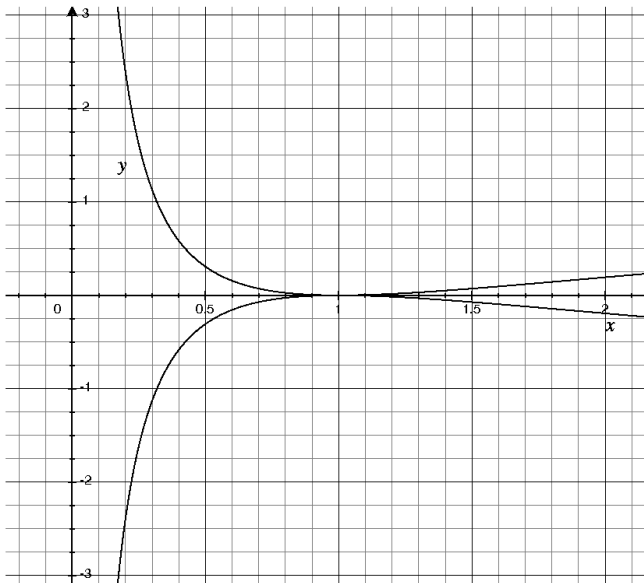


Fig. 2: Graphs of the normalized coupling potentials $V_p(r)/m_p c^2$ with $r_p = 1$ (upper curve), and $V_e(r)/m_e c^2$ with $r_e = 1$ (lower curve). ($r_e/r_p = 1836$)

2 Proton structure

The potential energy associated with the coupling forces (1) and (3) is defined as

$$V(r) = \int F(r)dr + V_0 \tag{5}$$

so that $dV/dr = F$ and $V(r_c) = 0$, where $r_c = e^*/mc^2$ is the force’s Compton radius. For the proton and electron this definition leads to

$$\frac{V_p(r)}{m_p c^2} = \frac{r_p}{r} - 1 - \ln\left(\frac{r_p}{r}\right) \tag{6}$$

and

$$\frac{V_e(r)}{m_e c^2} = 1 - \frac{r_e}{r} + \ln\left(\frac{r_e}{r}\right) \tag{7}$$

where (6) and (7) yield $V_p(r) \geq 0$ and $V_e(r) \leq 0$ over the entire range of the radius r (Figure 2).

The spirit of the Klein Paradox discussed in Appendix A is that, if a region of free space is subjected to a sufficiently large *positive* potential, then an electron impinging on that region can extract energy from the negative-energy vacuum state. The following assumes that this paradox reflects a real physical phenomenon, implying that the positive charge of the proton core (but not the negative charge of the electron core) can expose a small region of the PV to perturbations from free-space particles. This conclusion leads to a structured proton and a structureless electron.

Equation (6) yields the quadrature formula

$$x = 1 + \frac{V_p}{m_p c^2} + \ln x \quad \text{with} \quad x \equiv r_p/r \tag{8}$$

from which the proton structure can be derived, where x is defined in the open interval $(0, \infty)$. The proton-proton (p-p) overlap radius (Appendix A) is determined by setting $V_p = 2m_p c^2$ in (8) and results in

$$x = 3 + \ln x \tag{9}$$

which leads to $x = 4.50$ and the p-p overlap radius $r_1 (\equiv r_p/4.50)$. This is the radius where the negative-energy level $-m_p c^2$ of the vacuum state just enters the positive-energy level $m_p c^2$ of the free-space proton in its rest frame.

The negative energy maximum associated with the PV is $-m_e c^2$. Thus the proton electron-proton (e-p) overlap radius results from $V_p = m_p c^2 + m_e c^2$ and yields

$$\begin{aligned} x &= 1 + \frac{(m_p c^2 + m_e c^2)}{m_p c^2} + \ln x \\ &= 2 + \frac{r_p}{r_e} + \ln x \approx 2 + \ln x \end{aligned} \tag{10}$$

where $m_e/m_p = r_p/r_e = 1/1836$. Solving (10) leads to $x = 3.15$ and $r_2 (\equiv r_p/3.15)$ for the e-p overlap radius. The sphere within the outer overlap radius $r_2 (> r_1)$ represents the total exposed portion of the PV, and the surface of that sphere takes on a positive polarization charge due to the proton-core charge.

The size of the core $(-e_*, m_e)$ in the Dirac electron is no larger than $r_e/39,000$ [6] [7, pp. 402-403]; so it is reasonable to conclude that the proton core is similarly reduced in size below r_p . From the preceding the following picture of the proton structure emerges: the “point charge” proton core has a radius $r_0 (< r_p/39,000)$; the p-p overlap radius is r_1 ; and the e-p overlap radius is r_2 . The e-p surface at r_2 sustains a polarization charge caused by the core polarizing the exposed PV within that radius.

3 Charge spread

The core-charge polarization of the PV in the proton case leads to an apparent spread in the proton charge that can be roughly expressed in the proton electric field as

$$E(r) = \frac{e(r)}{r^2} \tag{11}$$

where the spread is

$$e(r) = \begin{cases} e_*, & r < r_0 \\ < e_*, & r_0 < r < r_2 \\ \sim e, & r_2 < r < r_p \\ e = \alpha^{1/2} e_*, & r_p < r \end{cases} \tag{12}$$

and $\alpha (\approx 1/137)$ is the fine structure constant. An important characteristic of this result is the large charge gradient

$$\frac{\Delta e}{\Delta r} = \frac{e_* - e}{r_2 - r_0} \approx \frac{e_*(1 - \sqrt{\alpha})}{r_p/3.15} \approx \frac{2.9e_*}{r_p} \tag{13}$$

between the core charge e_* and the polarization charge at r_2 . This result explains a similar gradient in the QED spread depicted in Figure 11.6 of [8, p. 319].

Appendix A: Overlap radii

In the Klein Paradox [9, p. 127], a free electron propagates in the positive z -direction until it collides with the free-space region II in which the negative energy vacuum has been distorted by the *positive* step-potential

$$e\phi = \begin{cases} 0 & \text{for } z < 0 \text{ (region I)} \\ V_0 & \text{for } z > 0 \text{ (region II)} \end{cases} \quad (\text{A1})$$

that is externally applied to the half-space $z > 0$. The Klein Paradox demonstrates that a sufficiently strong positive free-space potential can expose a portion of the vacuum state to “attack” by free-space particles.

For $V_0 = 0$, the positive energy continuum for an electron in regions I and II increases from $m_e c^2$ in the positive energy direction, while the negative-energy vacuum continuum decreases from $-m_e c^2$ in the negative-energy direction. When the positive step-potential is imposed on the $z > 0$ half-space, however, the negative energy continuum in region II is increased as a whole by V_0 . The electron positive energy continuum and the vacuum negative energy continuum can then overlap in region II. The plane at $z = 0$ is referred to in the present paper as an overlap boundary, and region II as the corresponding overlap region.

Upon collision with the step, the electron excites electron-positron pairs, the electrons and positrons propagating in the negative and positive z -directions respectively. In order for there to be pair excitation, the perturbing potential V_0 must satisfy the inequality

$$V_0 > E + m_e c^2 = (m_e^2 c^4 + c^2 p^2)^{1/2} + m_e c^2 \quad (\text{A2})$$

where E and p are the relativistic energy and momentum of the incident electron.

In the proton rest frame, the proton core (e_*, m_p) is responsible (via the coupling force (1)) for distorting the PV and for exposing the negative energy continuum to the free space around the core. The free-space spherical surfaces where the various positive and negative energy continua begin to overlap are defined in the present paper as *overlap radii*. The surface at the e-p overlap radius develops a positive polarization charge due to the polarizing effect of the positive core charge.

Submitted on January 7, 2015 / Accepted on January 12, 2015

References

1. Daywitt W.C. Why the proton is smaller and heavier than the electron. *Progress in Physics*, 2014, v. 10 (3), 175.
2. Daywitt W.C. The Planck vacuum. *Progress in Physics*, 2009, v. 5 (1), 20. See also www.planckvacuum.com.
3. Daywitt W.C. The electron and proton Planck-vacuum coupling forces and the Dirac equation. *Progress in Physics*, 2014, v. 10 (2), 114. The minus sign in equation (17) of this paper should be replaced by a positive sign.
4. Daywitt W.C. The strong and weak forces and their relationship to the Dirac particles and the vacuum state. *Progress in Physics*, 2015, v. 11 (1), 18.
5. Carroll B. W., Ostlie D. A. An Introduction to Modern Astrophysics. Addison-Wesley, San Francisco-Toronto, 2007.
6. Daywitt W.C. The source of the quantum vacuum. *Progress in Physics*, v. 5 (1), 27. There is a error in Appendix A of this paper: in the first line of the last paragraph “ $p = \hbar/r_L$ ” should read “ $m_p c = \hbar/r_L$ ”.
7. Milonni P.W. The Quantum Vacuum – an Introduction to Quantum Electrodynamics. Academic Press, New York, 1994.
8. Aitchison I.J.R., Hey A.J.G. Gauge Theories in Particle Physics, Vol. 1. Taylor & Francis, New York, London, 2003.
9. Gingrich D.M. Practical Quantum Electrodynamics. CRC, The Taylor & Francis Group, Boca Raton, London, New York, 2006. – In the Klein Paradox V_0 is assumed to be a positive electrostatic potential, whereas the nonnegative potential $V_p(r)$ includes both charge (e_*) and mass (m_p). The difference between the two potentials is of no interest to the present paper, the salient point being the positive nature of both potentials.

“The Theory of Heat Radiation” Revisited: A Commentary on the Validity of Kirchhoff’s Law of Thermal Emission and Max Planck’s Claim of Universality

Pierre-Marie Robitaille¹ and Stephen J. Crothers²

¹Department of Radiology, The Ohio State University, 395 W. 12th Ave, Columbus, Ohio 43210, USA

²Queensland, Australia

E-mails: robitaille.1@osu.edu, steve@plasmaresources.com

Affirming Kirchhoff’s Law of thermal emission, Max Planck conferred upon his own equation and its constants, h and k , universal significance. All arbitrary cavities were said to behave as blackbodies. They were thought to contain black, or normal radiation, which depended only upon temperature and frequency of observation, irrespective of the nature of the cavity walls. Today, laboratory blackbodies are specialized, heated devices whose interior walls are lined with highly absorptive surfaces, such as graphite, soot, or other sophisticated materials. Such evidence repeatedly calls into question Kirchhoff’s Law, as nothing in the laboratory is independent of the nature of the walls. By focusing on Max Planck’s classic text, “*The Theory of Heat Radiation*”, it can be demonstrated that the German physicist was unable to properly justify Kirchhoff’s Law. At every turn, he was confronted with the fact that materials possess frequency dependent reflectivity and absorptivity, but he often chose to sidestep these realities. He used polarized light to derive Kirchhoff’s Law, when it is well known that blackbody radiation is never polarized. Through the use of an element, $d\sigma$, at the bounding surface between two media, he reached the untenable position that arbitrary materials have the same reflective properties. His Eq. 40 ($\rho = \rho'$), constituted a dismissal of experimental reality. It is evident that if one neglects reflection, then all cavities must be black. Unable to ensure that perfectly reflecting cavities can be filled with black radiation, Planck inserted a minute carbon particle, which he qualified as a “catalyst”. In fact, it was acting as a perfect absorber, fully able to provide, on its own, the radiation sought. In 1858, Balfour Stewart had outlined that the proper treatment of cavity radiation must include reflection. Yet, Max Planck did not cite the Scottish scientist. He also did not correctly address real materials, especially metals, from which reflectors would be constructed. These shortcomings led to universality, an incorrect conclusion. Arbitrary cavities do not contain black radiation. Kirchhoff’s formulation is invalid. As a direct consequence, the constants h and k do not have fundamental meaning and along with “Planck length”, “Planck time”, “Planck mass”, and “Planck temperature”, lose the privileged position they once held in physics.

... That the absorption of a particle is equal to its radiation, and that for every description of heat.

Balfour Stewart, 1858 [1]

1 Introduction

Seldom does discovery bring forth scientific revolution [2]. In this regard, there can be no greater exception than Max Planck’s [3] introduction of the quantum of action, at the beginning of the twentieth century [4, 5]. Within “*The Theory of Heat Radiation*” [5] Planck outlined the ideas which gave life both to this revolution and to the concept that fundamental constants existed which had universal significance throughout nature. The pillars which supported his ideas included: 1) Kirchhoff’s Law of thermal emission [6, 7], 2) the irreversibility of heat radiation, and 3) the adoption of dis-

crete states.* He utilized Kirchhoff’s Law not only to assist in the derivation of his equation, but to infer universality. Max Planck concluded that all cavities, irrespective of experimental evidence, would eventually become filled with blackbody, or normal, radiation. He argued that, if a cavity did not contain black radiation, the cause was a lack of thermal equilibrium, which could be easily rectified by the introduction of a minute particle of carbon [8]. For Max Planck, as for his teacher Gustav Kirchhoff [9], cavity radiation was independent of the nature of the enclosure. In reality, such ideas were not supported by experiment, as arbitrary cavities do not contain black, or normal, radiation. By applying his law to all cavities, the father of quantum theory detached his equation from physical reality itself. In truth, Planck’s equation was only valid for laboratory blackbodies constructed from highly

**The Theory of Heat Radiation* is readily available online [5].

absorbing materials.

As a direct consequence, Planck's equation was never linked to a particular physical process and he did not provide physics with a cause for thermal emission. In fact, Kirchhoff's Law prevented him from advancing such a link [8, 10]. The exact nature of the oscillators responsible for thermal radiation could not be identified. Planck emphasized that [5, § 111],

“... to attempt to draw conclusions concerning the special properties of the particles emitting the rays from the elementary vibrations in the rays of the normal spectrum would be a hopeless undertaking”.

Studying Planck's classic text, the reader is eventually brought to the equation which governs specific intensity \mathbf{K}_ν [5, Eq. 300],

$$\mathbf{K}_\nu = \frac{h \nu^3}{c^2} \frac{1}{e^{\frac{h\nu}{kT}} - 1}, \quad (1)$$

wherein ν , c , h , k and T represent the frequency of interest, the speed of light,* Planck's constant, Boltzmann's constant, and absolute temperature, respectively. The validity of this equation appears to have been established for blackbodies; namely those specialized heated cavities whose interior is always lined with good absorbers over the frequency of interest, such as graphite, soot, carbon black, or other specialized materials (see [8] and references therein). Max Planck recognized that blackbodies were complex devices, as the data provided for his analysis had been obtained by some of the premier experimentalists in Germany [11–13].

He relied on the work of Rubens and Kurlbaum [11, 13] to secure the data which led to Eq. 1. In this regard, it is important to note the elaborate experimental setup used [11, 13]. It was very far from a simple cavity. These results made use of “the method of residual rays”, a process which actually took place well beyond the confines of the cavity [11, 13]. Repeated reflections were supported by using crystals of quartz, fluorite, rocksalt, and sylvine, each for a given frequency of interest [11, 13]. The desired data points could only be obtained with an apparatus used to select the frequency of interest at the proper intensity.

In themselves, such extreme experimental methods confirmed that not all enclosures were filled with black radiation. Surely, if arbitrary cavities contained black radiation, there should have been no need for the use of these sophisticated approaches [13].

In this regard, it is also interesting to note that when faced with non-compliant experimental facts, scientists often invoke the inability to reach thermal equilibrium. This is especially true when cavities are constructed from materials with a low emissivity. Such arguments are not reasonable, given

the speed of light and the relative ease of maintaining temperature equilibrium in metallic objects through conductive processes. Laboratory findings do not support Planck's position relative to Kirchhoff's Law.

Clearly, real blackbodies were much more than simple arbitrary cavities [11–13]. Yet, Max Planck believed with certainty in the universality of Kirchhoff's Law. It is this aspect of Planck's work which must be carefully considered. For if it holds true, then Eq. 1 continues to have far-reaching consequences. It can be applied to any thermal spectrum, whether on Earth in the laboratory, or within any astrophysical context, provided of course, that thermal equilibrium can be demonstrated.[†] However, if Kirchhoff's Law can be shown to be false, then Planck's equation, while still valid for laboratory blackbodies, loses all universal significance [8, 10, 14–19].

It could no longer be used indiscriminately outside of the laboratory, at least if the observer could not ensure that the source of the observed spectrum originated from a known solid. Hence, all applications of Planck's law in astronomy would very likely constitute violations of its required setting. In addition, the fundamental nature of Planck's constant, Boltzmann's constant, and of “Planck length”, “Planck time”, “Planck mass”, and “Planck temperature” would forever be lost. All would have ordinary significance. They would be no more fundamental for physics than the mile versus the kilometer. Everything simply becomes a question of the scale physics chooses to select, rather than scales being imposed upon mankind by nature itself. Consequently, Max Planck's conclusion that Eq. 1 could be applied to all arbitrary cavities had great implications.

It remains an experimental fact that good reflectors, such as silver, are never utilized to construct blackbodies, in direct contradiction to Kirchhoff's claim that cavity radiation is independent of the nature of the walls from which it is comprised. Silver walls would prefer to increase their temperature when confronted with an influx of heat, such as that typically used to drive blackbodies in the laboratory (see [8] and references therein). They would not easily maintain their temperature while building a radiation field within a cavity using reflection (see [19] for a discussion). It has also not been established that cavities constructed from walls of low emissivity can contain Lambertian emission. These are some of the reasons why Kirchhoff's Law fails.

As such, how could this law have survived for so long? In order to answer this question, it is important to revisit both the experimental and theoretical foundations which brought forth Kirchhoff's Law. For this exposition, the journey will begin with the experiments of Balfour Stewart [1] in keeping with the reality that experiments [10], not solely theory, govern the laws of physics. At this point, the work of Gus-

*The United Nations has declared that 2015 will be the “Year of Light”.

[†]There must be radiative equilibrium, no temperature changes, and no conduction or convection taking place in the system of interest.

tav Kirchhoff [6, 7] must be discussed, especially as related to his treatment of reflection. Then, finally, a detailed analysis of Max Planck's derivation of Kirchhoff's Law, as outlined in "*The Theory of Heat Radiation*" [5], will be presented. It will be demonstrated that Planck's derivation suffers, not only with minor problems, but with significant departures from experimental reality.

2 Balfour Stewart and the Law of Equivalence

Balfour Stewart was a Scottish physicist. In 1858, one year before Kirchhoff's Law was proposed [6, 7], Stewart published what can be considered one of the most important works in the history of thermal emission [1]. His analysis of radiation was entirely based on experimental grounds. Hence, he never claimed, as law, principles which could not be proven experimentally [1]. Using actual measurements with material plates made of various substances, Stewart formulated the Law of Equivalence, first in §19 of his work [1],

"The absorption of a plate equals its radiation, and that for every description of heat",

and then in §33 [1],

"That the absorption of a particle is equal to its radiation, and that for every description of heat".

At the same time, he addressed cavity radiation, arriving at a general principle by considering a single theoretical argument. For Stewart, this principle did not rise to the level of a law, precisely because the conclusion had not been experimentally verified. He treated cavity radiation purely from a theoretical perspective and highlighted that the radiation which should come to fill the cavity resulted from the radiation emitted, in addition to the radiation which had been built up by reflection. The arguments advanced, being theoretical and not experimental, prevented him from formally proposing a new law with respect to cavity radiation. Rather, he spoke of a general principle [1],

"Although we have considered only one particular case, yet this is quite sufficient to make the general principle plain. Let us suppose we have an enclosure whose walls are of any shape, or any variety of substances (all at a uniform temperature), the normal or static condition will be, that the heat radiated and reflected together, which leaves any portion of the surface, shall be equal to the radiated heat which would have left that same portion of the surface, if it had been composed of lampblack. . . Let us suppose, for instance, that the walls of this enclosure were of polished metal, then only a very small quantity of heat would be radiated; but this heat would be bandied backwards and forwards between surfaces, until the total amount of radiated and re-

flected heat together became equal to the radiation of lampblack".

The problem is that good reflectors do not readily emit radiation. As such, in order to drive the reflection term, one must try to inject heat into the walls of these cavities, while hoping that additional photons will be produced. But, if one attempts to pump heat into their walls using conduction, for instance, the temperature of the walls can simply increase [18, 19]. Nothing dictates that new photons can become available for the buildup of the reflective term, while maintaining the cavity at the same temperature. One can infer that good reflectors can easily move away from the temperature of interest and fall out of thermal equilibrium. As a result, they cannot easily be filled with the desired radiation, even if theoretical arguments suggest otherwise. In the real world, nothing is independent of the nature of the materials utilized.

Stewart recognized that, if one could "drive the radiation" in a cavity made from arbitrary materials, by permitting the slow buildup of reflected radiation, the interior could eventually contain black radiation. The argument was true in theory, but not demonstrated in practice. Stewart remained constrained by experimental evidence. The situation could not be fully extended in the laboratory.

From Balfour Stewart, we gain three important lessons. First, he correctly supplied the Law of Equivalence: *Given thermal equilibrium, the emission of an object is equal to its absorption*. Second, he outlined the principle that cavity radiation can become black, in theory, in the event that the reflective term can be driven. Third, and most importantly, he did not advance a new law of physics without experimental confirmation.

3 Gustav Kirchhoff: Physics from Theory Alone

Soon after Balfour Stewart formulated the Law of Equivalence [1], Gustav Kirchhoff published his law of thermal emission [6, 7]. Almost immediately, the work was translated into English by F. Guthrie [7] and Kirchhoff's paper was then re-published in the same journal where Stewart had presented his law the year before. At this point, a battle ensued between Kirchhoff and Stewart.* The problem centered on Kirchhoff's attempt to dismiss Stewart's priority claims for the Law of Equivalence. Kirchhoff did so by arguing that Stewart had not brought forth sufficient theoretical support for his law. As for Stewart, he believed that the law had been experimentally proven, even if his mathematical treatment might have lacked sophistication.

In any event, Kirchhoff's paper went much beyond the Law of Equivalence. Thus, Stewart, who had outlined the principle that arbitrary cavities might come to hold black radiation, did not insist that this was always true [1]. Conversely, Kirchhoff formulated this conclusion as a law of physics, but

*An excellent treatment of this incident has already been published [20] and one of the authors has also addressed the issue [8].

he did so without recourse to a single experiment. Both of his proofs were theoretical [6, 7].

To begin his investigation, Kirchhoff, in the first section of his text, defined a blackbody as follows [7, § 1]:

“This investigation will be much simplified if we imagine the enclosure to be composed, wholly or in great part, of bodies which, for infinitely small thickness, completely absorb all rays which fall upon them”.

Note the emphasis on the absorption by an element of infinitely small thickness. The contrast between Kirchhoff’s definition of a blackbody and that adopted by Max Planck was profound [5], as will be discovered below. In any event, in §3 of his classic paper [7] Kirchhoff presented his law as follows,

“The ratio between the emissive power and the absorptive power is the same for all bodies at the same temperature”.

In § 13, he explicitly wrote the following form,

$$\frac{E}{A} = e. \quad (2)$$

Kirchhoff eventually set $A = 1$ [7, § 3]. In modern notation,* one could express Kirchhoff’s Law as follows:

$$\frac{E_\nu}{\alpha_\nu} = f(T, \nu), \quad (3)$$

where $f(T, \nu)$ corresponds to the right side of Eq. 1 above, as first defined by Max Planck [4, 5]. In §17 of his classic paper [7], Kirchhoff outlined his law as follows,

“When a space is surrounded by bodies of the same temperature, and no rays can penetrate through these bodies, every pencil in the interior of the space is so constituted, with respect to its quality and intensity, as if it proceeded from a perfectly black body of the same temperature, and is therefore independent of the nature and form of the bodies, and only determined by the temperature. The truth of this statement is evident if we consider that a pencil of rays, which has the same form but the reverse direction to that chosen, is completely absorbed by the infinite number of reflections which it successively experiences at the assumed bodies. In the interior of an opaque glowing hollow body of given temperature there is, consequently, always the same brightness whatever its nature may be in other respects.”

*Though Kirchhoff speaks of absorptive power, A , he was actually referring to the unitless absorptivity, α_ν . Conversely, when referring to emissive power, E , he was, in fact, referring to this quantity, even in modern terms. That is, Kirchhoff’s “ E ” has the same units as his “ e ” and neither is equal to 1. Kirchhoff, stated that “ e ” was a universal function and believed that its elucidation was a matter of great scientific importance.

Relative to Kirchhoff’s formulation, three important concerns must be raised. First, the law becomes undefined in the perfect reflector, as $\alpha_\nu = 0$ under that condition. Planck himself recognized this fact [5, § 48], but might not have exercised proper care relative to its consequences. Second, it is clear that Kirchhoff lacked an accurate understanding of what was happening within his cavity, as an “infinite number” of reflections will never amount to absorption. An “infinite number” of reflections does not involve the exchange of energy. Conversely, when absorption occurs, energy is exchanged between the field in the interior of the cavity and the walls. Third, and the most serious objection to Kirchhoff’s Law, centers upon his improper treatment of reflection. One of the authors has previously addressed these problems in detail [16].

In brief, within his first proof, Kirchhoff utilized transmissive plates to accomplish the proof, even if blackbody cavities must always be opaque. He addressed transmission by positioning mirrors behind his plates. In so doing, it appeared that Kirchhoff had properly treated reflection, because the mirrors did, in fact, reflect radiation. However, he had dismissed the possibility that the plates considered could possess differing surface reflection [16]. As shall be discovered below, Max Planck committed the same error, when he attempted to formulate Kirchhoff’s Law [5, § 36–38]. In his second proof, Kirchhoff unknowingly permitted the cavity to fall out of thermal equilibrium, depending on the order in which operations were performed (see [16] for a detailed presentation).

It is evident that no valid theoretical proof of Kirchhoff’s Law existed before Max Planck formulated his law of emission (see [21] for an excellent presentation). In fact, physicists continued to argue about a proper theoretical proof for Kirchhoff’s Law until well after Planck’s ideas became accepted [21]. Thus, in search of a proof, those provided by Planck, Hilbert, or Pringsheim may be the most relevant [21]. Yet, the proofs provided by Pringsheim and Hilbert have their own shortcomings [21].[†] It has even been claimed that, by applying Einstein coefficients to arrive at Planck’s law, physics could dispense with the proof of Kirchhoff’s Law [21]. However, Einstein’s derivation utilized the energy density associated with a Wien radiation field, something which could only be found within a blackbody. Surely, Wien had not dispensed with Kirchhoff. In truth, it appears that those concerned with bringing forth a proper proof for Kirchhoff’s Law were never able to reach their goal. The problem of finding a valid proof, seems to have simply been displaced by “more exciting physics”, as the long sought definitive formulation of Kirchhoff’s Law could no longer provide sufficient interest. The entire issue appears to have come to a slow death, without proper resolution.

It is certain that all theoretical proofs of Kirchhoff’s Law

[†]The authors have not been able to locate an analysis of the proof advanced by Max Planck within “*The Theory of Heat Radiation*”.

will be found to contain significant misapplications of experimental facts. The inability to provide a proper proof before the days of Planck [21], has not been easily overcome by some new insight into the nature of materials, after Planck. It remains true that all theoretical proofs of Kirchhoff's Law suffer from one or more of the following: 1) an improper treatment of reflection, absorption, or transmission; 2) the invocation of polarized light, when heat radiation is always unpolarized; 3) the use of transmissive materials, when Kirchhoff's Law refers to opaque enclosures; and 4) the existence of hypothetical objects which can have no place in the physical world.

However, the central proof of Kirchhoff's Law must always be the one outlined by Max Planck himself (see [5, § 1–51]), forty years after Kirchhoff [6,7]. For it is upon this proof (see [5, § 1–51]) that Eq. 1 was derived and through which Planck would ultimately attempt to lay the foundation for universality. Hence, it is best to forgo Kirchhoff's own derivations, as the theoretical validity of Kirchhoff's Law now rests with Max Planck [5, § 1–51].

4 Max Planck and Departure from Objective Reality

Having held such reverence for Max Planck over the years [3], it is with some regret that the following sections must be composed, outlining his sidestep of known experimental physics in the derivation of Kirchhoff's Law. Fortunately, in Planck's case, the validity of his equation is preserved, but only within the strict confines of the laboratory blackbody. The quantum of action continues to hold an important place in physics. Yet, the loss of universality cannot be taken lightly, as this aspect of Planck's work was the pinnacle of his career. In fact, above all else, it was universality which Planck sought, believing that he had discovered some great hidden treasure in nature [5, § 164],

“Hence it is quite conceivable that at some other time, under changed external conditions, every one of the systems of units which have so far been adopted for use might lose, in part or wholly, its original natural significance. In contrast with this it might be of interest to note that, with the aid of the two constants h and k which appear in the universal law of radiation, we have the means of establishing units of length, mass, time, and temperature, which are independent of special bodies or substances, which necessarily retain their significance for all times and for all environments, terrestrial and human or otherwise, and which may, therefore, be described as ‘natural units’ ”.

This was an illusion. With the collapse of Kirchhoff's Law, there are no “natural units” and all the constants of physics become a manifestation of the scales which the scientific community chooses.

4.1 Planck's Derivation of Kirchhoff's Law: Part I

Throughout his derivation of Kirchhoff's Law (see [5, § 1–51]), Max Planck sub-optimally addressed reflection, transmission, and absorption. This can be seen in the manner in which he redefined a blackbody, in an array of quotations [5, § 4],

“Strictly speaking, the surface of a body never emits rays, but rather it allows part of the rays coming from the interior to pass through. The other part is reflected inward and according as the fraction transmitted is larger or smaller, the surface seems to emit more or less intense radiation”.

For Planck, photons were being released from an object, not because they were emitted by its surface, but simply because they managed to be transmitted throughout, or beyond, its interior. The blackbody became a sieve. Planck stated [5, § 10],

“A rough surface having the property of completely transmitting the incident radiation is described as ‘black’ ”.

Planck continued [5, § 12],

“Thus only material particles can absorb heat rays, not elements of surfaces, although sometimes for the sake of brevity, the expression absorbing surfaces is used.

Note the contrast, with Kirchhoff, which can be repeated for convenience [7, § 1],

“This investigation will be much simplified if we imagine the enclosure to be composed, wholly or in great part, of bodies which, for infinitely small thickness, completely absorb all rays which fall upon them”.

Planck acknowledged in a footnote that Kirchhoff considered a blackbody as absorbing over an infinitely thin element. He stated [5, § 10],

“In defining a blackbody Kirchhoff also assumes that the absorption of incident rays takes place in a layer ‘infinitely thin’. We do not include this in our definition.”

With his words, Planck redefined the meaning of a blackbody. The step, once again, was vital to his derivation of Kirchhoff's Law, as he relied on transmissive arguments to arrive at its proof. Yet, blackbody radiation relates to opaque objects and this is the first indication that the proofs of Kirchhoff's Law must not be centered on arguments which rely upon transmission. Planck ignored that real surface elements must possess absorption, in apparent contrast with Kirchhoff and without any experimental justification. Planck would expand on his new concept for a blackbody with these words [5, § 10],

“... the blackbody must have a certain minimum thickness depending on its absorbing power, in order to insure that the rays after passing into the body shall not be able to leave it again at a different point of the surface. The more absorbing a body is, the smaller the value of this minimum thickness, while in the case of bodies with vanishingly small absorbing power only a layer of infinite thickness may be regarded as black.”

Now, he explicitly stated that bodies which are poor absorbers can still be blackbodies. Yet, we do not make blackbodies from materials which have low absorptivities, because these objects have elevated reflectivities, not because they are not infinite. Planck had neglected the important effects of absorption and reflection when formulating his new definition for a blackbody. This may have consequences throughout physics and astronomy [8, 17, 22].

In the end, Planck’s surface elements must be composed of material particles. Since Planck was a theoretical physicist, he cannot work solely in the vacuum of a mathematical world. His derivations and conclusions must be related to physical reality. Yet, Planck’s treatment had moved away from laboratory experiments with thin plates. These experiments were vital to the development of blackbody radiation science from the days long before Balfour Stewart [1]. Planck stated that [5, § 12],

“Whenever absorption takes place, the heat ray passing through the medium under consideration is weakened by a certain fraction of its intensity for every element of path traversed.”

Clearly, Planck’s element at the “bounding surface”, as will soon be discovered, was an “element of path traversed”. He therefore cannot neglect its absorption. Planck was well aware of this fact [5, § 12]:

“We shall, however, consider only homogeneous isotropic substances, and shall therefore suppose that α_ν has the same value at all points and in all directions in the medium, and depends on nothing but the frequency ν , the temperature T , and the nature of the medium.”

and again [5, § 32],

“Consider then any ray coming from the surface of the medium and directed inward; it must have the same intensity as the opposite ray coming from the interior. A further immediate consequence of this is that the total state of radiation of the medium is the same on the surface as in the interior.”

Still, at every turn, he attempted to include the effect of transmission, when it had no proper place in the treatment of blackbody radiation, as found in opaque bodies [5, § 14],

“Let $d\sigma$ be an arbitrarily chosen, infinitely small element of area in the interior of a medium through which radiation passes.”

Planck thereby included the transmissive properties of the element, $d\sigma$, though he should have avoided such an extension. In the end, his definition of a blackbody was opposed to all that was known in the laboratory. Blackbodies are opaque objects without transmission, by definition. By focusing on transmission, Planck prepared for his move to universality, as will now be discussed in detail.

4.2 Planck’s Derivation of Kirchhoff’s Law: Part II

In the first section of his text, leading to his Eq. 27, [5, Eq. 27], Planck chose to formally neglect reflection, even though the total energy of the system included those rays which are both emitted/absorbed and those which would have been maintained by driving reflection [18, 19]. Such an approach was suboptimal. Planck must have recognized that the reflective contributions could eventually be canceled. Perhaps, that is why he simply neglected these terms, but the consequence was that insight was lost. In addition, by adopting this approach, Max Planck explicitly prevented the newcomer to the field of thermal radiation from appreciating the crucial importance of reflection within cavity radiation, as Balfour Stewart had well demonstrated [1, 18, 19].

In order to properly follow Planck’s work, it is important to recognize his unusual conventions with respect to symbols. Dimensional analysis reveals that even though he spoke of a coefficient of emission (Emissionskoeffizienten) and utilized the symbol now reserved for emissivity, ϵ_ν , he was not referring to the emissivity in this instance. Rather, he was invoking the emissive power, \mathbf{E} , an entity with units. Conversely, when he spoke of the coefficient of absorption (Absorptionkoeffizienten), α_ν , he was truly referring to the dimensionless absorptivity, as we know it today. Insufficient attention relative to Planck’s notation has, in fact, caused one of the authors to revise some of his previous works [18, 19]. Suffice it to note for the time being that, in order to remain consistent with Planck’s notation, the following conventions will now be adopted: The symbol ϵ_ν , will represent emissive power, \mathbf{E} , and not emissivity. The symbols α_ν and ρ_ν will retain their modern meaning and represent dimensionless absorptivity and reflectivity, respectively. This is in keeping with Planck’s notation. At the same time, we shall add the symbol η_ν , in order to deal with dimensionless emissivity, since Max Planck had already utilized the needed symbol when expressing emissive power.*

*In § 44, Planck presented Kirchhoff’s Law in the following form [5, Eq. 48],

$$\frac{E}{A} = I = d\sigma \cos \theta d\Omega \mathbf{K}_\nu dv,$$

where A is actually the unitless absorptivity. Then, in § 45, Planck set $A = 1$. But, he also set, $E = A$. In so doing, he removed dimensionality from the emissive power, E .

At the outset, Max Planck considered the radiation within the interior of an isotropic medium. Inside this material, the total energy emitted from a volume element, $d\tau$, in frequency range of interest, $\nu + d\nu$, and in time, dt , in the direction of a conical element, $d\Omega$, was given by [5, Eq. 1],

$$dt d\tau d\Omega d\nu 2\epsilon_\nu, \quad (4)$$

from which Planck immediately surmised, by integrating over all directions and frequencies, that the total energy emitted corresponded to [5, Eq. 2],

$$dt d\tau 8\pi \int_0^\infty \epsilon_\nu d\nu. \quad (5)$$

He then moved to present the same equation, in slightly modified form in § 25 as,

$$dt v 8\pi \int_0^\infty \epsilon_\nu d\nu, \quad (6)$$

where v now corresponded to the volume element.

But since this element was contained within the medium of interest, it must also be reflecting radiation from other elements within the medium. That is because, as Balfour Stewart correctly highlighted, the total radiated power measured from a particle is to that portion which was emitted by the particle itself and that portion which it reflected [1]. This reflective component corresponds to the reflection coefficient, ρ_ν , multiplied by the specific intensity, \mathbf{K}_ν , of the radiation leaving the second element, $d\tau'$, positioned at the end of Planck's conical section. The proper form of Eq. 4 [5, Eq. 1], including all of the radiation which leaves the particle, becomes,

$$dt d\tau d\Omega d\nu 2(\epsilon_\nu + \rho_\nu \mathbf{K}_\nu). \quad (7)$$

This expression, rather than leading to Eq. 6, results in,

$$dt v 8\pi \int_0^\infty (\epsilon_\nu + \rho_\nu \mathbf{K}_\nu) d\nu. \quad (8)$$

Similarly, Planck characterized the fate of the radiation which strikes the volume element, by including only absorption [5, Eq. 25],

$$dt v 8\pi \int_0^\infty \alpha_\nu \mathbf{K}_\nu d\nu. \quad (9)$$

If however, one considers that the radiation incident to the volume element, v , can be either absorbed or reflected, then Eq. 9 [5, Eq. 25] becomes,

$$dt v 8\pi \int_0^\infty (\alpha_\nu + \rho_\nu) \mathbf{K}_\nu d\nu. \quad (10)$$

Equating Eqs. 6 and 9, Planck obtained,

$$dt v 8\pi \int_0^\infty \epsilon_\nu d\nu = dt v 8\pi \int_0^\infty \alpha_\nu \mathbf{K}_\nu d\nu, \quad (11)$$

which led to [5, Eq. 27],

$$\mathbf{K}_\nu = \frac{\epsilon_\nu}{\alpha_\nu}. \quad (12)$$

Note that in this expression, Planck, like Kirchhoff, removed all consideration of reflection. Conversely, by combining Eqs. 8 and 10, we obtain that,

$$dt v 8\pi \int_0^\infty (\epsilon_\nu + \rho_\nu \mathbf{K}_\nu) d\nu = dt v 8\pi \int_0^\infty (\alpha_\nu + \rho_\nu) \mathbf{K}_\nu d\nu. \quad (13)$$

This expression leads to the following relation,

$$\epsilon_\nu + \rho_\nu \mathbf{K}_\nu = \alpha_\nu \mathbf{K}_\nu + \rho_\nu \mathbf{K}_\nu. \quad (14)$$

If one eliminates the terms involving reflection, this expression immediately leads to Eq. 12 [5, Eq. 27]. More importantly, since $\alpha_\nu + \rho_\nu = 1$ at thermal equilibrium, then a second expression, which retains the importance of reflectivity, is obtained,

$$\epsilon_\nu = (1 - \rho_\nu) \mathbf{K}_\nu. \quad (15)$$

Since Eq. 14 leads directly to Eq. 12, it now becomes clear why Max Planck chose to ignore the contribution of reflection in his derivation. He adopted a physically incomplete picture, but without mathematical consequence, at least in this instance. It could also be argued that Eq. 12 and Eq. 15 do not differ from one another, since at thermal equilibrium $1 - \rho_\nu = \alpha_\nu$. However, mathematically this is not the case. Eq. 12 becomes undefined when the absorptivity, α_ν , is set to zero. This is precisely what happens in the perfect reflector. Conversely, Eq. 15 is never undefined, as long as the reflective term is retained. As such, the prudent course of action for Max Planck might have been to adopt Eq. 15.

At this point, a trivial observation can be easily advanced. As mentioned above, given thermal equilibrium, then $1 - \rho_\nu = \alpha_\nu$. But at the same time, $\alpha_\nu = \eta_\nu$. This is the Law of Equivalence, first presented by Balfour Stewart [1]. As a result, it can be readily noted that Eq. 15 can be expressed as,

$$\epsilon_\nu = \eta_\nu \mathbf{K}_\nu \quad \text{or} \quad \mathbf{E}_\nu = \eta_\nu \mathbf{K}_\nu, \quad (16)$$

which is similar to Planck's Eq. 26 [5, Eq. 26]. In this case, \mathbf{K}_ν is given by Planck [5, Eq. 300]. It corresponds to a Planck function multiplied by the square of the index of refraction of the medium. Note what Eq. 16 is stating: *The emissive power of an arbitrary cavity at thermal equilibrium is equal to the emissivity of the material which makes up the cavity multiplied by a function.* This constitutes a proper and direct contradiction of universality. The nature of the radiation within the cavity becomes dependent on the nature of the cavity itself.

Thus, if the derivation is accomplished while including reflection, additional insight is gained. If given the choice, a function which is never undefined, like Eq. 15, must always take precedence over a function which can become undefined,

like Eq. 12. Then, consider Eq. 16. This relationship is important, because, like the form presented by Kirchhoff (Eq. 2) and Planck (Eq. 12), it is devoid of the consideration of reflection. But, when confronted with Eq. 16, it is impossible to conclude that arbitrary cavities contain black radiation.

In this initial treatment, Planck had not yet formally introduced Kirchhoff's Law. In order to accomplish this feat, he had to explore more than one medium at a time. Nonetheless, in this initial exposition of Planck's derivation, an important lesson has been learned: it is vital to recognize that the manner in which a result is presented can have a great deal of influence on its interpretation. Nowhere is this more applicable than in Planck's formal presentation of Kirchhoff's Law, as he leads the reader from Eq. 27 to Eq. 42 [5, Eq. 27–42]. It is here that Planck sidestepped experimental reality.

4.3 Planck's Derivation of Kirchhoff's Law: Part III

Heat radiation is unpolarized, by definition [23, p. 450]. In § 4 of *The Theory of Heat Radiation* [5], Planck considered a homogeneous isotropic emitting substance. Any volume element of such a material necessarily emits heat radiation uniformly in all directions. In § 5 Planck admitted that homogeneous isotropic media emit only natural or normal, i.e. unpolarized, radiation [5, § 5]:

“Since the medium was assumed to be isotropic the emitted rays are unpolarized.”

This statement alone, was sufficient to counter all of the arguments which Planck later utilized to arrive at Kirchhoff's Law [5, Eq. 42]. That is because the important sections of Planck's derivation, namely § 35–37 make use of plane-polarized light. These steps were detached from experimental reality, relative to heat radiation [5, § 35],

“Let the specific intensity of radiation of frequency ν polarized in an arbitrary plane be \mathbf{K}_ν in the first substance ... and \mathbf{K}'_ν in the second substance ...”

Planck also stated [5, § 36],

“...we have for the monochromatic plane-polarized radiation...”

As such, to prepare for his use of polarized light in later sections, Planck resolved, in § 17, the radiation into its two polarized components. However, note that he could have arrived at Eq. 12 [5, Eq. 27] without ever resolving the radiation into its components. Nonetheless, his proof for the universality of Kirchhoff's Law [5, Eqs. 27–42] depended upon the use of polarized light [5, § 35–37]. Planck utilized polarized light in an isotropic medium, even though he had already recognized in § 5, that such radiation must be unpolarized. He clearly remarked in § 107,

“For a plane wave, even though it be periodic with a wave lying within the optical or thermal

spectrum, can never be interpreted as heat radiation.”

In order to arrive at Kirchhoff's Law, in § 35–37, Planck placed two different homogeneous isotropic media in contact with one another, as illustrated in Figure 1. The whole system was “*enclosed by a rigid cover impermeable to heat*”. He then considered two arbitrary plane-polarized waves, one from each of the media, incident upon an element of area $d\sigma$ at the *bounding surface* of the two media. It can be seen in § 38, that Planck initially endowed this element with differing reflectivities, depending on whether the incident rays approached from medium 1 or medium 2. For Planck, both waves underwent reflection and refraction. He sidestepped that the ray could be absorbed, a decision vital to his ability to derive Kirchhoff's law [5, § 9],

“... a discontinuous change in both the direction and the intensity of a ray occurs when it reaches the boundary of a medium and meets the surface of a second medium. The latter, like the former, will be assumed to be homogeneous and isotropic. In this case, the ray is in general partly reflected and partly transmitted.”

Planck invoked a small element of area $d\sigma$ at the boundary of his two contiguous media. This element had no consistent meaning in Planck's analysis. First, in § 36 and § 42 Planck placed this element in the *bounding surface* and, in so doing, allocated it properties characteristic of medium 1 on one half and medium 2 on the other. However, in § 43, he placed the element firmly within the surface of medium 2,

“... and falls on the surface element $d\sigma$ of the second medium.”

Note that Planck had already introduced three causes for objection. First, what exactly was the location of $d\sigma$? In reality it must rest in one of the two media. Second, Planck neglected the fact that real materials can possess finite and differing absorptivities. While these can be ignored within the medium when treating propagation, because of the counter effect of emissivity, they cannot be dismissed at the boundary. Third, the simplest means of nullifying the proof leading to Planck's Eq. 42, is to use a perfect reflector as the second medium. In that case, a refractive wave could never enter the second medium and Planck's proof fails. The same objection can be raised using any fully opaque material for the second medium (i.e. $\alpha_\nu + \rho_\nu = 1$), as for all of them, $\tau_\nu=0$. This would include many materials typically used to construct real blackbodies in the laboratory. Consequently, for his proof of Kirchhoff's Law, Planck eliminated, by definition, virtually all materials of interest. In fact, he even excluded the perfect reflector, the very material he had chosen to consider throughout much of his text [5].

In § 36 Planck considered a monochromatic plane-polarized ray of frequency ν , emitted in time dt . In order to

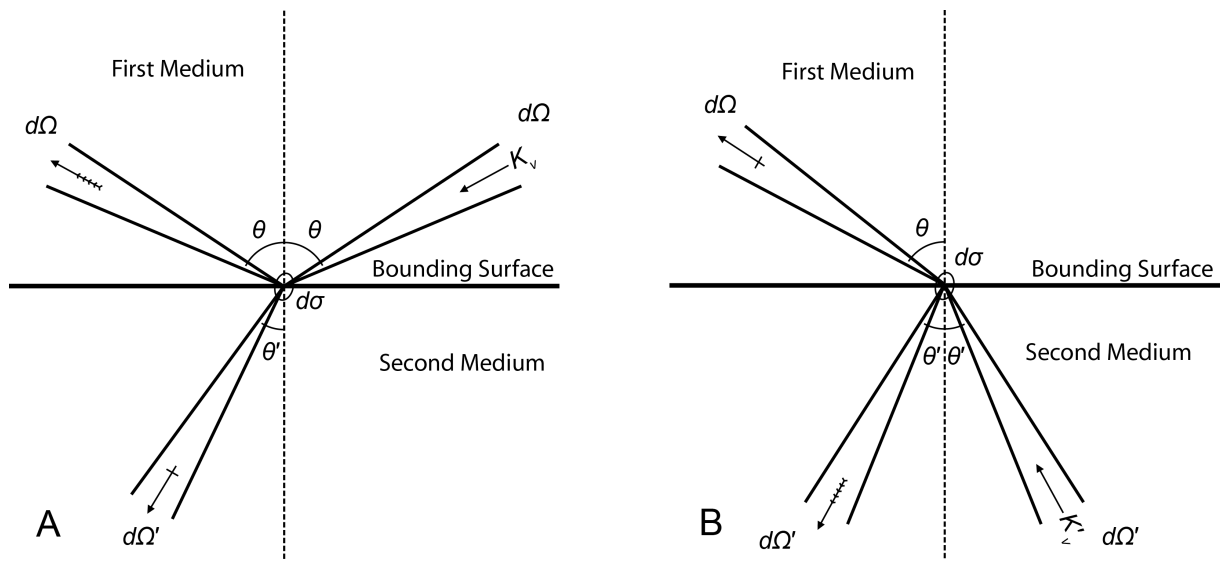


Fig. 1: Expansion of Figure 3 in “The Theory of Heat Radiation” [5] depicting the full complement of rays involved in treating the interaction between two media separated by a “bounding surface” which contained a hypothetical element of interest, $d\sigma$. Planck considered the reflective nature of $d\sigma$ to ascertain whether its reflection coefficients were identical depending on whether the incident ray originated from medium 1, (A), or medium 2, (B). A) Schematic representation of the incident specific intensity, \mathbf{K}_v (plain arrow), at an angle θ , contained in the conical section, $d\Omega$, of the first medium (upper right quadrant) which is reflected by the bounding surface into the conical section $d\Omega$ in the upper left quadrant and refracted into the conical section $d\Omega'$ of the second medium, at an angle θ' , in the lower left quadrant. Note that in order to preserve the proper specific intensities, \mathbf{K}_v , in the upper left quadrant, Planck must sum the reflected portion of the incident specific intensity of medium 1, $\rho_v \mathbf{K}_v$, with the refracted portion of the incident specific intensity of medium 2, $(1 - \alpha'_v - \rho'_v) \mathbf{K}'_v$, depicted in B. This fact is represented by the feathered arrow. However, he neglected to include that part of the specific intensity in the upper left quadrant was being produced by emission in that direction, η_v , by $d\sigma$. B) Schematic representation of the incident specific intensity, \mathbf{K}'_v (plain arrow), at an angle θ' , contained in the conical section, $d\Omega'$, of the second medium (lower right quadrant) which is reflected by the bounding surface into the conical section, $d\Omega'$, in the lower left quadrant and refracted into the conical section, $d\Omega$, of the first medium, at an angle θ , in the upper left quadrant. Note that, in order to preserve the proper specific intensities, \mathbf{K}'_v , in the lower left quadrant, Planck must sum the reflected portion of the incident specific intensity of medium 2, $\rho'_v \mathbf{K}'_v$, with the refracted portion of the incident specific intensity of medium 1, $(1 - \alpha_v - \rho_v) \mathbf{K}_v$, as depicted in A. This fact is represented by the feathered arrow. However, he neglected to include that part of the specific intensity in the lower left quadrant was being produced by emission in that direction, η'_v , by $d\sigma$.

address absorption at the “bounding surface”, as mentioned under the second objection above, the total radiation which was both emitted and reflected by an element within the medium of interest (i.e. the incident ray) towards the “bounding surface” must be considered, as illustrated in Figure 2.

Note in this case, that the ray which is approaching the bounding surface will be transformed into three components: 1) that which will be absorbed at the “bounding surface” and then re-emitted in the direction of reflection; 2) that which will be reflected into the same medium; and 3) that which will be refracted into the other medium. The distinction is important, for Planck inferred that $\rho_v + \tau_v = 1$, whereas the correct expression involves $\rho_v + \tau_v + \alpha_v = 1$.^{*} Planck permitted himself to state that $\tau_v = 1 - \rho_v$, whereas he should have

^{*}Note that in §36 Planck referred to frequency dependent reflectivity, ρ_v , but chose to write it simply as ρ . In this case, since he was dealing with the frequency dependent value, the subscripted form will be utilized throughout the presentation which follows. As such, the equations presented by Max Planck will be modified such that ρ is replaced with ρ_v in accordance with his description that the term was frequency dependent.

obtained $\tau_v = 1 - \rho_v - \alpha_v$. Again, this completely prevents further progress towards Kirchhoff’s Law [5, Eq. 42].

Planck considered the reflected rays in the first medium, of specific intensity \mathbf{K}_v at incidence [5, Eq. 38],

$$\rho_v dt d\sigma \cos \theta d\Omega \mathbf{K}_v dv, \tag{17}$$

which were augmented by rays of incident specific intensity \mathbf{K}'_v refracted from the second medium [5, Eq. 39],

$$(1 - \rho'_v) dt d\sigma \cos \theta' d\Omega' \mathbf{K}'_v dv. \tag{18}$$

In this setting, the resultant rays in medium 1 consist of components from both media, the reflected and the refracted rays. Planck then obtained the following equation, at the end of his § 36,

$$\frac{\mathbf{K}_v}{\mathbf{K}'_v} \cdot \frac{q^2}{q'^2} = \frac{1 - \rho'_v}{1 - \rho_v}, \tag{19}$$

where q and q' correspond to speeds of light in first and second media, respectively. He rapidly moved to [5, Eq. 40],

$$\rho_v = \rho'_v, \tag{20}$$

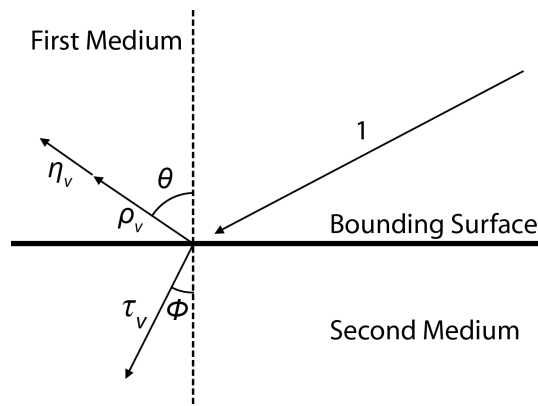


Fig. 2: Schematic representation of the fate of an incident ray, 1, which strikes a bounding surface. The ray will be split into three components: 1) the reflected ray, ρ_v ; 2) the refracted ray, τ_v ; and 3) that portion of the ray which is first absorbed, α_v , then immediately re-emitted, η_v , in order to preserve energy balance, in the direction of the reflected ray ($\alpha_v = \eta_v$). Thus, it is possible to describe this problem mathematically as $1 = \rho_v + \tau_v + \alpha_v$.

The result was stunning. Max Planck had determined that the reflectivities of all arbitrary media were equal. Yet, he attempted to dismiss such a conclusion by stating relative to Eq. 20 [5, Eq. 40]:

“The first of these two relations, which states that the coefficient of reflection of the bounding surface is the same on both sides, is a special case of a general rule of reciprocity first stated by Helmholtz.”

Planck provided for the element of the bounding surface two separate coefficients of reflection. These must, in fact, correspond to those of the media utilized. Planck has already stated in § 35 that

“... let all quantities referring to the second substance be indicated by the addition of an accent.”

Consequently, ρ and ρ' can only take meaning with respect to the media under consideration. Thus, how did Planck possibly reach the conclusion that these values must be equal? At the onset in Eq. 19 [5, § 35], Planck sought to force $\rho_v = \rho'_v$, in general, by first making $\rho_v = \rho'_v = 0$, in particular. To accomplish this feat, he considered rays that were,

“polarized at right angles to the plane of incidence and strike the bounding surface at the angle of polarization” [5, § 37].

Again, such rays could never exist in the context of heat radiation [23, p. 450].

The “plane of incidence” is that containing the unit normal vector from the surface of incidence and the direction of the incident ray. There are two natural ways by which the orientation of an electromagnetic wave can be fixed; by the electric vector \vec{E} or the magnetic vector \vec{B} . Contemporary

convention is to use the electric vector \vec{E} [24, § 1.4.2]. Planck used the erstwhile magnetic vector convention.

The “angle of polarization” is Brewster’s angle [23, p. 450]. The angle between reflected and refracted rays resulting from a given incident ray is then 90° . The reflected wave is entirely plane-polarized*, as shown in Figure 3,

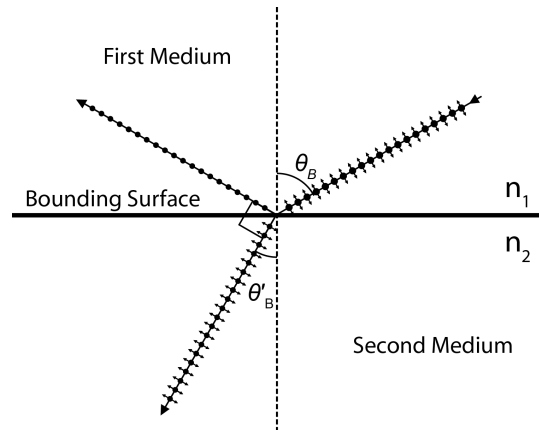


Fig. 3: Schematic representation of Brewster’s Law. The dots correspond to the electric vector perpendicular to the page, whereas the double-headed arrows represent the electric vector in the plane of the page. An unpolarized, or arbitrarily plane-polarized, incident ray (upper right quadrant), strikes a surface at an angle of incidence, θ_B , corresponding to the Brewster’s angle, or the angle of polarization. The reflected ray, depicted in the upper left quadrant will be entirely plane-polarized in such a way that it has no component of its electric vector in the plane of incidence. The transmitted ray produced at the angle of refraction, θ'_B , depicted in the lower left quadrant, will be partially polarized. The angle between the reflected and refracted rays is 90° . The angles, θ_B and θ'_B are complementary ($\theta + \theta'_B = 90^\circ$). This process depends on the refractive indices of the two media involved, n_1 and n_2 , such that the process is defined by Snell’s Law, $n_1 \sin \theta_B = n_2 \sin (90^\circ - \theta_B)$, which in turn becomes $n_1 \sin \theta_B = n_2 \cos \theta_B$, or $\tan \theta_B = n_2/n_1$.

Planck’s medium 2 has a Brewster’s angle complementary to the Brewster’s angle of his medium 1 ($\theta_B + \theta'_B = 90^\circ$). Brewster’s angle is defined in terms of a reflected and a refracted beam. Unpolarized light, and plane-polarized light that is not “at right angles to the plane of incidence”, produce reflected and refracted beams, in accordance with Brewster’s Law. Planck invoked Brewster’s Law [23, p. 450] with the special condition that incident rays are orthogonal to the plane of incidence. In this case, there could be no reflection, but only refraction, in accordance with Snell’s Law. He simultaneously applied these same restricted conditions to medium 2.

“Now in the special case when the rays are polarized at right angles to the plane of incidence and strike the bounding surface at the angle of polarization, $\rho = 0$, and $\rho' = 0$.”

*The reflected ray has no \vec{E} component in the plane of incidence.

However, Planck's two contiguous media were homogeneous and isotropic. They could only emit unpolarized light and not plane-polarized light. Since the entire system was enclosed by a barrier impermeable to heat, there was no external source of any incident plane-polarized rays. All incident rays considered must be unpolarized and all resultant composite rays, at best, partially polarized. This implied that the reflectivities of both media were never zero. Yet, Planck made all rays plane-polarized and, in this special case, orthogonal to the plane of incidence (magnetic vector convention). Since plane-polarized rays in both media were chosen orthogonal to their common plane of incidence, they had no components which could be reflected. The conclusion that the reflectivities were equal was therefore never properly tested, as Planck had offered no possibility of any reflection taking place. Consequently, Planck's conclusion, that $\rho_v = 0$, and $\rho'_v = 0$ cannot be true. Thus, Planck becomes unable to move to Kirchhoff's Law, as presented in his Eq. 42 [5, Eq. 42].

The situation was actually more complex, as Planck did not provide the proper form for Eqs. 17, 18, and 19. In reality, he neglected the contribution from emission or absorption in Eqs. 17 and 18. He had already redefined the blackbody as possessing a purely transmissive surface, in contradiction to Kirchhoff, as seen above. This was a critical error. The proper form of Eq. 17 [5, Eq. 38] must also include a term for emissivity, η_v , in the direction of the conical element,

$$(\eta_v + \rho_v) dt d\sigma \cos \theta d\Omega \mathbf{K}_v dv. \quad (21)$$

The proper form of Eq. 18 [5, Eq. 39] must also include a term for absorptivity of the second medium, α'_v ,

$$(1 - \rho'_v - \alpha'_v) dt d\sigma \cos \theta' d\Omega' \mathbf{K}'_v dv. \quad (22)$$

That is because the intensity of the ray from medium 2 which is refracted into medium 1 corresponds to the transmissivity ($\tau'_v = 1 - \rho'_v - \alpha'_v$). Clearly, the intensity of the transmitted ray must account for the reduction of the incident ray within medium 2 as a result of *both* reflection and absorption. Planck cannot ignore the absorption of the surface. Consequently, Eq. 19 should have included the emissivity of the first medium, η_v , and the absorptivity of the second medium, α'_v . If one considers that the emissivity of the first medium, η_v , is equal to its absorptivity, α_v , then Eq. 19 becomes,

$$\frac{\mathbf{K}_v}{\mathbf{K}'_v} \cdot \frac{q^2}{q'^2} = \frac{1 - \rho'_v - \alpha'_v}{1 - \rho_v - \alpha_v}. \quad (23)$$

This equation can never lead to Kirchhoff's Law [5, Eq. 42].

As a consequence, it is readily apparent that Planck, through Eqs. 17-20, adopted a presentation which selectively applied the rules of reflection and refraction to polarized rays, irrelevant to the discussion of heat radiation. Furthermore, he then arbitrarily chose the plane of polarization such that when the waves were incident at Brewster's angle, there would be

no reflection. Nonetheless, if there could be no reflection, then Brewster's angle, or the angle of polarization, could have no meaning. That is because such an angle depends on the reflected and refracted rays being at 90° to one another. But since Planck insisted that no reflection occurred, then clearly the reflected and refracted rays could not form a 90° angle. Importantly, not only did Planck advance Eq. 20 (i.e. Planck's Eq. 40) by neglecting absorptivity and emissivity, he thereby selected materials which have little or no relevance to heat radiation. Planck could not neglect absorption and emission, treating only transmission and reflection, if he wished to have any relevance to actual blackbodies. In addition, he hypothesized a *bounding surface* without any true physical meaning. Given this array of shortcomings, this derivation of Kirchhoff's law can never be salvaged. Planck's claims for universality were without proper theoretical confirmation.

5 Planck's Perfectly Reflecting Cavities and the Carbon Particle

Throughout "*The Theory of Heat Radiation*", Planck had recourse to a perfectly reflecting cavity, in which he placed a minute carbon particle (see [8] for a detailed treatment). Obviously, cavities comprised solely of perfectly reflecting surfaces, can never contain black radiation, as such materials cannot emit photons [16]. Nonetheless, Planck believed that these cavities contained radiation. He was careful however, not to state that this radiation was black [5, § 51],

"...in a vacuum bounded by totally reflecting walls any state of radiation may persist."

This statement, by itself, was a violation of Kirchhoff's Law. Nonetheless, Planck believed that he could transform the radiation contained in all cavities into the thermodynamically stable radiation by inserting a carbon particle [5, § 51],

"If the substance introduced is not diathermanous for any color, e.g., a piece of carbon however small, there exists at the stationary state in the whole vacuum for all colors the intensity \mathbf{K}_v of black radiation corresponding to the temperature of the substance".

and later [5, § 52],

"It is therefore possible to change a perfectly arbitrary radiation, which exists at the start in the evacuated cavity with perfectly reflecting walls under consideration, into black radiation by the introduction of a minute particle of carbon. The characteristic feature of this process is that the heat of the carbon particle may be just as small as we please, compared with the energy of radiation contained in the cavity of arbitrary magnitude. Hence, according to the principle of the conservation of energy, the total energy of radiation remains essentially constant during the

change that takes place, because the changes in the heat of the carbon particle can be entirely neglected, even if its changes in temperature should be finite. Herein the carbon particle exerts only a releasing (auslösend) action” .

Recall however, that Stewart’s law insisted that [1],

“... That the absorption of a particle is equal to its radiation, and that for every description of heat.”

When Planck moved the carbon particle into the cavity, clearly the emissive field of the particle also entered the cavity provided the former had some real temperature. However, if one assumes that the particle was at $T=0\text{K}$, then no radiation from the carbon particle could enter the cavity. At the same time, if the particle was allowed to come into physical contact with the walls of the cavity, then energy could flow from the walls into the particle by conduction. Hence the particle, being perfectly emitting, would fill the entire cavity with black radiation. Alternatively, if the carbon particle could be suspended within the cavity, with no thermal contact to its walls, then the only radiation entering the system, would be that which accompanied the carbon particle itself [16]. That is because the walls of the cavity would not be able to “drive” the carbon particle, since they could emit no radiation. In that case, the radiation density within the cavity would remain too low and characterized only by the carbon particle. Unlike what Planck believed, the carbon particle could never be a simple catalyst, as this would constitute a violation of Stewart’s law [1]. Catalysts cannot generate, by themselves, the product sought in a reaction. They require the reactants. Yet, the carbon particle was always able to produce black radiation, in accordance with Stewart’s findings [1]. This was evidence that it could not be treated as a catalyst.

6 Planck’s Treatment of Two Cavities

Planck’s suboptimal treatment of the laws of emission continued [5, § 69],

“Let us finally, as a further example, consider a simple case of a irreversible process. Let the cavity of volume V , which is everywhere enclosed by absolutely reflecting walls, be uniformly filled with black radiation. Now let us make a small hole through any part of the walls, e.g., by opening a stopcock, so that the radiation may escape into another completely evacuated space, which may also be surrounded by rigid, absolutely reflecting walls. The radiation will at first be of a very irregular character; after some time, however, it will assume a stationary condition and will fill both communicating spaces uniformly, its total volume being, say, V' . The presence of a carbon particle will cause all conditions of black radiation to be satisfied in the new state. Then,

since there is neither external work nor addition of heat from the outside, the energy of the new state is, according to the first principle, equal to that of the original one, or $U' = U$ and hence from (78)

$$T'^4 V' = T^4 V$$

$$\frac{T'}{T} = \sqrt[4]{\frac{V}{V'}}$$

which defines completely the new state of equilibrium. Since $V' > V$ the temperature of the radiation has been lowered by the process.”

This thought experiment was unsound. First, both cavities were made of perfectly reflecting walls. As such, Planck could not assume that the second cavity contained no radiation. To do so, constituted a violation of the very law he wished to prove. Kirchhoff’s Law stated that the second cavity could not be empty. Therefore, Planck could not surmise that the temperature had dropped.

If one accepted that Kirchhoff’s Law was false, as has been demonstrated above, then both cavities must be viewed as empty, other than the minute contribution made by the carbon particle. Here again, Max Planck had moved beyond the confines of reality, for he advanced a result which could not be correct, whether or not Kirchhoff’s Law was true. The cavities were either both empty (i.e. Kirchhoff’s Law was not valid), or both filled with radiation (i.e. Kirchhoff’s Law was valid). One could not be filled, while the other was empty. Planck’s equation, in the quote above, was incorrect.

7 Conclusion

Throughout “*The Theory of Heat Radiation*” [5] Planck employed extreme measures to arrive at Kirchhoff’s Law. First, he redefined the nature of blackbodies, by adopting transmission as a central element of his derivation. Second, he neglected the role of absorption at the surface of such objects, in direct contradiction to experimental findings and Kirchhoff’s understanding of blackbodies. While it could be argued that absorption does not take place entirely at the surface, Planck could not assume that no absorption took place in this region. He was bound to include its contribution, but failed to meet this requirement. Third, he sidestepped reflection, by neglecting its presence in arriving at Eq. 12 [5, Eq. 27]. Nonetheless, the energy of the system under investigation included both that which was involved in emission/absorption and that associated with the reflection terms. Stewart has well highlighted that such terms are central to the nature of the radiation within arbitrary cavities [1] and the concept has recently been re-emphasized [18, 19]. Fourth, Planck had recourse to plane-polarized light, whereas blackbody radiation is never polarized.

In the end, Planck’s presentation of Kirchhoff’s Law did not properly account for the behavior of nature. Arbitrary

cavities are not always black and blackbodies are highly specialized heated objects. Planck's characterization of the carbon particle as a simple "catalyst" constituted a dismissal of Stewart's Law [1]:

"... That the absorption of a particle is equal to its radiation, and that for every description of heat."

Planck could not transform a perfect absorber into a catalyst. Yet, without the carbon particle [8], the perfectly reflecting cavities, which he utilized throughout "*The Theory of Heat Radiation*" for the derivation of his famous Eq. 1 [4, 5], remained devoid of radiation. Perfectly reflecting cavities are incapable of producing radiation, precisely because their emissivity is 0 by definition. Planck can only properly arrive at Eq. 1 by having recourse to perfectly absorbing materials, a truth which he did not acknowledge. The presence of reflection must always be viewed as suboptimal to the creation of a blackbody, since significant reflection acts as a hindrance to the generation of photons through emission. It is never clear that the reflection term can easily be driven to arrive at the desired radiation, since thermal equilibrium, under these circumstances, can easily be violated, as the temperature of the cavity increases.

Planck's detachment from experimental findings relative to Kirchhoff's Law was evident in his presentation of Eq. 20 [5, Eq. 40]. His conclusion, with respect to the equivalence of the reflection in arbitrary materials, was false. Obviously, if reflection was always the same, then all opaque cavities would become identical. Eq. 20 [5, Eq. 40] became the vital result in Planck's derivation of Kirchhoff's Law. Unfortunately, the conclusion that $\rho = \rho'$ [5, Eq. 40] constituted a distortion of known physics and, by extension, so did Kirchhoff's formulation.

Without a proper proof of Kirchhoff's Law, Planck's claim for universality loses the role it plays in science. This has significant consequences in both physics and astronomy [8, 17, 24]. The constants h and k do not have fundamental meaning. Along with "Planck length", "Planck time", "Planck mass", and "Planck temperature", they are to be relegated to the role of ordinary and arbitrary constants. Their value has been defined by our own selection of scales, not by nature itself.

Dedication

This work is dedicated to the memory of Balfour Stewart [1].

Submitted on: January 24, 2015 / Accepted on: January 25, 2015

First published online on: January 28, 2015

References

1. Stewart B. An account of some experiments on radiant heat, involving an extension of Prévost's theory of exchanges. *Trans. Royal Soc. Edinburgh*, 1858, v. 22, no. 1, 1–20.
2. Kuhn T.S. *The Structure of Scientific Revolutions*. University of Chicago Press, Chicago, IL, 1962.
3. Robitaille P.-M. Max Karl Ernst Ludwig Planck: (1858–1947). *Progr. Phys.*, 2007, v. 4, 117–120.
4. Planck M. Über das Gesetz der Energieverteilung im Normalspektrum. *Annalen der Physik*, 1901, v. 4, 553–563.
5. Planck M. *The theory of heat radiation*. P. Blakiston's Son & Co., Philadelphia, PA, 1914, <http://gutenberg.org/ebooks/40030>.
6. Kirchhoff G. Über den Zusammenhang zwischen Emission und Absorption von Licht und Wärme. *Monatsberichte der Akademie der Wissenschaften zu Berlin*, sessions of Dec. 1859, 1860, 783–787.
7. Kirchhoff G. Über das Verhältnis zwischen dem Emissionsvermögen und dem Absorptionsvermögen der Körper für Wärme und Licht. *Poggendorfs Annalen der Physik und Chemie*, 1860, v. 109, 275–301.
8. Robitaille P.-M. Blackbody radiation and the carbon particle. *Progr. Phys.*, 2008, v. 3, 36–55.
9. Agassi J. The Kirchhoff–Planck radiation law. *Science*, 1967, v. 156(3771), 30–37.
10. Robitaille P.-M. Kirchhoff's Law of thermal emission: 150 Years. *Progr. Phys.*, 2009, v. 4, 3–13.
11. Hoffmann D. On the experimental context of Planck's foundation of quantum theory. In: *Revisiting the Quantum Discontinuity*, Max Planck Institute for the History of Science, Preprint 150, 2000, 47–68.
12. Lummer O. and Pringsheim E. Kritisches zur schwarzen Strahlung. *Annalen der Physik*, 1901, v. 6, 192–210.
13. Rubens H. and Kurlbaum F. Anwendung der Methode der Reststrahlen zur Prüfung der Strahlungsgesetzes. *Annalen der Physik*, 1901, v. 2, 649–666; Rubens H. and Kurlbaum F. On the heat radiation of long wave-length emitted by black bodies at different temperatures. *Astro-phys. J.*, 1901, v. 74, 335–348.
14. Robitaille P.M. On the validity of Kirchhoff's Law of thermal emission. *IEEE Trans. Plasma Sci.*, 2003, v. 31, no. 6, 1263–1267.
15. Robitaille P. M. L. An analysis of universality in blackbody radiation. *Progr. Phys.*, 2006, v. 2, 22–23; arXiv: physics/0507007.
16. Robitaille P.-M. A critical analysis of universality and Kirchhoff's Law: A return to Stewart's law of thermal emission. *Progr. Phys.*, 2008, v. 3, 30–35 (also in arXiv: 0805.1625).
17. Robitaille P.-M. Blackbody Radiation and the Loss of Universality: Implications for Planck's Formulation and Boltzmann's Constant. *Progr. Phys.*, 2009, v. 4, 14–16.
18. Robitaille P.-M. On the equation which governs cavity radiation. *Progr. Phys.*, 2014, v. 10, no. 2, 126–127; (see also Errata – Notice of Revision. *Progr. Phys.*, 2015, v. 11, no. 1, 88.)
19. Robitaille P.M. On the equation which governs cavity radiation II. *Progr. Phys.*, 2014, v. 10, no. 3, 157–162; (see also Errata – Notice of Revision. *Progr. Phys.*, 2015, v. 11, no. 1, 88.)
20. Siegel D.M. Balfour Stewart and Gustav Robert Kirchhoff: Two independent approaches to Kirchhoff's Law. *Isis*, 1976, v. 67, no. 4, 565–600.
21. Schirrmacher A. Experimenting theory: the proofs of Kirchhoff's radiation law before and after Planck. *Hist. Stud. Phys. Biol. Sci.*, 2003, v. 33, 299–335.
22. Robitaille P.M. Forty lines of evidence for condensed matter – The Sun on trial: Liquid metallic hydrogen as a solar building block. *Progr. Phys.*, 2013, v. 4, 90–142.
23. Jenkins F.A. and White H.E. *Fundamentals of Optics* (4th Edition), McGraw-Hill, Inc, New York, 1976.
24. Born M. and Wolf E. *Principles of Optics* (6th edition), Cambridge University Press, 1980.

Scaling of Body Masses and Orbital Periods in the Solar System

Hartmut Müller

Advanced Natural Research Institute in memoriam Leonhard Euler, Munich, Germany
E-mail: admin@anr-institute.com

The paper shows that the sequence of sorted by value body masses of planets and largest planetoids is connected by a constant scaling exponent with the sequence of their sorted by value orbital periods.

1 Introduction

In [1] we have shown that the observable mass distribution of large celestial bodies in the Solar system continues the mass distribution of elementary particles that can be understood as contribution to the fundamental link between quantum- and astrophysics via scaling.

Within the last ten years several articles [2–6] were published which confirm our statement that scaling is a widely distributed phenomenon. Possibly, natural oscillations of matter generate fractal distributions of physical properties in very different processes. Fractal scaling models [7] of oscillation processes in chain systems are not based on any statements about the nature of the link or interaction between the elements of the oscillating system. Therefore, the model statements are quite general, that opens a wide field of possible applications.

In this paper we will show, that the connection between the body mass distribution and the distribution of orbital periods of planets and largest planetoids in the solar system can be described by the scaling law (1):

$$M = \mu \cdot T^D, \quad (1)$$

where M is a celestial body mass, T is a celestial body orbital period and μ and D are constants.

We will show, that for sorted by value couples of a body mass M and an orbital period T the exponent D is quite constant and is closed to $3/2$. Furthermore, for M in units of the proton rest mass $m_p \approx 1.67 \times 10^{-27}$ kg [8] and T in units of the proton oscillation period $\tau_p = \hbar/m_p c^2 \approx 7.02 \times 10^{-25}$ s [9], the constant $\mu = 1$.

2 Methods

Already in the eighties the scaling exponent $3/2$ was found in the distribution of particle masses [10]. In [11] we have shown that the scaling exponent $3/2$ arises as consequence of natural oscillations in chain systems of harmonic oscillators.

Within our fractal model [1] of matter as a chain system of oscillating protons and under the consideration of quantum oscillations as model mechanism of mass generation [9], we interpret the exponent D in (1) as a Hausdorff [12] fractal dimension of similarity (2):

$$D = \frac{\ln M/m_p}{\ln T/\tau_p}. \quad (2)$$

The ratio M/m_p is the number of model protons, the ratio T/τ_p is the number of model proton oscillation cycles.

3 Results

If we sort by value the body masses and the orbital periods of planets and largest planetoids of the Solar system, then we can see that for sequently following couples of a body mass M and an orbital period T the fractal dimension D is quite constant and closed to the model value of $3/2$.

Table 1 contains properties of planets and of the most massive planetoids in the Solar system. On the left side the bodies are sorted by their masses, on the right side the bodies are sorted by their orbital periods. Within the Solar system the average empiric value $D \approx 1.527$ is a little bit larger than the model value of $3/2$.

Based on the empiric value $D \approx 1.527$, Table 2 continues the Table 1 until the Jupiter body mass. The orbital period of Eris corresponds well to the Uranus body mass, but the smaller transneptunian orbits, occupied by Pluto, Haumea and Makemake, ask for additional bodies. Possibly, the three vacant body masses and the three vacant orbital periods in Table 2 are properties of bodies which are still to be discover.

4 Resume

Celestial bodies are compressed matter which consist of nucleons over 99%. Possibly, the model approximation of $D = 3/2$ and $\mu = 1$ in (1) for proton units is a macroscopic quantum physical property, which is based on the baryon nature of normal matter, because $\mu = 1$ means that $M/T^D = m_p/\tau_p^D$.

The scaling law (1) seems a true system property, because it describes a connection between masses and orbital periods of different celestial bodies (Mercury and Jupiter, Earth and Neptune, etc.) within the Solar system.

5 Acknowledgements

I'm thankful to my friend Victor Panchelyuga, my son Erwin and my partner Leili for the great experience to work with them, for the deep discussions and permanent support. I'm thankful to my teacher Simon Shnoll.

Submitted on January 26, 2015 / Accepted on January 27, 2015

Bodies, sorted by M	Body mass M , kg	$\ln(M/m_p)$	D	$\ln(T/\tau_p)$	Orbital period T , years	Bodies, sorted by T
Ceres	9.5000×10^{20}	109.9584	1.5387	71.4603	0.2408	Mercury
Makemake	2.1000×10^{21}	110.7516	1.5298	72.3980	0.6152	Venus
Haumea	4.0100×10^{21}	111.3985	1.5284	72.8839	1.0000	Earth
Pluto	1.3000×10^{22}	112.5746	1.5313	73.5156	1.8808	Mars
Eris	1.7000×10^{22}	112.8429	1.5165	74.4099	4.6000	Ceres
Mercury	3.3020×10^{23}	115.8094	1.5368	75.3573	11.8626	Jupiter
Mars	6.4191×10^{23}	116.4741	1.5272	76.2665	29.4475	Saturn
Venus	4.8690×10^{24}	118.5003	1.5327	77.3149	84.0168	Uranus
Earth	5.9742×10^{24}	118.7049	1.5221	77.9885	164.7913	Neptune

Table 1: For sorted by value couples of a body mass M and an orbital period T the fractal dimension $D(2)$ is quite constant and closed to the model value $3/2$. Data come from [8, 13–16].

Bodies, sorted by M	Body mass M , kg	$\ln(M/m_p)$	D2	$\ln(T/\tau_p)$	Orbital period T , years	Bodies, sorted by T
vacant	1.6358×10^{25}	119.7122	1.5270	78.3970	247.9207	Pluto
vacant	2.0281×10^{25}	119.9271	1.5270	78.5378	285.4000	Haumea
vacant	2.2999×10^{25}	120.0529	1.5270	78.6201	309.9000	Makemake
Uranus	8.6849×10^{25}	121.3816	1.5325	79.2064	557.0000	Eris
Neptun	1.0244×10^{26}	121.5467	1.5270	79.5984	824.2881	vacant
Saturn	5.6851×10^{26}	123.2605	1.5270	80.7207	2532.1227	vacant
Jupiter	1.8987×10^{27}	124.4664	1.5270	81.5104	5577.7204	vacant

Table 2: Continues Table 1 until the Jupiter body mass. The masses and orbital periods for vacant bodies are calculated, based on the empiric average value $D \approx 1.527$.

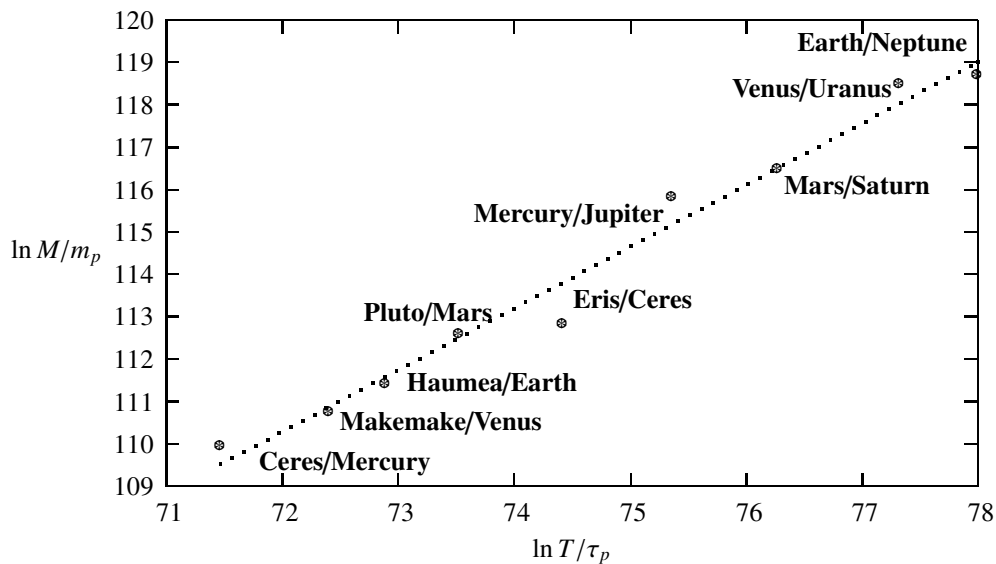


Fig. 1: Graphic representation of Table 1. For sorted by value couples of a body mass M and an orbital period T the fractal dimension D is quite constant. The dotted line is drawn for the average $D \approx 1.527$.

References

1. Müller H. Fractal scaling models of natural oscillations in chain systems and the mass distribution of the celestial bodies in the Solar System. *Progress in Physics*, 2010, issue 3, 61–66.
2. Fook M.V.L., Ries A. Fractal Structure of Nature's Preferred Masses: Application of the Model of Oscillations in a Chain System. *Progress in Physics*, 2010, issue 4, 82–89.
3. Fook M.V.L., Ries A. Application of the Model of Oscillations in a Chain System to the Solar System. *Progress in Physics*, 2011, issue 1, 103–111.
4. Wu K.K.S., Lahav O., Rees M.J. The large-scale smoothness of the Universe. *Nature*, 1999, v. 397.
5. Barenblatt G.I. *Scaling*. Cambridge University Press, 2003.
6. Tatischeff B. Fractals and log-periodic corrections applied to masses and energy levels of several nuclei. arXiv: 1107.1976v1, 2011.
7. Müller H. Fractal scaling models of resonant oscillations in chain systems of harmonic oscillators. *Progress in Physics*, 2009, issue 2, 72–76.
8. Physical constants. Particle Data Group. www.pdg.lbl.gov
9. Müller H. Emergence of Particle Masses in Fractal Scaling Models of Matter. *Progress in Physics*, 2012, issue 4, 44–47.
10. Kolombet V. Macroscopic fluctuations, masses of particles and discrete space-time. *Biofizika*, 1992, v. 36, 492–499.
11. Müller H. Fractal Scaling Models of Natural Oscillations in Chain Systems and the Mass Distribution of Particles. *Progress in Physics*, 2010, issue 3, 61–66.
12. Hausdorff F. *Dimension und äußeres Maß*, 1919, v. 79.
13. Ragozzine D., Brown M. Orbits and Masses of the Satellites of the Dwarf Planet Haumea = 2003 EL61. *Astronomical Journal*, 2009. arXiv: 0903.4213v1.
14. Brown M., Schaller E. The Mass of Dwarf Planet Eris. *Science*, 2007, v. 316 (5831), p. 1585.
15. Neptune System Nomenclature Table Of Contents. Gazetteer of Planetary Nomenclature. USGS Astrogeology, 2009.
16. Malhotra R., Showman A. The Galilean Satellites. *Science*, 1999, v. 286, 77–84.

EDITORIAL MESSAGE**In Memoriam of Joseph C. Hafele (1933–2014)**

Joseph Carl Hafele was born on July 25, 1933, in Peoria, Illinois, in the large family of Carl Louis Hafele and Thelma Loeb Hafele. He grew up among his many brothers and sisters.

In 1951, after serving in the US Army, he attended the University of Illinois at Urbana-Champaign. At the University, he got a BSc in engineering physics in 1959, and was bestowed the PhD degree in nuclear physics in 1962. After the graduation, during 1964–1966, he worked at the Los Alamos National Laboratory, wherein he conducted research in particle physics. After that, during 1966–1972, he worked within the Physics Faculty of Washington University at St. Louis, Missouri.

In 1958, he married Carol Hessling, and they raised four daughters.

In October 1971, Joseph C. Hafele commonly with Richard E. Keating, an astronomer from the US Naval Observatory, conducted the around-the-world-clock experiment which is one of the main experimental tests of the Theory of Relativity. Four Cesium atomic clocks were transported on board of a jet plane around the Globe twice, toward and against the direction of the Earth's rotation. The around-the-world-clock experiment showed, with high measurement precision, both gravitational and relativistic effects of Einstein's theory in the local space of the Earth. This experiment gave both of them world fame. Later, it became known as *Hafele-Keating experiment*.

Commencing in 1972, Joseph C. Hafele worked in different positions. He conducted some developments for Caterpillar Inc., lectured at Eureka College (1985–1991), was a visiting researcher for NASA at Langley AFB in Hampton, Virginia, lectured at Christopher Newport University in Newport News, Virginia. He retired in 1996, and settled in common with his wife Carol in Laramie, Wyoming.

Upon retirement, Joseph C. Hafele did not cease his scientific activity. Having no longer a physics laboratory for conducting experiments, he undertook deep theoretical research studies of the anomalous experiments which were unexplained in the frameworks of both modern classical mechanics and relativistic mechanics. He published a number of excellent papers in scientific journals, including our journal. It was a great honour for us to communicate with him and publish his research papers. Many of his scientific ideas still remain undeveloped until now.

In Laramie, Wyoming, he lived a modest life in common with his wife Carol, in their home where he grew tomatoes in



Joseph C. Hafele and Richard E. Keating on board of a jet plane while performing the around-the-world-clock experiment (1971).

his garden, and spent some astronomical observations at the telescope installed in his home observatory at the back yard.

Joseph C. Hafele passed away in November 15, 2014, being 81 years old. His heart suddenly stopped during surgery for an aortic aneurism at the Medical Center of the Rockies in Loveland, Colorado.

Let his memory live for ever!

Dmitri Rabounski and Larissa Borissova

LETTERS TO PROGRESS IN PHYSICS**Solar-Time or Sidereal-Time Dependent? The Diurnal Variation in the Anisotropy of Diffusion Patterns Observed by J. Dai (2014, Nat. Sci.)**

Felix Scholkmann

Bellariarain 10, 8038 Zürich, Switzerland. E-mail: felix.scholkmann@gmail.com

In this correspondence an additional analysis is reported about the anisotropic diffusion patterns of a toluidine blue colloid solution in water measured by J. Dai (*Nat. Sci.*, 2014, v. 6 (2), 54–58). In the previous analysis (Scholkmann, *Prog. in Phys.*, 2014, v. 10 (4), 232–235) it could be shown that the anisotropy data contain a diurnal and annual periodicity. This novel analysis investigated whether this periodicity is also present when the data were analyzed according to the sidereal time. The analysis revealed that the daily periodicity is present in the data scaled with the solar as well the sidereal time. When using solar time an oscillation with a diurnal period appears, when using sidereal time the oscillation is semidiurnal. In addition, the novel analysis revealed that the data of the maximum diffusion trend show a quantization of unknown origin.

Recently in this journal (v. 10 (4), [1]), I present a reanalysis of the data of J. Dai [2] that investigated fluctuations in anisotropic diffusion patterns of a toluidine blue colloid solution in water. It could be shown that the fluctuation of anisotropy, i.e. the maximum diffusion trend (MDT), clearly exhibits a diurnal and annual periodicity. Responding to this article, Prof. R. Cahill (Flinders University, Adelaide, Australia) suggested that it would be interesting to analyse if the observed periodicity is associated with the solar or the sidereal time (i. e. the time based on the Earth's rotation with respect to the fixed stars). In order to investigate this issue, the following new analysis was performed: (i) The time information given in the data of Dai was converted from the local solar time to the local sidereal time using the information of the location where the experiment was conducted (Wuhan City, China, latitude: N $\sim 30^{\circ}35'35.1168''$, longitude: E $\sim 114^{\circ}18'18.6192''$). (2) The data were analyzed by calculating the median and the median absolute deviation (MAD) for every hourly time interval (24 in total). (3) The function $f(\text{MDT}) = \alpha_0 + \alpha_1 \cos(\text{MDT} \omega)$ (with the free parameters α_0 , α_1 and ω) was fitted to the daily grouped data using the Trust-Region-Reflective Least Squares Algorithm. For the fitting, the MAD values were taken into account to increase the precision of the fit (which is an improvement to the fitting approach used in the previous analysis [2]).

The individual MDT values plotted against the solar time and sidereal time are shown in Figure 1(a) and (e), respectively. Fitting the periodic (sinusoidal) function to the MDT data showed that the fit functions differ depending on the time scaling (solar vs. sidereal) used. When using the solar time the best fit is a function with a diurnal periodicity (see Figure 1(b)) whereas when using the sidereal time the best fit has a semidiurnal periodicity (See Figure 1(f)). The goodness-of-fit (quantified by the squared Pearson correlation coefficient, r^2 , and the root-mean-square error, RMSE) for both

cases were: (i) MDT data with solar time: $r^2 = 0.5028$, RMSE = 3.191, and (ii) MDT data with sidereal time: $r^2 = 0.4838$, RMSE = 3.04. A visualization of the r^2 and RMSE values for both cases is shown in Figure 1(d) and Figure 1(h). To visualize the density distribution of the MDT values the density at each point of the grid was calculated as $1/z$ with z the sum of squared distance from each point. For this the Matlab function "DataDensityPlot" written by M. McLean was used. The density plots are shown in Figure 1(c) and Figure 1(g).

From this new analysis results we can conclude that (i) in both cases (solar and sidereal time scaling) the MDT data show a periodicity, (ii) the periodicity has a frequency depending on the time scaling: diurnal for solar time (oscillation maximum: at approx. 0.00 a.m.) and semidiurnal for sidereal time (oscillation maxima: at approx. 0.00 a.m. and 12.00–1.00 p.m.), (iii) the goodness-of-fit of the fitted function for both data sets (MDT vs. solar or sidereal time) is similar. The correlation is higher for the solar time scaling but the RMSE value lower for the sidereal time scaling. This can be interpreted as meaning that the MDT values contain an oscillation correlated with the solar as well as with the sidereal time. A related observation was obtained by Shnoll who found a solar and sidereal oscillation in the similarity of histograms of radioactive decay of ^{239}Pu [3, 4].

The detected oscillations indicate that there is possibly cosmophysical factor influencing the diffusion process. This factor might be influencing the process from a preferred direction in space such as determined for example by Miller (right ascension, $\alpha = 4^{\text{hr}} 54^{\text{min}}$, declination, $\delta = -70^{\circ} 33'$ [5]; $\alpha = 4^{\text{hr}} 56^{\text{min}}$, $\delta = -70^{\circ} 33'$ [6]), Cahill ($\alpha = 4.92^{\text{hr}}$, $\delta = -75.0^{\circ}$) [7], Múnera et al. ($\alpha = 16^{\text{hr}} 40^{\text{min}}$, $\delta = -75^{\circ}$ [8]; $\alpha = 5^{\text{hr}} 24^{\text{min}}$, $\delta = +79^{\circ}$ [9]), and Baurov ($\alpha = 19^{\text{hr}} 32^{\text{min}} \pm 40^{\text{min}}$, $\delta = 36^{\circ} \pm 10^{\circ}$) [10].*

*The value for the right ascension is originally given by Baurov as $\alpha =$

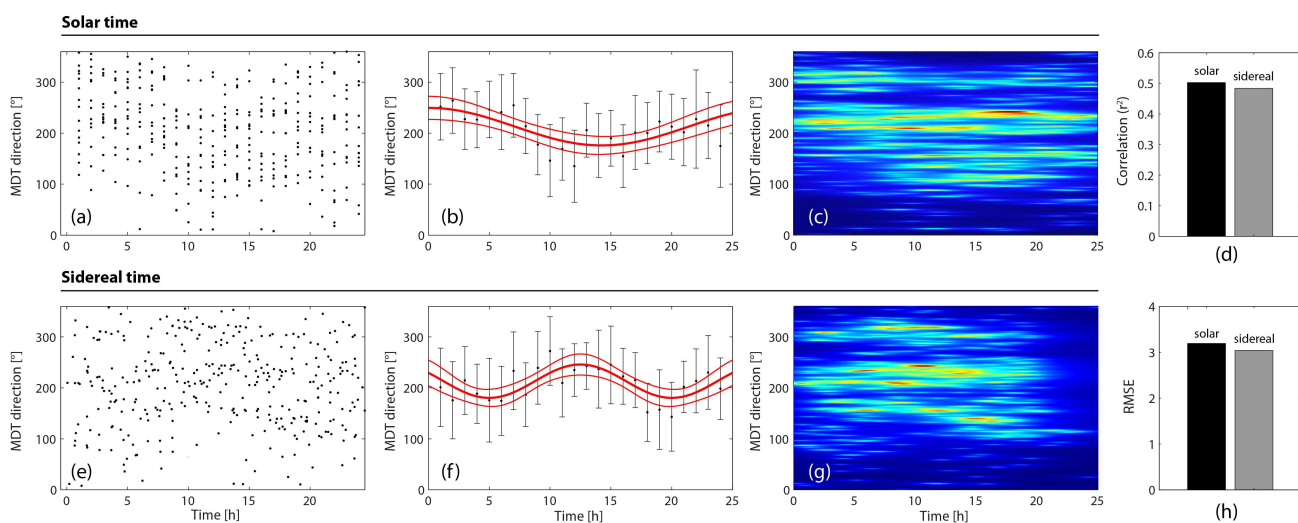


Fig. 1: Raw data plotted against solar (a) or sidereal (e) time. Fitted sinusoidal function to the MDT scaled using the solar (b) or sidereal (f) time. Density plot of the MDT values plotted against solar (c) or sidereal (g) time. The values for the correlation and RMSE value of the fit are shown in (d) and (h).

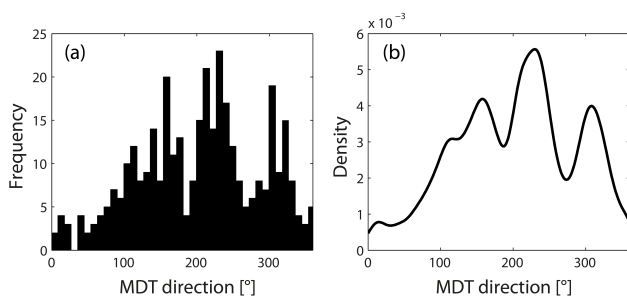


Fig. 2: (a) Histogram and Kernel density (b) of the MDT values.

As an additional analysis the characteristics of the distribution of the MDT from all 15 days were investigated by computing the histogram (number of bins: 40) and the Kernel density according to the method of Shimazaki & Shinomoto [5]. This analysis revealed an interesting pattern: the occurrence of MDT values shows three distinct peaks. The strongest peak is at 230° , the second at 158° and the third at 303° (see Figure 2). This quantization of diffusion anisotropy is another interesting feature of Dai's data that awaits explanation.

In conclusion, the new analysis performed shows novel features of the MDT data of Dai. Further MDT measurements and investigations into the cause of the observed effects would be an interesting next step in this area of research.

Submitted on January 28, 2015 / Accepted on February 5, 2015

$293^\circ \pm 10^\circ$ and was converted to $\alpha = 19^{\text{hr}} 32^{\text{min}}$ by the author using the equality $360^\circ = 24 \text{ h}$.

References

- Scholkmann F. Indications for a diurnal and annual variation in the anisotropy of diffusion patterns – A reanalysis of data presented by J. Dai (2014, Nat. Sci.). *Progress in Physics*, 2014, v. 10 (4), 232–235.
- Dai J. Macroscopic anisotropic Brownian motion is related to the directional movement of a “Universe field”. *Natural Science*, 2014, v. 6 (2), 54–58.
- Shnoll S. E., Rubinstein I. A. Regular changes in the fine structure of histograms revealed in the experiments with collimators which isolate beams of alpha-particles flying at certain directions. *Progress in Physics*, 2009, v. 2, 83–95.
- Shnoll S. E., Astashev M. E., Rubinstein I. A., Kolombet V. A., Shapovalov S. N., Bokalenko B. I., Andreeva A. A., Kharakoz D. P., Melnikov I. A. Synchronous measurements of alpha-decay of 239 Pu carried out at north pole, antarctic, and in Puschino confirm that the shapes of the respective histograms depend on the diurnal rotation of the earth and on the direction of the alpha-particle beam. *Progress in Physics*, 2009, v. 3, 11–16.
- Miller D. C. The ether-drift experiment and the determination of the absolute motion of the earth. *Reviews of Modern Physics*, 1933, v. 5 (3), 203–242.
- Miller D. C. The ether-drift experiment and the determination of the absolute motion of the earth. *Nature*, v. 133, 162–164.
- Cahill R. T. Combining NASA/JPL one-way optical-fiber light-speed data with spacecraft Earth-flyby Doppler-shift data to characterise 3-space flow. *Progress in Physics*, v. 5 (4), 50–64.
- Múnera H. A., Hernández-Deckers D., Arenas G., Alfonso E. Observation of a significant influence of Earth's motion on the velocity of photons in our terrestrial laboratory. *Proceedings of the SPIE, The Nature of Light: What Are Photons?*, v. 6664.
- Múnera H. A., Hernández-Deckers D., Arenas G., Alfonso E., López I. Observation of a non-conventional influence of earth's motion on the velocity of photons, and calculation of the velocity of our galaxy. *PIERS Proceedings, Beijing, China, 2009, March 23–27*.
- Baurov Yu. A. *Global Anisotropy of Physical Space*. Nova Science Publishers, New York (USA), 2004.

Energy from Swastika-Shaped Rotors

Michael Edward McCulloch

University of Plymouth, Plymouth, PL4 8AA, UK
E-mail: mike.mcculloch@plymouth.ac.uk

It is suggested here that a swastika-shaped rotor exposed to waves will rotate in the direction its arms are pointing (towards the arm-tips) due to a sheltering effect. A formula is derived to predict the motion obtainable from swastika rotors of different sizes given the ocean wave height and phase speed and it is suggested that the rotor could provide a new, simpler method of wave energy generation. It is also proposed that the swastika rotor could generate energy on a smaller scale from sound waves and Brownian motion, and potentially the zero point field.

1 Introduction

With the recent awareness of the environmental damage caused by fossil fuels, there is a need to find renewable sources of energy. There are many possible sources of energy: sunlight, the wind, ocean tides and also the energy stored in ocean surface waves, and other types of waves. Ocean waves are particularly relevant for the island of Great Britain. It has been estimated that between 7 and 10 GW of energy might be extractable from the waves in UK waters by Wave Energy Converters (WECs), compared with the UK peak demand estimated at 65 GW, so that 15% of UK peak demand could be met by wave power [1].

One of the first viable techniques for the generation of ocean wave power was Salter's Duck which rotated along a horizontal axis under the undulation of waves and generated energy using dynamos. The result was an 81% conversion of wave energy into power [2], but this method extracts energy from waves only in one direction.

Another problem with Salter's duck and other wave energy converters is that they have many moving parts which can degrade with time. The new wave energy generation method proposed here is far simpler in structure and has only one moving part: the rotor. It can also be deployed far from the coast, and, as discussed later in the paper, is applicable to all kinds of waves or fluctuations and not just ocean waves, maybe also the zero point field.

Part of the inspiration for this paper was the proposal of Boersma [3] that two ships at sea will produce a wave shadow zone between them, so that more waves will hit the ships from outside than from between them and so the ships will tend to move together. This is an analogy to the well-known Casimir effect in quantum physics [4] which involves the suppression of the zero point field between two parallel conducting plates which are then forced together. The Casimir force has been measured [5]. The effect due to ocean waves is predicted to be small, but has recently also been measured by [6].

2 Method & results

This proposal uses a swastika, or Greek letter Chi, see Figure 1. The idea is that if waves arrive from all directions,

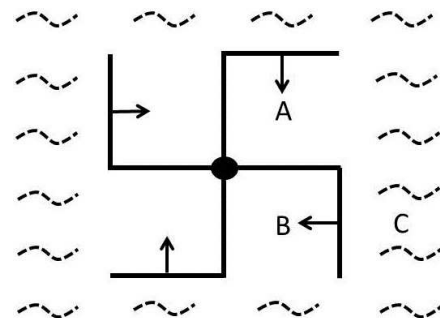


Fig. 1: Schematic showing the swastika rotor, the surrounding wave field (dashed lines) and the resulting forces (arrows).

more waves hit the outer sides of the swastika's arms, then hit the sheltered inner-facing sides of the arms, producing a torque that rotates the swastika about its axis.

To explain this more clearly and estimate the force that can be extracted from this shape we can consider three square areas that interact with the southeast arm: areas A, B and C as shown in Fig. 1. The assumption is that the areas A and B are sheltered zones rather like harbours and that only certain waves can exist between the walls, those with a wavelength that has nodes at the walls. If we then assume that the particular wavelength in the ocean does not fit, then there will be fewer waves in areas A and B, but there will of course be waves in area C since there is no closed boundary, it is open to the ocean. The maximum force obtainable from this shape can be found by looking at the net force on the southeast arm of the swastika and multiplying it by four. For the inner half of the southeast arm, between areas A and B, there is no net force since there are either no waves, or more likely the same intensity of waves, on either side, but for the outer half of the arm between B and C there will be a force on the arm pushing it westward because there are waves on the open east side, but not on the enclosed west side.

According to [7, 8] the impact pressure or slamming force (P) due to wave impacts is

$$P = \frac{F}{A} = K\rho C^2, \quad (1)$$

where A is the area of impact, K is an empirical constant between 3 and 10, ρ is the water density and C is the wave phase speed. For the southeast arm of the swastika this is

$$F = KA\rho C^2 \quad (2)$$

and A is the area hit by the waves which is the half-length of the arm (D) times the wave height h

$$F = KDh\rho C^2. \quad (3)$$

The force and resulting rotation will be clockwise, towards the arm-tips. Since $F = ma$, then the acceleration of the arm will be

$$a = \frac{KDh\rho C^2}{m}. \quad (4)$$

Equation 4 predicts the maximum acceleration obtainable from the swastika, neglecting friction, if its dimensions are such that it cancels the waves in areas A and B completely. The acceleration increases as a function of the wave height (h), length of the arms (D) and the phase speed (C). The acceleration, of course, decreases as the mass increases (m). The effect missing here is friction, which will slow the rotational acceleration as soon as it begins.

3 Discussion

This rotor is only a proposal at this stage. It requires testing in a wave tank big enough so that interactions between the swastika and the wave tank's walls are reduced and also so that the waves in area C are not damped. The waves should be a similar wavelength to the width of the arms of the swastika or shorter. Longer waves than this will not be able to resolve the shape of the arms so there will be no rotation. Eqs. 3 and 4 imply that to get the maximum rotation, the test should use a light rotor with arms projecting enough from the water to intercept the waves, subject to high waves with a large phase speed. Since the effect may be subtle, care will have to be taken to reduce the effects of residual rotational flows.

The swastika rotor has advantages over current wave energy devices in that it is simple and has only one moving part: the axle, it does not require wave impacts from any particular direction and can work just as well with isotropic random waves, and it will also rotate if a surface ocean current exists, but the opposite way, since it is then similar in design to an anemometer.

One intriguing possibility is that the rotation of the swastika shape in a wave field could also be applied at a much smaller scale. A smaller-scale swastika may be spun by sound waves, Brownian motion or even on the nanoscale by the zero-point field allowing perhaps that source of energy to be tapped for the first time.

On the Brownian scale [9] have shown that boomerang-shaped colloidal particles move towards their concave sides when subjected to Brownian motion: random collisions with

atoms or molecules. A sheltering process similar to that described in this paper, might explain their results since, due to sheltering, these boomerang particles would see fewer impacts from atoms in the concave gap between their arms and more impacts on their convex side, so they should move towards their concave side, or towards their arm-tips, just as observed.

A light-driven swastika-shaped rotor on the nanoscale has already been demonstrated. It does not utilise the zero point field, but is driven by an applied beam of light and works in a different manner since the light photons interact with the electrons in the conducting shape [10].

4 Conclusions

It is predicted that a rotor in the shape of a swastika will rotate in the direction its arms are pointing, i.e.: towards the arm-tips, in the presence of isotropic waves, due to the sheltering effect of the arms.

It is proposed that such a rotor can be used to convert wave energy to electricity by using its axle to drive a dynamo. Its advantage over existing wave energy generating devices is its simplicity, its response to isotropic waves and its (reversed) response to surface currents. It now needs to be tested experimentally.

The swastika shape could also be used on smaller scales to generate energy from sound waves or Brownian motion: for example it may explain the observed motion of Boomerang-shaped particles. It may be possible to use nanoscale swastika rotors to extract energy from the hitherto untapped zero point field.

Submitted on February 1, 2015 / Accepted on February 4, 2015

References

1. Drew B., Plummer A.R., Sahinkaya M.N. A review of wave energy converter technology. *Proc. Inst. Mechanical Engineers, Part A: Journal of Power and Energy*, 2009, v. 223, no. 8, 887–902.
2. Falnes J. A review of wave-energy extraction. *Marine Structures*, 2007, v. 20(4), 185–201.
3. Boersma S.L. A maritime analogy of the Casimir effect. *Am. J. Phys.*, 1996, v. 64(5).
4. Casimir H.B.G. On the attraction between two perfectly conducting plates. *Proc. Kon. Nederland Akad. Wetensch.*, 1948, v. B51, 793.
5. Lamoreaux S.K. Demonstration of the Casimir force in the 0.6 to 6 μm range. *Phys. Rev. Lett.*, 1997, v. 78, 5–8.
6. Denardo B.C., Puda J.J. and Larazza A. A water wave analog of the Casimir effect. *Am. J. Phys.*, 2009, v. 77(12).
7. Bea R.G., Xu T., Stear J., Ramos R. Wave forces on decks of offshore platforms. *Journal of Waterway, Coastal and Ocean Engineering*, May/June 1999, 136–144.
8. Chen E.S and Melville W.K. Deep-water plunging wave pressure on a vertical plane wall. *Proc. R. Soc. Lond.*, 1988, v. A417, 95–131.
9. Chakrabarty A., Konya A., Wang F., Selinger J.V., Sun K., Wie Q.-H. Brownian motion of boomerang colloidal particles. *Phys. Rev. Lett.*, 2013, v. 111, 160603.
10. Liu M., Zentgraf T., Liu Y., Bartal G., Zhang X. Light-driven nanoscale plasmonic motors. *Nature Nanotechnology*, 2010, v. 5, 570–573.

Nuclear Phase Transition from Spherical to Axially Symmetric Deformed Shapes Using Interacting Boson Model

A. M. Khalaf¹, N. Gaballah², M. F. Elgabry³ and H. A. Ghanim¹

¹Physics Department, Faculty of Science, Al-Azhar University, Nasr City 11884, Cairo, Egypt.
E-mail: ali_khalaf43@hotmail.com hussein00848@gmail.com

²Physics Department, Faculty of Science (Girls branch), Al-Azhar University, Nasr City 11884, Cairo, Egypt.
E-mail: nermgaballah@yahoo.com

³Mathematics and Physics Department, Faculty of Engineering, Al-Azhar University, Nasr City 11884, Cairo, Egypt.
E-mail: ererereg@yahoo.com

The interacting boson model (sd-IBM1) with intrinsic coherent state is used to study the shape phase transitions from spherical U(5) to prolate deformed SU(3) shapes in Nd-Sm isotopic chains. The Hamiltonian is written in the creation and annihilation form with one and two body terms. For each nucleus a fitting procedure is adopted to get the best model parameters by fitting selected experimental energy levels, B(E2) transition rates and two-neutron separation energies with the calculated ones. The U(5)-SU(3) IBM potential energy surfaces (PES's) are analyzed and the critical phase transition points are identified in the space of model parameters. In Nd-Sm isotopic chains nuclei evolve from spherical to deformed shapes by increasing the boson number. The nuclei ¹⁵⁰Nd and ¹⁵²Sm have been found to be close to critical points. We have also studied the energy ratios and the B(E2) values for yrast band at the critical points.

1 Introduction

The interacting boson model (IBM) [1] describes the low energy quadruple collective states of even-even nuclei in terms of bosons with angular momentum 0 and 2 so called s and d bosons. The bosonic Hamiltonian is assumed to have a general form with one- and two-body terms and must be invariant under some fundamental symmetries. The algebraic formulation of the IBM allows one to find analytical solutions associated with breaking the U(6) into three dynamical symmetries called U(5), SU(3) and O(6) limits of the model, corresponding to spherical (vibrational), axially symmetric prolate deformed (rotational) and soft with respect to axial symmetric (γ -unstable) shapes respectively.

Phase transitions between the three shapes of nuclei are one of the most significant topics in nuclear structure research [2-11]. These shape phase transitions were considered in the framework of the geometric collective model [12], resulting in the introduction of the critical point symmetries E(5) [13] X(5) [14], Y(5) [15], Z(5) [16] and E(5/4) [17]. The E(5) corresponds to the second order transition between U(5) and O(6), while X(5) corresponds to the first order transition between U(5) and SU(3). The symmetry at the critical point is a new concept in the phase transition theory, especially for a first order transition. From the classical point of view, in a first order transition, the state of the system changed discontinuously and a sudden rearrangement happens, which means that there involves an irregularity at critical point [18].

Empirical evidence of these transitional symmetries at the critical points has been observed in several isotopes. The study of the shape phase transitions in nuclei can be best

done in the IBM, which reproduces well the data in several transitional regions [8, 11].

In this paper we use the IBM with intrinsic coherent states to study the spherical to prolate deformed shape transition in the Nd-Sm isotopic chains. Section 2 outlines the theoretical approach and the main features of the U(5)-SU(3) model, the model Hamiltonian under study is introduced in subsection 2.1. In subsection 2.2 the intrinsic coherent states are given as energy states of the model Hamiltonian. In section 3 we present the numerical results of PES's for Nd-Sm isotopic chains and gives some discussions. Finally a conclusion is given in section 4.

2 Outline of the theoretical approach

2.1 The general Hamiltonian of the sd-IBM

In order to study the geometric shapes associated with the sd-IBM, we consider the most standard one and two body IBM Hamiltonian [1]

$$\begin{aligned}
 H = & \epsilon_s \hat{n}_s + \epsilon_d \hat{n}_d \\
 & + \sum_L \frac{1}{2} \sqrt{2L+1} C_L \left[[d^\dagger \times d^\dagger]^{(L)} \times [\tilde{d} \times \tilde{d}]^{(L)} \right]^{(0)} \\
 & + \frac{1}{\sqrt{2}} v_2 \left(\left[[d^\dagger \times d^\dagger]^{(2)} \times \tilde{d} s \right]^{(0)} + \left[s^\dagger d^\dagger \times [\tilde{d} \times \tilde{d}]^{(2)} \right]^{(0)} \right) \\
 & + \frac{1}{2} v_0 \left(\left[[d^\dagger \times d^\dagger]^{(0)} \times s s \right]^{(0)} + \left[s^\dagger s^\dagger \times [\tilde{d} \times \tilde{d}]^{(0)} \right]^{(0)} \right) \\
 & + u_2 [d^\dagger s^\dagger \times \tilde{d} s]^{(0)} + \frac{1}{2} u_0 [d^\dagger s^\dagger \times s s]^{(0)}
 \end{aligned} \quad (1)$$

with

$$C_L = \langle ddL|v|ddL\rangle, \quad (2)$$

$$v_2 = \sqrt{\frac{5}{2}} \langle dd2|v|ds2\rangle, \quad (3)$$

$$v_0 = \langle dd0|v|ss0\rangle, \quad (4)$$

$$u_2 = 2\sqrt{5} \langle ds2|v|ds2\rangle, \quad (5)$$

$$u_0 = \langle ss0|v|ss0\rangle, \quad (6)$$

where $s^\dagger(s)$ and $d^\dagger(\tilde{d})$ are the creation and annihilation operators of the s and d bosons. \tilde{d} is the annihilation operator of the d boson with the time reversal phase relation $\tilde{d}_{2k} = (-1)^{2+k}d_{2,-k}$.

2.2 The intrinsic coherent state

The geometric picture of the IBM can be investigated by introducing the intrinsic coherent state which is expressed as a boson condensate [19]:

$$|N\beta\gamma\rangle = \frac{1}{\sqrt{N!}}(b_c^\dagger)^N|0\rangle, \quad (7)$$

$$b_c^\dagger = \frac{1}{\sqrt{1+\beta^2}} \left[s^\dagger + d_0^\dagger \beta \cos \gamma + \frac{1}{\sqrt{2}}(d_2^\dagger + d_{-2}^\dagger)\beta \sin \gamma \right], \quad (8)$$

where N is the boson number, β and γ are the intrinsic deformation parameters which determine the geometrical shape of the nucleus. $|0\rangle$ is the boson vacuum. Here $\beta \geq 0$, $0 \leq \gamma \leq \frac{\pi}{3}$.

2.3 The Potential Energy Surface (PES)

The PES associated with the classical limit of IBM Hamiltonian (1) is given by its expectation value in the intrinsic coherent state (7)

$$\begin{aligned} E(N, \beta, \gamma) = \langle N\beta\gamma|H|N\beta\gamma\rangle = & \epsilon_s \frac{N}{1+\beta^2} + \epsilon_d \frac{N\beta^2}{1+\beta^2} + \\ & \left(\frac{1}{10}C_0 + \frac{1}{7}C_2 + \frac{9}{35}C_4 \right) N(N-1) \frac{\beta^4}{(1+\beta^2)^2} - \\ & \frac{2}{\sqrt{35}}v_2N(N-1) \frac{\beta^3 \cos 3\gamma}{(1+\beta^2)^2} + \frac{1}{\sqrt{5}}(v_0 + u_2)N(N-1) \\ & \frac{\beta^2}{(1+\beta^2)^2} + \frac{1}{2}u_0N(N-1) \frac{1}{(1+\beta^2)^2}. \end{aligned} \quad (9)$$

If the parameter $v_2 = 0$, then the PES is independent of γ . If $v_2 \neq 0$ then for every $\beta > 0$ the PES has a minimum at $\gamma = 0$, if $v_2 > 0$ (axially symmetric case with prolate shape) or $\gamma = \frac{\pi}{3}$ if $v_2 < 0$ (oblate shape).

The PES equation (9) can be written in another form as:

$$\frac{E(N, \beta, \gamma)}{N} = \frac{A_2\beta^2 + A_3\beta^3 \cos 3\gamma + A_4\beta^4}{(1+\beta^2)^2} + A_0 \quad (10)$$

Table 1: Equilibrium values of the parameters A_2, A_3, A_4 in the large N limit for transition from dynamical symmetry limit U(5) to dynamical symmetry limit SU(3) as an illustrative example.

Set	A_2	A_3	A_4
a	500	-283	850
b	102	-508	703
c	91	-514	727
d	0	-566	700
e	-250	-707	625
f	95	-512	728
g	85	-517	725

with

$$A_2 = \epsilon_d - \epsilon_s - u_0 + (N-1) \frac{1}{\sqrt{5}}(u_2 + v_0), \quad (11)$$

$$A_3 = -\frac{2}{\sqrt{35}}(N-1)v_2, \quad (12)$$

$$A_4 = \epsilon_d - \epsilon_s - \frac{1}{2}u_0 + (N-1) \left(\frac{1}{10}C_0 + \frac{1}{7}C_2 + \frac{9}{35}C_4 \right), \quad (13)$$

$$A_0 = \frac{1}{2}u_0. \quad (14)$$

To determine the critical values of the order parameters of the system, one needs to determine the locus of points for which the conditions $\frac{\partial E}{\partial \beta} = 0$ and $\frac{\partial^2 E}{\partial \beta^2} = 0$ are fulfilled.

The equilibrium value of β is determined by:

$$\frac{\partial E(N, \beta)}{\partial \beta} = 0, \quad (15)$$

leading to

$$\beta \left[2A_2 + 3A_3\beta + (4A_4 - 2A_2)\beta^2 - A_3\beta^3 \right] = 0. \quad (16)$$

Figure (1) (with the parameters listed in table (1)) illustrates the critical points: For $A_2 = 1, A_3 = A_4 = 0$, the nucleus is in the symmetric phase since the PES has a unique minimum at $\beta = 0$ when A_3 and A_4 not vanish and A_2 decreases, a second nonsymmetric minimum arises (set b) at $\beta \neq 0$. This non symmetric minimum take the same depth of the symmetric one at the critical point (set c). Beyond this value, the symmetric minimum at $\beta = 0$ becomes unstable point (set d). (Sets g, h) show two cases in the coexistence region.

3 Application to Nd–Sm isotopic chains

Nuclei in rare-earth region are well-known examples of the U(5)-SU(3). The validity of the present technique is examined for the rare earth isotopic chains $^{144-154}\text{Nd}$ and $^{146-162}\text{Sm}$. The optimized values of the nine parameters of the Hamiltonian $\epsilon_s, \epsilon_d, C_0, C_2, C_4, u_0, u_2, v_0, v_2$ which are truncated to four parameters A_2, A_3, A_4, A_0 are adjusted by fitting

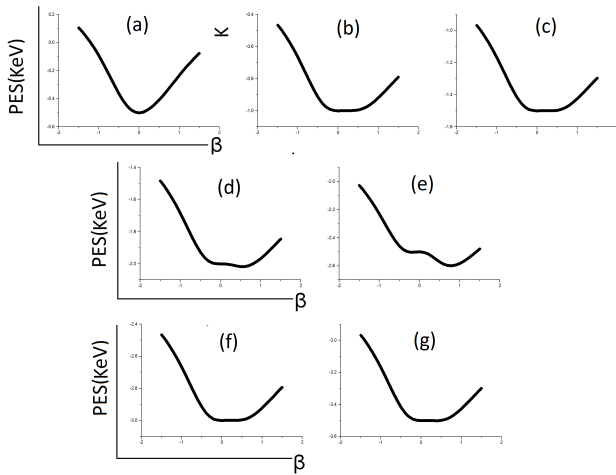


Fig. 1: The scaled PES's as a function of the deformation parameter β for the model parameters listed in table (1). The curves (b, c, d) represents the spinodal, critical and antispinodal points respectively. The curves (f, g) show two cases on the coexistence region.

procedure using a computer simulated search program in order to describe the gradual change in the structure as neutron number varied (number of bosons) and to reproduce ten positive parity experimental levels namely $(2_1^\dagger, 4_1^\dagger, 6_1^\dagger, 8_1^\dagger, 0_2^\dagger, 2_3^\dagger, 4_3^\dagger, 2_2^\dagger, 3_1^\dagger$ and $4_2^\dagger)$, the $B(E2)$ values and the two neutron separation energies for each nucleus in each isotopic chain. The effect of ϵ_s be ignored also the parameter u_0 is kept zero because it can be absorbed in the three parameters. The resulting model parameters are listed explicitly in Table (2). The PES's $E(N, \beta)$ as a function of the deformation parameter β for our Nd-Sm isotopic chains evolving from spherical to axially symmetric well deformed nuclei are illustrated in the Figures 2, 3. At the critical points (^{150}Nd , ^{152}Sm) the spherical and deformed minima must coexist and be degenerated in order to obtain a first order phase shape transition. To identify the shape phases and their transition it is helpful to examine the correspondence between the interaction strengths in the microscopic model and the dynamical symmetry in the IBM.

Phase transitions in nuclei can be tested by calculating the energy ratios

$$R_{I/2} = E(I_1^\dagger)/E(2_1^\dagger). \quad (17)$$

For $I = 4$, the ratio $R_{4/2}$ varied from the values which correspond to vibrations around a spherical shape $R_{4/2} = 2$ to the characteristic value for excitations of a well deformed rotor $R_{4/2} = 3.33$. Figure (4) shows the $R_{I/2}$ for ^{150}Nd and ^{152}Sm compared to U(5) and SU(3) prediction.

Now, we discuss the electric quadrupole transition probabilities. The general form of the E2 operator was used

$$T^{(E2)} = \alpha \left([d^\dagger \times \tilde{s} + s^\dagger \times d^\dagger]^{(2)} + \beta [\tilde{d} \times \tilde{d}]^{(2)} \right) \quad (18)$$

where α is the boson effective charge and β is the structure

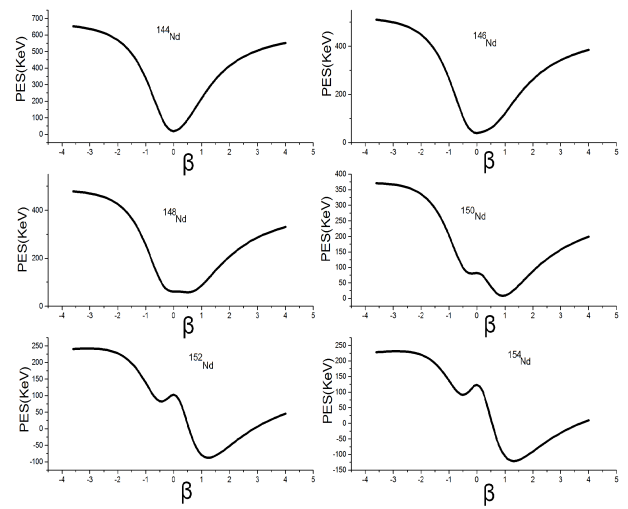


Fig. 2: The PES's (in the $\gamma = 0$ plane given by the IBM as a function of deformation parameter β , to describe the U(5)-SU(3) transition in $^{144-154}\text{Nd}$ isotopic chain. The calculations are for $\chi = -\sqrt{7}/2$.

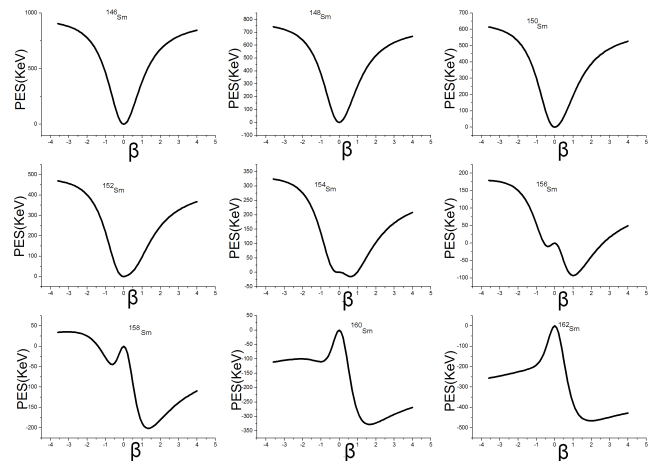


Fig. 3: The same as Fig.2 but for $^{146-162}\text{Sm}$ isotopic chain.

parameter. The parameters α and β have been determined directly from the least square fitting to the observed $\beta(E2)$. $\alpha = 0.135$ and $\beta = -0.115$. The ratios of the E2 transition rates for the U(5) and SU(3) are given by

$$\begin{aligned} B_{(I+2)/2} &= B(E2, I+2 \rightarrow I) / B(E2, 2_1^\dagger \rightarrow 0_1^\dagger), \\ &= \frac{1}{2}(I+2) \left(1 - \frac{I}{2N}\right) \quad \text{for U(5),} \\ &= \frac{15}{2} \frac{(I+2)(I+1)}{(2I+3)(2I+5)} \left(1 - \frac{I}{2N}\right) \left(1 + \frac{I}{2N+3}\right) \\ &\quad \text{for SU(3).} \end{aligned} \quad (19)$$

In Figure (5), the $B_{(I+2)/2}$ ratios are shown for the best candi-

Table 2: The adopted best model parameters in (keV) for our selected Nd-Sm isotopic chains.

	N_B	A_2	A_3	A_4	A_0
^{144}Nd	6	400.132	-242.551	636.717	18.936
^{146}Nd	7	168.175	-291.061	452.077	39.874
^{148}Nd	8	54.518	-339.571	385.737	60.812
^{150}Nd	9	-140.338	-388.081	238.197	81.751
^{152}Nd	10	-359.495	-436.591	66.357	102.689
^{154}Nd	11	-452.052	-485.102	21.117	123.627
^{146}Sm	7	748.245	-160.541	946.905	0.0
^{148}Sm	8	554.405	-187.298	786.175	0.0
^{150}Sm	9	360.565	-214.055	625.445	0.0
^{152}Sm	10	166.725	-240.812	464.715	0.0
^{154}Sm	11	-27.115	-267.569	303.985	0.0
^{156}Sm	12	-220.955	-294.326	143.255	0.0
^{158}Sm	13	-414.795	-321.083	-17.475	0.0
^{160}Sm	14	-608.635	-347.839	-178.205	0.0
^{162}Sm	15	-802.475	-374.596	-338.935	0.0

date ^{152}Sm compared to the U(5) and SU(3) predictions and the experimental data.

4 Conclusion

The shape transition U(5)-SU(3) in $^{144-154}\text{Nd}$ and $^{146-162}\text{Sm}$ isotopic chains in the rare earth region is studied in the framework of sd IBM1 using the most general Hamiltonian in terms of creation and annihilation operators using the method of the intrinsic states.

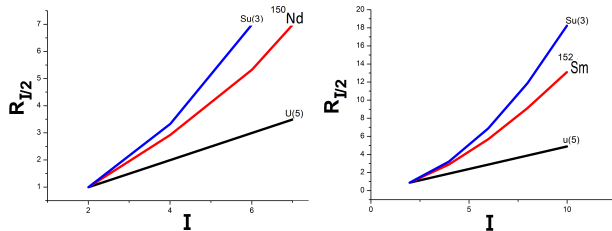


Fig. 4: Normalized excitation energies $R_{I/2} = E((I_1^\dagger)/E((I_2^\dagger))$ for ^{150}Nd and ^{152}Sm nuclei compared to U(5) and SU(3) predictions.

The optimized model parameters have been deduced by using a computer simulated search program in order to obtain a minimum root mean square deviation of the calculated some excitation energies, the two neutron separation energies and some B(E2) values from the measured ones. The PES's are analyzed and the location of the critical points are obtained. In our Nd and Sm chains, nuclei evolve from spherical to prolate deformed shape transition. The lighter nuclei are spherical and the heavier are well deformed. The ^{150}Nd and the ^{152}Sm have been found to be critical point nuclei, that is the

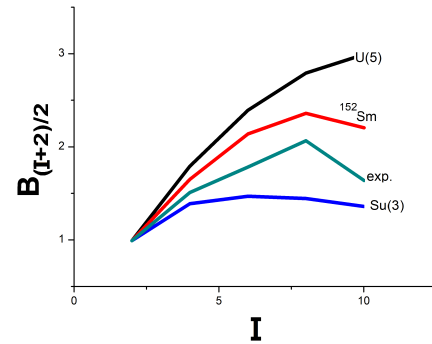


Fig. 5: Comparison of the $B_{I+2/2} = B(E2, I+2 : I)/B(E2, (2_1^\dagger, 0_1^\dagger))$ ratios of the ground state band in ^{152}Sm (N=11) compared to the U(5) and SU(3) predictions and the experimental ratio.

transition from the spherical to deformed occurs between boson number N=9 and N=10. The energy ratios and the B(E2) values are also studied.

Submitted on January 18, 2015 / Accepted on February 2, 2015

References

1. Iachello F. & Arima A. The Interacting Boson Model. Cambridge University Press, Cambridge, (1987).
2. Liu Y.X., Mu L.Z. and Wei H. Approach to the Relation Driven Vibrational to Axially Rotational Shape Phase Transition along the yrast line of a Nucleus. *Phys. Lett.* 2006, v. 633 B, 49–53.
3. Rowe D.J. *Nuc. Phys.* 2004, v. A745, 47; Rosenstiel G. and Rowe D.J. *Nuc. Phys.* 2005, v. A759, 92.
4. S.Heinze et al. Evolution of spectral properties along the O(6)-U(5) transition in the interacting boson model. I. Level dynamics – Heinze, Stefan et al. *Phys. Rev.*, 2006, v. C73, 014306.
5. Zhang J.F., Lü L.J. and Bai H.B. Critical behaviour in nuclear structure from spherical to axially symmetric deformed shape in IBM. *Chinese Physics*, 2007, v. 16, 1941–2006.
6. Hellemans v. et al. Phase Transition in the Configuration Mixed Interacting Boson Model u(5)-O(6) Mixing. *Acta Physica Polonica*, 2007, v. 38B, 1599.
7. Casten R.F. *Nucl. Phys.* 2009, v. A62, 183.
8. Khalaf A.M. and Awwad T.M. A Theoretical description of U(5)-SU(3)Nuclear Shape Transitions in the Interacting Boson Model. *Progress In Physics*, 2013, v. 1, 7–11.
9. Khalaf A.M. and Ismail A.M.,The Nuclear Shape Phase Transition Studied within the Geometric Collective Model. *Progress in Physics*, 2013, v. 2, 51–55; Structure Shape Evaluation in Lanthenide and Actinide Nuclei, *Prgress in Physics*, 2013, v. 2, 98–104.
10. Khalaf A.M. et al, Nuclear Potential Enrgy Surfaces and Critical Point Symmetry within the Geometric Collective Model. *Progress in Physics*, 2014, v. 10, 12–15.
11. Khalaf A.M., Hamdy H.S. and El-Sawy M.M. Nuclear Shape Transition using Interacting Boson Model with the Intrinsic Coherent State. *Progress in Physics*, 2013, v. 3, 44–51.
12. Bohr A. and Mottelson B. Nuclear Structures Benjamin, New York, 1975, Vol.2.

13. Iachello F. Dynamic Symmetries at the Critical point. *Phys. Rev. Lett.*, 2000, v. 85, 3580–3583.
 14. Iachello F. Analytic Prescription of Critical Point Nuclei in a Spherical Axially Deformed Shape Phase Transition. *Phys. Rev. Lett.*, 2001, v. 87, 052502–052506.
 15. Iachello F. Phase Transition on Angle variables. *Phys. Rev. Lett.*, 2003, v. 91, 132502–132507.
 16. Bonatsos O. et al. Z(5): Critical Point Symmetry for the Prolate to Oblate Nuclear Shape Phase Transition. *Phys. Lett.*, 2004, v. 588B, 172–179.
 17. Iachello F. *Phys. Rev. Lett.*, 2005, v. 95, 0525203.
 18. Landau L.D. and Lifshitz F.M. *Statistical Physics*, Butterworth-Heinemann, Oxford, 2001, Part 1.
 19. Dieprink A.E.L., Soholten O. and Iachello F. Classical Limit of the Interacting Boson Model. *Phys. Rev. Lett.*, 1980, v. 44, 1747–1750.
-

Planck's Radiation Law: Thermal Excitations of Vacuum Induced Fluctuations

Fernando Ogiba

E-mail: ogiba@cpovo.net

The second Planck's radiation law is derived considering that "resonators" induced by the vacuum absorb thermal excitations as additional fluctuations. The maximum energy transfer, as required by the maximum entropy equilibrium, occurs when the frequencies of these two kind of vibrations are equal. The motion resembles that of the coherent states of the quantum oscillator, as originally pointed by Schrödinger [1]. The resulting variance, due to random phases, coincides with that used by Einstein to reproduce the first Planck's radiation law from his thermal fluctuation equation [2].

1 Introduction

In 1901, Planck derived the spectral distribution of radiant heat, simply calculating entropy from the number of ways that thermal energy can be distributed among all blackbody resonators (maximum entropy). This forced him to interpret the possible energies of the resonators, for a given mode and temperature, as multiples of a fixed energy; the quantum of electromagnetic energy [3]. In such approach, the appearance of a collection of resonators — with all sort of frequencies — depends only on thermal excitations, that is, for $T = 0$ they do not exist. However, in 1912 Planck realized that *thermal equilibrium with radiation* would make sense only if the resonators remain even for $T = 0$ [4]. In this new approach the quantization of the first Law was preserved, but only in the emissions, that is, oscillators in equilibrium with radiation absorbs continuously until a certain $nh\nu$ is reached, and then they emit or continues absorbing. From this semi-classical derivation, one concludes that exists vibrations not induced by thermal excitations. In this way, arose the concept of zero-point energy (ZPE), which is a term of the second Planck's radiation law, i.e.

$$\langle E \rangle = \frac{1}{2} \hbar\omega + \frac{\hbar\omega}{e^{\hbar\omega/k_B T} - 1}. \quad (1)$$

At the time, the ZPE was a controversial concept; at best, it was accepted as "virtual photons due to nearby matter". The concept of a radiation field permeating the vacuum, and then inducing "matter-oscillators" with an energy given by the first term of Eq. (1), only gained credibility after the predictions of the quantum field theory (quantum vacuum states) and the experimental proof of the Casimir's force [5]. In fact, around the middle of the last century they begin appear works that assume explicitly that the matter (elementary electrical charges or agglomerates of them) are in permanent interaction with a zero-point radiation field (ZPF); absorbing and emitting electromagnetic radiation in a conservative way, independently of temperature.

In accordance with the experimentally proved work of Casimir [6] and the proponents of the stochastic electrodynamics [7], the ZPF is a homogeneous and isotropic distribution of electromagnetic plane waves pervading all space; each

one carrying energy proportional to its frequency (ranging from zero to infinite, or a big cutoff value), $\hbar\omega/2$. Moreover, its spectral energy density is proved to be a Lorentz invariant. As the phases of such waves are randomly distributed in the range $[0, 2\pi]$, then electrical charges (or any agglomerate of them) are permanently receiving unpredictable impulses with the following features: First, the ZPF isotropy ensures zero net momentum transfer. Second, the emitted radiation, due to non uniform acceleration, responds by the local energy conservation. Third, the symmetric distribution of emissions ensures zero net self-momentum (no liquid radiation reaction). Fourth, the permanent nature of the absorption-emission process imply a remnant random trembling motion, whose energy in the particle-bound reference frame, in the case of a free electron, is the well-known rest energy

$$m_0 c^2 = \frac{\hbar\omega_Z}{2}, \quad (2)$$

where ω_Z is the zitterbewegung frequency [8, 9].

This zitterbewegung, strongly correlated with the translational motion trough the de Broglie's periodicity, prevent such particles to follow predictable paths (quantum randomness). Even so, the overall motion obeys the dynamical principle founded on trajectories. Non relativistically, this obedience means that the center of mass of the particle's vibrations can be found — instantly — over any one of the trajectories dictated by the stochastic Hamilton-Jacobi-Bohm equation, which is implicit in the Schrödinger's equation [10].

What follows is a derivation of Planck distribution, which replaces the quantization a priori by the presence of the ZPF, which, therefore, is the responsible by "resident blackbody resonators". Nevertheless, quantization is implied. Indeed, the zero-point energy ε_0 , besides being a fixed quantity for each mode, is indispensable to get a discrete Boltzmann's distribution from a continuous one [12].

2 Thermal excitations of vacuum induced fluctuations

The energy absorbed (emitted) from (to) the ZPF in order to form temperature independent primordial matter-oscillators (or "Blackbody resonators") is

$$\varepsilon_0(\omega) = \frac{1}{2} \hbar\omega. \quad (3)$$

When particles absorbs such vibrant energy, conservatively, it is expected that its coordinates fluctuates as

$$q_0(t, \phi) = \sqrt{\frac{2\mathcal{E}_0(\omega)}{m\omega^2}} \cos(\omega t + \phi), \quad (4)$$

which differs from a typical classical oscillation only by the presence of random phases ϕ (ZPF randomness), which imply that this equation does not describe the actual path followed by particles, but simply obedience to the dynamic principle at each occupied position. Indeed, this is the main feature of the Schrödinger's equation, as argued elsewhere.

Notice, now $\varepsilon_0(\omega)$ is the energy of the matter-oscillator (the zero-point energy), which, as can be seen by simple substitution of Eq. (4), obey the equality

$$\varepsilon_0(\omega) = \frac{1}{2\pi} \int_0^{2\pi} \left[(2) \frac{2\pi}{\omega} \int_0^{2\pi/\omega} \frac{1}{2} m \left(\frac{dq_0(t, \phi)}{dt} \right)^2 dt \right] d\phi, \quad (5)$$

where the factor (2) refers to equal contributions from kinetic and potential energies of the harmonic oscillator, ω is the angular frequency of the absorbed radiation, the integral in t is an average over the radiation period, and the integral in ϕ is an average over random phases.

Given the permanent nature of the interactions, the ZPE must be viewed as a remnant energy. It is indispensable to compose the ground state energy of quantum systems. The exact shape, as it should be, only appears in the case of the harmonic oscillator.

For $T \neq 0$, there are thermal excitations, which manifest as additional vibrations that increase the amplitude of existing fluctuations. In a sense, this can be inferred from the thermal dilatation of bodies. In other words, the center of mass of the matter-fluctuations, as expressed by Eq. (4), fluctuates due to thermal excitations. This implies the superposition

$$q_{\phi, \Phi}(t) = \sqrt{\frac{2\mathcal{E}_0(\omega)}{m\omega^2}} \cos(\omega t + \phi) + \sqrt{\frac{2\mathcal{E}_T(\Omega)}{m\Omega^2}} \cos(\Omega t + \Phi), \quad (6)$$

where $\mathcal{E}_T(\Omega)$ is the vibrational energy induced by thermal excitations at the temperature T , Φ is a random phase, and, for the sake of generality, Ω is an arbitrary frequency.

It is worth informing, the assumption of the last paragraph is in full agreement with what is inferred from the coherent states of the quantum harmonic oscillator (the perfect framework to derive the Planck's law); that is, the statistical Gaussian of the ground state (here, the primordial oscillator) is moved, as a whole, by classical oscillations [11, see p. 104].

Averaging the energy

$$(2) \times \frac{\omega}{2\pi} \int_0^{2\pi/\omega} \frac{1}{2} m \left(\frac{dq_{\phi, \Phi}(t)}{dt} \right)^2 dt$$

over random phases, both ϕ and Φ , yields the energy absorbed (emitted) by this superposition of vibrations, i.e.

$$E(\omega, \Omega) = \varepsilon_0(\omega) + \mathcal{E}_T(\Omega), \quad (7)$$

where Ω still continues unknown.

Now, averaging the square deviation from $\varepsilon_0(\omega)$,

$$\left[(2) \times \frac{2\pi}{\omega} \int_0^{2\pi/\omega} \frac{1}{2} m \left(\frac{dq_{\phi, \Phi}(t)}{dt} \right)^2 dt - \varepsilon_0(\omega) \right]^2,$$

over both random phases, emerges the variance

$$\sigma_{\omega, \Omega}^2 = \frac{2\hbar\omega^3 (\omega^2 + \Omega^2) \sin^2(\pi\Omega/\omega) E_T(\Omega)}{\pi^2 (\omega^2 - \Omega^2)} + \frac{[\omega^2 + 16\pi^2\Omega^2 - \omega^2 \cos^2(4\pi\Omega/\omega) E_T(\Omega)] E_T(\Omega)}{16\pi^2\Omega^2} \quad (8)$$

which seems to diverges when $\Omega \rightarrow \omega$. In true, there is the maximum variance

$$\sigma^2 = \lim_{\Omega \rightarrow \omega} \sigma_{\omega, \Omega}^2 = E_T^2(\omega) + \hbar\omega E_T(\omega), \quad (9)$$

which can also be obtained replacing Ω by ω in the starting Eq. (6), and then performing the indicated operations.

Maximum variance implies maximum entropy (or thermodynamical equilibrium). Indeed, calculating entropy from Gaussian or exponential distribution (like Boltzmann's distribution) one find that entropy is proportional to $[\ln(\sigma^2) + cte]$.

From another point of view, the Eq. (9) also means that maximum energy transfer occurs when thermal vibrations are tuned with that induced by the ZPF, in full agreement with a well-known result of the theory of oscillations; that is, maximum energy transfer occurs at the natural frequency of the absorbing oscillator.

Therefore, from this tuned behavior — thermodynamical equilibrium — it follows that each possible energy, considering Eq. (7), obey

$$E = \frac{\hbar\omega}{2} + E_T(\omega), \quad (10)$$

and are distributed in such a way that the corresponding distribution has the variance σ^2 .

It is crucial emphasizing, such ensemble of random energies is justified by a variance arising from random phases, ϕ and Φ . The first is a well-known feature of the ZPF (masterfully interpreted in the quantum mechanics framework), and the second is related to the myriad of ways that thermal excitations can move an elementary constituent of a body.

3 Thermal fluctuations and the Planck's radiation law

The variance expressed by Eq. (9) ensures that for each ω -mode at the remperature T there is a collection of random energies E , Eq. (10). From a thermodynamical point of view, the equilibrium involving such energy fluctuations must be treated in terms of the Boltzmann's statistics.

Deriving the moments of such distribution,

$$\langle E^r \rangle = \frac{\int_0^\infty dE E^r e^{-\beta E}}{\int_0^\infty dE e^{-\beta E}} = r! \langle E \rangle^r,$$

with respect to $\beta = 1/k_B T$, we obtain the Einstein's thermal fluctuation equation

$$\sigma_E^2 = k_B T^2 \frac{d\langle E \rangle}{dT}, \quad (11)$$

where, in the present calculations, $\langle E \rangle$ is the thermal average of the energies expressed by Eq. (10), i.e.

$$\langle E \rangle = \frac{\hbar\omega}{2} + \langle E_T \rangle, \quad (12)$$

and the thermal variance (thermal fluctuation) σ_E^2 is, therefore, the thermal average of Eq. (9):

$$\sigma_E^2 = \langle E_T \rangle^2 + \hbar\omega \langle E_T \rangle. \quad (13)$$

Combining the last three equations, we get the differential equation

$$k_B T^2 \frac{d\langle E_T \rangle}{dT} = \langle E_T \rangle^2 + \hbar\omega \langle E_T \rangle, \quad (14)$$

whose solution, considering $\langle E_T \rangle = 0$ for $T = 0$, is

$$\langle E_T \rangle = \frac{\hbar\omega}{e^{\hbar\omega/k_B T} - 1}. \quad (15)$$

Therefore,

$$\langle E \rangle = \frac{\hbar\omega}{2} + \frac{\hbar\omega}{e^{\hbar\omega/k_B T} - 1}. \quad (16)$$

Submitted on February 10, 2015 / Accepted on February 14, 2015

References

1. Schrödinger E. Collected Papers on Wave Mechanics, Blackie Son Limited, 1929
2. Einstein A. Zum gegenwertigen Stand des Strahlungs-problems. *Physikalische Zeitschrift*, 1900, v. 10, 185–193. Published in The Collected Papers of Albert Einstein, v. 2: The Swiss Years: Writings, 1900–1909 (English translation supplement), Princeton University Press, 1989, 357–369.
3. Planck M. The Theory of Heat Radiation, Dover, New York, 1959.
4. Milonni P.W. The Quantum Vacuum: An Introduction to Quantum Electrodynamics, Academic Press, 1994.
5. Casimir H. B. G. On the attraction between two perfectly conducting plates. *Proceedings of the Royal Netherlands Academy of Arts and Sciences*, 1948, v. B51, 793–795.
6. Lamoroux S. K. Demonstration of the Casimir Force in the 0.6 to 6m Range. *Physical Review Letters*, 1997, v. 78, n. 1, 5–8.
7. Boyer T. H. Random electrodynamics: The theory of classical electrodynamics with classical electromagnetic zero-point radiation. *Physical Review D*. 1975, v. 11, n. 4, 790–808.
8. Dirac P. A. M. The Principles of Quantum Mechanics, 4ed. Oxford University Press, 1999.
9. Sidharth B. G. Revisiting Zitterbewegung. *International Journal of Theoretical Physics*, 2009, v. 48, 497–506.
10. Ogiba F. Addendum to Phenomenological Derivation of the Schrödinger Equation. *Progress in Physics*, 2014, v. 1, 108–110.
11. Burkhardt C. E., Leventhal J. J. Foundations of Quantum Physics, Springer, 2008.
12. de la Peña L., Ceto A. M. The Quantum Dice: An Introduction to the Stochastic Electrodynamics, Kluwer Academic, Dordrecht, 1996

Diffusion Equations, Quantum Fields and Fundamental Interactions

Sebastiano Tosto

Retired physicist. E-mail: stosto44@gmail.com, stosto@inwind.it

The paper concerns an “ab initio” theoretical model based on the space-time quantum uncertainty and aimed to identify the conceptual root common to all four fundamental interactions known in nature. The essential information that identifies unambiguously each kind of interaction is inferred in a straightforward way via simple considerations involving the diffusion laws. The conceptual frame of the model is still that introduced in previous papers, where the basic statements of the relativity and wave mechanics have been contextually obtained as corollaries of the quantum uncertainty.

1 Introduction

Understanding the fundamental interactions of nature is certainly one among the most challenging topics of the modern physics; a unified theory able to account for the fundamental forces is a dream of the physicists since a long time [1, 2]. The science of the fundamental interactions progressed with the advancement of the physics of the elementary particles [3], whose properties could be tested by examining their way of interacting with other particles. The theoretical models bridging quantum and relativistic theories [4, 5] progressed along with the merging of the physics of the elementary particles and quantum fields [6] with that of the fundamental interactions. All this culminated with the formulation of the standard model [7] and with the superstring theory [8]. The way the particles interact involves significantly even the cosmology [9, 10]. The GU theories [11, 12] share some general concepts about the four fundamental interactions, their basic idea to model the force between quantum particles is in principle simple: to exchange appropriate elementary particles that transfer momentum and energy between the interacting partners. The vector bosons are acknowledged to mediate the forces between particles according to their characteristic features of lifetime and action range [13]. These messenger particles, quanta of the respective fields, are said to mediate the interaction that propagates with finite velocity and perturbs the space-time properties. This way of thinking suggests reasonably the key role of the displacement mechanism of the particles that propagate the interaction, e.g. the different transport rates of massive or massless messengers; this means, in particular, that the space in between a set of interacting particles is filled with the vector bosons mutually exchanged. As clouds of these latter flow throughout the space-time, it is reasonable to expect that the global properties of the resulting interaction should depend on the ability of the messengers to spread around the respective partners. Eventually, since the mutual positions of each particle in the set are in general functions of time, even random local density gradients of these messengers are expectedly allowed to form throughout the space-time.

These preliminary considerations feed the idea of imple-

menting a model of fundamental interactions based on a appropriate mechanism of transport of matter/energy, sufficiently general to be suitably extended from sub-nuclear to infinite range interactions. Among the possible transport mechanisms deserves attention the particle diffusion, driven by a gradient law originated by a non-equilibrium situation; as it has been shown in a previous paper [14], this law is strictly connected with the global entropy increase of an isolated thermodynamic system, the diffusion medium plus the diffusing species both tending to the equilibrium configuration in the state of maximum disorder. So the driving force of the diffusion process is actually the second principle of thermodynamics, i.e. a law so general to hold at the nano-micro-macro scales of interest in the present context. As a matter of fact, it has been found that this law allows describing not only the concentration gradient driven mass transport but also other important laws of physics: for instance Ohm’s electric conductivity or Fourier’s heat conductivity or Poiseuille pressure laws [14]. So, in agreement with the quantum character of the approach therein introduced, appears stimulating in principle the idea of testing via the diffusion laws even the exchange of vector bosons to describe the fundamental interactions. This hint leads in a natural way to the idea of dynamical flux of messenger particles, by consequence of which are exchanged momentum and energy of the interacting partners. This assumption merely requires that the messengers of the forces are exchanged as clusters of particles randomly flowing through the space-time and thus characterized in general by local concentration gradients. The physics of the four fundamental interactions has been already concerned in a dedicated paper [15]; in that paper the interactions have been described starting directly from the concept of space-time uncertainty. Here this problem is reformulated via the diffusion laws only in a surprisingly simple way. This paper aims to show that the key features of the fundamental forces are obtained by elaborating purposely the diffusion laws; it will be emphasized that these laws provide interesting hints also for relativistic and thermodynamic considerations. Of course the purpose of the paper is not that of providing an exhaustive description of the fundamental interactions, which would require a much longer review of the huge amount of literature

existing about each one of them; the paper intends instead to emphasize an even more crucial aspect of this topic, i.e. how to infer the essential features of all known interactions from a unique fundamental principle; in other words, the aim is to focus on a unique conceptual root from which follow contextually as corollaries all fundamental interactions. The paper introduces an “ab initio” model via considerations limited to the minimum necessary to infer the distinctive features of the various forms of interaction that identify unambiguously each one of them. Despite this topic is usually tackled via heavy computational ways, the present theoretical model is conceptual only but surprisingly straightforward. While the idea of interactions due to a diffusion-like flux of vector bosons has been early introduced [16], in the present paper this hint is further implemented. The model concerned in this paper exploits first the quantum origin of the diffusion laws, shortly reported for completeness of exposition, to infer next the interactions directly via the diffusion laws. Some concepts already published [14, 15, 16] are enriched here with further considerations in order to make this paper as self-contained as possible. It is clear the organization of the paper: the section 2 introduces the quantum background of the model and both Fick diffusion laws, plus ancillary information useful in the remainder sections; the section 3 introduces some thermodynamic considerations; the section 4 concerns the fundamental interactions, whereas the section 5 concerns a few additional remarks on the gravity force.

2 Physical background

The statistical formulation of the quantum uncertainty reads in one dimension

$$\Delta x \Delta p_x = n\hbar = \Delta \varepsilon \Delta t, \quad \Delta \varepsilon = v_x \Delta p_x, \quad v_x = \Delta x / \Delta t. \quad (1)$$

The subscript indicates the component of momentum range along an arbitrary x -axis. The second equality is actually consequence of the former merely rewritten as $(\Delta x / v_x)(\Delta p_x v_x)$, being Δt the delocalization time lapse necessary for the particle to travel throughout Δx ; so this definition leaves unchanged the number n of quantum states allowed to the concerned system. Since the local coordinates are waived “a priori”, i.e. conceptually and not as a sort of approximation aimed to simplify some calculation, these equations focus the physical interest on the region of the phase space accessible to the particle rather than on the particle itself. As these equations link the space range Δx to the time range Δt via n , any approach based on these equations is inherently four-dimensional by definition. The sizes of the uncertainty ranges are arbitrary, unknown and unknowable; it has been shown that they do not play any role in determining the eigenvalues of the physical observables [17], as in effect it is known from the operator formalism of the wave mechanics. Actually it is possible to show that the wave formalism can be inferred as a corollary of the Eqs. (1) [17], coherently with the fact that

n plays just the role of the quantum number in the eigenvalues inferable via these equations only [18, 19]. The Eqs. (1), early introduced in these papers to provide a possible way to describe the quantum systems in alternative to the solution of the pertinent wave equations, have been subsequently extended to the special and general relativity [20]. It has been shown for instance that a straightforward consequence of the space time uncertainty is

$$c^2 \Delta p_x = v_x \Delta \varepsilon. \quad (2)$$

The demonstration is so short and simple to deserve of being mentioned here for completeness: this equation and the next Eq. (3) are enough for the purposes of the present paper. Consider a free particle delocalized in Δx . If this particle is a photon in the vacuum, then $\Delta x / \Delta t = c$; i.e. the time range Δt is necessary by definition for the photon to travel Δx . Yet, trusting to the generality of the concept of uncertainty, the Eqs. (1) must be able to describe even the delocalization of a massive particle moving at slower rate $v_x = \Delta x / \Delta t < c$. Let us examine now this problem according to the Eqs. (1), i.e. starting from $\Delta x \Delta p_x = \Delta \varepsilon \Delta t$ to infer $\Delta \varepsilon / \Delta p_x = \Delta x / \Delta t$; as c represents the maximum velocity allowed to any particle, it must be true that $\Delta x / \Delta t \leq c$, whence $\Delta \varepsilon / \Delta p_x \geq c$. The inequality therefore constrains the ratio of the range sizes $\Delta \varepsilon$ and Δp_x depending on whether the delocalized particles are massive or not. Anyway both chances are considered writing $\Delta \varepsilon / \Delta p_x = (c / v_x) c$. One finds thus the sought Eq. (2), which implies the local functional dependence $c^2 p_x = v_x \varepsilon$ between energy and momentum and velocity components of the massive particles. Also note that the Eq. (2) implies the concept of mass simply introducing the limit

$$\lim_{v_x \rightarrow 0} \frac{\Delta p_x}{v_x} = \frac{\Delta \varepsilon_{rest}}{c^2} = m. \quad (3)$$

As there is no compelling reason to expect a vanishing $\Delta \varepsilon_{rest}$ for $v_x \rightarrow 0$, one concludes that the left hand side is in general finite and corresponds to the definition of mass. Both signs are allowed in principle to v_x and thus to Δp_x ; yet squaring $c^4 \Delta p_x^2 = v_x^2 \Delta \varepsilon^2$ and implementing again $v_x < c$, one finds $c^2 \Delta p_x^2 < \Delta \varepsilon^2$ i.e. $\Delta \varepsilon^2 = c^2 \Delta p_x^2 + \Delta \varepsilon_o^2$; thus the local functional dependence $\varepsilon^2 = c^2 p_x^2 + \varepsilon_o^2$, well known, combined with the Eq. (3) yields $\varepsilon_o = mc^2$ and also the explicit expressions of ε and p_x compliant with the respective Lorentz transformations.

2.1 Quantum basis of the diffusion laws

This subsection assumes that the diffusion medium is an isotropic body of solid, liquid or gas matter at constant and uniform temperature. The following considerations shortly summarize the reasoning introduced in [14]. Let us divide both sides of the Eq. (2) by $v_o V$, being v_o an arbitrary velocity and V an arbitrary volume. So one finds

$$v_x C = \Delta J_x, \quad C = \frac{\Delta p_x}{v_o V}, \quad \Delta J_x = \frac{\Delta \varepsilon / c^2}{V} v_x. \quad (4)$$

As C has physical dimensions *mass/volume*, it represents the average concentration of a mass m in the volume V , whereas ΔJ_x is the net change of the flux of particles moving at average rate v_x through V . So ΔJ_x , whose physical dimensions are *mass/(time \times surface)*, describes the net flux of matter entering in and leaving out two opposite surfaces delimiting V ; the first Eq. (4) also implies that the functional dependence of any J_x within its uncertainty range ΔJ_x upon the corresponding local flux of m fits the classical definition $J_x = C v_x$. Assuming that $\Delta \varepsilon/c^2$ is the energy equivalent of mass, the last equation inferred with the help of the Eq. (2) extends the definition of flux of the first equation to the change of energy density inside V . Write now $V = \Delta x^3$, which is certainly possible regardless of the particular geometric shape because both V and Δx are arbitrary; so any shape factor, e.g. $4\pi/3$ for spherical V , is inessential because it would still yield $V = \Delta x'^3$ once included in $\Delta x'$. Since $\Delta x^{-3} = -\partial \Delta x^{-2}/2\partial \Delta x$, one finds

$$\Delta J_x = \frac{\Delta p_x}{\Delta x^3} = -\frac{\Delta p_x}{2} \frac{\partial \Delta x^{-2}}{\partial \Delta x}.$$

Moreover $\Delta x^{-2} = \Delta p_x^2/(n\hbar)^2$, so that

$$\Delta J_x = -\frac{\Delta p_x^2}{(n\hbar)^2} \frac{\partial \Delta p_x}{\partial \Delta x} = -\frac{1}{3(n\hbar)^2} \frac{\partial \Delta p_x^3}{\partial \Delta x}$$

which yields in turn

$$\Delta J_x = -\frac{n\hbar}{3} \frac{\partial(1/\Delta x^3)}{\partial \Delta x} = -\frac{n\hbar}{3m} \frac{\partial(m/\Delta x^3)}{\partial \Delta x}. \quad (5)$$

The last equality holds under the reasonable assumption of constant mass m in the volume Δx^3 : as both V and m are arbitrary, the former can be conveniently chosen in order to fulfil the requirement that the latter is simply redistributed within Δx^3 during an assigned diffusion time Δt related to ΔJ_x . Indeed the fact of having defined C as the average concentration of a constant amount of diffusing mass does not exclude the existence of a concentration gradient within V ; in effect ΔJ_x results in the Eq. (5) as the concentration gradient driven mass flux at the boundary surfaces of V . Also note that \hbar/m has the same physical dimensions, *length²/time*, of a diffusion coefficient D ; so, as shown in [14], it is possible to write $D = qn\hbar/m$ being q an appropriate numerical coefficient able to fit the experimental value of D of any species moving in any diffusion medium. Owing to the generality of the Eqs. (1), no specific hypothesis is necessary about whether the concerned diffusion process occurs in gas or liquid or solid phase or even in the vacuum; also, this holds at any temperature and value of C . So the last equation (5) reads

$$\Delta J_x = -D \frac{\partial C}{\partial \Delta x}, \quad C = \frac{m}{\Delta x^3}, \quad \Delta x = \frac{\Delta x}{q}, \quad D = \frac{qn\hbar}{m}. \quad (6)$$

Of course the inessential factor 3 has been included into q . Here C is related to the given amount of mass m redistributed

within V ; so it depends not only on m itself, but on the space extent through which this redistribution was allowed to occur. This result is nothing else but the well known first Fick gradient law, now straightforward consequence of the fundamental Eqs. (1). So far, for simplicity has been concerned the one-dimensional case, symbolized by the subscript x denoting the actual vector components of momentum and displacement velocity of m along an arbitrary x -axis. Yet it is useful to account explicitly for the vector nature of the equations above summarizing the Eqs. (4) and (6) as follows:

$$\Delta \mathbf{J} = C \mathbf{v} = -D \nabla C. \quad (7)$$

For the following purposes, it is interesting to extend these first results. Given an arbitrary function $f(x, t)$ of coordinate and time, express its null variation $\delta f(x, t) = 0$ as $(\partial f/\partial x)\delta x + (\partial f/\partial t)\delta t = 0$ that reads $v_x(\partial f/\partial x) + (\partial f/\partial t) = 0$ i.e. $\mathbf{v} \cdot \nabla f + \partial f/\partial t = 0$; this yields $\nabla \cdot (f\mathbf{v}) - f\nabla \cdot \mathbf{v} = -\partial f/\partial t$. It is convenient in the present context to specify this result putting $f = C$, in which case $f\mathbf{v} = \mathbf{J}$; thus

$$\nabla \cdot \Delta \mathbf{J} = -\nabla \cdot (D \nabla C) = -\frac{\partial C}{\partial t} + C \nabla \cdot \mathbf{v} \quad C = C(x, y, z, t). \quad (8)$$

In the particular case where \mathbf{v} is such that the second addend vanishes, one obtains a well known result, the second Fick equation subjected to the continuity boundary condition required by $\delta f = 0$ i.e.

$$\nabla \cdot \Delta \mathbf{J} = -\frac{\partial C}{\partial t} \quad \nabla \cdot \mathbf{v} = 0. \quad (9)$$

The condition on \mathbf{v} is satisfied if in particular:

(i) $\mathbf{v} = \mathbf{i}v_1(y, z, t) + \mathbf{j}v_2(x, z, t) + \mathbf{k}v_3(x, y, t)$ or (ii) $\mathbf{v} = \mathbf{v}(t)$ or (iii) $\mathbf{v} = \text{const}$.

Anyway, whatever the general analytical form of \mathbf{v} might be, this condition means that the vector \mathbf{v} is solenoidal, which classically excludes sinks or sources of matter in the volume Δx^3 enclosing m . Note however that since the boundaries of any uncertainty range are arbitrary and unknown, introducing the range $\Delta \mathbf{J} = \mathbf{J} - \mathbf{J}_0$ means implementing the actual \mathbf{J} as change of the flux in progress with respect to a reference flux \mathbf{J}_0 appropriately defined. For instance \mathbf{J}_0 could be a constant initial value at an initial time t_0 of $\Delta t = t - t_0$ where the diffusion process begins, in which case \mathbf{J}_0 can be put equal to zero by definition; this means determining the initial boundary condition $\mathbf{J}_0 = 0$ at $t_0 = 0$. Yet more in general is remarkable the fact that, according to the Eq. (8), the usual classical form $\mathbf{J} = C\mathbf{v}$ is also obtained if \mathbf{J}_0 is regarded as a reference flux as a function of which is defined \mathbf{J} that fulfils the condition

$$\nabla \cdot \mathbf{J} = -\frac{\partial C}{\partial t} \quad \nabla \cdot \mathbf{J}_0 = -C \nabla \cdot \mathbf{v}. \quad (10)$$

The quantum chance of expressing the diffusion equations considering $\Delta \mathbf{J}$ instead of \mathbf{J} emphasizes that the classical view point is a particular case of, and in fact compatible with, the Eqs. (1).

This section has shown that the usual Fick equation (8) written as a function of \mathbf{J} and C does not hold necessarily in the absence of sinks or sources of matter only, it includes also the chance $\nabla \cdot \mathbf{v} \neq 0$ provided that the boundary condition about the reference flux gradient $\nabla \cdot \mathbf{J}_0$ is properly implemented. In this subsection it has been also shown that all this has a general quantum basis.

2.2 Diffusion and relativistic velocity addition rule

Let us consider the Eq. (7) $\Delta\mathbf{J} = C\mathbf{v}$ and express the change $\delta\Delta\mathbf{J}$ of $\Delta\mathbf{J}$ as a function of the variations of $\delta\mathbf{v}$ and δC

$$\delta\Delta\mathbf{J} = \mathbf{v}\delta C + C\delta\mathbf{v} \quad \mathbf{v} = \mathbf{v}_x + \mathbf{v}_y + \mathbf{v}_z \quad \mathbf{v} = \mathbf{v}(\Delta t) \quad (11)$$

to calculate the scalar product of $\delta\Delta\mathbf{J}$ by one component of \mathbf{v} , e.g. \mathbf{v}_x :

$$\mathbf{v}_x \cdot \delta\Delta\mathbf{J} = \mathbf{v}_x \cdot \mathbf{v}\delta C + C\mathbf{v}_x \cdot \delta\mathbf{v}. \quad (12)$$

It is interesting to define in particular $\delta\mathbf{v}$ orthogonal to this component \mathbf{v}_x for reasons clarified below; hence

$$\mathbf{v}_x \cdot \delta\mathbf{v} = 0, \quad \mathbf{v}_x = \delta\mathbf{v} - (\delta\mathbf{v})^2 \frac{\mathbf{v}_o}{\mathbf{v}_o \cdot \delta\mathbf{v}}. \quad (13)$$

The second equation shows the form of \mathbf{v}_x that satisfies the former condition whatever the ancillary vector \mathbf{v}_o might be. So, owing to the Eqs. (7) and (12), one finds

$$\mathbf{v}_x \cdot \delta\Delta\mathbf{J} = \mathbf{v}_x \cdot \mathbf{v}\delta C = \delta\Delta\mathbf{J} \cdot \delta\mathbf{v} - (\delta\mathbf{v})^2 \frac{\mathbf{v}_o \cdot \delta\Delta\mathbf{J}}{\mathbf{v}_o \cdot \delta\mathbf{v}}. \quad (14)$$

As concerns the second equality, eliminating $(\delta\mathbf{v})^2$ between the Eqs. (14) and (13) one finds

$$\mathbf{v}_x = \delta\mathbf{v} - \frac{(\delta\mathbf{v} - \mathbf{v}_x) \cdot \delta\Delta\mathbf{J}}{\mathbf{v}_o \cdot \delta\Delta\mathbf{J}} \mathbf{v}_o. \quad (15)$$

As concerns the first equality (14), it is possible to write

$$\begin{aligned} \mathbf{v}_x \cdot \delta\Delta\mathbf{J} &= \pm v_x \delta\Delta J_x, \\ \delta\Delta J_x &= \pm \frac{\mathbf{v} \cdot \mathbf{v}_x \delta x}{v_x} \frac{\delta C}{\delta x} = \pm (v_x \delta x) \frac{\delta C}{\delta x}, \end{aligned} \quad (16)$$

being $\delta\Delta J_x$ the modulus of the component of $\delta\Delta\mathbf{J}$ along \mathbf{v}_x . Note that $\mathbf{v} \cdot \mathbf{v}_x \delta x / v_x = \mathbf{v} \cdot \mathbf{u}_x \delta x$, where \mathbf{u}_x is a unit vector oriented along \mathbf{v}_x , has the physical dimensions of a diffusion coefficient D ; so, being $|v_x|$ arbitrary, the Eq. (16) reads

$$\delta\Delta J_x = \pm D \frac{\delta C}{\delta X}, \quad D = q v_x \delta x, \quad \delta X = q \delta x, \quad (17)$$

with q again proportionality coefficient, as previously introduced. With the minus sign, the first equation fits the quantum result (6); this sign therefore is that to be retained. Also, this agreement supports the usefulness of the condition (13) and introduces a further result in the quantum frame of the present approach. Put $\mathbf{v}_x = \xi \mathbf{v}_o + \mathbf{v}_1$, being ξ an arbitrary constant and \mathbf{v}_1 another arbitrary vector; in this way \mathbf{v}_x has been

simply redefined through a linear combination of two vectors, as it is certainly possible. So the second Eq. (13) reads

$$\mathbf{v}_o = \frac{\delta\mathbf{v} - \mathbf{v}_1}{\xi - \frac{\xi(\delta\mathbf{v})^2}{\mathbf{v}_1 \cdot \delta\mathbf{v}}}.$$

Multiplying both sides of this equation by the unit vector \mathbf{u}_z one finds

$$v_{oz} = \frac{\delta v_z}{\xi - \frac{\xi(\delta\mathbf{v})^2}{\mathbf{v}_1 \cdot \delta\mathbf{v}}}, \quad v_{oz} = \mathbf{v}_o \cdot \mathbf{u}_z, \quad \delta v_z = (\delta\mathbf{v} - \mathbf{v}_1) \cdot \mathbf{u}_z. \quad (18)$$

It is natural at this point to express the terms with physical dimensions of velocity and square velocity appearing in the last result as follows

$$\delta v_z / \xi = u_a - u_b, \quad (\delta\mathbf{v})^2 = u_a u_b, \quad \mathbf{v}_1 \cdot \delta\mathbf{v} = c^2,$$

being u_a and u_b two arbitrary velocities; then one obtains

$$v_{oz} = \frac{u_a - u_b}{1 - \frac{u_a u_b}{c^2}}. \quad (19)$$

The physical meaning of this result is acknowledged by reasoning "a posteriori", i.e. by assessing its implications. Trivial considerations show that, whatever the actual numerical value of c might be, if $u_a = u_b = c$ then $v_{oz} = c$; also, the right hand side never exceeds c . Knowing that c is the upper value of velocity accessible to any particle [16], and so just for this reason invariant in different inertial reference systems in reciprocal motion [17], the Eq. (19) must have the physical meaning of addition velocity rule; the appropriate notation should be therefore $v_{oz} = u'_a$ with u'_a corresponding to u_a in another reference system, which is possible because \mathbf{v}_o has not been specifically defined. Also this conclusion is a corollary of the quantum principle of uncertainty, Eqs. (1), from which started the present reasoning.

Let us summarize the results achieved in this subsection. The Eqs. (6) and (7) introduce the laws of physics where the gradient of some non-equilibrium property, e.g. the non-uniform concentration of matter or charges and even temperature or pressure field gradients, generates the respective mass or charge or heat flows and related driving forces; this expresses the tendency of nature towards an equilibrium configuration corresponding to the maximum entropy [14]. Next the Eq. (12) enabled to infer the x -component of $\delta\Delta\mathbf{J}$ corresponding to that of the Eq. (6), thus emphasizing the connection of the present analysis with the straightforward quantum result. Eventually the orthogonality position of the Eq. (13) was also necessary to ensure that $\delta\mathbf{v}$ associated to $\delta\Delta\mathbf{J}$ does not imply the change of \mathbf{v}_x to which is related D of the Eq. (17); so the Eq. (19) results pertinent to the Eq. (6) although obtained via $\delta\mathbf{v}$. This last result, Eq. (19), is a well known relativistic equation: the addition of the velocities, here expressed through

one velocity component along an arbitrary axis identified by \mathbf{u}_z , cannot overcome the limit speed c despite u_a or u_b or both are themselves equal to c . All of these results have been obtained via the first equation (13) only, which is straightforward consequence itself of the Eqs. (1). Besides the concrete importance of these results, however, the question arises at this point: what is the physical connection between the gradient laws of physics and the relativistic composition of the velocities? Otherwise stated: if the gradient law describes the tendency of physical systems towards the equilibrium state, why this result has been inferred contextually to the velocity addition rule of the special relativity? This question can be further extended also considering the dimensional properties of the flux of matter of the Eq. (7), whose time derivative obtained differentiating the Eq. (7) yields

$$\frac{\delta\Delta\mathbf{J}}{\delta\Delta t} = C\dot{\mathbf{v}} + \mathbf{v}\dot{C}, \quad \dot{\mathbf{v}} = \frac{\delta\mathbf{v}}{\delta\Delta t}, \quad \dot{C} = \frac{\delta C}{\delta\Delta t}; \quad (20)$$

as explained in [17], the derivatives are defined in the present model via the Eqs. (1) only, i.e. as ratios of the uncertainty ranges therein introduced. In the present context the ratio regards the change $\delta\Delta\mathbf{J}$ during $\delta\Delta t$. Being $C = \text{mass}/\text{volume}$ and noting that $\Delta\mathbf{J}$ is *force/volume*, one infers that $\mathbf{F} \approx m\mathbf{a}$ in the case where $\mathbf{v}\dot{C}$ can be neglected with respect to the former addend. As it is known, force and acceleration are parallel vectors in the non-relativistic approximation only; since both C and \mathbf{v} are arbitrary, in general they are expected to contribute at increasing \mathbf{v} to the relativistic limit $|\mathbf{v}| \rightarrow c$ where reasonably the second addend becomes important. In effect is sensible the fact that $\mathbf{v}\dot{C}$ somehow surrogates the relativistic consequences of the space-time deformation, recalling that $C = m/V$; writing $V = \Delta x^3$ and regarding the time derivative as that due to the change of V pertinent to a fixed amount m of mass, in agreement with the Eq. (5), one infers $\dot{C} = -3C\Delta\dot{x}/\Delta x$. In fact $\Delta\dot{x}/\Delta x$ is a deformation of the space-time uncertainty range Δx , being by definition $\Delta\dot{x} = \delta\Delta x/\delta\Delta t$; so, at least in principle, the involvement of relativistic concepts like the deformation of the space-time in the presence of the mass is understandable. In effect, is not accidental the fact that just this space-time deformation is the relativistic contribution to the Newtonian term $m\dot{\mathbf{v}}$.

In conclusion, the actual quantum origin of the diffusion equations stimulates the question about why relativistic implications, apparently dissimilar, have been contextually obtained without any ‘‘ad hoc’’ hypothesis. The only possible answer is that the mere context of the quantum uncertainty contains itself the intimate connection that underlies fundamental laws even of apparently different nature. All considerations have been carried out by elaborating the Eqs. (1), which are thus the common root of these results: so this conclusion is not surprising because, as shown in [17], even the basic statements of quantum mechanics and special and general relativity are obtained as corollaries of the Eqs. (1). Therefore further considerations are expectedly hidden in this

kind of approach, even as concerns the field gradient driven forces.

2.3 Diffusion and driving forces

The second equality (7) reads $\mathbf{v} = -D\nabla \log(C)$ and suggests a reasonable link with the known expression of the chemical potential $\mu = k_B T \log(C)$; this hint yields

$$\mathbf{v} = -\frac{D}{k_B T} \nabla k_B T \log(C) \quad \mathbf{F} = -\nabla k_B T \log(C); \quad (21)$$

then merging the thermodynamic definitions of μ and mobility β , i.e. $\mathbf{v} = \beta\mathbf{F}$, one finds contextually the force $\mathbf{F} = -\nabla\mu$ acting on the diffusing species and the Einstein equation $D = \beta k_B T$ linking mobility and diffusion coefficient. Note however that it is convenient to define μ as

$$\mu = k_B T \log(C/C_j) \quad C_j = C_j(t) \quad (22)$$

which leaves unaffected \mathbf{F} and \mathbf{v} and is still consistent with the asymptotic limits $\mathbf{F} \rightarrow 0$ and $\mathbf{v} \rightarrow 0$ for $C \rightarrow \text{const}$: i.e. the driving force of the diffusion process vanishes when C evolves as a function of time to reach any constant concentration. This limit implies a gradient free distribution of matter attained for $C \rightarrow C_j$ evolving as well e.g. to fit the limit value of C . Further information is also inferred with the help of the Eq. (2); dividing both sides by Δt , this equation reads in vector form $\mathbf{F} = \Delta\mathbf{p}/\Delta t = (\Delta\varepsilon/c^2\Delta t)\mathbf{v}$, which yields with the help of the Eqs. (1)

$$\mathbf{F} = \frac{n\hbar(c\Delta t)\mathbf{v}}{(c\Delta t)^3} = \frac{n\hbar}{\delta x^3} \mathbf{v}\delta x, \quad \delta x = c\Delta t, \quad \beta = \frac{c^2\Delta t}{\Delta\varepsilon} = \frac{(c\Delta t)^2}{n\hbar}.$$

Calculate the component of \mathbf{F} along the arbitrary direction of a unit vector \mathbf{u} ; owing to the Eq. (17) the scalar $\mathbf{v} \cdot \mathbf{u}\delta x$ at right hand side defines the diffusion coefficient D , so

$$\frac{F_u}{D} = \frac{n\hbar}{V}, \quad V = \delta x^3, \quad D = \mathbf{v} \cdot \mathbf{u}\delta x. \quad (23)$$

Merging the last equation with the Eq. (6), one finds $\mathbf{v} \cdot \mathbf{u}\delta x = qn\hbar/m$, which reads $mv_u\delta X = n\hbar$ and thus is just nothing else but the first equality (1). Implementing again the idea of expressing D via $n\hbar/m$ by dimensional reasons, see the Eqs. (6), the Eq. (23) reads

$$F_u = \frac{(n\hbar)^2}{mV}; \quad (24)$$

this step of the reasoning introduces diffusing mass and volume in the expression of the driving force of the macroscopic process whose diffusion coefficient is D . Interesting evidence about the importance of this result has been already emphasized in [16]; this point is so simple that it is worth being shortly summarized here for completeness.

The Eqs. (1) and (6) yield $qF_u/D = n\hbar/V$ and thus $qF_u/D = \Delta\varepsilon/\nu V$ having defined $\nu = \Delta t^{-1}$; so the right hand

side is an energy range per unit frequency and unit volume. Putting $\Delta\varepsilon = h\nu$ one finds thus $qF_u/D = nh/V$. Let now V be the volume of a cavity in a body filled with radiation in equilibrium with its internal walls, whose size is able to contain the longest wavelength $\lambda = c/\nu$ of the steady radiation field; of course λ is arbitrary. Then $V = (2c/\nu)^3$, where the factor 2 accounts for λ with nodes just at the boundaries of the cavity, whose size is thus one half wavelength. Hence $F_u/D = 8h(\nu/c)^3 n/q$. Is significant here the physical meaning of the ratio F_u/D , which has physical dimensions $h/volume$, regardless of the specific values of F_u and D separately; thus, being F_u/D the component of the vector \mathbf{F}/D along the arbitrary direction defined by \mathbf{u} , regard this latter as a unit vector drawn outwards from the surface of the body at the centre of the cavity. As \mathbf{u} represents any possible path of the radiation leaving the cavity, let q be defined in this case in agreement with $\int(F_u/D)d\Omega = \pi nh/V$. Actually F_u/D is taken out of the integral because it has no angular dependence, whereas the integral $\int d\Omega$ is carried out over the half plane above the surface of the cavity only, which yields 2π ; a factor 1/2 is also necessary as this is the probability that one photon at the surface of the cavity really escapes outwards instead of being absorbed inwards within the cavity. So $\int(F_u/D)d\Omega = 8\pi h(\nu/c)^3 n$ yields the Planck black body formula once replacing the number n of states allowed to the radiation field with the factor $(\exp(h\nu/k_B T) - 1)^{-1}$ of the Bose distribution statistics of all oscillators: as an arbitrary number of particles is allowed in each state, n is also representative of any number of particles concerned by the statistical distribution.

Implement now the definition of mobility to write $\delta\mathbf{v} = \beta\delta\mathbf{F} + \mathbf{F}\delta\beta$; dividing both sides by $\delta\beta$ one finds $\delta\mathbf{v}/\delta\beta - \mathbf{F}' = \mathbf{F} = -\nabla\mu$, having put $\mathbf{F}' = \beta\delta\mathbf{F}/\delta\beta$. By analogy with \mathbf{F} , let us introduce the position $\mathbf{F}' = -\nabla Y$ with Y appropriate energy function related to $\delta\mathbf{F}$; thus the result is

$$\frac{\delta\mathbf{v}}{\delta\beta} = -\nabla(Y + \mu). \quad (25)$$

The physical meaning of this result is highlighted thinking that the physical dimensions of β are *time/mass*; considering in particular a volume V of matter where the mass is conserved and simply redistributed, exactly as assumed in the Eq. (5), $\delta\mathbf{v}/\delta\beta$ is proportional to *mass* \times $\delta\mathbf{v}/\delta t$, i.e. it is nothing else but the law of dynamics previously found via $\partial\mathbf{J}/\partial t$. The Eq. (25), which agrees with the additive character of the force vectors, could be also obtained via Euler's homogeneous function theorem. Here \mathbf{F}' is regarded as if it would be a function of β , whereas it is usually implemented as a function of the position vector \mathbf{r} defined in an appropriate reference system. To this purpose it is enough to put the modulus $r = a\beta$, being a a parameter that controls the local values of mobility as a function of r , to write $\mathbf{F}(a\beta) = a^k\mathbf{F}(\beta)$. So calculating $\partial\mathbf{F}(a\beta)/\partial a\beta = \beta\partial\mathbf{F}(a\beta)/\partial a = ka^{k-1}\mathbf{F}(\beta)$ and putting then in particular $a = 1$, as shown in standard textbooks, one

finds $\beta\delta\mathbf{F}/\delta\beta = k\mathbf{F}(\beta)$; this is the essence of the Euler theorem. Eventually, once having inferred $\mathbf{F}' = \beta\delta\mathbf{F}/\delta\beta = a^k\mathbf{F}(\beta)$, similarly to $\mathbf{F} = -\nabla\mu$ one concludes $\mathbf{F}' = -\nabla Y$ too. An example to elucidate Y could be the familiar force $\nabla Y = -ze\nabla\phi$ to which is subjected an ion of charge ze under the electric potential gradient $\nabla\phi$, in which case $Y + \mu = ze\phi + \mu$ is the well known electro-chemical potential controlling the working conditions of a fuel cell. The result (25) is in fact possible because $\delta\mathbf{F} = \mathbf{F}_2 - \mathbf{F}_1$ is an arbitrary force; whatever \mathbf{F}_2 and \mathbf{F}_1 might be, their arbitrariness ensures the general physical meaning of \mathbf{F}' and thus its ability to be specified according to some particular physical condition. Suppose known for instance C , solution of the Eq. (8) with or without the condition (9). This solution provides one with information about the momentum pertinent to the mass transfer involved by the diffusion process. Indeed $\Delta\mathbf{J}$ represents from the dimensional point of view the momentum change per unit volume related to the redistribution of the mass within V . Thus, collecting the Eqs. (2) and (7), one finds $\Delta\mathbf{J} = \Delta\mathbf{p}/V = \mathbf{v}\Delta\varepsilon/c^2 V = C\mathbf{v}$ being $\Delta\varepsilon/c^2 = m$ and $mC = V$ by definition. Putting then $\Delta\mathbf{p} = \mathbf{p} - \mathbf{p}_o$, trivial manipulations with the help of the first Eq. (21) yield

$$\frac{\mathbf{p}}{m} = \frac{\mathbf{p}_o}{m} - D\nabla\log(C).$$

The ratios involve the velocities \mathbf{v} and \mathbf{v}_o in agreement with the Eqs. (21); for instance, the former is the rate with which occurs the redistribution of m in V , the latter is the initial velocity of the concerned species before the redistribution. In summary, this section has shown that the diffusion equations imply the transfer of matter, energy and momentum; moreover, the velocity addition rule shows that the particles responsible of the mass transfer move in agreement with the relativistic requirements under the condition (13). Eventually the fact of having inferred $\mathbf{F} \approx m\mathbf{a}$ without precluding, at least in principle, even its possible generalization to the relativity, suggests that the quantum basis of these preliminary results is appropriate to carry out further tasks to describe the fundamental interactions too.

3 Entropy and chemical potential

As concerns μ of the Eq. (22) it is known that [21]

$$\left(\frac{\partial\mu}{\partial T}\right)_{P,n} = -\left(\frac{\partial S}{\partial n}\right)_{T,P}, \quad (26)$$

being dS the entropy change calculated keeping constant the pressure and temperature during the time necessary to increase n by dn ; here n is a dimensionless amount of the concerned substance, e.g. a number of atoms or molecules, whereas dn can be approximately treated as a differential for large n only. The following considerations aim to integrate the Eq. (26) with respect to dn with the help of the Eq. (22).

Let m consist of a cluster of n_m atoms or molecules randomly distributed over an arbitrary number of elementary volumes V_j forming V , i.e. such that $V = \sum_j V_j$; so the given

amount m of mass in the actual volume V is in fact distributed into several elementary volumes $V_j = V_j(t)$. Regard thus each V_j as a possible state allowed to one or more particles among the n_m available: if for instance V_j would be all equal, then each ratio $V_j/V = 1/n_j$ would yield the probability $\Pi_j = 1/n_j$ of each state accessible to m , being by definition $\sum_j n_j^{-1} = 1$. Moreover the possible distributions of n_m objects into the various V_j are functions of time related to the corresponding number N_j of allowed quantum configurations: whatever N_j might be in general, depending on the kind of statistical distribution compliant with the possible spin of the n_m particles, V_j/V is in fact a parameter related to the degree of disorder characteristic of m in V . Hence integrating the Eq. (26) with respect to dn means summing over all of the probabilities n_j^{-1} consistent with all possible V_j compatible with V ; this also means integrating over $d(V_j/V)$ while keeping constant the total number of particles n_m in V , as required at left hand side of the Eq. (26) and in agreement with the Eq. (5). Putting therefore $C_j = m/V_j$ by analogy with $C = m/V$, one infers $C/C_j = V_j/V$ and then

$$S_j = S_o - \int (\partial\mu_j/\partial T)_{P,n} dn = S_o - k_B \int \log(V_j/V) d(V_j/V) = S_o - k_B (V_j/V) (\log(V_j/V) - 1).$$

Clearly the reasoning about the j -th states in V can be repeated for the j' -th states pertinent to the ratios V_j'/V' concerning the volume V' , which consists of related elementary volumes V_j' such that $\sum_{j'} V_j'/V' = 1$. The same holds also for a volume V'' defined as sum of elementary volumes V'' and so on; in this way it is possible to define the resulting extensive entropy collecting together all integrals on V_j/V plus that on V_j'/V' and V_j''/V'' , with $V + V' + V'' + \dots = V_{tot}$ and the respective masses $m + m' + m'' + \dots = m_{tot}$ each one of which is that already concerned in the Eq. (5). Then since by definition $\sum_{j'} V_j'/V' = \sum_{j''} V_j''/V'' = 1$ and thus $\sum_j V_j/V + \sum_{j'} V_j'/V' + \sum_{j''} V_j''/V'' + \dots = j_{tot}$, summing over all elementary volumes of which consist the total mass and volume of the body yields

$$S = (S_o + j_{tot}k_B) - k_B \sum_j \frac{V_j}{V} \log\left(\frac{V_j}{V}\right). \quad (27)$$

The first addend is clearly a constant. This result defines an extensive function that collects all possible configurations N_j corresponding to all distributions of the various m in the respective volumes V_j compatible with each V where holds the Eq. (5). In principle V is arbitrary; yet it must be sufficiently large to be subdivided into V_j whose n_j allow considering dn_j as differentials. Note that the Eq. (27) has been early obtained in [14] elaborating directly the Eqs. (5). Appears clear the link between diffusion, regarded as the way through which the nature drives a thermodynamic system towards the equilibrium state, and entropy, $-\sum_j \pi_j \log \pi_j$, which measures the tendency towards states of progressively increasing disorder:

this link is the underlying chemical potential μ , strictly connected with the concentration gradient of the diffusing species on the one side and with the related entropy change on the other side. If in the Eq. (26) $d\mu = 0$, which corresponds to $\mathbf{F} = -\nabla\mu = 0$ for uniform distribution of C , then $dS = 0$ reveals that the concerned system is in the state of maximum disorder. The diffusion of matter and energy is thus the driving force that puts into action the second law.

4 Diffusion and fundamental interactions

This is the central section of the paper. The fact of having inferred the results of the previous section from the fundamental Eqs. (1) along with relativistic implications, suggests that additional outcomes should be obtainable elaborating further the concepts hitherto introduced. For the following considerations it is useful to remark that the physical dimensions of \mathbf{J} imply $flux/velocity = density = \rho$ and $flux \times velocity = energy\ density = \eta$. The interactions are thus described by a flux \mathbf{J} of messenger particles, the respective boson vectors, displacing at rate \mathbf{v} and characterized by mass and energy densities ρ and η . The starting point of this section is again the initial Eq. (9) identically rewritten as

$$\nabla \cdot \Delta\mathbf{J} + \frac{\partial C}{\partial t} = +\nabla \cdot \nabla \times \mathbf{U}_+,$$

which holds whatever the arbitrary vector \mathbf{U}_+ might be; indeed the last addend is anyway null. Let us rewrite this equation with the help of the position $\nabla \cdot \mathbf{U}_- = C$, which in turn yields

$$\nabla \cdot \left(\Delta\mathbf{J} + \frac{\partial \mathbf{U}_-}{\partial t} - \nabla \times \mathbf{U}_+ \right) = 0. \quad (28)$$

So the vector within parenthesis must be a constant or a function of time only; then in general

$$\Delta\mathbf{J} + \frac{\partial \mathbf{U}_-}{\partial t} - \nabla \times \mathbf{U}_+ = \mathbf{J}_w, \quad \mathbf{J}_w = \mathbf{J}_w(t), \quad \nabla \cdot \mathbf{U}_- = C. \quad (29)$$

The physical dimensions of \mathbf{U}_- and \mathbf{U}_+ are $mass \times surface^{-1}$ and $mass \times time^{-1} \times length^{-1}$, whence $\mathbf{U}_+ = \mathbf{U}_-c$ from dimensional point of view; c is the pertinent constant velocity. The homogeneous differential equation obtained from the Eq. (29) is

$$\Delta\mathbf{J} + \frac{\partial \mathbf{U}_-}{\partial t} - \nabla \times \mathbf{U}_+ = 0, \quad \mathbf{J}_w = 0. \quad (30)$$

Starting from this quantum groundwork, the next subsections aim to highlight the steps ahead toward the goal of inferring the four fundamental interactions of nature as contextual corollaries.

4.1 The Maxwell equations

This subsection summarizes the reasoning reported in [15]; it is emphasized in the next subsection 4.2 how to include also the weak interaction still in the frame of the same approach.

Consider first the homogeneous differential equation inferred from the Eq. (30)

$$\nabla \times \mathbf{U}_+ = \Delta \mathbf{J} + \frac{\partial \mathbf{U}_-}{\partial t}, \quad \nabla \cdot \mathbf{U}_- = C. \quad (31)$$

The first equation (31) defines the vector \mathbf{U}_+ as a function of \mathbf{U}_- , the second one defines the vector \mathbf{U}_- as a function of C . Putting $\Delta \mathbf{J} = \mathbf{J}_2 - \mathbf{J}_1$, it is reasonable to expect also $\mathbf{U}_- = \mathbf{U}_2 - \mathbf{U}_1$ and thus $C = C_2 - C_1$. Moreover, besides the dimensional link, appears now a preliminary reason to define \mathbf{U}_+ via the same vectors that implement \mathbf{U}_- : there is no compelling necessity to introduce further vectors additional to \mathbf{U}_1 and \mathbf{U}_2 , about which specific hypotheses would be necessary to solve both Eqs. (31). This choice simply requires $\mathbf{U}_+ = (\mathbf{U}_2 + \mathbf{U}_1)\xi$, being ξ an appropriate proportionality factor. The vectors \mathbf{U}_1 and \mathbf{U}_2 just introduced are arbitrary, likewise the respective C_1 and C_2 ; for this reason both \mathbf{U}_+ and \mathbf{U}_- have been defined with coefficients of the linear combinations of \mathbf{U}_1 and \mathbf{U}_2 equal to 1 without loss of generality. Hence, combining these definitions with the dimensional requirements, one finds

$$\mathbf{U}_+ = c(\mathbf{U}_2 + \mathbf{U}_1), \quad \mathbf{U}_- = \mathbf{U}_2 - \mathbf{U}_1, \quad (32)$$

$$\mathbf{U}_2, \mathbf{U}_1 = \text{mass/surface},$$

so that the second Eq. (31) yields

$$\nabla \cdot \mathbf{U}_2 = C_2, \quad \nabla \cdot \mathbf{U}_1 = C_1, \quad (33)$$

whereas the first Eq. (31) takes the form

$$c\nabla \times \mathbf{U}_2 + c\nabla \times \mathbf{U}_1 - \mathbf{J}_2 + \mathbf{J}_1 - \frac{\partial \mathbf{U}_2}{\partial t} + \frac{\partial \mathbf{U}_1}{\partial t} = 0. \quad (34)$$

Now the problem arises about how could be rearranged the terms appearing in this equation. For instance the chance

$$c\nabla \times \mathbf{U}_2 - \mathbf{J}_2 - \frac{\partial \mathbf{U}_2}{\partial t} = \mathbf{J}' = -c\nabla \times \mathbf{U}_1 - \mathbf{J}_1 - \frac{\partial \mathbf{U}_1}{\partial t} \quad (35)$$

separates the quantities with subscript "2" from those with subscript "1"; the ancillary arbitrary vector \mathbf{J}' that satisfies both equalities (35) can be in general different from zero. If so, then one obtains two equations

$$c\nabla \times \mathbf{U}_2 - \mathbf{J}'_2 - \frac{\partial \mathbf{U}_2}{\partial t} = 0, \quad -c\nabla \times \mathbf{U}_1 - \mathbf{J}'_1 - \frac{\partial \mathbf{U}_1}{\partial t} = 0, \quad (36)$$

$$\mathbf{J}'_2 = \mathbf{J}_2 + \mathbf{J}', \quad \mathbf{J}'_1 = \mathbf{J}_1 + \mathbf{J}'.$$

Note that it is possible to change the physical meaning of the mass concentrations C_1 and C_2 of the Eqs. (33) simply multiplying both sides by q_m/m and q_e/m respectively; q_e is the total amount of electric charge possibly owned by the mass m , the physical meaning of q_m will be explained later in analogy with that of q_e . The multiplicative factors convert the mass density C_2 into the q_e charge density C_2^* , whereas

C_1 turns into the q_m density C_1^* ; analogously \mathbf{U}_1 and \mathbf{U}_2 turn into \mathbf{U}_1^* and \mathbf{U}_2^* in the Eqs. (33), whereas the same holds for \mathbf{J}'_2 and \mathbf{J}'_1 that turn respectively into charge and q_m flows \mathbf{J}_2^* and \mathbf{J}_1^* in the Eqs. (36). This means having converted \mathbf{U}_1 and \mathbf{U}_2 into quantities corresponding to the respective \mathbf{J}_1^* and \mathbf{J}_2^* . Indeed the Eqs. (33) and the last two equations read

$$\nabla \cdot \mathbf{U}_1^* = C_1^*, \quad \nabla \cdot \mathbf{U}_2^* = C_2^*,$$

$$C_1^* = C_1 \frac{q_m}{m}, \quad C_2^* = C_2 \frac{q_e}{m}, \quad (37)$$

whence

$$c\nabla \times \mathbf{U}_2^* - \mathbf{J}_2^* - \frac{\partial \mathbf{U}_2^*}{\partial t} = 0, \quad \mathbf{U}_2^* = \mathbf{U}_2 \frac{q_e}{m}, \quad \mathbf{J}_2^* = \mathbf{J}'_2 \frac{q_e}{m}, \quad (38)$$

and

$$-c\nabla \times \mathbf{U}_1^* - \mathbf{J}_1^* - \frac{\partial \mathbf{U}_1^*}{\partial t} = 0$$

$$\mathbf{U}_1^* = \mathbf{U}_1 \frac{q_m}{m}, \quad \mathbf{J}_1^* = \mathbf{J}'_1 \frac{q_m}{m}. \quad (39)$$

The Eqs. (38) and (39) have physical meaning different from that of the respective Eqs. (36); subtracting side by side these latter one of course finds again the initial Eq. (34), whereas the same does not hold for the Eqs. (38) and (39) that have been multiplied by the respective factors implemented in the Eqs. (37).

Exploit now the fact that the Eqs. (38) and (39) can be still merged together because anyway $c\nabla \times \mathbf{U}_2^* - \mathbf{J}_2^* - \partial \mathbf{U}_2^*/\partial t = -c\nabla \times \mathbf{U}_1^* - \mathbf{J}_1^* - \partial \mathbf{U}_1^*/\partial t$. Note however that the vectors $\mathbf{U}_1^*(\mathbf{J}_1^*)$ and $\mathbf{U}_2^*(\mathbf{J}_2^*)$ obtained solving separately the Eqs. (38) and (39) have scarce physical interest, because the boundaries of the initial uncertainty range $\Delta \mathbf{J}$ are arbitrary; whatever their form might be, they provide two independent solutions that are functions of their own flux vectors only. More interesting seems instead a general solution like $\mathbf{U}_1^*(\mathbf{J}_1^*, \mathbf{J}_2^*)$ and $\mathbf{U}_2^*(\mathbf{J}_1^*, \mathbf{J}_2^*)$, in fact also prospected by the initial Eqs. (35) themselves: this hint appears sensible because \mathbf{U}_+ and \mathbf{U}_- consist by definition of the same vectors \mathbf{U}_1 and \mathbf{U}_2 in the Eq. (31). So rewrite the last result as

$$c\nabla \times \mathbf{U}_1^* - \mathbf{J}_2^* - \partial \mathbf{U}_2^*/\partial t = 0 = -c\nabla \times \mathbf{U}_2^* - \mathbf{J}_1^* - \partial \mathbf{U}_1^*/\partial t,$$

where we have simply exchanged the sides where appear the curl vectors. For simplicity of notation, but without loss of generality, has been omitted the new flux vector \mathbf{J}'' possibly shared by both equalities; indeed, as previously done with \mathbf{J}' to infer the Eqs. (36) from the Eq. (35), \mathbf{J}'' would have been once more incorporated within \mathbf{J}_2^* and \mathbf{J}_1^* . In conclusion one obtains from the Eqs. (37) to (39)

$$\nabla \cdot \mathbf{U}_1^* = C_1^*, \quad \nabla \cdot \mathbf{U}_2^* = C_2^*, \quad (40)$$

$$c\nabla \times \mathbf{U}_1^* - \mathbf{J}_2^* - \frac{\partial \mathbf{U}_2^*}{\partial t} = 0, \quad c\nabla \times \mathbf{U}_2^* + \mathbf{J}_1^* + \frac{\partial \mathbf{U}_1^*}{\partial t} = 0.$$

Despite the notations, mere consequence of the fact that the starting point to attain the Eqs. (40) were the diffusion equations of the section 2, is evident the conceptual equivalence of these equations with the well known ones

$$\begin{aligned} \nabla \cdot \mathbf{H} &= 0, & \nabla \cdot \mathbf{E} &= \rho_{ch}, \\ \nabla \times \mathbf{H} - \frac{\partial \mathbf{E}}{\partial t} - \mathbf{J}_{ch} &= 0, & \nabla \times \mathbf{E} + \frac{\partial \mathbf{H}}{\partial t} &= 0, \end{aligned} \quad (41)$$

simply regarding $\mathbf{U}_2^* \equiv \mathbf{E}$ and $\mathbf{U}_1^* \equiv \mathbf{H}$ together with the charge density $C_2^* \equiv \rho_{ch}$ and $C_1^* = 0$. So, being \mathbf{J}_2^* by definition identified with the charge current density \mathbf{J}_{ch} , the Eqs. (41) are nothing else but the Maxwell equations, usually written putting $C_1^* = \rho_{qm} = 0$ and $\mathbf{J}_1^* = \mathbf{J}_{qm} = 0$; these positions, due to $q_m = 0$, acknowledge the lack of experimental evidence of magnetic monopoles. Since these monopoles have not yet been observed experimentally, the correspondence has been emphasized as in the Eqs. (41), despite it would be very attracting and convincing to consider $q_m \neq 0$ too in the equations (41) by formal symmetry: it is worth emphasizing indeed that the reasoning hitherto carried out does not exclude at all the theoretical existence of the magnetic monopoles, rather this approach suggests explicitly them. The positions above that read now

$$\mathbf{U}_+^*/c = \mathbf{E} + \mathbf{H}, \quad \mathbf{U}_-^* = \mathbf{E} - \mathbf{H},$$

entail four more reasons to validate the positions (32), according which \mathbf{U}_- and \mathbf{U}_+ can be expressed through the same vectors they introduce:

- (i) $\mathbf{U}_+^*/c + \mathbf{U}_-^* = 2\mathbf{H}$ and $\mathbf{U}_+^*/c - \mathbf{U}_-^* = 2\mathbf{E}$;
- (ii) the same holds for the scalars $\mathbf{U}_+ \cdot \mathbf{U}_-/c = H^2 - E^2$ and $U_+^2/c^2 - U_-^2 = 4\mathbf{E} \cdot \mathbf{H}$;
- (iii) $\mathbf{U}_- \times \mathbf{U}_+/c = 2\mathbf{E} \times \mathbf{H}$;
- (iv) $U_+^2/c^2 + U_-^2 = 2(H^2 + E^2)$.

Once having specified in particular \mathbf{H} and \mathbf{E} as vectors proportional to magnetic and electric fields, then the proposed definitions of \mathbf{U}_- and \mathbf{U}_+ entail the well known features: the scalars (ii) define two invariants with respect to Lorentz transformations, whereas the vector (iii) is proportional to the Poynting vector and defines the energy density flux; moreover the point (iv) defines a scalar proportional to the energy density of the electromagnetic field; finally, the integral $c^{-1} \int \mathbf{U}_+ \cdot \mathbf{U}_- dV$ over the volume previously introduced is proportional to the Lagrangian of a free field. As the only velocity that appears in these equations is c , one must conclude that the carriers of this kind of interaction are the photons. Despite these last considerations are well known, their mentioning here is not redundant: indeed these outcomes of the diffusion laws come from and complete the quantum frame of the Maxwell equations.

4.2 The weak interactions

The starting point of this subsection is the non-homogeneous Eq. (29) which concerns $\mathbf{J}_w \neq 0$. Of course even the results of

the previous subsection hold when $\mathbf{J}_w \neq 0$ is negligible with respect to $\Delta \mathbf{J}$; so the content of this subsection is not to be regarded separately from the previous one, rather as its completion and generalization. Note that the Eq. (29) results formally similar to the Eqs. (35); the only difference is that \mathbf{J}' is in general function of x, y, z, t , as no hypothesis has been necessary about it, whereas \mathbf{J}_w is instead by definition function of time only in agreement with the Eq. (28). So this case can be formally handled as before, simply rewriting the Eq. (29) as

$$\Delta \mathbf{J}' + \frac{\partial \mathbf{U}_-}{\partial t} - \nabla \times \mathbf{U}_+ = 0, \quad \Delta \mathbf{J}' = \Delta \mathbf{J} - \mathbf{J}_w, \quad \mathbf{J}_w = \mathbf{J}_w(t). \quad (42)$$

Once replacing the previous change of flux $\Delta \mathbf{J} = \mathbf{J}_2 - \mathbf{J}_1$ with $\Delta \mathbf{J}' = \mathbf{J}_2 - \mathbf{J}_1 - \mathbf{J}_w$, is attracting the idea that in the present problem \mathbf{J}_w describes a quantum time fluctuation of energy range $\Delta \varepsilon_w$ and time length Δt_w consistent with the uncertainty equations (1). To highlight the link between the flux modulus $J_w = |\mathbf{J}_w|$ and $\Delta \varepsilon_w$, let $\eta_w = \mathbf{v} \cdot \mathbf{J}_w$ be the energy density transient of time length $\Delta t_w = \hbar/\eta_w V$, being $V = \Delta x^3$ the volume within which is generated the mass density transient $\rho_w = m_w/V = J_w/v$; of course $v = |\mathbf{v}|$ is the modulus of the velocity with which the messenger particles propagate this kind of interaction, whereas $\Delta \varepsilon_w$ is the fluctuation energy change necessary to create messengers with lifetime Δt_w . It is possible to express the mass flux J_w of m_w as $\hbar/\Delta x_w^4$ by dimensional reasons; so $J_w = \xi \hbar/\Delta x_w^4$, being ξ a proportionality constant. Hence $\xi \hbar/\Delta x_w^4 = m_w v/\Delta x_w^3$ yields

$$\zeta \frac{\hbar}{\Delta x_w} = m_w c, \quad v = \gamma c, \quad \zeta = \frac{\xi}{\gamma};$$

so the range of this interaction force is $\Delta x_w = (\xi/\gamma)(\hbar c/m_w c^2)$. Let us estimate Δx_w putting preliminarily $\xi/\gamma \approx 1$, according to the reasonable idea that a proportionality constant correlating two quantities should be of the order of the unity; otherwise some further physical effect should be identified and implemented to justify $\xi/\gamma \gg 1$. So one expects

$$\Delta x_w \approx \frac{\hbar c}{m_w c^2}, \quad \Delta x_w \approx 10^{-16} \text{ cm}, \quad m_w c^2 \approx 250 \text{ GeV}. \quad (43)$$

The estimates have been guessed to exemplify the correlation between space range and energy scale; the figures are plausibly typical of the weak interactions. This preliminary estimate aimed merely to show that the positions $J_w \approx \hbar/\Delta x_w^4$ and $\rho_w \approx J_w/v$ and mass m_w of the messenger particles are reasonable; this result must be however better assessed and more thoroughly justified.

The basic idea is that during the time transient described by \mathbf{J}_w , the range of the related interaction cannot be very wide; a long distance travel of messenger particles would require an extended time length, incompatible with the short-lasting transient Δt_w during which the classical energy conservation is temporarily replaced by the related quantum en-

ergy uncertainty $\Delta\varepsilon_w$. The next reasoning attempts to introduce a short range force mediated by massive particles created somewhere in the space-time by the energy fluctuation $\Delta\varepsilon_w$ and moving at rate $v_w < c$: once having waived in the Eqs. (1) the local time and space coordinates, it is possible to say that at an arbitrary time t_0 the quantum fluctuation nucleates at the arbitrary point x_0, y_0, z_0 the total mass m_w that flows along with \mathbf{J}_w within a volume V with average density ρ_w .

To confirm the existence of massive particles describing this interaction, divide the Eqs. (1) by Δt so that $v_x \Delta p_x = \hbar/\Delta t = \Delta\varepsilon$ with $\Delta p_x \approx (m' - m)v_x$ according to the Eq. (3): hence the uncertainty prospects the chance of two kinds of vector bosons of different masses describing the interaction.

Consider first the carrier of mass m and implement the Eq. (24), noting that the volume V defining the density ρ_w can be written as $V = \Delta x^2 \delta x_u$ without loss of generality; introducing indeed V via an arbitrary coefficient ξ is actually irrelevant, because $\xi \Delta x^2 \delta x_u$ would be handled exactly like $V = \Delta x^2 \delta x'_u$ simply rewriting $\delta x'_u = \xi \delta x_u$. So the actual geometric shape of V is waived because the sizes of Δx and δx_u are arbitrary in the conceptual frame based on the uncertainty Eqs. (1) only. Let us write the Eq. (24) as $\varepsilon_u = (n\hbar)^2/m\Delta x^2$ with $\varepsilon_u = F_u \delta x_u$ and then identify ε_u with the energy mc^2 necessary to create just the concerned rest mass m by virtue of the quantum energy fluctuation only; so one finds with $n = 1$ the reduced Compton length associated to m

$$\lambda = \Delta x, \quad \lambda = \frac{\hbar}{mc}. \quad (44)$$

This expression holds for any particle free and neutral: the former condition assumes that m does not directly interact with m' , the latter requires that no additional net charge is created during Δt_w because of the total charge conservation with respect to that early concerned by the Maxwell equations before the quantum fluctuation.

Analogous considerations hold for m' , in particular as concerns the condition of charge conservation during the fluctuation time of \mathbf{J}_w . So m' either describes another neutral particle or it could actually consist of a couple of particles having equal mass and opposite charges; as in the latter case the charges interact to form an electromagnetic interaction driven Coulomb system with gain of energy, let therefore m' consist of two particles of equal reduced mass $m'_r = m'/2$. The energy ε_{em} and Bohr radius r_{em} of a hydrogenlike system are well known: considering the ground energy state with $n = 1$ only, they are $\varepsilon_{em} = -\alpha^2 m'_r c^2 / 2 = -e^2 / 2r_{em}$ with $r_{em} = \alpha^{-1} \hbar / m'_r c$; thus ε_{em} is defined by the diametric delocalization distance $2r_{em}$ only of the system of charges orbiting around their centre of mass [18]. Express r_{em} via the condition of steady circular waves $2\pi r_{em} = n_w \lambda_w$ early introduced to account for the stability of the old Bohr atom, whence $\varepsilon_{em} = -\pi e^2 / n_w \lambda_w$ with $n_w \geq 1$ an arbitrary integer. Define then the new energy $\varepsilon_w = n_w \varepsilon_{em} = -\pi e^2 / \lambda_w$. Clearly

$n_w = 1$ still implies the electromagnetic energy $\varepsilon_w = \varepsilon_{em}$, whereas $n_w > 1$ implies $\varepsilon_w > \varepsilon_{em}$ since $\lambda_w < r_{em}$: this shows that actually ε_{em} and ε_w are both allowed and thus coexisting. On the one hand ε_w is hidden into and closely related to ε_{em} : having merely replaced r_{em} with the wavelengths λ_w allowed to the circular waves of charge, ε_w appears as a sort of short range high energy compatible with the electromagnetic interaction from which it differs for $n_w > 1$, rather than the energy of a separate form of interaction. On the other hand, if really the masses of all three particles correspond to the available energy ε_w , it should be true that $\varepsilon_w \approx 3m_w c^2$ for three equal masses m_w . In fact this expectation is compatible with $-\pi e^2 / \lambda_w$ putting $m_w c^2 \approx e^2 / \lambda_w$ while $\lambda_w \approx \lambda \approx \lambda'$; the replacement of r_{em} with the smaller λ_w accounts for the increase of energy necessary to create short range massive boson vectors, whereas the factor π replacing the expected factor 3 simply reveals that the masses of the neutral and charged boson vectors should actually be slightly different. Otherwise stated, regarding this result as $(m_0 + m_+ + m_-)c^2 = \pi e^2 / \lambda_w$ with obvious meaning of symbols, one infers

$$m_0 c^2 + 2m_{\pm} c^2 = \pi \frac{e^2}{\lambda_w}, \quad m_{\pm} c^2 = \frac{e^2}{\lambda_w},$$

$$m_0 c^2 = (\pi - 2) \frac{e^2}{\lambda_w}, \quad m_+ = m_- = m_{\pm}. \quad (45)$$

Hence, it should be true that

$$m_0 / (m_0 + m_+ + m_-) = (\pi - 2) / \pi,$$

$$m_{\pm} / (m_0 + m_+ + m_-) = 1 / \pi.$$

Compare this last conclusion with the experimental data

$$m_{Z^0} = 91.19 \text{ GeV}, \quad m_{W^{\pm}} = 80.39 \text{ GeV},$$

$$m_{tot} = m_{Z^0} + 2m_{W^{\pm}} = 251.97 \text{ GeV}.$$

Indeed $m_0 / m_{tot} = 0.36$ and $m_{\pm} / m_{tot} = 0.32$ agree well with $(\pi - 2) / \pi = 0.363$ and $1 / \pi = 0.318$; despite the non-relativistic approach, this agreement supports the idea that the energy gain ε_w due to the charge system accounts for the creation of its own mass plus a further neutral particle as well. The experimental energies support the idea that contracting λ_w from $2\pi r_{em}$ down to $2\pi r_{em} / n_w$ implies the chance of a new form of interaction correlated to and coexisting with the familiar electromagnetic interaction at increasing values of the quantum number n_w .

Let us put now

$$m' c^2 \approx \frac{\hbar}{\Delta t_w} \quad (46)$$

being Δt_w the characteristic lifetime of the vector bosons.

This result is reasonable, as m' is proportional to the characteristic energy $\hbar / \Delta t_w$. To calculate this expression, let us also assume $m' \propto \Delta t_w$: as any process in nature requires a

definite time to be completed, it is natural to expect that the amount of mass creatable during the fluctuation of \mathbf{J}_w is proportional to the time length of this fluctuation. In other words: the longer the fluctuation, the greater the transient amount of energy and thus of mass that can be created. Putting then $m' = k_w \Delta t_w$, where k_w is an appropriate proportionality constant, there are two chances: either $k_w \approx 1$ or $k_w \neq 1$. In general the latter chance means that some physical effect is still hidden in k_w , whereas the former chance means that in fact k_w accounts for the concerned physical correlation without need of further considerations. Let us guess that $k_w \approx 1$ effectively represents the fluctuation lifetime; then, replacing into the Eq. (46), one finds

$$k_w(c\Delta t_w)^2 = \hbar, \quad k_w \approx 1\text{g/s}, \quad (47)$$

which yields $\Delta t_w \approx 10^{-24}\text{s}$. Note that the second Eqs. (45) reads $m_{\pm}c^2 = \hbar\alpha c/\lambda_w$, which suggests that αc is the actual displacement rate of the charged vector bosons having energy $\hbar\nu/\lambda_w$ and that the same holds for the neutral boson. Assuming therefore that $v = \alpha c$ is the actual displacement rate of the massive bosons, the characteristic range of this interaction should be of the order of $\Delta x_w \approx \alpha c\Delta t_w = 2 \times 10^{-16}\text{cm}$, whereas $\hbar c/\Delta x_w \approx 0.15\text{erg} = 98\text{GeV}$ in agreement with the Eq. (43) previously found.

In conclusion we have introduced three particles of comparable mass, of the order of 90 GeV, two of which with opposite charges and the third neutral, that propagate the interaction within the sub-nuclear space range Δx_w during a characteristic time range Δt_w . These results are the fingerprint of the weak interaction, which has been inferred as a generalization of the Maxwell equations inherent the homogeneous diffusion equation (30) via the transient fluctuation term $\mathbf{J}_w(t)$ appearing in the more general Eq. (29). So this kind of interaction differs in principle from, but it is strictly related to, the electromagnetic interactions of the Maxwell equations; it is simply an extension of these latter to the transient formation of three further short range carriers consistent with the time flux function \mathbf{J}_w additional to the electric and magnetic fields described by \mathbf{J}_2^* and \mathbf{J}_1^* , consequences themselves of the early Fick diffusion equations. It is worth emphasizing once again that the existence of magnetic monopoles does not conflict with, rather comes directly from, all of these outcomes and their quantum origin.

4.3 The gravity force

Exploit the dimensional relationship

$$\pm \mathbf{J} \cdot \mathbf{v} = \frac{|\mathbf{F}|}{\text{surface}}; \quad (48)$$

of course \mathbf{v} is the rate with which propagate the carriers of the force \mathbf{F} at right hand side and \mathbf{J} their flux. The double sign takes into account either chance of sign in principle possible at left hand side, being the modulus of force positive by

definition. The gravitons are acknowledged to be the carriers of the gravity force at the light speed; anyway, whatever the actual physical nature of these boson vectors and their displacement rate might specifically be, is enough for the present purposes to introduce a one-dimensional reference system R to which will be referred the scalars of the Eq. (48). This assumption on R is consistent with the chance of describing the gravitational interaction between two masses placed arbitrarily apart along one coordinate. Imposing this condition and thus introducing an arbitrary x -axis, write $|\mathbf{F}| = \xi F_x$: the x -component of \mathbf{F} has been related to its modulus $|\mathbf{F}|$ via the dimensionless proportionality factor ξ , which obviously is an unknown variable quantity. Moreover, being $J_x = \hbar/\Delta x^4$, it is possible to write in an analogous way $\mathbf{J} \cdot \mathbf{v} = \pm \zeta J_x v_x = \pm \zeta \hbar c/\Delta x^4$: once more the dimensionless proportionality factor ζ relating the scalar $\mathbf{J} \cdot \mathbf{v}$ to its arbitrary component $J_x v_x$ is an unknown variable quantity. In this way, whatever v_x and the interaction carriers might be, $J_x v_x$ can be expressed via ζ as a function of the constant quantity $\hbar c$. Of course, even *surface* reduces to Δx^2 in R . These positions are useful to rewrite the initial Eq. (48) as $\zeta \hbar c/\Delta x^4 = \pm \xi F_x/\Delta x^2$ and thus $\zeta m_o^2 G/\Delta x^4 = \pm \xi F_x/\Delta x^2$ in R , having put $\hbar c = Gm_o^2$ by dimensional reasons; this is surely possible by defining appropriately the value of the constant mass m_o . Yet the specific value of m_o is not essential: the term $m_o^2 \zeta/\xi$ yields indeed $m_1 m_2$, with $m_1 = m_o \zeta$ and $m_2 = m_o/\xi$ because of the arbitrary values of the proportionality factors ζ and ξ . In this way m_1 and m_2 are two arbitrary inputs defining F_x , which indeed owing to the Eq. (48) reads

$$F_x = \pm G \frac{m_1 m_2}{\Delta x^2}.$$

Note that the Δx^{-2} law could be directly inferred from the Eqs. (1), since in the present model the derivatives are defined as mere ratios of uncertainty ranges. Differentiating the Eqs. (1) at constant n yields $\delta \Delta p_x = -(n\hbar/\Delta x^2)\delta \Delta x$, then dividing both sides by $\delta \Delta t$ corresponding to $\delta \Delta x$ one finds $\delta \Delta p_x/\delta \Delta t = -n\hbar v_x/\Delta x^2$ with $v_x = \delta \Delta x/\delta \Delta t$: at left hand side appears the x -component of a force, at right hand side the concept of mass is hidden in the physical dimensions of the factor $\hbar v_x$, which reveals its physical meaning of space-time deformation rate of $\delta \Delta x$ during $\delta \Delta t$. Of course v_x is positive or negative depending on whether $\delta \Delta x$ represents expansion or contraction of Δx .

This short note aims to emphasize that in the present model the concept of gravity force is still linked to that of space-time deformation; yet the force also explicitly follows from the diffusion equations. In conclusion, taking the minus sign, we have found the Newton gravity law. Note however three remarks:

- (i) this result is not new, it has been inferred in different ways directly from the Eqs. (1) in [20, 23];
- (ii) here even the anti-gravity with the plus sign is allowed, as it has been repeatedly found elsewhere [22, 23];

(iii) the Newton law is actually an approximation of a more general gravity law, as found previously when concerning $\mathbf{F} \approx m\mathbf{a}$.

In fact one could guess an expression of *surface* like $\Delta x'^2 = \Delta x^2(1 + a_1 \Delta x_o/\Delta x + a_2(\Delta x_o/\Delta x)^2 + \dots)$; the series expansion is dimensionally compatible with the Eq. (48) and reduces to Δx^2 previously considered for $\Delta x \rightarrow \infty$ only, i.e. for weak gravity fields at large distances between the masses. This expansion defines a more general scalar component $\zeta J'_x v_x = \pm \xi F'_x/\Delta x'^2$ defining a more complex force component $\pm F'_x$ that coincides, as a particular case, with that F_x previously found simply putting equal to zero the higher order coefficients $a_{j \geq 1}$ of the series expansion. Note that $F_x \rightarrow 0$ for $\Delta x \rightarrow \infty$. The present choice to express the series expansions of *surface* has been purposely assumed in order that even the non-Newtonian $F'_x \rightarrow 0$ satisfies the same condition of the Newtonian F_x .

4.4 The strong interaction

The starting point and the subsequent reasoning are still that of the subsection 4.3. Note however that the dimensional equation (48) does not compel defining *force* as purposely done before; as a subtle and possible alternative, nothing hinders defining in the one dimensional R the right hand side as

$$\pm \mathbf{J} \cdot \mathbf{v} = \frac{|\mathbf{F}|}{\Delta x^2} + \frac{\text{energy}}{\Delta x^3}. \quad (49)$$

Proceeding as before, we merge again $\mathbf{J} \cdot \mathbf{v}$ with the concerned force per unit surface at the right hand side of the Eq. (48); one finds $\pm \xi \hbar c/\Delta x^4 = F_x/\Delta x^2 + \varepsilon_o/\Delta x^3$ i.e. $F_x = \pm \xi \hbar c/\Delta x^2 - \varepsilon_o/\Delta x$, where ε_o is a constant. This force component is derivable from a potential energy U having the form

$$U = \pm \frac{\xi \hbar c}{\Delta x} + \varepsilon_o \log(\Delta x/\Delta x_o), \quad (50)$$

which in turn, putting $\Delta x = \Delta x_o \pm \delta x$, reads

$$U \approx \pm \left(\frac{a}{\Delta x} \pm b \delta x \right), \quad \Delta x = \Delta x_o \pm \delta x, \\ a = \xi \hbar c, \quad b = \frac{\varepsilon_o}{\Delta x_o}, \quad \frac{\delta x}{\Delta x_o} \ll 1. \quad (51)$$

This is certainly possible because, being both Δx and Δx_o arbitrary, the necessary inequality can be actually verified at short distances $\Delta x \gtrsim \Delta x_o$ or $\Delta x \lesssim \Delta x_o$. This result with the minus sign at right hand side reads

$$U \approx -\frac{a}{\Delta x} + b \delta x,$$

i.e. it leads to the sought interaction energy of interest here.

It is however also interesting to note that attractive and repulsive strong forces are in principle allowed in this model.

The physical dimensions of the constants a and b are *energy* \times *length* and *energy/length*, so that $ab = \text{energy}^2$ and

$a/b = \text{length}^2$: write then $\hbar/\sqrt{ab} = \Delta t_s$ whence $\hbar c/\sqrt{ab} = \lambda_s = c\Delta t_s$. The chance of introducing the characteristic range λ_s directly via c agrees with the idea of massless vector bosons mediating this kind of interaction, which follows in turn from the lack of a compelling motivation to introduce a slower velocity of heavy particles. Thus, putting reasonably $\lambda_s = \sqrt{a/b}$ too, one finds

$$a = \hbar c, \quad \xi = 1, \quad (52)$$

i.e. a sensible value of the proportionality constant ξ . Moreover holds also now the reasoning previously introduced about the proportionality between mass and characteristic lifetime of particles mediating the interaction. Let us repeat therefore an identical approach, concerning however the energy of the messengers instead of their mass to rewrite the proportionality condition $m \propto \Delta t$ as $\sqrt{ab}/c^2 \propto \Delta t_s$; introducing once more a proportionality constant k one finds $\sqrt{ab} = kc^2\Delta t_s$, which reads in turn $\sqrt{ab} = kc^2\hbar/\sqrt{ab}$ so that $ab = k\hbar c^2$. Hence, owing to the Eq. (52),

$$b = kc, \quad k \approx 1\text{g/s}. \quad (53)$$

The last position, coherent with that of the Eq. (47), is justified by the same hint of the previous section about the physical meaning of any proportionality constant correlating two physical amounts. The values of these constants are therefore

$$a = 3 \times 10^{-17} \text{erg cm} = 0.2 \text{ GeV fm}, \\ b \approx 10^{10} \text{dyn} = 10^5 \text{N}. \quad (54)$$

These figures yield therefore the characteristic length Δx_o defined by $a/\Delta x_o = b\Delta x_o$ and the characteristic interaction time as a function of the characteristic energy \sqrt{ab} ; one obtains

$$\Delta x_o = \sqrt{a/b} \approx 10^{-13} \text{cm}, \quad \Delta t_s = \hbar/\sqrt{ab} \approx 10^{-24} \text{s},$$

$$\sqrt{ab} = \sqrt{k\hbar c^2} \approx 10^{-3} \text{erg} = 0.6 \text{GeV}.$$

Note that $a/\Delta x$ reads $\hbar c/\Delta x_o = \alpha^{-1} e^2/\Delta x_o$, i.e. the strength of this kind of interaction is α^{-1} times greater than that of the electromagnetic interaction. The form of U in the Eq. (51) and these figures are fingerprints of the strong interaction.

5 Connection between gravity and electromagnetism

Note that in the cgs system (*charge/mass*)² has physical dimensions l^3/m^2 , i.e. the same as the gravity constant. Yet, what has to do the electromagnetism with the gravity force? The possible answer relies just on the hint suggested by the question itself, i.e. the link between $(e/m_G)^2$ and G . It is interesting the possibility of specifying m_G directly as follows

$$G = \frac{\hbar c}{m_G^2} = \frac{1}{\alpha} \left(\frac{e}{m_G} \right)^2,$$

which defines $m_G = 2.2 \times 10^{-5} \text{g}$ as a function of the value of G assumed known; moreover, introducing m_G via its reduced Compton length λ_G , one finds

$$G = \frac{1}{\alpha} \left(\frac{e\lambda_G c}{\hbar} \right)^2 = \frac{e}{\alpha} \frac{e}{m_G^2}, \quad \lambda_G = \frac{\hbar}{m_G c}. \quad (55)$$

It is interesting the fact that the gravity constant is linked: (i) to the electromagnetism via the electric charge, (ii) to the relativity via c and (iii) to the quantum theory via \hbar ; also, λ_G results to be of the order of the Planck length. However we acknowledge gravity and electromagnetism as two separate forces despite their common origin from the diffusion equations, whence the question: how and why does actually the nature split the electromagnetic and gravity forces? The starting point to answer this question is the Newton law itself previously found. Rewrite first the Newton law with the help of the Eq. (55) as

$$F = G \frac{m_1 m_2}{\Delta x^2} = \frac{e}{\alpha} \frac{e}{\Delta x^2} \frac{m_1}{m_G} \frac{m_2}{m_G}. \quad (56)$$

The only term of the second equality that does not depend neither upon Δx nor upon m_1 and m_2 is e/α . Let us split therefore this equation via a proportionality constant k as follows

$$G = k \frac{e}{\alpha}, \quad \frac{m_1 m_2}{\Delta x^2} = \frac{F}{G} = \frac{1}{k} \frac{e}{\Delta x^2} \frac{m_1}{m_G} \frac{m_2}{m_G}. \quad (57)$$

Note now that the masses m_1 and m_2 appear in this equation as dimensionless ratios m_1/m_G and m_2/m_G ; these pure numbers yield therefore

$$\begin{aligned} \frac{F}{G} &= \frac{r_2}{k} \frac{Q_{e1}}{\Delta x^2} = \frac{1}{\alpha G} \frac{Q_{e2} Q_{e1}}{\Delta x^2}, & Q_{e1} &= r_1 e, & Q_{e2} &= r_2 e, \\ \frac{m_1}{m_G} &= r_1, & \frac{m_2}{m_G} &= r_2. \end{aligned} \quad (58)$$

In practice we have eliminated the concept of mass from the right hand side of F : the arbitrary variable r_1 , which depends on the arbitrary value of m_1 , converts the fixed charge e of the second equation (57) into the arbitrary total charge Q_{e1} . The ratio r_2/k involves an arbitrary number r_2 and a factor k that is reasonably related to the measure units of the modulus $Q_{e1}/\Delta x^2$ of a new quantity we call electric field strength due to the charge Q_{e1} at a distance Δx : hold indeed for Q_{e2} the same considerations highlighted for Q_{e1} , i.e. Q_{e2} is an arbitrary charge in the field of Q_{e1} . In fact the first Eq. (58) turns into

$$F = \frac{Q_{e2} Q_{e1}}{\alpha \Delta x^2}. \quad (59)$$

From numerical and dimensional points of view, the factor α^{-1} is immaterial: since both Q_{e1} and Q_{e2} are arbitrary, one could identically write F as $Q'_{e2} Q_{e1}/\Delta x^2$ with $Q'_{e2} = Q_{e2}/\alpha$ without loss of generality. Conceptually, however, α^{-1} replaces in fact G : the latter describes the interaction between

m_1 and m_2 , the former that between Q_{e1} and Q_{e2} . This also shows that the analogous analytical form of the Coulomb and Newton laws is not at all accidental, as already shown in [23]. It is clear that the key step of this conclusion is the position $G = k(e/\alpha)$ of the Eq. (57). It is instructive to calculate e/α and compare it with the experimental values of G in the cgs and SI systems

$$G = 6.68 \times 10^{-8} \text{cm}^3 \text{g}^{-1} \text{s}^{-2} = 6.68 \times 10^{-11} \text{m}^3 \text{Kg}^{-1} \text{s}^{-2};$$

while being

$$e_{cgs} = 4.8 \times 10^{-10} \text{esu}, \quad e_{SI} = -1.6 \times 10^{-19} \text{C}.$$

One finds

$$k_{cgs} \frac{e_{cgs}}{\alpha} = k_{cgs} 6.6 \times 10^{-8} \text{cm}^3 \text{g}^{-1} \text{s}^{-2},$$

$$k_{SI} \frac{e_{SI}}{\alpha} = k_{SI} 2.1 \times 10^{-12} \text{m}^3 \text{Kg}^{-1} \text{s}^{-2}.$$

Of course $k_{SI} \neq k_{cgs}$ for two reasons: (i) because of the different measure units and (ii) because in the cgs system the charge is directly defined via the electric force, in the SI the charge is defined in an independent way via the Ampere; thus k_{SI} requires an additional multiplicative factor k_0 to match G calculated simply changing the mass and length units of the proportionality constants k_{cgs} and k_{SI} . As the physical dimensions of k_{cgs} are $(\text{length}/\text{mass})^{3/2}/\text{time}$, one expects $k_{SI} = (10^{3/2} k_{cgs}) k_0$; the factor in parenthesis accounts for the different metric units only. Hence

$$G = k_{cgs} 6.6 \times 10^{-8} \text{cm}^3 \text{g}^{-1} \text{s}^{-2},$$

$$G = k_{cgs} k_0 6.6 \times 10^{-11} \text{m}^3 \text{Kg}^{-1} \text{s}^{-2}. \quad (60)$$

This result clearly shows that the actual value of the gravity constant is well described by the dimensionless proportionality constant $k_{cgs} \approx 1$ and that $k_{cgs} k_0 \approx 1$ is also true; actually $k_0 \approx 1$ is not surprising, it is consequence of having implemented e_{SI} by including the Coulomb factor in the second Eq. (60). As repeatedly stated, a proportionality factor of the order of the unity shows that the correlation between two quantities is physically correct; no hidden effect is to be expected. What is significant is that the dimensionless values $k_{cgs} \approx 1$ and $k_0 \approx 1$ fit the experimental values of G in both systems.

To conclude this section, it is worth noticing that the value of G had been correctly calculated in several ways as a function of the fundamental constants of nature in the previous paper [20]; moreover more details about the connection between gravity and electric forces have been emphasized in a recent paper [23].

6 Discussion

The idea of linking the diffusion laws to the fundamental interactions was suggested by their generality and by the various implications inherent their basic concepts. Regarding the formulae of the section 2 as strictly related to the mere displacement of chemical elements, thus with outcomes pertinent to the solid state physics only, is certainly reductive. Actually some concepts can be extrapolated beyond the plain domain of the materials science, e.g. as they concern even the fields. This aspect, evidenced by the first and last Eqs. (4), has been emphasized considering for instance that the heat transfer Fourier law has formal physical analogy with the displacement of matter [14]. The connection with the fundamental interactions appears thus natural once acknowledging that these latter consist of the exchange of messenger particles, the vector bosons, that propagate throughout the space-time.

Follow the idea that any body of matter is surrounded by a cloud of bosons randomly flowing towards another body with which it interacts, and that in general both bodies are moving by effect of the interaction itself; consequently transients of local concentration gradients of these carriers throughout the space-time are also allowed to form. If so, the ability of the carriers to mediate the pertinent interaction reduces basically to the diffusion laws governing the displacement of clusters of these carriers. It has been evidenced that the concept of particle flux is crucial in finding the correlation between density gradient of the carriers and strength and kind of interaction; as the flux related to the concept of diffusion concerns intrinsically a non-equilibrium situation, even the interactions fit the idea of dynamical universe evolving towards a thermodynamic steady state.

Obviously the results introduced here are not exhaustive in describing themselves all features of the fundamental forces of the nature; this detailed investigation about each form of interactions is not the actual purpose of the model, which instead aims merely to identify their common root only by merging diffusion laws and quantum uncertainty only. On the one hand, the present conclusions must be regarded having already in mind also previous results, obtained starting directly from the Eqs. (1) to explain the significant features of the various interactions [15]. On the other hand, the fact that the same results are also obtainable via the diffusion laws is informative of the physical mechanism upon which these latter rely: otherwise stated, all interactions are consequences of the second law, i.e. the vector bosons transfer the interaction moving likewise chemical elements of a non-equilibrium thermodynamic system to increase the global internal entropy of the system. Are significant in this respect the considerations of the section 3. A further implication of the present model relies on the possibility of demonstrating that the magnetic monopoles can in fact exist, being compatible with the basic ideas from which the interactions are inferred: at the present stage of development, the model does not prospect

any reason to reject their existence. The isotropy of the space-time is essential to introduce the pertinent diffusion coefficient as a numerical value D without requiring instead a tensor matrix; even without excluding that actually this position could be an oversimplification only, the results indicate that the assumption is acceptable at least at the present level of development of the model. Moreover no necessity of extra-dimensions appears in this context, which however does not exclude that these latter might actually exist.

A short remark is useful to explain why the diffusion equations are the key to infer contextually and in a surprisingly simple way the basic aspects of the fundamental interactions. A partial answer is that the concept of uncertainty does not require hypotheses or information about the kind of diffusion medium, kind of vector bosons and strength and range of the interactions; as the Eqs. (1) have a primary significance regardless of any ancillary information, their consequences are expected to match different kinds of interaction just because of their generality. Yet a more comprehensive answer is that the quantum Eqs. (1) are inherently consistent with the general relativity [17], so any reasoning based on these equations leads consequently to relativistic conclusions as well; this explains why some valuable relativistic implications have been contextually found as side outcomes throughout the paper. Previous and present results demonstrate the validity of the theoretical model where uncertainty ranges replace the local values of the dynamical variables; ignoring these latter means accepting that the former only have true physical meaning. On the one hand, it is worth recalling the key role of the arbitrary boundaries of the uncertainty ranges to demonstrate that the quantum origin of the Maxwell equations and related consequences, e.g. the Gauss theorem and the Faraday law, rely on the concept of space-time ranges: \mathbf{E} and \mathbf{H} were contextually introduced implementing just both boundaries of ranges to express via the Eqs. (1) the flux of vector bosons that mediate the electromagnetic interaction between charged particles. On the other hand, the most interesting aspect of the formalism based on ranges concerns its conceptual meaning that merges quantum theory and relativity: so the usefulness of the results presently achievable is not the only support to their validity.

In the wave mechanics the dynamical variables of the classical formulae are replaced by operators that constitute the wave equations, whose solutions provides the eigenvalues of the observables; in the present model the dynamical variables are replaced by the respective uncertainty ranges, the eigenvalues are inferred by elementary manipulations of the classical formulae while the quantization is introduced via n . The present model reverts thus fundamental inputs and outcomes of the standard wave mechanics: the uncertainty is no longer consequence of the commutation rules of postulated quantum operators, it becomes instead the fundamental statement as a function of which the operator formalism is inferred by consequence of the range formalism. Several papers, e.g.

[18, 19] show that this way of thinking is a valid alternative to the standard wave mechanics: the expressions of the eigenvalues are identical in all cases where the wave equations can be solved analytically without the need of numerical procedures. The intriguing advantage of the present approach is thus that it not only agrees with the wave formalism, in fact inferable as a corollary so that the present model is in principle compliant with any quantum results today known, but contextually implies even the conceptual foundations of the special and general relativity [17]; so are not surprising the chance of having obtained the Eq. (19) and recognized the approximate character of the Newton law $\mathbf{F} \approx m\mathbf{a}$, preliminarily obtainable as in the Eq. (20), without the relativistic correction involving the space-time deformation in the presence of mass.

The quantum space-time uncertainty has profound implications in relativity, whose formulae result indeed expressed themselves via uncertainty ranges; although the formulae are seemingly identical, however their physical meaning is definitely different. E.g., it has been emphasized that the Eq. (2) entails the functional dependence $p_x = v_x \varepsilon / c^2$ of the local dynamical variables: the latter equation is well known, the former seems a redundant and pretextuous attempt to rewrite the standard relativistic result. Yet just in this way, introducing ranges that replace local variables, the relativity is made compliant with the quantum theory. The local dynamical variables are incompatible with the Heisenberg principle, the uncertainty ranges do by definition; so the usual formulae of the standard relativity are mere classical limit cases of range sizes tending to zero, in agreement with the classical character of the relativity itself.

In short, the present paper is a further contribution confirming that the Eqs. (1) represent the common root underlying quantum theory and relativity.

7 Conclusion

The necessity of skipping a detailed analysis about the specific features of all forms of interaction, outside of the scope of this paper, ranks the significance of the essential outcomes provided by the model; the value of results already known relies on the fact of being obtained contextually in the frame of a unique idea, which emphasizes the validity of the theoretical basis so far implemented. The approach proposed here suggests that an appropriate basic assumption about the displacement mechanism of the vector bosons has priority importance with respect to the detailed speculation about the single interactions themselves; moreover the scalar $\mathbf{J} \cdot \mathbf{v}$ was proven effective as a common basis to infer distinguishing information even without introducing explicit hypotheses on the pertinent vector bosons. The analytical form of the gravity force was inferred waiving the specific nature of the gravitons; the well known form (51) of the strong force has been inferred waiving the features of the gluons and their property of ex-

changing the colour force between quarks, whereas the electromagnetic interaction was found related to the photons as a particular case of a more general electro-weak interaction involving massive vector bosons. The weak interaction only required considering explicitly the displacement velocity of the carriers, which cannot travel at the light speed as their masses affect the characteristic space range and lifetime. Yet the basic features of all interactions depend primarily on the diffusion like behaviour of vector bosons described case by case through the form of the respective scalars $\mathbf{J} \cdot \mathbf{v}$. Although such theoretical approach is seemingly classical, indeed the section 2 exploits standard vector calculus, relativistic implications are anyway evident and occasionally even unexpected; this is because the Eqs. (1) contain an obvious quantum character that however encloses also relativistic implications, which therefore appear by consequence while implementing them. Considering the quantum origin of the diffusion laws, it is not surprising that the implications of the model are general enough to span not only the solid state physics but also the fundamental interaction physics.

Submitted on February 11, 2015 / Accepted on February 14, 2015

References

- Weinberg S. *Dreams of a Final Theory*. Vintage Books, London, 1993.
- Davies P. *The Forces of Nature*. Cambridge Univ. Press 2nd ed., 1996.
- Braybant S., Giacomelli G., Spurio M. *Particles and Fundamental Interactions. An Introduction to Particle Physics*. Springer, Dordrecht, 2012.
- Bjorken J.D., Drell S.D. *Relativistic Quantum Mechanics*. New York, McGraw-Hill, 1964.
- Abers E.S., Lee B.W. Gauge theories. *Physics Reports*, 1973, v. 9, 1–141.
- Feynman R.P., Weinberg S. *Elementary Particles and the Laws of Physics*. Cambridge University Press, Cambridge, 1987.
- Baak M. The Electroweak Fit of the Standard Model after the Discovery of a New Boson at the LHC. *The European Physical Journal C*, 2012, v. 72, no. 11, 1–2.
- Kaku M. *Introduction to Superstring and M-Theory*. 2nd ed., Springer-Verlag, New York, USA, 1999.
- Narlikar J.V. and Padnababhand T. *Gravity, Gauge Theories and Cosmology*. Reidel Publishing Company, Dordrecht, Holland, 1986.
- Weinberg S. Quantum contribution to cosmological correlation. *Phys. Rev. D*, 2005, Vol 72, 4, 43514–43533.
- Ross G. *Grand Unified Theories*. Westview Press, 1984.
- Buras A.J., Ellis J., Gaillard M.K., Nanopoulos D.V. Aspects of the grand unification of strong, weak and electromagnetic interactions. *Nuclear Physics B*, 1978, v. 135(1), 66–92.
- Wilczek F. Quantum field theory. *Reviews of Modern Physics*, 1999, v. 71, S83–S95.
- Tosto S. Fundamentals of diffusion for optimized applications. *EAI*, 2012, no. 4–5, part 1, 94–107.
- Tosto S. Quantum uncertainty and fundamental interactions. *Progress in Physics*, 2013, v. 2, 56–81.
- Tosto S. Quantum Uncertainty and Relativity. *Progress in Physics*, 2012, v. 2, 58–81.
- Tosto S. Quantum Uncertainty, Relativity and Cosmology. *International Journal of Physics and Astronomy*, 2014, v. 27, Issue 1, 1136–1157.

18. Tosto S. An analysis of the states in the phase space: the energy levels of quantum systems. *Il Nuovo Cimento B*, 1996, v. 111, no. 2, 193–215.
 19. Tosto S. An analysis of the states in the phase space: the diatomic molecules. *Il Nuovo Cimento D*, 1996, v. 18, 1363–1394.
 20. Tosto S. An analysis of states in the phase space: from quantum uncertainty to general relativity. arXiv gr-qc/0807.1011
 21. Job G., Hermann F. Chemical potential - a quantity in search of recognition. *European Journal of Physics*, 2006, v. 27, 353–371.
 22. Tosto S. Quantum standpoint for a more understandable universe. *American Journal of Space Science*, 2013, v. 1(1), 22–32.
 23. Tosto S. Quantum approach to the gravitational waves. *Physics International*, 2013, v. 4(2), 135–151
-

Scaling of Moon Masses and Orbital Periods in the Systems of Saturn, Jupiter and Uranus

Hartmut Müller

Advanced Natural Research Institute in memoriam Leonhard Euler, Munich, Germany
E-mail: admin@anr-institute.com

The paper shows, that the sequence of sorted by value masses of the largest moons in the systems of Saturn, Jupiter and Uranus is connected by constant scaling exponents with the sequence of their sorted by value orbital periods.

1 Introduction

In [1] we have shown, that the connection between the body mass distribution and the distribution of orbital periods of planets and planetoids in the Solar System can be described by the scaling law:

$$M = \mu \cdot T^D, \quad (1)$$

where M is a celestial body mass, T is a celestial body orbital period and μ and D are constants. We have shown, that for sorted by value couples of a body mass M and an orbital period T the exponent D is quite constant and is closed to the model value $3/2$. Furthermore, for M in units of the proton rest mass $m_p \approx 1.67 \times 10^{-27}$ kg [2] and T in units of the proton oscillation period $\tau_p = \hbar/m_p c^2 \approx 7.02 \times 10^{-25}$ s, the constant $\mu = 1$.

In this paper we will show, that the scaling law (1) describes also the distribution of masses and orbital periods in the moon systems of Saturn, Jupiter and Uranus.

2 Methods

In [3] we have shown that the scaling exponent $3/2$ arises as consequence of natural oscillations in chain systems of harmonic oscillators.

Within our fractal model [4] of matter as a chain system of oscillating protons and under the consideration of quantum oscillations as model mechanism of mass generation [5], we interpret the exponent D in (1) as a Hausdorff [6] fractal dimension of similarity (2):

$$D = \frac{\ln M/m_p}{\ln T/\tau_p}. \quad (2)$$

The ratio M/m_p is the number of model protons, the ratio T/τ_p is the number of model proton oscillation cycles.

Already in the eighties the scaling exponent $3/2$ was found in the distribution of particle masses [7]. Possibly, the model approximation of $D \approx 3/2$ and $\mu = 1$ in (1) for proton units is a macroscopic quantum physical property, which is based on the baryon nature of normal matter, because $\mu = 1$ means that:

$$M/T^D = m_p/\tau_p^D \quad (3)$$

In [1] we have shown, that for planets and the most massive planetoids the average empiric value $D \approx 1.527$ is a little bit

larger than the model value $3/2$. If we interpret the deviation of the empiric value $D \approx 1.527$ in comparison with the model value $3/2$ as a consequence of the fractality of the mass distribution in the system, then we can represent (1) in the form:

$$M^\Delta/T^2 = 1 \quad (4)$$

where $\Delta = 2/D$ is the fractal dimension of the mass distribution, the constant of proportionality is 1 for proton units m_p and τ_p . The model value of Δ is $2/(3/2) = 4/3$.

3 Results

The tables 1-3 contain properties of the largest moons of the Saturn, Jupiter and Uranus systems. Always on the left side the moons are sorted by their masses, on the right side the moons are sorted by their orbital periods. The tables show, that within each moon system the fractal dimension Δ (4) is quite constant, but different from the average empiric value $\Delta = 2/D = 2/1.527 \approx 1.31$ for planets and planetoids [1]. This fact we interpret as criterion of different levels of fractality of the mass distribution in these systems. Furthermore, the tables show, that for the systems of Saturn and Uranus the fractal dimension Δ is nearly of the same average value, which is quite different of Δ for the system of Jupiter.

4 Resume

Within our fractal model [8], the scaling law (4) arises in chain systems of many harmonic oscillators and can be understood as fractal equivalent of the Hooke law. The scaling law (4) is valid for sorted by value couples of system properties. The Saturn system shows, that the scaling law (4) can be valid for one and the same body. The Jupiter and Uranus systems shows, that the scaling law (4) can be valid also for couples of different bodies. This may mean, that in general, the orbital period of each body does not depend only on its own mass, but depends on the body mass distribution in the system.

5 Acknowledgements

I'm thankful to my friend Victor Panchelyuga, my son Erwin and my partner Leili for the great experience to work with them, for the deep discussions and permanent support.

Submitted on February 15, 2015 / Accepted on February 17, 2015

Saturn moons, sorted by M	Body mass M , kg	$\ln(M/m_p)$	Δ	$\ln(T/\tau_p)$	Orbital period T , years	Saturn moons sorted by T
Mimas	3.7493×10^{19}	106.7277	1.2541	66.9235	0.9420	Mimas
Enceladus	1.0802×10^{20}	107.7858	1.2487	67.2983	1.3702	Enceladus
Tethys	6.1745×10^{20}	109.5291	1.2347	67.6187	1.8878	Tethys
Dione	1.0955×10^{21}	110.1024	1.2350	67.9901	2.7369	Dione
Iapetus	1.8056×10^{21}	110.6022	1.2385	68.4914	4.5182	Rhea
Rhea	2.3065×10^{21}	110.8470	1.2585	69.7524	15.9450	Titan
Titan	1.3452×10^{23}	114.9130	1.2419	71.3568	79.3215	Iapetus

Table 1: For sorted by value couples of a body mass M and an orbital period T the fractal dimension $\Delta(4)$ is quite constant within the Saturn moon system. The Saturn moon system average $\Delta = 1.2445$. Data comes from [9].

Jupiter moons, sorted by M	Body mass M , kg	$\ln(M/m_p)$	Δ	$\ln(T/\tau_p)$	Orbital period T , years	Jupiter moons sorted by T
Europa	4.7998×10^{22}	113.8824	1.1864	67.5538	1.7691	Io
Io	8.9319×10^{22}	114.5035	1.1921	68.2506	3.5512	Europa
Callisto	1.0759×10^{23}	114.6896	1.2024	68.9510	7.1546	Ganymede
Ganymede	1.4819×10^{23}	115.0098	1.2138	69.7980	16.6890	Callisto

Table 2: For sorted by value couples of a body mass M and an orbital period T the fractal dimension $\Delta(4)$ is quite constant within the Jupiter moon system. The Jupiter moon system average $\Delta = 1.1987$. Data comes from [12].

Uranus moons, sorted by M	Body mass M , kg	$\ln(M/m_p)$	Δ	$\ln(T/\tau_p)$	Orbital period T , years	Uranus moons sorted by T
Miranda	6.5900×10^{19}	107.2916	1.2551	67.3294	1.4135	Miranda
Umbriel	1.1720×10^{21}	110.1700	1.2328	67.9076	2.5200	Ariel
Ariel	1.3530×10^{21}	110.3136	1.2402	68.4050	4.1440	Umbriel
Oberon	3.0140×10^{21}	111.1145	1.2446	69.1473	8.7062	Titania
Titania	3.5270×10^{21}	111.2717	1.2507	69.5833	13.4632	Oberon

Table 3: For sorted by value couples of a body mass M and an orbital period T the fractal dimension $\Delta(4)$ is quite constant within the Uranus moon system. The Uranus moon system average $\Delta = 1.2447$. Data comes from [10, 11].

References

- Müller H. Scaling of Body Masses and Orbital Periods in the Solar System. *Progress in Physics*, 2015, v. 2, 133–135.
- Physical constants. Particle Data Group. www.pdg.lbl.gov
- Müller H. Scaling Models of Natural Oscillations in Chain Systems and the Mass Distribution of Particles. *Progress in Physics*, 2010, v. 3, 61–66.
- Müller H. Scaling models of Natural Oscillations in Chain Systems and the Mass Distribution of the Celestial Bodies in the Solar System. *Progress in Physics*, 2010, v. 1, 62–66.
- Müller H. Emergence of Particle Masses in Fractal Scaling Models of Matter. *Progress in Physics*, 2012, v. 4, 44–47.
- Hausdorff F. Dimension und äußeres Maß, 1919, v. 79.
- Kolombet V. Macroscopic fluctuations, masses of particles and discrete space-time. *Biofizika*, 1992, v. 36, 492–499.
- Müller H. Fractal scaling models of Resonant Oscillations in Chain systems of Harmonic Oscillators. *Progress in Physics*, 2009, v. 2, 72–76.
- Bordi J., Jacobson R., Antreasian P. et al. The Gravity Field of the Saturnian System from Satellite Observations and Spacecraft Tracking Data. *Astronomical Journal*, 2006, v. 132, 2520–2526.
- Uranus System Nomenclature Table Of Contents. Gazetteer of Planetary Nomenclature. USGS Astrogeology, 2009.
- Taylor A., Synnott S., Jacobson R., Campbell J. The masses of Uranus and its major satellites from Voyager tracking data and Earth based Uranian satellite data. *Astronomical Journal*, 1992, v. 103, 2068–2078.
- Malhotra R., Showman A. The Galilean Satellites. *Science*, 1999, v. 286, 77–84.

Birkeland Currents: A Force-Free Field-Aligned Model

Donald E. Scott

Department of Electrical Engineering (Retired), University of Massachusetts, Amherst, MA, USA.
e-mail: dascott3@cox.net

The fundamental vector calculus definition of a force-free, field-aligned current in space is expanded in cylindrical coordinates to directly obtain the Bessel partial differential equation that specifies the magnetic field created by such a current. This result is often called the Lundquist solution. A simple but detailed derivation is included here. The physical properties of the resulting intricate magnetic field structure are described. The cause of its characteristic counter-rotation and counter-flows are identified. The describing equations are put into state-variable form and a step-wise approximation is applied. This solution reveals the primary effect of the force-free parameter, α , as being a scale factor of radial distance. We show that: 1) both the axial and azimuthal magnetic and current density components cyclically reverse their directions with radial distance from the central axis of the current; 2) the magnetic field extends farther from the central axis within a force-free field than it would if produced by a current in a long straight conductor. The total magnetic field magnitude and current density are shown to vary inversely as the square root of r . For large r , outside the plasma, the azimuthal magnetic field is shown to vary as $1/r$. These results are shown to be consistent with laboratory and astronomical observations.

1 Introduction

After Kristian Birkeland [1] (1867-1917) suggested in 1908 that Earth's auroras were powered by corpuscular rays emanating from the Sun that become deflected into Earth's polar regions by the geomagnetic field, the existence of such magnetic field-aligned currents was strongly disputed based partially on the idea that currents could not cross the presumed "vacuum" of space [2, p. 181]. Birkeland's main problem, however, was that having made detailed measurements of Earth's geomagnetic field on the ground, he then wanted to extrapolate that knowledge into a description of the current-density distribution that caused those magnetic effects. This is not possible because a given magnetic field value can be produced by more than one distribution of current-density.

A level of interest did, however, develop regarding the Sun's photosphere and plasma properties of the solar corona. For example, a mathematical model of a force-free magnetic field was proposed as early as 1950 by Lundquist [3, 4]. He investigated whether magnetic fields could exist in an electrically conducting liquid and his results included presentation of the now well-known Bessel solution for force-free fields. Later in 1957, investigators such as Chandrasekhar and Kendall [5] applied a similar analysis to the spherical geometry of the Sun.

NASA scientists and many other investigators worked on Birkeland currents and flux rope observations since the mid-to-late 1960's [6–18], with substantial activity on this topic after the late 1980's [19–24]. A few researchers have sought cylindrical coordinate solutions [25] but almost always in reference to intricate quasi-cylindrical solar surface or coronal applications. Potemra [24] concluded that Birkeland currents and Alfvén waves are fundamental to an understanding of

the Earth's plasma environment. It is now generally assumed that magnetic fields inside interplanetary magnetic clouds and flux ropes in the solar photosphere are force-free [26]. In 2009, space probe Themis discovered a flux rope pumping a 650,000 A current down into the arctic auroral region [27]. This strong observational evidence supports the existence of Birkeland Currents.

Consistent with this, the major goals of this paper are:

1. To present a simple, but complete derivation of Lundquist's equations that describe the magnetic field structure of a field-aligned current.
2. To fully describe the physical (not only magnetic, but also both the electrical and structural) consequences of those equations; to develop a model.
3. To demonstrate the correspondence between the properties of that model and observational evidence gathered from both plasma laboratories and astronomical images.

First we show that the basis of any model of a Birkeland current is what is called a force-free, field-aligned current.

2 Definition of a force-free field-aligned current

Consider a stream of moving charged particles (an electrical current) in a plasma that is not subject to any external forces. A useful mathematical idealization of such a physical cosmic current is a vector field of current density, \mathbf{j} , that, when viewed in a cylindrical coordinate system, creates an overall average current vector, \mathbf{I} , which, by definition determines the direction of the z -axis. The magnitude of \mathbf{I} is assumed to be everywhere independent of the z coordinate. The coordinate system defines a point, p , represented by (r, θ, z) , as illustrated in Figure 1.

The basic structure of such a cosmic magnetic field is controlled by the momentum equation of ideal magneto-hydrodynamics [25, 28–30],

$$(\nabla \times \mathbf{B}) \times \mathbf{B} = \mu_0 \nabla p \quad (1)$$

where μ_0 is the permeability of free-space.

The left hand side of this expression represents the compressive magnetic (Lorentz) force and the right side is the expansive force (pressure gradient multiplied by the permeability of the plasma). We distinguish between force-free fields with $\nabla p = 0$ and pressure balanced fields with $\nabla p \neq 0$. On the photosphere and within the lower chromosphere of the Sun the energy of the plasma motion dominates the magnetic energy and therefore the field is swept passively along with the plasma. This condition is characterized as a high- β plasma [31], where the parameter β is defined as the ratio between the plasma pressure p and the magnetic pressure,

$$\beta = 2\mu_0 \frac{p}{B^2}. \quad (2)$$

Higher up in the corona, in interplanetary and in cosmic space, a lower pressure (lower ion and electron densities), low- β plasma often exists depending on local field pressure. Here the plasma can take on a force-free character [6,32,33]. However, care must be exercised in assuming low- β properties. For example, “the extensive magnetosheath flow downstream of Earth’s bow shock is a high-beta plasma. Along a radial cut of the plasma coming inward from the Sun near the day-side sub-solar point, the solar wind and magnetosheath flow is high-beta, the magnetopause and immediate (thin) plasma boundary provides a high to low beta transition, and immediately within the low-latitude boundary layer (within the outer magnetosphere) plasma is low-beta. Then with lower radial distance the plasma again becomes high-beta.” [34]. We now present here a model that requires a low- β plasma environment.

The electromagnetic force experienced by each charge within such a plasma is given by,

$$\mathbf{F} = q(\mathbf{E} + \mathbf{v} \times \mathbf{B}). \quad (3)$$

The first term, $q\mathbf{E}$, is the *electric force* and the second term, $q(\mathbf{v} \times \mathbf{B})$, is called the *magnetic force*. The name *Lorentz force* is used to describe expression (3). The plasma region contains the cylindrical current stream. No initial assumptions are made about the distribution of the current density across the cross-section.

A flow of charge creates its own magnetic field through which the charge flows. The site at which each charged particle, q , in the stream is located is the point of origin of two local vectors: $\mathbf{j} = q\mathbf{v}$ (current density) and \mathbf{B} (magnetic field). The current density vector \mathbf{j} at each point inherently creates a $\text{curl}(\mathbf{B})$ vector given by Maxwell [35]:

$$\nabla \times \mathbf{B} = \mu \left(\mathbf{j} + \epsilon \frac{\partial \mathbf{E}}{\partial t} \right). \quad (4)$$

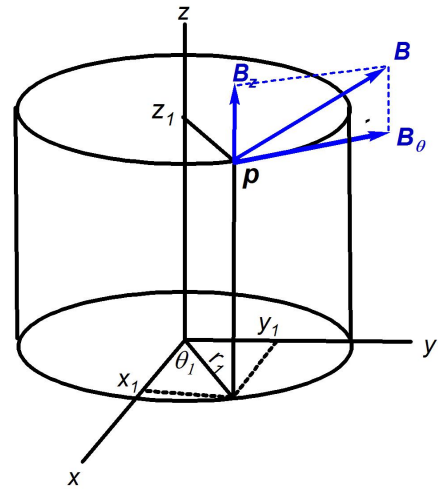


Fig. 1: Total magnetic field vector $\mathbf{B} = \mathbf{B}(r, \theta, z)$, and its two components B_z and B_θ at a particular location; $B_r = 0$. Note that at any point r , the pitch angle of the vector \mathbf{B} measured upward from the horizontal plane is defined as the arctan $[B_z(r) / B_\theta(r)]$.

The derivative term in (4) which was added by Maxwell is called the displacement current. It is often considered to be zero valued, as we do here, when it can be assumed there are no time-varying electric fields in the region. Integrating the $\text{curl}(\mathbf{B})$ vectors over a cross-section of the cylindrical stream (Stoke’s theorem) yields,

$$\int_S \nabla \times \mathbf{B} \cdot d\mathbf{S} = \int_S \mu \mathbf{j} \cdot d\mathbf{S} = \oint_C \mathbf{B} \cdot d\mathbf{l} \quad (5)$$

where S is any cross-section of the plasma, and μ and ϵ are the permeability and permittivity respectively of the plasma medium. The second term in (5) is equivalently $\mu \mathbf{I}$ where \mathbf{I} is the total current carried by the plasma. If the cross-section is circular with radius r , then the last term in (5) is $2\pi r \mathbf{B}$ where \mathbf{B} is in the azimuthal, θ , direction, not aligned with \mathbf{I} and the z -axis. Thus the \mathbf{B} field produced by a cylindrical plasma at its outer boundary, $r = R$, is

$$\mathbf{B}_\theta = \frac{\mu \mathbf{I}}{2\pi R}. \quad (6)$$

Expression (4) is the *point form* and (5) is the *integral (macroscopic) form* of that Maxwell equation. Expression (4) is valid at any point. The integral forms given in (5) and (6) imply that \mathbf{B} is a vector sum of the effects of all the \mathbf{j} vectors on the surface S that is enclosed by C . \mathbf{B} is not directly produced by any single \mathbf{j} . In (4) it is clear that \mathbf{j} , the current density at a point, creates only a single $\text{curl}(\mathbf{B})$ vector, not a \mathbf{B} vector. In general, there can be (and often is) a non-zero valued \mathbf{B} vector at points at which $\mathbf{j} = \mathbf{0}$.

Prior to the time a cosmic current system, free of externally applied forces or fields, reaches a steady-state config-

uration, the \mathbf{j} and \mathbf{B} vectors are interacting – all the \mathbf{j} 's are creating $\text{curl}(\mathbf{B})$ vectors that sum to form the local \mathbf{B} vectors. At any point in the plasma where $\mathbf{j} \neq \mathbf{0}$ a force can exist between that current density vector and its local magnetic \mathbf{B} -field vector. This force is a magnetic *Lorentz force* given by the second term in (3). This vector cross product of a moving charge's velocity vector \mathbf{v} and the local vector \mathbf{B} implies that the scalar value (magnitude) of the resulting Lorentz force on each q is given by,

$$F_L = qvB \sin \varphi \quad (7)$$

where φ is the smallest angle between the vectors \mathbf{v} and \mathbf{B} , with scalar values v and B . We call φ the Lorentz angle. If this angle is zero or 180 degrees, the magnetic Lorentz $\mathbf{v} \times \mathbf{B}$ force at that point is zero-valued.

The *magnetic intensity* (symbol \mathbf{H}) is often used to describe the macroscopic forcing function that creates a magnetic field,

$$\mathbf{H} = \frac{\mathbf{B}}{\mu} = \frac{N\mathbf{I}}{l}. \quad (8)$$

The dimensions of \mathbf{H} are A/m. (The number of turns, N , is dimensionless). \mathbf{H} has also been called the *magnetic field strength*, and the *magnetizing force*.

The scalar magnitude, B , in (8) arises from the integral form (5). In that expression, B is shown to be the result of the total current, I . It follows that H is not a point form variable.

It may be shown that the energy density, W_B (Joules/m³), stored in the magnetic field of such a current stream is given by,

$$W_B = \frac{\mu}{2} H^2. \quad (9)$$

Using (8) in (9), the total energy stored, ψ (Joules), in the magnetic field of a cosmic current is given by,

$$\psi = \frac{1}{2} \left(\frac{\mu N^2 A_c}{l} \right) I^2 \quad (10)$$

where A_c is the cross-sectional area and the *inductance* of the current stream is defined by the factor in parentheses. This shows that the only way to reduce the entire stored energy to zero is to completely cut off the current (set $I = 0$); in which case the entire cosmic current structure would cease to exist.

However, we assume that in unconstrained plasma in cosmic space, the current stream is free to move and distribute itself so as to minimize the internally stored potential energy due to the stresses resulting from magnetic Lorentz forces everywhere throughout the plasma. In fact space plasmas are uniquely situated to obey the *minimum total potential energy principle* [36], which asserts that a system or body shall deform or displace to a position and/or morphology that minimizes its total potential (stored) energy (a formalization of the idea that "water always flows downhill.").

The energy described in (10) is irreducible because it is caused by the fixed quantity, I . But the Lorentz energies can

be eliminated because they do not depend on the value of I , only on the cross-products between local \mathbf{B} and \mathbf{j} vectors.

If and when the process of shedding the internal magnetic-force energy reaches a steady-state equilibrium, this structure is called a *force-free current* and is defined by the relation between the magnetic field vector, \mathbf{B} , and the current density vector, \mathbf{j} , at every location at which a charge, q , exists in the current stream:

$$q(\mathbf{v} \times \mathbf{B}) = \mathbf{j} \times \mathbf{B} = 0. \quad (11)$$

It follows from (11) that the Lorentz forces are everywhere equal to zero in a force-free current because every \mathbf{j} is collinear with its corresponding \mathbf{B} . This arrangement is therefore also called a *field-aligned current* (FAC).

It follows directly from (4) and (11) that, if there is no time-varying electric field present, then (11) is equivalent to

$$(\nabla \times \mathbf{B}) \times \mathbf{B} = 0 \quad (12)$$

which is identical to (1) with $\nabla p = 0$. This is the basic defining property of a force-free, field-aligned current.

Expression (4) implies that, if at any point in an otherwise field-aligned current, $\mathbf{j} = \mathbf{0}$, (12) is automatically fulfilled even if \mathbf{B} is non-zero. The value of the magnitude and direction of \mathbf{B} at any given point is generally not sufficient information to determine the magnitude, direction, or even the existence of \mathbf{j} at that point. This is the problem that confronted Birkeland in his attempts to identify the currents responsible for the magnetic field variations he measured. However, from (4), knowledge of the direction and magnitude of the $\nabla \times \mathbf{B}$ vector at any given point does identically determine the value of $\mu\mathbf{j}$ there.

Field-aligned, force-free currents represent the lowest state of stored magnetic energy attainable in a cosmic current [31]. We seek an expression for the magnetic field, $\mathbf{B}(r, \theta, z)$, in such a current/field structure.

3 Quantitative model of a force-free field-aligned current

Equation (12) can be expanded into differential equation form using the cylindrical coordinate definition of curl and the 3-dimensional vector product determinant. However, this leads to an expression of little utility. Because (12) is satisfied if the current density, \mathbf{j} , has the same direction (except for sign) as \mathbf{B} (and with no requirements on its magnitude), it was suggested (Lundquist [3, 4] and many others) that,

$$\nabla \times \mathbf{B} = \alpha \mathbf{B} \quad (13)$$

which from (4) is equivalently,

$$\mu \mathbf{j} = \alpha \mathbf{B} \quad (14)$$

where α is any non-zero valued scalar, which is equivalent to (12). This leads to a simple solution, but it is important

to note that accepting (14) as a substitute for (12) assumes *a priori* that, for any non-zero α , a non-zero valued \mathbf{B} at any point requires the existence of a current density $\mathbf{j} \neq \mathbf{0}$ at that same point. This is in general, an unwarranted presumption. This is especially so in light of the well-known tendency of plasmas to form filaments (creating regions where $\mathbf{j} = \mathbf{0}$ but \mathbf{B} is not). There are many examples in the study of electromagnetism, such as: Given that, in otherwise empty space, a current, $I_x = +1$ A exists in a straight, infinitely long conductor lying along the x -axis, find the value of the resulting magnetic field vector, \mathbf{B} , at the point ($x = y = 0, z = 1$). The goal of this exercise is to find a value of \mathbf{B} at a point where \mathbf{j} is explicitly zero-valued. The answer is not zero.

However, most investigators start unhesitatingly with (13) and therefore (14) as givens. (This rules out applying the solution to a filamented plasma.) For example, Wiegelmann [37] does this and derives a vector Helmholtz equation which he states, can be solved by a separation *ansatz*, a Green's function method [8] or a Fourier method [18].

An *ansatz* is the establishment of the starting equation(s), the theorem(s), or the value(s) describing a mathematical or physical problem or solution. After an *ansatz* has been established (constituting nothing more than an assumption), the equations are solved for the general function of interest (constituting a confirmation of the assumption). That the mathematical solution accurately describes the physics is assumed.

In his 1950 paper Lundquist (after accepting the validity of (13)), without further explanation or derivation states that the solution of (14) with constant α is,

$$\begin{aligned} H_z &= A J_0(\alpha r) \\ H_\theta &= A J_1(\alpha r). \end{aligned} \quad (15)$$

Lundquist thus presents α as being a radial distance scale factor in the argument of his Bessel function solution. No evaluation of the coefficient A is offered. He also presents an image similar to Figure 6 below, but does not derive the current density or the physical consequences of these functions such as periodic reversals with increasing radius or counter-rotation and counter-flows of the plasma within the current structure.

Other investigators [45] start with (13) and then take its curl to obtain,

$$\begin{aligned} \nabla(\nabla \cdot \mathbf{B}) - \nabla^2 \mathbf{B} &= \alpha(\nabla \times \mathbf{B}) \\ \nabla^2 \mathbf{B} &= -\alpha(\nabla \times \mathbf{B}). \end{aligned} \quad (16)$$

They then also present the solution of (16) as being that given in (15). This agrees with Lundquist.

One of the most extensive reviews of force-free currents in a cylindrical geometry by Botha & Evangelidis [25] contains several references to similar studies. However, none of these investigators make the simplest assumptions: adopt a piece-wise linear approach, assume α to be any scalar value,

and assume no variation of \mathbf{j} or \mathbf{B} in either the azimuthal or axial directions. Such simplifications may not be justified on the solar surface, but are in deep space. Therefore, we derive here a simple solution that follows from this and carefully note the effect of the parameter α on the resulting model.

Before beginning this derivation, we specify the dimensions of several involved quantities. Using (8),

$$[\mu] = \left[\frac{B}{H} \right] = \frac{\text{Wb m}}{\text{m}^2 \text{ A}} = \frac{\text{Wb}}{\text{mA}}. \quad (17)$$

Using (4) the following units obtain,

$$[\nabla \times \mathbf{B}] = [\mu \mathbf{j}] = \frac{\text{Wb A}}{\text{mA m}^2} = \frac{\text{Wb}}{\text{m}^3}. \quad (18)$$

Using (13),

$$\frac{\text{Wb}}{\text{m}^3} = [\alpha] \frac{\text{Wb}}{\text{m}^2} \quad (19)$$

or

$$[\alpha] = 1/\text{meter}. \quad (20)$$

Our derivation is as follows: The left side of (13) is expanded in cylindrical coordinates:

$$\begin{aligned} \nabla \times \mathbf{B} &= \left(\frac{1}{r} \frac{\partial B_z}{\partial \theta} - \frac{\partial B_\theta}{\partial z}, \frac{\partial B_r}{\partial z} - \frac{\partial B_z}{\partial r}, \right. \\ &\quad \left. \frac{1}{r} \frac{\partial}{\partial r} (r B_\theta) - \frac{1}{r} \frac{\partial B_r}{\partial \theta} \right) \end{aligned} \quad (21)$$

and the right side of (13) is expressed as,

$$\alpha \mathbf{B} = (\alpha B_r, \alpha B_\theta, \alpha B_z). \quad (22)$$

In (21) and (22), all field components are functions of the position vector, \mathbf{p} . Given that there is no reason to assume any variation of current density \mathbf{j} in the θ or z directions in cosmic space, (14) implies the same is true for \mathbf{B} .

It follows from the absence of any externally applied forces other than possibly a static axial electric field to maintain \mathbf{I} (first term in (3)) and any time-varying electric fields, that all partial derivatives of \mathbf{B} with respect to θ and z are zero and, therefore, what remains of (13) after these simplifications in (21) are the following three expressions: In the radial direction,

$$\alpha B_r = 0. \quad (23)$$

There is no radial component of the \mathbf{B} vector. This is consistent with Maxwell's $\nabla \cdot \mathbf{B} = 0$. In the azimuthal direction,

$$\frac{\partial B_z}{\partial r} = -\alpha B_\theta \quad (24)$$

and in the axial direction,

$$\frac{1}{r} \frac{\partial}{\partial r} (r B_\theta) = \alpha B_z. \quad (25)$$

This results in two non-trivial coupled differential equations in the two dependent variables B_z and B_θ as shown in (24) and (25). The independent variable in both is radial distance, r .

4 Solution in closed form

Combining (24) and (25) yields a single second-order differential equation in a single dependent variable,

$$r^2 \frac{\partial^2 B_z(r)}{\partial r^2} + r \frac{\partial B_z(r)}{\partial r} + \alpha^2 r^2 B_z(r) = 0. \quad (26)$$

The dependent variable $B_z(r)$ is the axial component of the force-free steady-state magnetic field. The component field $B_z(r)$ is allowed to extend as far as the differential equation (26) provides for. No boundary condition at any non-zero value of r is introduced. There will be, in all real currents in space, a natural limit, $r = R$, to the extent of the current density $\mathbf{j}(r)$.

Having now fully specified the differential equation (26), it is recognized as being identical to Bessel's equation of order zero, with scalar parameter α (the units of which are (see (20)) the reciprocal of the units of r). We thus have a closed-form solution for the dependent variable in that differential equation that results from expanding equation (13). Its solution is,

$$y = AJ_0(\alpha x) + CY_0(\alpha x). \quad (27)$$

$J_0(x)$ is the Bessel function of the first kind and zeroth order, and $Y_0(x)$ is the Bessel function of the second kind (or sometimes called the Weber or Neumann function) of zeroth order.

The function $J_0(\alpha x)$ has the value unity at the boundary $x = 0$, and the function $Y_0(\alpha x)$ has a singularity at this same boundary. Because reality dictates that the magnetic field remain finite-valued, the value of arbitrary coefficient C must be set equal to zero. Thus, the solution to (26) is given by,

$$B_z(r) = B_z(0) J_0(\alpha r). \quad (28)$$

This Bessel function of the first kind and of order zero is used to produce Bessel functions of the first kind and orders 1, 2, 3, ... by simple differentiation. The recursion relation for the first-order Bessel function is,

$$J_1(x) = -\frac{dJ_0(x)}{dx}. \quad (29)$$

Thus, from (24) and (29), we obtain,

$$B_\theta(r) = B_z(0) J_1(\alpha r). \quad (30)$$

Consequently, from (28) and (30), the scale of the size, r , of the magnetic field in the radial direction is determined by the parameter α . Allowing $\alpha = \alpha(r)$ would distort the radial axis used to plot $B_z(r)$ and $B_\theta(r)$.

These Bessel functions approach damped trigonometric functions for large r , but the amplitude decrease is unusually gradual – varying inversely as the *square root* of αr , which is a more gradual decay than the typical exponential, or $1/\alpha r$, or $1/(\alpha r)^2$ damping.

This decay behavior is seen from the asymptotic forms shown here in (31) below,

$$\begin{aligned} J_0(x) &= \sqrt{\frac{2}{\pi x}} \left[\cos\left(x - \frac{\pi}{4}\right) + O\left(\frac{1}{x}\right) \right] \\ J_1(x) &= \sqrt{\frac{2}{\pi x}} \left[\cos\left(x - \frac{3\pi}{4}\right) + O\left(\frac{1}{x}\right) \right]. \end{aligned} \quad (31)$$

Therefore, $B_r(r)$, $B_z(r)$ and $B_\theta(r)$ shown in (23), (28), and (30) together provide a complete description of the magnetic field that surrounds and pervades the final force-free, minimum-energy, steady-state, cylindrical current. In this state, all Lorentz forces have been reduced to zero. The physical implications of these expressions are fully described in Section 8, below.

5 Euler method of solution

Another approach to solving (26), one that does not require that it be recognized as a Bessel equation, is to use an iterative numerical method. One such method is based on a *state-variable representation* of the differential equation – in this case the pair (24) and (25). In order to describe those differential equations in state-variable form, the product rule for derivatives is first applied to (25) as follows:

$$\frac{\partial(rB_\theta)}{\partial r} = r\alpha B_z \quad (32)$$

$$r \frac{\partial B_\theta}{\partial r} + B_\theta = r\alpha B_z. \quad (33)$$

Two state-variables may be defined as follows:

$$x_1 = B_z \quad (34)$$

$$x_2 = B_\theta \quad (35)$$

so that rewriting (24) and (25) in state-variable form yields,

$$\frac{dx_1}{dr} = -\alpha x_2 \quad (36)$$

$$\frac{dx_2}{dr} = \alpha x_1 - \left(\frac{1}{r}\right) x_2. \quad (37)$$

An Euler/Runge-Kutta algorithm for obtaining an approximate step-wise solution to (36) and (37) was implemented. The results, presented in Figure 2, show, as expected, the familiar shapes of Bessel functions J_0 and J_1 as $B_z(r)$ the axial component, and $B_\theta(r)$ the azimuthal component. Also shown is the total magnetic field strength $|\mathbf{B}|$ (the square root of the sum of the squares of the two component scalar fields, B_z and B_θ). This total field strength magnitude is strongest at a minimum radial value r and decreases monotonically with increasing r .

Specifically, in Figure 2, *total magnetic field magnitude* is shown to decrease with increasing radial distance from the

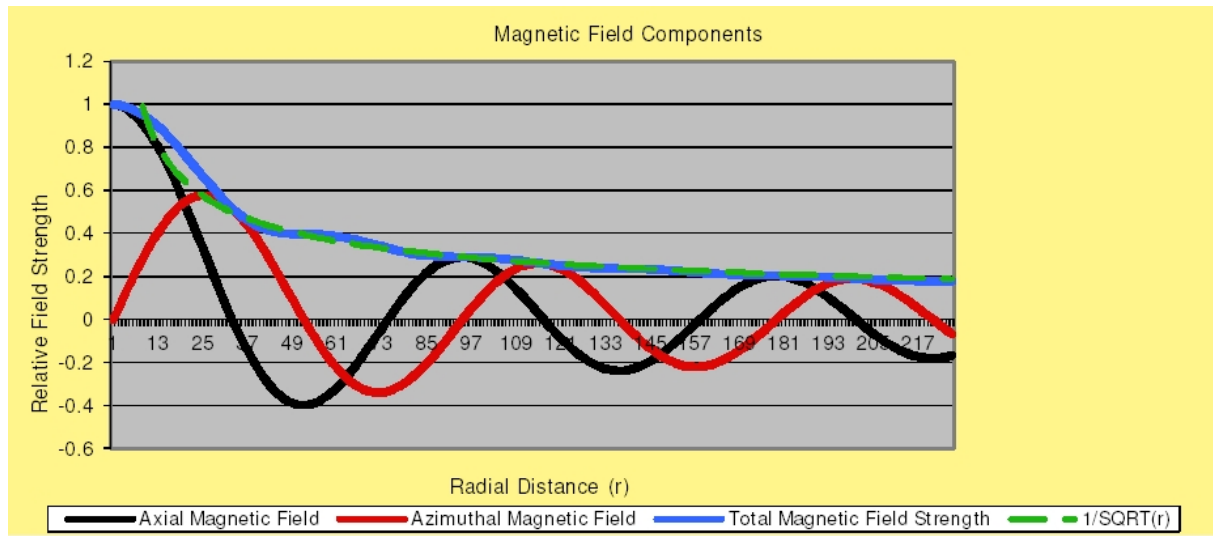


Fig. 2: Axial Magnetic Field component B_z , the Azimuthal Magnetic Field component B_θ , the magnitude of the Total Magnetic Field; and, for reference, a plot of $1/\sqrt{r}$ – all vs. radial distance quantized to integer multiples of the step-size $h = 0.1$. The value of α arbitrarily selected in (36) and (37) to achieve adequate resolution of the Bessel functions with this step-size is 0.075. The horizontal axis in this plot is the radius r -axis. Note in Table I that in every case (row) the inherently dimensionless Bessel function argument, $x = \alpha r$, thus demonstrating the scale factor utility of α . (e.g., $2.4048 = 0.075 \times 32$.)

central axis of the current as $(\alpha r)^{-1/2}$. This function is shown, for reference, as the fourth series plotted in Figure 2. This behavior was fully described in Section 4 (see (31)). Therefore, the magnetic fields within field-aligned cosmic currents clearly extend outward in space much farther and less diminished in strength than the magnetic field that would be generated by a simple straight-wire electric current (see (6)).

The parameter α appears as a scale factor operating on the radius variable, r . In the result shown in Figure 2, the value for that distance-scaling parameter was arbitrarily chosen to be $\alpha = 0.075$. The horizontal axis of Figure 2 is in units of actual radial distance, r . For example, the first zero of $J_0(x)$ is located at $x = 2.4048$. In Figure 2 it is shown to occur at $r = x/0.075 = 32$. This demonstrates the relationship between the non-dimensional argument of the Bessel functions, x , and the scaled variable, r : $x = \alpha r$. Nothing is inferred or implied about the current density vector field \mathbf{j} at this stage.

The step-wise Euler method described here can also be used in the event the state-equations are nonlinear due to choosing an arbitrary $\alpha = \alpha(r)$.

6 General validity of solution

A question remains regarding the generality of the solutions (23), (28), and (30), for $B_r(r)$, $B_\theta(r)$, and $B_z(r)$ respectively. Directly or indirectly all three of these quantities result from solving the Bessel equation (26), which, itself, is derived from the substitute equation (13), not from the fundamental, definition of a force-free current (12). This substitute, (13), was posited as being a valid alternative to (12), the defining property. Expressions (12) and (13) impose similar but not identical

Table 1: IMPORTANT VALUES FOR RADIAL MAGNETIC COMPONENTS

Radius Values $r = x/\alpha$	Zeros of $J_0(x)$ X	Zeros of $J_1(x)$ x	Description
0		0	B_z pos max, B_θ zero
32	2.4048		B_z zero, B_θ pos max
51		3.8317	B_z neg max, B_θ zero
74	5.5201		B_z zero, B_θ neg max
94		7.0156	B_z pos max, B_θ zero
116	8.6537		B_z zero, B_θ pos max
136		10.1735	B_z neg max, B_θ zero
158	11.7915		B_z zero, B_θ neg max
178		13.3237	B_z pos max, B_θ zero
199	14.9309		B_z zero, B_θ pos max

requirements on the magnetic field $\mathbf{B}(r, \theta, z)$ and the current density field $\mathbf{j}(r, \theta, z)$. Therefore, it has not yet been demonstrated that the vector field solutions of (13) listed in (23), (28) and (30) are also valid solutions of the fundamental definition, (12).

In order to demonstrate this, we insert those solutions back into (12) by writing the central three-dimensional cross product contained in that expression in determinant form:

$$(\nabla \times \mathbf{B}) \times \mathbf{B} = \begin{vmatrix} \hat{r} & \hat{\theta} & \hat{z} \\ (\nabla \times \mathbf{B})_r & (\nabla \times \mathbf{B})_\theta & (\nabla \times \mathbf{B})_z \\ B_r & B_\theta & B_z \end{vmatrix}. \quad (38)$$

Using the cylindrical curl expansion of (21),

$$|b_{ij}| = (\nabla \times \mathbf{B}) \times \mathbf{B} = \begin{vmatrix} \hat{r} & \hat{\theta} & \hat{z} \\ 0 & -\frac{\partial B_z}{\partial r} & \frac{1}{r} \frac{\partial}{\partial r} (r B_\theta) \\ B_r & B_\theta & B_z \end{vmatrix}. \quad (39)$$

We use (23), (28) and (30). Then in (39) the element b_{22} becomes,

$$\begin{aligned} b_{22} &= -\frac{\partial}{\partial r} [B_z(0) J_0(\alpha r)] \\ &= \alpha B_z(0) J_1(\alpha r). \end{aligned} \quad (40)$$

The element b_{23} becomes,

$$\begin{aligned} b_{23} &= \frac{1}{r} \left(r \frac{\partial B_\theta}{\partial r} + B_\theta \right) = \frac{\partial B_\theta}{\partial r} + \frac{1}{r} B_\theta \\ &= \alpha B_z(0) \left[\frac{\partial J_1(\alpha r)}{\partial r} + \frac{1}{\alpha r} J_1(\alpha r) \right]. \end{aligned} \quad (41)$$

Since

$$\frac{\partial J_1}{\partial x} = J_0 - \frac{1}{x} J_1, \quad (42)$$

(41) becomes,

$$\begin{aligned} b_{23} &= \alpha B_z(0) \left[J_0(\alpha r) - \frac{1}{\alpha r} J_1(\alpha r) + \frac{1}{\alpha r} J_1(\alpha r) \right] \\ &= \alpha B_z(0) J_0(\alpha r). \end{aligned} \quad (43)$$

Using the above expressions together with (23), (28), and (30), in (39) and omitting functions' arguments for clarity,

$$(\nabla \times \mathbf{B}) \times \mathbf{B} = \begin{vmatrix} \hat{r} & \hat{\theta} & \hat{z} \\ 0 & \alpha B_0 J_1 & \alpha B_0 J_0 \\ 0 & B_0 J_1 & B_0 J_0 \end{vmatrix} = \mathbf{0}. \quad (44)$$

(QED)

Thus, the components of $\mathbf{B}(r, \theta, z)$ given in (23), (28), and (30) are shown to be valid solutions of the original defining equation (12). That fact remains valid whether or not the alternative (13) had ever been suggested.

Regarding the practical evaluation of α when approximate observations of both \mathbf{B} and $\nabla \times \mathbf{B}$ are available, we have [31, p.107],

$$\alpha = \frac{(\nabla \times \mathbf{B}) \cdot \mathbf{B}}{B^2}. \quad (45)$$

Inserting the appropriate components from (23), (28), and (30) into (45) yields the identity,

$$\alpha = \alpha. \quad (46)$$

This indicates that the results presented here as (23), (28) and (30) are consistent with the formulation for α given in (45).

7 Current density of a field aligned current

Having accepted the postulated alternative definition (13) and (14) to determine the force-free magnetic-field solutions (28) and (30) (repeated below as (47) and (48)), it is then logically consistent to simply insert these into (14) to obtain the companion current-density relations (49) and (50):

$$B_z(r) = B_z(0) J_0(\alpha r) \quad (47)$$

$$B_\theta(r) = B_z(0) J_1(\alpha r) \quad (48)$$

$$j_z(r) = \frac{\alpha B_z(0)}{\mu} J_0(\alpha r) \quad (49)$$

$$j_\theta(r) = \frac{\alpha B_z(0)}{\mu} J_1(\alpha r). \quad (50)$$

A dimensional analysis of (49) and/or (50) using (18) and (20) shows the units of the constant term $\alpha B_z(0)/\mu$ to be A/m^2 as they must be.

In (49) and (50), it is clear that as the radial size of the model is increased (by decreasing the value of α), the magnitude of both current density components decrease proportionally.

Wiegmann [37] *defines* α as being $\alpha(x, y) = \mu_0 j_0 / B_0$ (see (49) and (50)). This definition also has units of $1/m$ (reciprocal of distance) (see (17)–(20)). Peratt [31, p.107] states that α is adjusted until reasonable agreement is obtained with observations (see (45) and (46)).

8 Consequences of the oscillatory nature of the Bessel (Lundquist) solution

Expressions (47)–(50) fully describe the structure of the model of a minimum (Lorentz force) energy, cylindrical, force-free, field-aligned current (FAC) under the assumption of equation (14). Thus:

1. There are no points within the plasma where $\mathbf{B} = \mathbf{0}$. A non-zero valued magnetic field exists at every point. In the first paragraph after (3) it was stated, nor are any assumptions made about the distribution of the current density across the cross-section. (49) and (50) now express that spatial distribution of $\mathbf{j}(\mathbf{p})$.
2. At every point in the plasma, \mathbf{j} and \mathbf{B} are collinear.
3. At every point in the plasma $\mu \mathbf{j} = \alpha \mathbf{B}$ (assumption, as discussed in Section 3).
4. The model expressions (47)–(50) remain valid only over the range $0 < r < R$. Farther out from the z -axis than $r = R$, $\mathbf{j} = \mathbf{0}$. From that point outward, the cylindrical plasma appears more and more like a single straight, isolated current-carrying wire. So beyond radius R , the magnetic field strength will decay approaching $1/r$. This is shown directly using (14): for $r > R$, $\mathbf{j} = \mathbf{0}$, $\alpha = 0$. Then using (32) and (33) yields:

$$B_\theta(r) = \frac{k_z}{r}. \quad (51)$$

This is consistent with (6).

Visualizing this field configuration with the aid of Figures 2, 3, and 5, reveals that, within the plasma, at increasing radial values, the magnetic field, together with its collinear current density, wrap the axis of the current stream with a continuously increasing helical pitch angle.

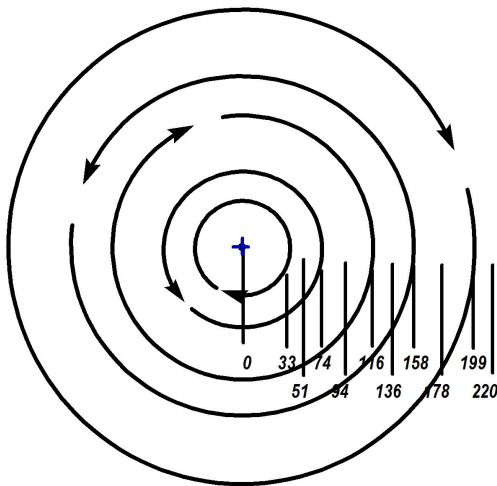


Fig. 3: Cross-section of a force-free current. In this view the reader is looking in the +z-direction, in the direction of main current flow. The radius values shown are plotted as values of $r = x/\alpha$ ($\alpha = 0.075$), which were used in the Euler iterative solution of (36) and (37). At the radius values shown, the axial \mathbf{B} -field is zero-valued so the total field is only azimuthal (either clockwise or counter-clockwise circles).

From (23), there is no outward radiation of the magnetic field (nor its collinear \mathbf{j}) from inside the plasma where $\alpha \neq 0$. There is no non-zero B_r or j_r component anywhere. Thus no matter escapes from the plasma. This preserves the structural integrity of the FAC over large axial distances.

Both solutions (closed-form and Euler) demonstrate repeated reversals in the directions of both the axial and the azimuthal magnetic field components with increasing radial distance. This implies the existence of a discrete set of virtual concentric cylindrical surfaces (see Figure 3). These surfaces are centered on the z-axis of the field-aligned current. At these discrete radial values, the axial field component, B_z is zero-valued and the azimuthal magnetic component, B_θ , is at alternately clockwise and counter-clockwise maxima. As a function of r the axial and azimuthal field strengths are observed to be in quadrature. For example in Figure 2, in a region such as that between radial distances 74 and 116, the axial field, B_z , is unidirectional (in the positive z-direction, attaining maximum strength at $r = 94$); whereas the azimuthal field reverses direction at $r = 94$, changing from the negative direction of θ to the positive direction. This results in a total magnetic field vector that wraps the current stream, its pitch angle rotating (with increasing r) in a clockwise direction when viewed looking inward in a radial direction, toward the central axis of the current (see Figure 5).

Thus, the axis of a cosmic, field-aligned current is wrapped with a compound helical magnetic field whose angle with respect to the +z-axis increases continuously with increasing radial distance, r . This gives rise to a structure suggestive of some ancient Roman fasces.

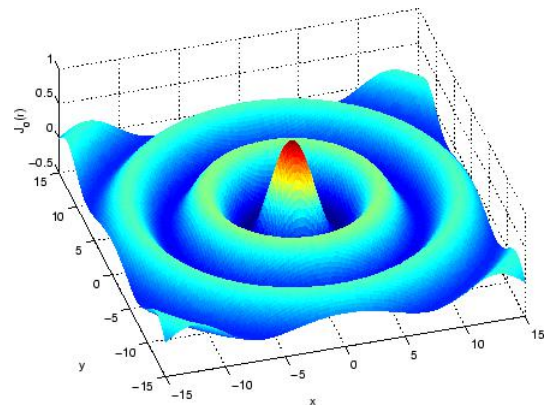


Fig. 4: Three-dimensional plot of the magnitude of the axial magnetic field component $B_z(r)$ and the current density $j_z(r)$. This demonstrates the relative strength of both those central (on-axis) fields. The magnitude scale of the horizontal axes used in this Figure are both x , the dimensionless arguments of the Bessel $J_0(x)$ and $J_1(x)$ functions.

In Figure 5, one cycle (0° – 360°) of the pitch angle is shown. The cycle is sketched at eleven incrementally increasing sample values of radius. The shaded arrows show the total magnetic field direction at each value of radius, r , and the white arrows show the field direction at an increment just below each of those values of radius. At every point in a stable force-free, field-aligned current, the current density \mathbf{j} is collinear with \mathbf{B} .

The Lundquist-Alfvén image shown in Figure 6, which is often used to describe the Birkeland current steady-state minimum-energy magnetic field, is in agreement with these results (47–50), but it only describes the morphology for small values of r . As r increases beyond what is shown in Figure 6, an uninterrupted rotation of the pitch angle of the magnetic/current helices continues (see Figure 5). The field rotation does not abruptly stop at 90° (where the total magnetic field is orthogonal to the direction of z) as might be inferred from Figure 6. The helical wrapping of the \mathbf{j} and \mathbf{B} fields continues with increasing radius values. This adds strength to the overall FAC structure. The tangent of the helical angle at any point, r , is the ratio (see Figure 1),

$$\frac{B_z(r)}{B_\theta(r)} = \frac{J_0(\alpha r)}{J_1(\alpha r)} = \frac{J_0(x)}{J_1(x)}. \tag{52}$$

Therefore if the value of the scale factor, $\alpha = x/r$ is, say, doubled, then that same pitch angle will occur at a value of r at half the original radius (x value unchanged). Thus the scale of the entire model will be halved (see Figure 6).

9 Effects of increased axial current

In a geomagnetic storm, a surge in the flux of charged particles (current increase) often temporarily alters Earth’s magnetic field.

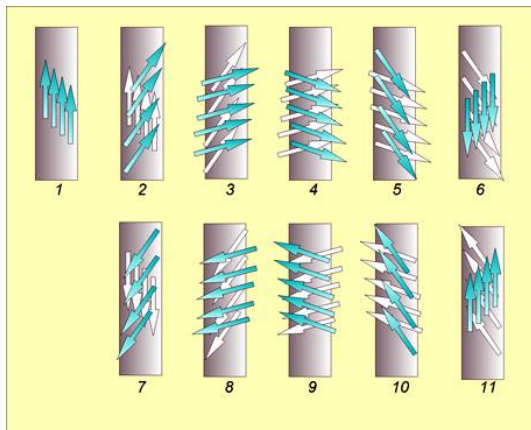


Fig. 5: The pitch angle of the helical total magnetic field, \mathbf{B} vector, that encircles a field-aligned current changes continuously with increasing radial distance from the central axis of the current. There are no abrupt quantum jumps or breaks in this angle's change or in the field's magnitude. One cycle (0° – 360°) of the pitch angle is shown. The cycle is sketched at eleven incrementally increasing sample values of radius. The shaded arrows show the total magnetic field direction at each value of radius, r , and the white arrows show the field direction at an increment just below each of those values of radius.

The entirety of this paper up to this point has been focused on the consequences of the reduction or possible elimination of the Lorentz $\mathbf{v} \times \mathbf{B}$ forces as defined in the second term of (3). But, the first term in that expression produces an independent, conduction component of the current density that may be added, via superposition, to the current density, \mathbf{j}_z , that has been derived above. This additional term is written as,

$$\mathbf{j}_{cond} = q\mathbf{E} \left(\sum_k n_k \mu_{ions}^{(k)} + n_e \mu_e \right) \quad (53)$$

where n_k is the ion density, with k = ionization number of the various ions, n_e is the electron density and $\mu_{ions}^{(k)}$ and μ_e are the respective mobilities of those ions and electrons in the plasma. Expression (53) is the point form of Ohm's Law. Another way that \mathbf{j}_z might become increased is by narrowing the cross-sectional area of a Birkeland current as it squeezes down into a polar cusp in a geomagnetic field.

It is not known if any actual, observed cosmic currents are in the complete minimum (Lorentz force) energy, field-aligned state. Several apparently show evidence of near-force-free behavior [31]. In the steady-state minimum energy FAC configuration, all Lorentz forces have been eliminated and charge simply follows the magnetic field structure. For example, in Figure 3, any positively charged matter located at $r = 158$, has counter-clockwise motion.

The image shown in Figure 8 was obtained in a plasma laboratory. Neither this nor the image of Saturn's north pole in Figure 7 represent force-free currents because they both are images of collisions of such currents with material objects.

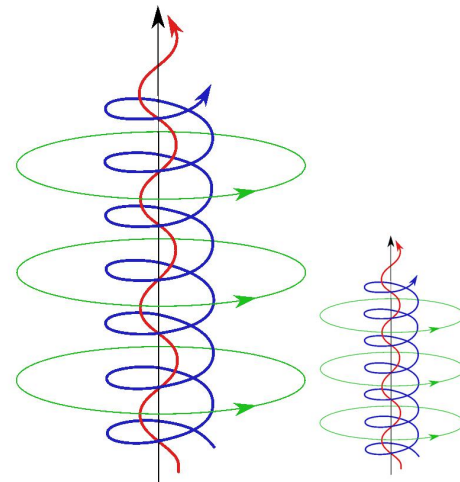


Fig. 6: Two different sized scale models of a FAC. These are both Lundquist-Alfvén-type images showing the helical structure of the collinear \mathbf{j} and \mathbf{B} vectors for small values of radius, r . (Left: Using $\alpha = \alpha_0$. Right: Using $\alpha = 2\alpha_0$.) This demonstrates why some investigators say that alpha controls the "tightness of twist". It only appears to do that as a secondary effect because it's primary effect is as a scale factor on the overall dimensional *size* (r, z) of the model's structure.

Figure 8 suggests what may occur if such an overall current density increase were to occur. The force-free structure would begin to undergo changes (if not be totally destroyed). Exactly what would happen is pure conjecture but if we start with Figure 3 and consider what might occur if and when a low intensity stream of positive charge begins to infuse the entire cross-section in a $+z$ direction (away from the reader), these additional positive charges would likely be deflected by Lorentz forces as follows (see Figure 3). At radii 33, 116, and 199 – deflection inward and clockwise. At radii 74, and 158 – deflection outward and counter-clockwise.

The two paths (inward and clockwise at $r = 116$ and the one at $r = 74$ moving outward and counter-clockwise) might appear to be a single path spiraling inward from $r = 116$ toward $r = 74$. Such pathways are suggested in Figure 8. Clearly in that state, the system is no longer at minimum energy – Lorentz forces are at work within the no-longer force-free plasma.

Another effect of an increase in the magnitude of the axial component of the current density, \mathbf{j}_z , would be to add a small incremental vector in the $+z$ -axis direction to each existing \mathbf{j}_z -vector. For example, consider sub-figures 2-5 in Figure 5. A small $+\mathbf{j}_z$ vector added to each of the shaded \mathbf{j} -vectors shown there would tend to twist them slightly counter-clockwise, away from being aligned with their corresponding \mathbf{B} -vector that remains fixed. The resulting Lorentz force ($\mathbf{j} \times \mathbf{B}$) would be directed inward (away from the viewer). However, if a similar small $+\mathbf{j}_z$ vector were to be added to each of the shaded \mathbf{j} -vectors shown in sub-figures 7-10 in Figure 5, this would

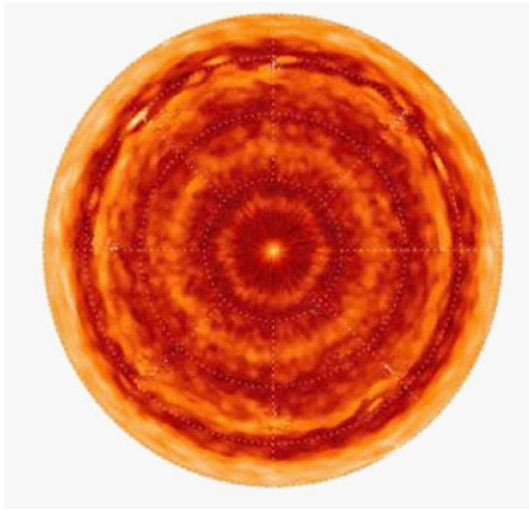


Fig. 7: Saturn's north pole, infrared Cassini image. Saturn is a gaseous planet composed mainly of hydrogen and helium. This image was obtained during the dark winter. The pole is encircled by a hexagonal feature in its atmosphere, which is thought to be caused by a planetary (atmospheric) wave. Image obtained using the infrared mapping spectrometer on board the Cassini Orbiter spacecraft. Courtesy of: NASA/JPL-Caltech/University of Arizona. The Cassini-Huygens mission is a cooperative project of NASA, the European Space Agency and the Italian Space Agency. Image Credit: NASA/JPL/GSFC/Oxford University/Science Photo Library [40].

twist them slightly clockwise and the Lorentz force would, at those points, be directed outward (toward the viewer). Ions, then, will be pushed inward over radial ranges wherever azimuthal magnetic field, \mathbf{B}_θ , is directed clockwise in Figure 3. Ions will be expelled outward wherever \mathbf{B}_θ is directed counter-clockwise in Figure 3. Matter (ions and neutral dust) will thus tend to congregate at intermediate radius values such as $r = 0, 94$, and 178 . These are radii defined by the *odd zeros* of $J_1 = J_1(x) = J_1(ar)$, ($x = 0, 7, 13, \dots$) (see Figure 4 and column 3 of Table I for values). Electrons moving in the $-z$ -direction will tend to be scavenged into the same r -regions. These are hollow cylindrical surfaces where $+j_z$ dominates.

10 Comparison of results with observations

Images in Figures 7, 9, and 10 are obtained from actual astronomical observations. The image shown in Figure 7 is consistent with the hypothesis that Saturn is receiving a flow of electric charge via a Birkeland current directed into its north pole much as Earth is known to be experiencing. It is well known that currents in plasma drag un-ionized (as well as ionized) matter along in their path [42]. Figure 3 and the discussion at the end of Section 9, above, imply that clockwise and counter-clockwise counter-rotating current paths such as those at $r = 33$ and 74 ought to exhibit such counter-rotation. But, for years it has been unknown whether the spiraling/circular paths appearing in Figures 7, 8 and 9 are really counter-rotating.

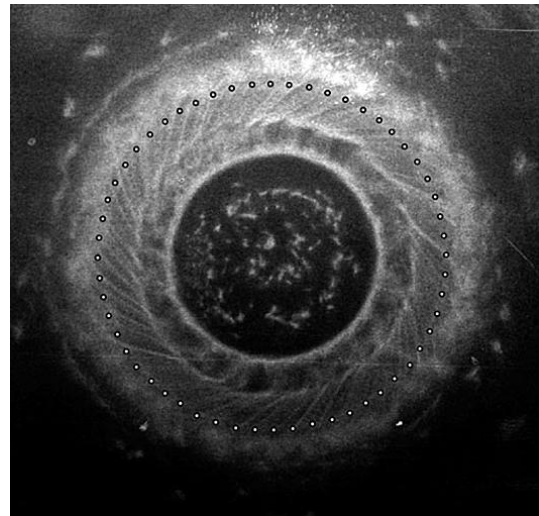


Fig. 8: Cross-section of a dense plasma focus Birkeland Current carrying $I = 174,000$ amperes. This image was captured by a witness plate placed in the discharge in a plasma lab. The spiral structure of the cross-section is visible. The 56-dot circular overlay shows the locations of the apparent spiral shaped paths of matter. Courtesy of A.L. Peratt, from Characteristics of a High-Current, Z-Pinch Aurora As Recorded in Antiquity, Part II Directionality and Source by Peratt, Directionality and Source. IEEE Transactions on Plasma Sci., August 2007 [41].

It would require a video to reveal that relative motion.

It so happens that NASA has produced exactly such a video clearly showing counter-rotating (plasma) clouds within what appears to be the hexagonal shape at Saturn's north pole (see: [43] NASA video - Saturn's Hurricane). In this video, the term hurricane is used repeatedly by the narrator who expresses concern about the fact that the "storm" is fixed to the planet's north pole and that no water ocean exists below it to cause it to exist. He does not mention that actual hurricane winds do not counter-rotate as these do.

In that video, in shear regions between counter-rotating shells, what appear to be diocotron instabilities are visible (see Figure 9). Without NASA's video, the counter-rotational motions of these areas in the Saturnian surface would not be observed and therefore their existence would go undiscovered. This recent motion picture is crucial evidence of part of what is being presented here. Many other edited versions of the original NASA video exist that do not show counter-rotation taking place. The uncut original does.

11 Conclusions

It has been well-known for decades that the Lundquist solution (15) constitutes a simple model of a cylindrical force-free, field-aligned current. This model:

1. Dictates that the two vector fields $\mathbf{j}(r, \theta, z)$ and $\mathbf{B}(r, \theta, z)$ be everywhere collinear;

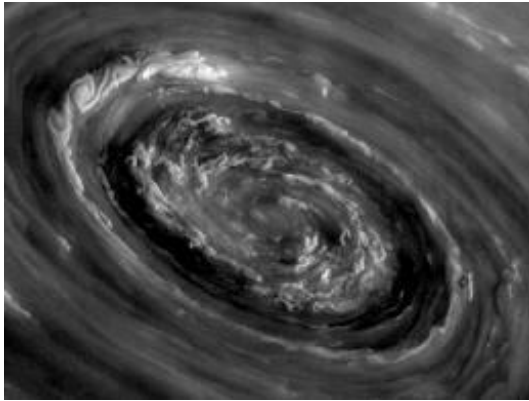


Fig. 9: Series of diocotron (shear) instabilities, especially obvious in the upper left of this image. This was taken from the NASA video [43] which clearly shows counter-rotation. From NASA Cassini mission video of Saturn's North Pole. Courtesy of: NASA/JPL-Caltech/University of Arizona. The Cassini-Huygens mission is a cooperative project of NASA, the European Space Agency and the Italian Space Agency. The imaging operations center is based at the Space Science Institute in Boulder, Colo. The Visual and Infrared Mapping Spectrometer team is based at the University of Arizona [43].

2. States that the overall solutions that specify the spatial dependence of those fields' magnitudes and directions are Bessel functions;
3. Assumes α is constant inside the plasma.

In this present paper we present a simple, but detailed derivation of this model of a force-free current and demonstrate, through straightforward mathematical analysis and strict adherence to the principles delineated in Maxwell's equations [35], a number of significant characterizations [44] of these field equations that are in strong agreement with reliable imagery obtained from both actual observations of phenomena in space and measurements in experiments in plasma laboratories. The most significant of those results are:

1. The complete mathematical model of a cylindrical, force-free FAC, including expressions for its current-density field is presented by (47)–(50), not just (15).
2. Magnetic fields produced by force-free currents stretch out radially from the central axis of the current stream much farther, and with greater effect, than previously thought. For radial distances, r , within the plasma ($r < R$) the amplitudes of those helical fields decay slowly *in inverse proportion to the square root of r* .
3. The fact that expression (23) requires that no component of the magnetic field, \mathbf{B} , can extend outward in the radial direction (and the fact that \mathbf{B} and \mathbf{j} are everywhere collinear) demonstrates that no dissipative currents or fields leave the cylindrical structure along its length. Birkeland's critics thought that the final, re-

laxed distribution would be an infinite dispersion, not a strong, tight cylinder (which it is).

4. The structural stability of the spiraling fascies-like wrapping of the magnetic field explains the observed enigmatic stability of Birkeland currents over long interplanetary, inter-stellar, and inter-galactic distances. For example, the cosmic current "jet" emanating from galaxy M87 remains collimated over a distance exceeding 5000 light years [46]. The stability of the flux-rope connecting the Sun and Earth is now better understood (see Section 8).
5. The angle of pitch of the helix varies smoothly and continuously with increasing radial distance, r , from the central axis of the current out as far as the plasma's current-carrying charge density extends. This causes cyclical reversals of direction (counter-flows) in both the axial and azimuthal magnetic field and its collinear current density. The magnitude of both the \mathbf{B} and \mathbf{j} -fields may be greater than zero for r values far beyond the first zero of $J_0(\alpha r)$ (which occurs at $r = 2.4048/\alpha$). Figure 6 is shown to be correct but incomplete, and thus potentially misleading.
6. Coupled with the new NASA video of Saturn's north polar region, this presentation strongly supports the hypothesis that a Birkeland current is feeding electric current into that region.
7. Parameter α controls the size of the resulting model in both the r and z dimensions (together – not separately). The value of α is arbitrary and is selected to enable the model to fit the size of the actual space-plasma being modeled.
8. The major difference between a field-aligned current (FAC) and a Birkeland current is that in a FAC the total current, \mathbf{I} , is a minimum. When the current density at any point, \mathbf{j} , increases for any reason above its minimal value, non-zero Lorentz forces begin to occur and the matter scavenging described in Section 9 takes place.
9. The mathematical procedure offered here is circumscribed to an extent not typical of other papers by caveats regarding the consequences of the universal unquestioning acceptance of the generality of the expression $\mu\mathbf{j} = \alpha\mathbf{B}$ (14). This is not applicable in filamented plasma.

The conclusions drawn from the analysis of the mathematical model derived in this paper have been tested against original motivating observations and measurements. Consistently strong agreement is found. Many otherwise enigmatic images stand witness to the potential benefits of considering possible electrical causation of other cosmic plasma phenomena.

The M2-9 Hourglass planetary nebula in Figure 10 is a prime case in point. We suggest that the narrowing of the

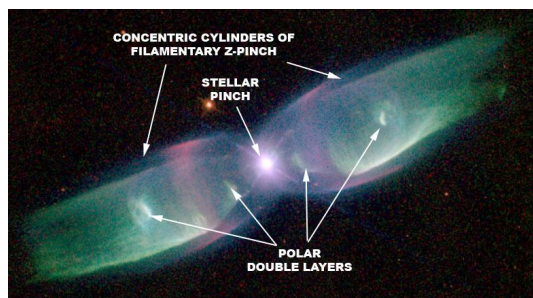


Fig. 10: The Hourglass (or Butterfly) planetary nebula, M2-9. In this image the separate hollow, cylindrical tubes of matter are clearly visible. The cross-sectional area of the structure diminishes near the center of the pinch. Since the total current is the same at every cross-section, this means regions near the central pinch have increased current density (A/m^2) and corresponding greater visual brightness. Courtesy of the Hubble Legacy Archive, NASA, ESA Processing *Judy Schmidt*. The Hubble Legacy Archive (HLA) is designed to optimize science from the Hubble Space Telescope by providing on-line, enhanced Hubble products and advanced browsing capabilities. The HLA is a joint project of the Space Telescope Science Institute (STScI), the Space Telescope European Coordinating Facility (ST-ECF), and the Canadian Astronomy Data Centre (CADC) [45].

plasma FAC channel due to the z-pinch creates an increased current density which causes a transition of the plasma from the dark mode into the visible glow and arc modes. The observed dual, concentric cylinders of excited plasma are consistent with the counter-rotation, matter scavenging, and reversing flows described in this paper.

Acknowledgements

The author wishes to express his sincere thanks to Dr. Jeremy Dunning-Davies for recognizing that the differential equation derived in this study is a Bessel Equation, whose solutions are given by the Bessel functions, J_0 and J_1 . He also gave the author much appreciated encouragement and very much needed advice.

Dr. Timothy Eastman, Wyle senior scientist at NASA Goddard, Dr. Ron DeLyser, EE Department U. of Denver, Dr. C. J. Ransom of Vemasat Labs, Dr. W. A. Gardner, and Dr. Michael Clarage gave freely and graciously of their time, advice, and assistance to help in this effort.

Submitted on: January 27, 2015 / Accepted on: February 17, 2015
First published online on: February 20, 2015

References

- Birkeland K. The Norwegian Polaris Expedition 1902–1903, Vol. 1, Sect. 1. Aschehoug, Oslo, Norway, 1908.
- Lerner E. The Big Bang Never Happened. New York, 1991. p. 181.
- Lundquist S. Magneto-hydrostatic fields. *Arch. Fys.*, 1950, v. 2, 361.
- Lundquist S. On the stability of magneto-hydrostatic fields. *Phys. Rev.*, 1951, v. 83 (2), 307–311. Available online: <http://link.aps.org/doi/10.1103/PhysRev.83.307>.
- Chandrasekhar S. and Kendall P. On force-free magnetic fields. *Astrophys. J.*, 1957, v. 12 (6), 457.
- Gold T. AAS-NASA Symposium on Physics of Solar Flares. Hess W. N., ed., NASA SP-50, 1964, p. 389.
- Alekseev I. and Shabansky V. A model of a magnetic field in the geomagnetosphere. *Planet. Space Sci.*, 1972, v. 20, 117.
- Chiu Y. and Hilton H. Exact Green's function method of solar force-free magnetic-field computations with constant alpha. I. Theory and basic test cases. *Astrophys. J.*, 1977, v. 212, 873–885.
- Cloutier P. and Anderson H. Observations of Birkeland currents. *Space Sci. Rev.*, 1975, v. 17, 563–587.
- Alfvén H. Evolution of the solar system. Scientific and Technical Information Office National Aeronautics and Space Administration, Washington, D.C., 1976.
- Hasegawa A. and Sato T. Generation of Field Aligned Current during Substorm in Dynamics of the Magnetosphere. Akasofu, S-I., ed., D. Reidel, Hingham, MA, 1979, p. 529.
- Nakagawa J. and Raadu M. A. On practical representation of magnetic field. *Solar Phys.*, 1972, v. 25, 127.
- Olson W. A model of distributed magnetospheric currents. *J. Geophys. Res.*, 1974, v. 79, 3731.
- Rostoker G., Armstrong J. C., and Zmuda A. J. Field-aligned current flow associated with intrusion of the substorm-intensified westward electrojet into the evening sector. *J. Geophys. Res.*, 1975, v. 80, 3571–3579.
- Zmuda A., Armstrong J. C., and Heuring F. Characteristics of transverse magnetic disturbances observed at 1100 kilometers in the auroral oval. *J. Geophys. Res.*, 1970, v. 75 (25), 4757–4762.
- Dessler A. Corotating Birkeland currents in Jupiter's magnetosphere - An Io plasma-torus source. *Plan. Space Sci.*, 1980, v. 28, 781–788.
- Harel M., Wolf R. A., Reiff P. H., Spiro R. W., Burke W. J., Rich F. J., and Smiddy M. Quantitative simulation of a magnetospheric substorm 1. Model logic and overview. *J. Geophys. Res.*, 1981, v. 86, 2217–2241.
- Alissandrakis C. On the computation of constant alpha force-free magnetic field. *J. Astron. Astrophys.*, 1981, v. 100 (1), 197–200.
- Burlaga L. Magnetic clouds and force-free fields with constant alpha. *J. Geophys. Res.: Space Phys.*, 1988, v. 93 (A7), 7217–7224.
- Durrant C. J. Linear force-free magnetic fields and coronal models. *Aust. J. Phys.*, 1989, v. 42, 317–329.
- Falthammer C. G. Magnetosphere-Ionosphere interaction. Near-Earth Manifestations of the plasma universe. *IEEE Trans. Plasma. Sci.*, 1986, v. 14 (6), 616–628.
- Potemra T. Birkeland Currents I. The Earth's Magnetosphere (From a special issue dedicated to Hannes Alfvén on his 80th Birthday). *Astrophys. Space Sci.*, 1988, v. 144 (1–2), 155–169.
- Potemra T. Observation of Birkeland currents with the TRIAD Satellite. *Astrophys. Space Sci.*, 1978, v. 58 (1), 207–226.
- Potemra T. Alfvén Waves and Birkeland Currents. *Physica Scripta*, 1995, v. T60, 107–112.
- Botha G. J. J. and Evangelidis E. A. Cylindrical linear force-free magnetic fields with toroidal flux surfaces. *Mon. Not. Roy. Astron. Soc.*, 2004, v. 350 (1), 375–384.
- Romashets E. and Vandas M. Force-free magnetic field in a cylindrical flux rope without a constant alpha. *Adv. Space Res.*, 2005, v. 36 (12), 2268–2272.
- Eastwood J. Flux ropes. NASA Goddard, 2009.
- Goedbloed J. and Poedts S. Principles of Magnetohydrodynamics: With Applications to Laboratory and Astrophysical Plasmas. Cambridge University Press, Cambridge, UK, 2004.
- Biskamp D. Nonlinear Magnetohydrodynamics. Cambridge University Press, Cambridge, UK, 1997.

30. Ferraro V. and Plumpton C. An Introduction of Magneto-Fluid Mechanisms. Clarendon Press, Oxford, 1966.
31. Peratt A. Physics of the Plasma Universe. Springer-Verlag, New York, 1992, p. 44. Republished ISBN 978-1-4614-7818-8, 2015, p. 406.
32. Titov V., Török T., Mikic Z., and Linker J. A. A method for embedding circular force-free ropes in potential magnetic fields. *Astrophys. J.*, 2014, v. 790 (2), 163.
33. Yang Y. Y., Shen C., Zhang Y. C., Rong Z. J., Li X., Dunlop M., Ma Y. H., Liu Z. X., Carr C. M., and Rème H. The force-free configuration of flux ropes in geomagnetotail: cluster observations. *J. Geophys. Res.: Space Phys.*, 2014, v. 119 (8), 6327–6341.
34. Eastman T. Wyle Senior Scientist at NASA Goddard, Personal communication, 5 February 2015.
35. Jackson J. Classical Electrodynamics, 2nd ed. John Wiley, New York, NY, 1975.
36. Callen H. Thermodynamics and an Introduction to Thermostatistics, 2nd ed. John Wiley, New York, NY, 1985.
37. Wiegelmann T. and Sakurai T. Solar force-free magnetic fields. *Living Rev. Solar Phys.*, 2012, v. 9 (5). Available online: <http://solarphysics.livingreviews.org/Articles/lrsp-2012-5/>.
38. Alfvén H. Cosmic Plasma. D. Reidel, Hingham, MA, 1981, p. 97.
39. Matlab, Bessel functions of the First and Second Kind. Available online: http://www.mhtlab.uwaterloo.ca/courses/me755/web_chap4.pdf.
40. Infrared image of Saturn's North pole. Available online: <http://www.sciencephoto.com/media/326994/view>, 4 February 2015.
41. Peratt A. Image: Penumbra from a dense plasma focus device. Available online: http://www.academia.edu/9156605/Neolithic_rock_art_associated_with_intense_auroral_currents, Figure 51, 4 February 2015.
42. Mehdipour H. and Foroutan G. The magnetized sheath of a dusty plasma with nanosize dust grains. *Phys. Plasmas*, 2010, v. 17, 083704.
43. NASA video of the Saturn hurricane. Available online: <http://www.jpl.nasa.gov/video/details.php?id=1213>, 4 February 2015.
44. Scott D. Real properties of electromagnetic fields and plasma in the cosmos. *IEEE Trans. Plasma Sci.*, 2007, v. 35 (4), 822–827.
45. High resolution NASA image of the Hour-Glass or Butterfly planetary nebula M2-9. Available online: <http://apod.nasa.gov/apod/ap130915.html>, 4 February 2015).
46. Messier 87 - SEDS catalog. Available online: <http://messier.seds.org/m/m087.html>.

LETTERS TO PROGRESS IN PHYSICS

An Eidetic Reflex and Moment of Breakthrough in Time and Scientific Creation: 10 Years of Progress in Physics, 100 Years of General Relativity, and the Zelmanov Cosmological Group

Indranu Suhendro

The Zelmanov Cosmological Group, Secretary of the Zelmanov Journal for General Relativity, Gravitation, and Cosmology

We celebrate the first 10-year momentous span of the solid body of critical scientific results and efforts delivered by the visionary editorial and founding team of the pioneering open new-millennium journal for advanced studies in theoretical and experimental physics, mathematics, astronomy, and cosmology, *Progress in Physics* (see the Editor-in-Chief's message: "Progress in Physics: 10 years in Print"), behind which is the core scientists and guardians of universal scientific creation, scientific revolution, and scientific-intellectual freedom and ethics: the few core scientists of the quintessential Zelmanov Cosmological Group, such as the founding editors and scientific creators Dmitri Rabounski and Larissa Borissova.

The Zelmanov Cosmological Group, which is also behind *The Abraham Zelmanov Journal* for General Relativity, gravitation, and cosmology, dedicates itself to the profound and extensive scope and depth of the works of the master theoretician "par excellence" of the Soviet-era general relativistic and cosmological school, Abraham Leonidovich Zelmanov, and to the most unique problems and possible extensions of General Relativity in general. Abraham Zelmanov's profundity "sine qua non" is reflected in the singular creation of the theories of chronometric, kinematic, and orthometric (monad) formalism in General Relativity, the Infinite Relativity Principle, the Anthropic Principle, the extensive classification of all possible cosmological models in the space-time of General Relativity (the Zelmanov Classification, including the possibility of absolute reference frames in a deforming, rotating, gravitating closed finite Universe), and many others (see the website of *The Abraham Zelmanov Journal* for details, and in particular the 2012 foreword to the book *Particles Here and Beyond the Mirror*). So, Zelmanov's theoretical mastery singularly encompasses the general fully non-linear, anisotropic, inhomogeneous, anholonomic, non-simply-connected space-time structure (and sub-structure) of General Relativity and the fabric of the cosmos, achieving the unification of the underlying structure of space-time, reference frame systems, and the fundamental observer. Zelmanov's few students and theoretical inheritors — such as Dmitri Rabounski and Larissa Borissova — have thereby preserved and extended his scientific and philosophical ideals as a whole, comprehensive, unitive scientific legacy: a singular univocity — "Zelmanovian Universum" — in the form of an ideologically most

unique and versatile platform for the most singular kind of meta-science and scientific creation, which is the embryo of the present Zelmanov Cosmological Group.

In the background of such unique origination, the general fundamental physics journal *Progress in Physics*, with a substantial portion of publications in General Relativity and differential geometry — in common with *The Abraham Zelmanov Journal*, is dedicated mostly to original, profound, critical, and challenging scientific works that potentially engage with the overall, far-reaching horizons and verizons of theoretical and experimental physics, mathematics, astronomy/cosmology, and of science as a whole, thereby expanding and synthesizing new scientific landscapes for both the present and the future. This is done mostly by identifying the pertinent objective quality and originality of the idea(s) in a submitted scientific work and the first and foremost crucial identification of the author as an essentially independent creative mind (whether specifically affiliated or not) and as a true person of integrity and clarity, therefore isolating the process of scientific judgement infinitely and decisively from the pervasively corruption-mongering, business-minded, pseudo-scientific (so, pseudo-objective) politics of typical modern academic practice and science administration (i.e., "big-wig scientism"). In specific cases where the editors and expert peer reviewers (who dare be non-anonymous) do not agree with the ideology and content of a submitted paper, a fidelity to pure scientific-intellectual freedom is still maintained as much as possible in the publication of the said work, as long as the basic technicality and competence (such as the mathematics and logical reasoning) is fulfilled. This is also true for some tremendous-looking extremely short papers that can subtly serve as an impetus for reflection and future scientific inspiration: they can be so short and still publishable in view of inspiring some pertinent new ideas in the future.

A word on a better peer-review system is at hand: above all, the journal categorically and distinctly promotes original thinkers and original scientific creators, along with fundamentally improving and transcending the largely deficient anonymously peer-review system, thus often allowing a work to be published with the potential for an on-going open peer-review (in the full critical vastness of time and space as regards judgement and validation): such as witnessed in the

forced, pioneering open peer-review case of Grisha Perelman's ground-breaking works on Ricci flow, manifold surgery, and the Poincaré conjecture. Thus, the journal employs a unique, more substantial form of peer-review system covering both immediate (pre-publication) and open-to-future-validation fully substantiated peer-review models. The journal does not welcome typical celebrity popularization and "celebrity fetishism/worship". Thus, it does not endorse exercising scientific judgement based on mere consensus and popularity, which is the malodorous, rotten, decadent business of politics and pseudo-science arising from the fact that there are too many people nowadays claiming to be "career scientists" (while careerism and science are most certainly two different things by way of subtle logical discernment) while essentially they are at large socially, inter-subjectively active opportunists and imitators. Such is to be compared to Einstein's time when scientists were truly still a rare breed or species — or say, before World War II, a war that changed so many ways of doing things in science and life, in science especially with the hijacking of some old journals and institutions by a plethora of powerful pseudo-scientists and pervasive mediocrity: certainly Einstein would not have survived today's popularity-concocting, narrow-minded, overly pretentious, intrinsically and extrinsically flawed scientific administration laden with closed-minded and pathetically rigid apathy against fundamental scientific novelty, individuality, and originality.

The common board of *Progress in Physics* and *The Abraham Zelmanov Journal* therefore comprises and welcomes scientific pioneers, as ethically liberal-democratic and inter-disciplinarily universal as possible: this, while the said board consists mostly of theoreticians and scientific creators in General Relativity, cosmology, and differential geometry at the heart of the Zelmanov Cosmological Group. While the journal is hosted by the said general relativists and differential geometers, it does not oppose alternative views: it acknowledges the two kinds of "alternative" (not one): the categorically superior "alternative" and the simple (ordinary) "alternative" (which can be either inferior or relatively on-par at times). Consequently, it promotes the fully open discussion of categorically different (often opposing) scientific views and ontologies, thus covering both the substance and event of all possible ideological presentations and representations.

In conducting a superior, alternative form of scientific peer-review, the board is also helped a great deal in dealing with radical, paradoxical, universal, inter-disciplinary scientific submissions and reasoning by the Smarandache Neutrosophy Group that extends the content, expression, and scope of logic and dialectics. This then is meant to be a fundamental platform for the creation of new physics, new mathematics, new cosmology, new phenomenology, new ontology, and new epistemology.

In other words, the journal aims at the rapid and transparent publication of uniquely qualified original scientific ideas

and impetuses: anything that is counter-productive, parasitic, and artificial to the true spirit of genuine scientific judgement (no matter how trendy), such as the extremely pernicious and popular trends and developments in the superficial politics of today's scientism, is not recognized by it. In addition to substantiating and upgrading peer-review, the journal also strives to help improve fully the genuine open-access system in all possible ways. This is the firmest future model for any true future science and scientific organization, where the quality of an individual original scientific work alone can reflect the journal's over-all stance as a whole, not simply the very superficial, idiotic, logically and semantically flawed concoction of "citation-only impact factor" (based merely on the number of citations) misused by so many "illiterate" (essentially quality-blind and quality-devoid) pretentious people in the typical administration nowadays. The journal philosophy as a whole serves in many ways as an absolute separator between real science and artificial politics, between originality and imitation, between profundity and superficiality, between integrity and hypocrisy. Any reader or any institution is absolutely free to download the materials (papers and books) published by both *Progress in Physics* and *The Abraham Zelmanov Journal*.

The year 2015 also marks the 100th anniversary of Einstein's geometric theory of space-time and gravitation, the General Theory of Relativity, since the final formulation of the generally covariant Einstein's field equations of gravitation in the last quarter of 1915 (during a very tragic and difficult time of World War I). It goes without saying that this was achieved by Einstein almost at the same time as Hilbert's final formulation of the field equations of gravitation, an axiomatic, lone, and colossal problem Hilbert rather spontaneously worked on upon witnessing Einstein's Göttingen lecture on the (at that time agonizingly stifled) progress of the formulation of the theory during the same year. It took well over 8 years of one of mankind's greatest intellectual (philosophical, physical, mathematical) struggles towards synthesis in history for the greatly isolated, independent, original, and visionary young scientific creator — Albert Einstein — to complete the task since 1907 when he first attempted the logical extension of the Special Theory of Relativity (born in 1905) to include gravitation and more general reference frames under the umbrella of differential geometry and general covariance (first with the help of Einstein's friend, Marcel Grossmann, who helped select and qualify Riemannian geometry for Einstein's new physics program, and also of Tullio Levi-Civita and Hermann Weyl upon the later publication of the final form of General Relativity). This was not so long after Poincaré and Minkowski (among Einstein's own teachers) proposed a basic four-dimensional space-time structure for the world, which later became incorporated into Special Relativity, and into particle physics and group theory via algebraic symmetry classification. Today, as per differential geometry and topology, both Riemannian and non-Riemannian

geometry (such as Finsler geometry) can be used in General Relativity to understand better its geometric-folitional structure (such as Riemannian sub-manifolds and singular spaces) as well as its extensions (most ontologically and epistemologically unique, though, would be General Relativity's orthometric extensions — not just any extension — as I have alluded to elsewhere).

Understood initially by very few in the world — and now genuinely and profoundly understood (truly in-depth, not merely in the popular and prevalent context) still by very few — General Relativity as such is a universal scientific construct and superstructure equivalent to a pure work of visual and musical art and a novel philosophical edifice of ontology and epistemology. I therefore would like to salute the truly small number of the world's most dedicated and original scientists (absolutely indifferent to mere popularity) whose field of work encompasses General Relativity, gravitation, cosmology, and the unified geometric theory of space-time and the physical fields (fundamental extension of Einstein's theory): those who singularly live Einstein's theory of General Relativity and generally the Einsteinian ideology of the geometrization of space-time, matter, and fields, i.e. those with real creative contributions to the field (excluding mere "toy models") and not simply those very many who opportunistically make a living out of it by hijacking Einstein's theory and name. Congratulations to the rarest and most universal kind of scientific creators in Einstein's name: those few scientific creators in possession of insight and ideation, originality and profundity, solitude and singularity, of new ideas in the unmistakable footsteps of Einstein himself.

Again, a disclaimer — a song of epistemic suffering and near-despair, arising from a saddest line and event of alienation in science — is immediately at hand also. It is a sad, tragic fact that Einstein's name today has been hijacked, misappropriated, and misused in the said way by the throngs of aggressively narrow-minded and self-promoting scientific imitators and popularizers (and "launderers" of shallow scientific outputs, opinions, and hypernarrations) the world over: they typically and consensually announce a plethora of trivial toy models of physics and the Universe and (by the blind forces of "status quo" consisting of greedy and petty power grabbers, false opinion manufacturers, and all their stooges) often force and entrench them as prevailing dogmas while hiding rather cowardly and manipulatively behind Einstein's stature. Such is a patently false misuse of power and a trivial, empty concoction of prestige, and an epitome of great prevalent hypocrisy, amounting to the greatest corruption done in the name of science: a categorical scientific abuse by way of mere opinion-making, large political and financial backing, and all sorts of flawed prestige and opinion manufacture absolutely without (and in contrast to) the first-principle ontic-epistemic determination of scientific profundity, quality, and reality with all its reflexively self-evident intrinsic logic, semantics, and syntax. It is clear that Einstein himself would

never take the side of those professing such a dogmatic and popular position, let alone those who pathetically suffer from — what I always call — utter ontic-epistemic shallowness, solipsistic folly, sycophant opportunism, and hypernarration (see the previous scientific letter "Meta-Epistemic Determination of Quality and Reality in Scientific Creation" as to how to epistemically qualify real quality science as simply genuine science and to disqualify bad popular science and its politics as simply bad science). I and my colleagues disassociate ourselves forever, once and for all, from such people who are the latent enemies and cancers of science. We care solely about the subtle and sublime spirit of science and scientific creation, and of scientific-intellectual freedom, not all the flawed manufactures of politics and such contingency.

The above diseased situation, often fogged and misunderstood in popular venues, has to be clearly understood by not only those working fundamentally in Einstein's theory, but also those who have engendered a relative (or absolute) opposition to Einstein and General Relativity. The latter group of people with certain alternative views — which we certainly usually can tolerate as long as science is the objective — ought not to mistake the flawed-in-mind opportunistic hijackers of Einstein's name and theory for Einstein himself (and General Relativity), so as to very arbitrarily and short-handedly fume out "war against Einstein". They have to at least understand the semantics and hermeneutics of Einstein and General Relativity a little better than usual: not from the said hijackers (who have no ontological, substantial relation to Einstein whatsoever), but from the solitary few who are real Einsteinian experts and inheritors. The Zelmanov Cosmological Group would welcome anyone who wants to understand Einstein and General Relativity better in a different way, as to disclose that great light in a solitary, often dark and hidden, true cosmic lane.

Finally, I salute once again the truly intellectually free — true scientists, minds symphonically swarthed with the cosmos and ideas, like true poets and artists — anywhere on this Earth and in the cosmos, on the most unique joint birthday occasion and resonance of Einstein's General Relativity and *Progress in Physics*.

Dedicated to Grisha Perelman and all the (few) truly free, courageous, revolutionary minds in the world of science. And to professors Brian Josephson and Sydney Brenner, and the late Joseph C. Hafele, from a silent observer on a distant but immediate star, as was Einstein unto Spinoza and as was Newton unto Copernicus: "... as this song of truth, this utter knowing — the poem — falls to the beautiful soul as dew to grass" (Pablo Neruda).

Submitted on February 25, 2015 / Accepted on February 26, 2015

Qualitative Prediction of Isotope Abundances with the Bipolar Model of Oscillations in a Chain System

Andreas Ries

Universidade Federal de Pernambuco (alumnus), Centro de Tecnologia e Geociências, Laboratório de Dispositivos e Nanoestruturas,
Rua Acadêmico Hélio Ramos s/n, 50740-330 Recife – PE, Brazil
E-mail: andreasries@yahoo.com

We analyzed the individual masses of non-radioactive isotopes of the chemical elements with an extended version of the bipolar model of oscillations in a chain system. When defining a small set of appropriate rules, the model is able to predict the isotope which possesses the highest abundance. This information can be read out from the continued fraction representations of the isotope masses. Isotopes with enhanced nuclear stability due to a magic number of neutrons in the nucleus were frequently found as exceptions from the model. The model is applicable to the di-, tri- and tetranuclidic chemical elements; it fails completely as soon as a chemical element is composed of 5 or more stable isotopes. From this we conclude that the bipolar model of oscillations in a chain system – in its present form – is not yet the final version; the model must still be extended.

1 Introduction

In a previous paper [1], the bipolar model of oscillations in a chain system was applied to the standard atomic weights of the chemical elements. The atomic weights of the 19 mononuclidic elements and Helium, which have the lowest standard deviations, were expressed in continuous fraction form without any outliers. This was the calibration (and determination of the phase shift) of the model. It was then found that the vast majority of atomic weights of the polynuclidic elements could be reproduced through continued fractions as well.

The underlying mathematical formalism worked as follows: the mean atomic weights were transformed into a continued fraction according to the equations

$$\ln \frac{m}{m_{electron}} = p_e + S, \quad \ln \frac{m}{m_{proton}} = p_p + S, \quad (1)$$

where p is the phase shift (it must hold $p_p = -p_e$) and S is the continued fraction (e is Euler's number)

$$S = n_0 + \frac{e}{n_1 + \frac{e}{n_2 + \frac{e}{n_3 + \dots}}}. \quad (2)$$

Numerically (if $\neq 0$), p_p was found to be -1.7918229 for the calibrating (low standard deviation) data set.

In this article we extend this previously established version of the model and demonstrate how to predict with an adequate set of rules, which isotope of a given chemical element has the highest abundance.

2 Data sources and computational details

All masses and percentage abundances of isotopes were taken from the web-site of the National Institute of Standards (NIST). An isotope mass is understood as the mass of the neutral atom in its nuclear and electronic ground state.

As in previous articles, the continued fraction representation $p + S$ is abbreviated as $[p; n_0 | n_1, n_2, n_3, \dots]$, where the free link n_0 is allowed to be $0, \pm 3, \pm 6, \pm 9, \pm 12, \pm 15 \dots$ and all partial denominators n_i can take the values $e+1, -e-1, \pm 6, \pm 9, \pm 12, \pm 15 \dots$

3 Results and discussion

3.1 Model extension

Within the originally presented form of the bipolar model (eq. 1) it is not possible to express all the nuclide masses through continued fractions within the accuracy of their standard deviations. Two adjustments are mandatory, one is related to the model itself, the other one to the data set.

First we introduce an additional phase shift δ , as it was already done in a previous article dealing with the electron density distribution in the Hydrogen atom [2]. We write

$$\ln \frac{m}{m_{electron}} = \delta_e + p_e + S, \quad \ln \frac{m}{m_{proton}} = \delta_p + p_p + S. \quad (3)$$

In the same manner as holds $p_p = -p_e$, must consequently hold $\delta_p = -\delta_e$, which means the bipolarity is strictly conserved. The only difference between δ and p is the fact that δ is a small phase shift ($\neq 0$, with either positive or negative sign) applying to *all* isotope masses, while the phase shift p varies among the data points. Some of the masses are associated to the phase shift zero, others to its non-zero value.

Second, in order to be able to express (almost) all the nuclide masses through continued fractions, we have to split the data set of non-radioactive nuclide masses into groups:

Group zero is the set of 19 mononuclidic elements, which was already analyzed in a previous article. Here the phase shift p was determined ($p_p = -1.7918229$) and a δ parameter was not considered, which means $\delta_p = 0$.

Group 1 is the set of dinuclidic elements. We require that the phase shift p remains the same for all nuclides, so only δ

must be adjusted in such a way that ideally all isotopes can be expressed through a continued fraction.

Group 2 is composed of all stable isotopes of the set of the trinuclear chemical elements.

Analogously the remaining chemical elements can be grouped. Every group of masses leads to the determination of a different numerical value of the parameter δ .

The first task (before making any abundance prediction) is the determination of δ , so that from the continued fraction representations (ideally) every isotope mass can be reproduced with a numerical error smaller than its standard deviation.

This means for every isotope mass we obtain 4 different continued fraction representations (eq. 3): two of them interpret the mass as a proton resonance and two others as electron resonances. In the case of no outliers, at least one of these continued fractions reproduces the mass value with an error smaller than its standard deviation.

3.2 Prediction rules

The following simple rules lead to a prediction of nature's preference for the one or the other isotope.

Rule 1:

The electrons contribute very little to the isotope mass, therefore the electron resonances are not decisive and we express the nuclide masses only as proton resonances, according to the equations

$$\ln \frac{m(\text{nuclide})}{m_{\text{proton}}} = \delta_p + 0 + S_0$$

and

$$\ln \frac{m(\text{nuclide})}{m_{\text{proton}}} = \delta_p + (-1.7918229) + S_p.$$

This means we calculate two continued fractions S_0 and S_p . In all the fractions below, the number -1.7918229 is abbreviated as p .

Rule 2:

It is obvious that now, due to the elimination of the electron resonances, many nuclide masses cannot be expressed anymore through a continued fraction with a numerical error smaller than the standard deviation. Consequently we ignore the standard deviation criterion and consider continued fractions leading to a numerical error up to 0.3 u as valid; whenever this error is greater, the result is interpreted as "no continued fraction found".

The choice of 0.3 u as the allowed numerical error is not fully arbitrary. It was adjusted in such a way to make it possible to express at least 95% of the masses through *valid continued fractions*. If the allowed error is too small, many masses fall out of the model, so the model automatically does not work for them. However, with increasing error also rises the probability that the continued fraction has no physical relation to the mass.

Rule 3:

The priority rule for continued fractions with different phase shifts: the fractions with phase shift zero have priority.

Rule 4:

Comparison rule: we can compare only continued fractions (of different masses) which were calculated considering the same phase shift.

Rule 5:

Abundant isotopes accumulate in nodes and sub-nodes with *high positive denominator*.

Rule 6:

A nuclide mass which cannot be expressed through a continued fraction is not abundant.

3.3 Model verification

These rules are now applied to the different groups of isotope masses. For simplicity, only the first four denominators of the fractions are given, which is sufficient for comparison purposes.

Group 1: dinuclear chemical elements, $\delta_p = 0.002919$.

1. Hydrogen:

^1H : [0; 0 | -1146, e+1, -e-1, e+1], 99.9885%

^2D : [0; 0 | e+1, 12, 9, 6], 0.0115%

Here we compare the first denominators: $e+1 > -1146$, so the model predicts that the isotope ^2D is more abundant than the isotope ^1H , which is not observed. The reason for the failure of the model is simply the fact that the isotope ^1H is directly linked to the proton, the reference mass of the model, always more abundant than any other nuclide mass.

2. Helium:

^3He : [p; 3 | -24, 12, -e-1, -9], 0.000134%

^4He : [p; 3 | 15, e+1, -e-1, e+1], 99.999866%

It is not possible to express the Helium isotope masses through continued fractions with phase shift zero. According to the priority rule for phase shifts we now consider the phase shifted fractions. As the first denominator (15) is higher than (-24), the isotope ^4He should be preferred by nature.

3. Lithium:

^6Li : [p; 3 | e+1, e+1, -e-1, e+1], 7.59%

^7Li : [p; 3 | e+1, 441, -6, -e-1], 92.41%

$441 > e+1$, therefore the isotope ^7Li should have the higher abundance, as observed. None of the Li isotope masses can be expressed via a continued fraction with phase shift zero.

4. Boron:

^{10}B : [0; 3 | -e-1, -21, 18, -15], 19.9%

^{11}B : [0; 3 | -e-1, -e-1, -150, 15], 80.1%
 $-e-1 > -21$, therefore preference to ^{11}B .

5. Carbon:
 ^{12}C : [0; 3 | -6, **e+1**, -6, -6], 98.93%
 ^{13}C : [0; 3 | -6, **-24**, -e-1, e+1], 1.07%
 e+1 > -24, therefore preference to ^{12}C .
6. Nitrogen:
 ^{14}N : [0; 3 | -6, -e-1, e+1, -e-1], 99.636%
 ^{15}N : [0; 3 | -9, 1137, -e-1, e+1], 0.364%
 -6 > -9, therefore preference to ^{14}N .
7. Chlorine:
 ^{35}Cl : [0; 3 | **6**, -e-1, e+1, -e-1], 75.76%
 ^{37}Cl : [0; 3 | **e+1**, e+1, -6, -e-1], 24.24%
 6 > e+1, therefore preference to ^{35}Cl .
8. Vanadium:
 ^{50}V : [0; 3 | e+1, -e-1, **-18**, e+1], 0.25%
 ^{51}V : [0; 3 | e+1, -e-1, **15**, e+1], 99.75%
 15 > -18, therefore preference to ^{51}V .
9. Copper:
 ^{63}Cu : [p; 6 | -**36**, 6, e+1, -e-1], 69.15%
 ^{65}Cu : [p; 6 | -**60**, -9, 9, e+1], 30.85%
 -36 > -60, therefore preference to ^{63}Cu .
10. Gallium:
 ^{69}Ga : [p; 6 | **186**, -e-1, 6, -6], 60.108%
 ^{71}Ga : [p; 6 | **63**, -15, 30, 6], 39.892%
 186 > 63, therefore preference to ^{69}Ga .
11. Bromine:
 ^{79}Br : [p; 6 | **18**, 24, -27, 21], 50.69%
 ^{81}Br : [p; 6 | **15**, 6, -e-1, 6], 49.31%
 18 > 15, therefore preference to ^{79}Br .
12. Rubidium:
 ^{85}Rb : [p; 6 | 12, **15**, 6, -e-1], 72.17%
 ^{87}Rb : [p; 6 | 12, **-e-1**, e+1, -e-1], 27.83%
 15 > -e-1, therefore preference to ^{85}Rb .
13. Silver:
 ^{107}Ag : [p; 6 | 6, **-375**, 12, e+1], 51.839%
 ^{109}Ag : [p; 6 | 6, **-12**, e+1, -9], 48.161%
 As -12 > -375, the model predicts the higher abundance for the isotope ^{109}Ag , which is not observed. So the element Silver is the first and only unexplained outlier where our model fails.
 It is completely impossible to express these masses through continued fractions with $p = 0$.
14. Indium:
 ^{113}In : [p; 6 | 6, -e-1, **-6**, 54], 4.29%
 ^{115}In : [p; 6 | 6, -e-1, **6**, 18], 95.71%
 6 > -6, preference to ^{115}In , as observed.
15. Antimony:
 ^{121}Sb : [p; 6 | e+1, e+1, -e-1, **e+1**], 57.21%
 ^{123}Sb : [p; 6 | e+1, e+1, -e-1, **-e-1**], 42.79%
 e+1 > -e-1, preference to ^{121}Sb , as observed.
16. Lanthanum:
 ^{138}La : [p; 6 | e+1, **24**, -e-1, e+1], 0.09%
- ^{139}La : [p; 6 | e+1, **33**, 6, -e-1], 99.91%
 33 > 24, preference to ^{139}La , as observed.
17. Europium:
 ^{151}Eu : [0; 6 | -e-1, e+1, -e-1, **e+1**], 47.81%
 ^{153}Eu : [0; 6 | -e-1, e+1, -e-1, **6**], 52.19%
 6 > e+1, preference to ^{153}Eu , as observed.
18. Lutetium:
 ^{175}Lu : [0; 6 | -e-1, 6, **-e-1**, -e-1], 97.41%
 ^{176}Lu : [0; 6 | -e-1, 6, **-6**, e+1], 2.59%
 -e-1 > -6, preference to ^{175}Lu , as observed.
19. Tantalum:
 ^{180}Ta : [p; 6 | e+1, -e-1, e+1, **-9**], 0.012%
 ^{181}Ta : [p; 6 | e+1, -e-1, e+1, **-6**], 99.988%
 -6 > -9, preference to ^{181}Ta , as observed.
20. Rhenium:
 ^{185}Re : [0; 6 | -e-1, **9**, e+1, -9], 37.40%
 ^{187}Re : [0; 6 | -e-1, **12**, -15, e+1], 62.60%
 12 > 9, preference to ^{187}Re , as observed.
21. Iridium:
 ^{191}Ir : [0; 6 | -e-1, **21**, -6, e+1], 37.3%
 ^{193}Ir : [0; 6 | -e-1, **33**, -27, -e-1], 62.7%
 33 > 21, preference to ^{193}Ir , as observed.
22. Thallium:
 ^{203}Tl : [0; 6 | -e-1, **-15**, -396, -e-1], 29.52%
 ^{205}Tl : [0; 6 | -e-1, **-12**, 6, e+1], 70.48%
 -12 > -15, preference to ^{205}Tl , as observed.
- Group 2:** trinucleidic chemical elements, $\delta_p = -0.016544$.
- Now we apply the same system to the set of 6 trinucleidic chemical elements. We see that (with one magic number exception) the model identifies the most abundant isotope.
1. Oxygen:
 ^{16}O : [0; 3 | -**12**, -6, -24, e+1], 99.757%
 ^{17}O : [0; 3 | -**18**, e+1, -36, -e-1], 0.038%
 ^{18}O : [0; 3 | -**27**, -33, -e-1, e+1], 0.205%
 -12 > (-18 or -27), preference to ^{16}O , as observed; however the model does not explain why the isotope ^{18}O is more abundant than ^{17}O .
2. Neon:
 ^{20}Ne : [0; 3 | **585**, -15, 18, 6], 90.48%
 ^{21}Ne : [0; 3 | **51**, -12, -e-1, 21], 0.27%
 ^{22}Ne : [0; 3 | **27**, 15, -e-1, e+1], 9.25%
 585 > (51 or 27), preference to ^{20}Ne , as observed.
3. Magnesium:
 ^{24}Mg : [0; 3 | **15**, -6, -18, -e-1], 78.99%
 ^{25}Mg : [0; 3 | **12**, -48, 12, -e-1], 10.00%
 ^{26}Mg : [0; 3 | **9**, e+1, -e-1, e+1], 11.01%
 15 > (12 or 9), preference to ^{24}Mg , as observed.
4. Silicon:
 ^{28}Si : [0; 3 | **9**, -e-1, e+1, -e-1], 92.223%

²⁹Si: no continued fraction found, 4.685%

³⁰Si: [0; 3 | 6, e+1, 6, -e-1], 3.092%

9 > 6, preference to ²⁸Si, as observed.

5. Argon:

³⁶Ar: [0; 3 | e+1, e+1, -e-1, e+1], 0.3365%

³⁸Ar: [0; 3 | e+1, 6, -6, 93], 0.0632%

⁴⁰Ar: [0; 3 | e+1, 15, 39, 6], 99.6003%

15 > (6 or e+1), preference to ⁴⁰Ar, as observed.

6. Potassium:

³⁹K: [0; 3 | e+1, 9, -e-1, -12], 93.2581%

⁴⁰K: [0; 3 | e+1, 15, 30, e+1], 0.0117%

⁴¹K: [0; 3 | e+1, 57, e+1, -6], 6.7302%

57 > (9 or 15), preference expected to ⁴¹K, which is against the experimental observations. Reason: Potassium is the element with atomic number 19. The isotope ³⁹K has 39 – 19 = 20 neutrons, which means a magic number of neutrons. This explains the increased abundance.

Group 3: tetranuclidic chemical elements, $\delta_p = 0.025770$.

1. Sulfur:

³²S: [0; 3 | 6, 9, 12, -429], 94.99%

³³S: [0; 3 | 6, -21, -e-1, e+1], 0.75%

³⁴S: [0; 3 | 6, -6, 9, -e-1], 4.25%

³⁶S: [0; 3 | 6, -e-1, e+1, -e-1], 0.01%

9 is the highest denominator, preference to the isotope ³²S, which is indeed observed.

2. Chromium:

⁵⁰Cr: [0; 3 | e+1, -e-1, -e-1, -6], 4.345%

⁵²Cr: [0; 3 | e+1, -e-1, 24, -15], 83.789%

⁵³Cr: [0; 3 | e+1, -e-1, 6, e+1], 9.501%

⁵⁴Cr: [0; 3 | e+1, -e-1, e+1, e+1], 2.365%

24 is the highest denominator, therefore preference to the isotope ⁵²Cr, as observed.

3. Iron:

When considering the phase shift zero, for both isotopes, ⁵⁷Fe and ⁵⁸Fe, no continued fraction is found. This is the only case where two isotopes of a chemical element could not be expressed as proton resonance simultaneously. A better description is found for the phase shifted fractions, here only ⁵⁴Fe turns out to be an outlier. The model is correct when going down the priority hierarchy and analyze these phase shifted fractions:

⁵⁴Fe: no continued fraction found, 5.845%

⁵⁶Fe: [p; 6 | -12, -6, e+1, -6], 91.754%

⁵⁷Fe: [p; 6 | -15, e+1, -e-1, e+1], 2.119%

⁵⁸Fe: [p; 6 | -15, 48, 150, 12], 0.282%

-12 > -15, therefore ⁵⁶Fe has the highest abundance.

4. Strontium:

⁸⁴Sr: [p; 6 | 15, -e-1, -e-1, e+1], 0.56%

⁸⁶Sr: [p; 6 | 12, e+1, -6, -e-1], 9.86%

⁸⁷Sr: [p; 6 | 12, 18, -9, -6], 7.00%

⁸⁸Sr: [p; 6 | 12, -6, -12, 9], 82.58%

15 > 12, so the model predicts the highest abundance for the isotope ⁸⁴Sr, which is not observed. Reason: Strontium is the element with atomic number 38. The most abundant nuclide ⁸⁸Sr has 88 – 38 = 50, a magic number of neutrons, which explains the failure of our model.

5. Cerium:

¹³⁶Ce: [p; 6 | e+1, 9, -e-1, e+1], 0.185%

¹³⁸Ce: [p; 6 | e+1, 12, -e-1, e+1], 0.251%

¹⁴⁰Ce: [p; 6 | e+1, 15, e+1, -e-1], 88.450%

¹⁴²Ce: [p; 6 | e+1, 30, e+1, e+1], 11.114%

Our model predicts the highest abundance for the isotope ¹⁴²Ce. However, the most abundant isotope ¹⁴⁰Ce has a magic number of 140 – 58 = 82 neutrons, so its abundance is increased.

6. Lead:

²⁰⁴Pb: [0; 6 | -e-1, -33, 6, e+1], 1.4%

²⁰⁶Pb: [0; 6 | -e-1, -21, e+1, -e-1], 24.1%

²⁰⁷Pb: [0; 6 | -e-1, -18, e+1, -e-1], 22.1%

²⁰⁸Pb: [0; 6 | -e-1, -15, e+1, 6], 52.4%

-15 is the highest denominator, the model predicts the highest abundance for ²⁰⁸Pb, as observed.

Higher groups: unfortunately, the model fails completely when predicting the most abundant nuclide for all chemical elements consisting of more than four isotopes. Despite the fact that the grouping scheme still allows the expression of the nuclide masses through continued fractions (with few outliers), no correlation between the maximum abundance and the denominators is visible.

4 Conclusions

We have shown that a minor extension of the bipolar model of oscillations in a chain system allows a satisfactory prediction of the most abundant isotope for a given chemical element. Most outliers occur when one of the isotopes has a magic number of neutrons in the nucleus. From its total failure for elements with 5 or more stable isotopes, we conclude that our model is still incomplete and must be extended.

Acknowledgments

The author greatly acknowledges the financial support from the Brazilian governmental funding agencies FACEPE and CNPq.

Submitted on March 2, 2015 / Accepted on March 3, 2015

References

1. Ries A. Atomic weights confirm bipolar model of oscillations in a chain system. *Progress in Physics*, 2013, v. 9(4), 63–67.
2. Ries A. The radial electron density in the Hydrogen atom and the model of oscillations in a chain system. *Progress in Physics*, 2012, v. 8(3), 29–34.

LETTERS TO PROGRESS IN PHYSICS

Addenda to My Paper “New Possible Physical Evidence of the Homogeneous Electromagnetic Vector Potential for Quantum Theory. Idea of a Test Based on a G. P. Thomson-like Arrangement”

Spiridon Dumitru

(Retired) Department of Physics, “Transilvania” University, B-dul Eroilor 29, 500036 Brasov, Romania
E-mail: s.dumitru42@unitbv.ro

This is addenda to my paper entitled “New Possible Physical Evidence of the Homogeneous Electromagnetic Vector Potential for Quantum Theory. Idea of a Test Based on a G. P. Thomson-like Arrangement”, which was published in *Progress in Physics*, 2014, v. 10, Issue 3, 196–200.

1 On the special coil able to create a homogeneous vector potential $\mathbf{h} - \vec{A}$

Some experimenters potentially interested in evaluating the test suggested in my article communicated me comments like:

- ‘It is practically difficult to realize with a desired level of geometrical accuracy the special annular coil designed in [1]. Then it arises the question if it is possible to imagine another system (of coils) able to create also a $\mathbf{h} - \vec{A}$ and which can be manufactured more easily and with a required precision’ .★

Here we wish to note shortly that a system of alluded type can be devised in form of a set consisting in two parallel flat coils pictured below in Fig. 3b. Each such a coil has the aspect shown in Fig. 3a. Note that here we were indexing figures and equations by the consecutive numbers from [1].

In the case of coils system from Fig. 3b the expression of the $\mathbf{h} - \vec{A}$ in an interior point P is given by

$$A = A_z(P) = \mu_0 \cdot I \cdot n \cdot d \tag{11}$$

where n denote the number of conductors per unit length along the coil (in direction of Ox axis).

The expression (11) can be achieved through a set of several simple calculations and the reasoning done in the following sequence of items

- α : Taking into account the equation (6) and its motivation from [1] as starting elements;
- β : Imagining a scheme of infinitely long conductors, located in xOz plane and mutually parallel with the Oz axis. The conductors are crossed by currents of same value I ;
- γ : Evaluation of the $\mathbf{h} - \vec{A}$ field generated by the respective currents in a point P situated on the Oy axis at some distance h of xOz plane;
- δ : The respective evaluation can be done by integration over the Ox -axis and using formula (2.733) from [2];

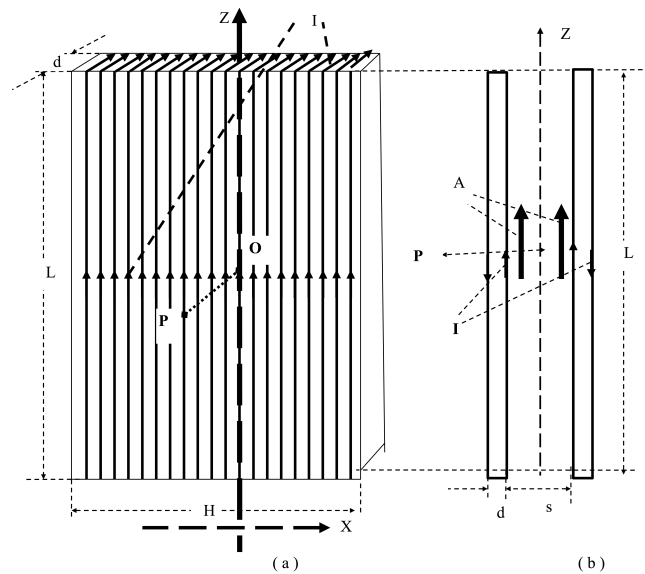


Fig. 3: Schemas with special flat coils. (a) Frontal image of a single coil. (b) Side view of a couple of coils

η : Consideration in Fig. 3 that the quantities L and H are much larger than the dimensions d and s specific to the set of flat and finite coils from Fig. 3b. One requires also that the respective coils to satisfy the conditions specified in note “From the ideal coil to a real one” from [1];

τ : Then, through some modest calculations, by using the evaluation mentioned in item δ one obtains the formula (11).

So, if one uses the coils-system from Fig. 3b, for evaluating the quantity i_{eff}^{dB} (A) mentioned in relation (5) from [1], become of interest the result (11). This means that for the value of $\mathbf{h} - \vec{A}$ must be taken the value $A = \mathfrak{K} \cdot I$ with $\mathfrak{K} = \mu_0 \cdot n \cdot d$. Then instead of relation (5) from [1] the

test in question has to check the formula

$$\frac{1}{i_{eff}^{dB}(A)} = \frac{a\sqrt{2me}}{hD} \sqrt{U} + \frac{ae}{hD} A = \frac{a\sqrt{2me}}{hD} \sqrt{U} + \frac{ae\mathfrak{R}}{hD} I. \quad (12)$$

The last formula points out the fact that the quantity $(i_{eff}^{dB})^{-1}$ (inverse of effective interfringe distance) shows linear dependence of the value of the $\mathbf{h} - \vec{A}$ (and of course of the current I which crosses the coils set). Such a fact can be significant in checking the plausibility of the proposed test.

2 On the G. P. Thomson-like arrangement

As instrument for testing the possible distinct physical signification of $\mathbf{h} - \vec{A}$ in [1] we suggested to use a G. P. Thomson-like arrangement. Such an arrangement can be designed and manufactured as a new apparatus specially dedicated to the concerned test. But one can appreciate that for such a device it is possible to use with sufficient confidence some scientific equipments already existent on the specialized market. As example of such an equipment can be taken into account the set “*Electron diffraction P2511300*” manufactured by the PHYWE company [3]. The main piece of the alluded set is in fact a G. P. Thomson-like device. In the respective device the role of diffraction grating (crystal lattice) mentioned in [1] is played by a graphite foil with interatomic spacing a and D as distance between crystalline foil and observational screen.

Usually [3] the respective device is used for measuring the diameter Q of the first (and eventually of second) smallest diffraction ring at different anode voltages U . Note that, in terms used by us in [1], the diameter Q of first such a ring is twofold of interfringe width i that is $Q = 2 \cdot i$. The interplanar spacing of graphite used in [3] is nothing but the interatomic spacing a in the crystal lattice (diffraction grating) mentioned in Fig.1 from [1]. Also a quantity D plays the role of distance between graphite foil and observational screen.

Notice: Putting into practice the test [1] by using the PHYWE-device can be performed by eluding the concrete values of a and D . Such a performance can be done as follows. In a first step is completed a measurement in absence of $\mathbf{h} - \vec{A}$ field (i.e. when in (12) $A = 0$ and $I = 0$). From the respective measurement is possible to evaluate a couple of values U_0 and $Q_{eff}^{dB}(0)$ for the quantities U and Q . So accordingly with (12) can be calculated device parameter

$$\Gamma = \frac{a}{hD} = \left[Q_{eff}^{dB}(0) \sqrt{\frac{meU_0}{2}} \right]^{-1}. \quad (13)$$

Take into account the fact that in the case of the PHYWE-device the values of quantities a , D and Γ as well as the permitted range for the voltages U_0 and U are predetermined by manufacturer. The respective fact must be considered when one operates with the alluded device and the set of numerical estimations from Section 4 of [1] are not important.

With the aid of parameter Γ the relation (12) can be transcribed as

$$\left[Q_{eff}^{dB}(A) \right]^{-1} = \Gamma \sqrt{\frac{meU}{2}} + \Gamma \frac{eA}{2} = \Gamma \sqrt{\frac{meU}{2}} + \Gamma \frac{e\mathfrak{R}}{2} I. \quad (14)$$

By using the above relations the mentioned PHYWE-device can be put in practice in order to check the proper evidence of the $\mathbf{h} - \vec{A}$ field.

Submitted on March 6, 2015 / Accepted on March 8, 2015

References

1. Dumitru S. New possible physical evidence of the homogeneous electromagnetic vector potential for quantum theory. Idea of a test based on a G. P. Thomson-like arrangement. *Progress in Physics*, 2014, v. 10, issue 3, 196–200.
2. Gradshteyn I.S., Ryzhik I.M. Table of Integrals, Series, and Products. Seventh Edition, Elsevier, 2007.
3. Electron diffraction P2511300, Physics University Experiments, Oct. 2013, PHYWE Systeme GmbH and Co. KG. http://www.phywe.com/index.php/fuseaction/download/lrn_file/TEP_2013_Final_low2.pdf

The de Broglie Relations Derived from the Electron and Proton Coupling to the Planck Vacuum State

William C. Daywitt

National Institute for Standards and Technology (retired), Boulder, Colorado. E-mail: wcdawitt@me.com

This paper argues that the de Broglie relations for the electron and proton are the result of their coupling to the Planck vacuum state, the continuum nature of that state impressing a wave-like behavior onto the free-space-particle aspect of the two particles. Lorentz transforming the vanishing of their corresponding particle/vacuum coupling forces at their respective Compton radii, treated as Lorentz invariant constants, leads to their space-direction and time-direction de Broglie relations. Results: explain the peculiar form of the relativistic particle energy $\sqrt{m^2c^4 + c^2p^2}$; define the de Broglie waves for the electron and proton as periodic undulations within the Planck vacuum in the vicinity of the electron and proton cores; and easily explain the double-slit electron-diffraction thought experiment.

1 Force transformation

The electron and proton cores, $(-e_*, m_e)$ and (e_*, m_p) , exert the two-term coupling forces [1]

$$\pm \left(\frac{e_*^2}{r^2} - \frac{mc^2}{r} \right) \quad (1)$$

on the Planck vacuum (PV) negating-energy continuum, where the plus and minus signs refer to the electron and proton respectively and mc^2 represents the rest energy of either particle. The bare charge e_* is assumed to be a massless point charge. The massive particle cores, however, possess a small spherical extension due to the zero-point formation of their derived masses [2].

The coupling force vanishes

$$\frac{e_*^2}{r_c^2} - \frac{mc^2}{r_c} = 0 \quad (2)$$

at the Compton radius $r_c (= e_*^2/mc^2)$ of either particle, leading to the Compton relations

$$r_c \cdot mc^2 = e_*^2 \quad \longrightarrow \quad r_e m_e c^2 = r_p m_p c^2 = e_*^2 \quad (3)$$

for the electron ($r_e m_e$) and proton ($r_p m_p$), and the (reduced) Planck constant $\hbar = e_*^2/c$. It is noted that (1) is a force acting between a free-space particle and the vacuum state – it is not a free-space/free-space force as are the Coulomb and Newton forces. The Compton relations and $\hbar = e_*^2/c$ are used throughout the following calculations.

The vanishing force (2) can be expressed as a tensor 4-force difference. In the primed rest frame of the particle where these static forces apply, this vanishing force difference $\Delta F'_\mu$ is ($\mu = 1, 2, 3, 4$)

$$\Delta F'_\mu = \left[\mathbf{0}, i \left(\frac{e_*^2}{r_c^2} - \frac{mc^2}{r_c} \right) \right] = [0, 0, 0, i0] \quad (4)$$

where $i = \sqrt{-1}$. Thus the vanishing of the component $\Delta F'_4 = 0$ in (4) can be thought of as the source of the Compton relations in (3).

The force difference in the laboratory frame (in which the rest frame travels at velocity v along the z-axis) [3]

$$\Delta F_\mu = a_{\mu\nu} \Delta F'_\nu = 0_\mu \quad (5)$$

follows from the tensor nature of (4) and the Lorentz transformation $x_\mu = a_{\mu\nu} x'_\nu$, where $x_\mu = (x, y, z, ict)$,

$$a_{\mu\nu} = \begin{pmatrix} 1 & 0 & 0 & 0 \\ 0 & 1 & 0 & 0 \\ 0 & 0 & \gamma & -i\beta\gamma \\ 0 & 0 & i\beta\gamma & \gamma \end{pmatrix} \quad (6)$$

and $\mu, \nu = (1, 2, 3, 4)$. Thus (5) yields

$$\begin{aligned} \Delta F_\mu &= \left[0, 0, \beta\gamma \left(\frac{e_*^2}{r_c^2} - \frac{mc^2}{r_c} \right), i\gamma \left(\frac{e_*^2}{r_c^2} - \frac{mc^2}{r_c} \right) \right] \\ &= \left[0, 0, \frac{1}{r_c} \left(\frac{e_*^2}{r_d} - c \cdot m\gamma v \right), \frac{i}{r_c} \left(\frac{e_*^2}{r_L} - c \cdot m\gamma c \right) \right] \\ &= [0, 0, 0, i0] \end{aligned} \quad (7)$$

where

$$r_d = \frac{r_c}{\beta\gamma} \quad \text{and} \quad r_L = \frac{r_c}{\gamma} \quad (8)$$

are the de Broglie radii for the space and time directions respectively; and where $\beta = v/c < 1$ and $\gamma = 1/\sqrt{1-\beta^2}$.

The force difference $\Delta F_3 = 0$ in (7) gives the de Broglie relation

$$r_d \cdot cp = e_*^2 \quad \text{or} \quad r_d = \frac{\hbar}{p} \quad (9)$$

in the space direction, where $p = m\gamma v$ is the relativistic particle momentum. The force difference $\Delta F_4 = 0$ gives the de Broglie relation

$$r_L \cdot E = e_*^2 \quad \text{or} \quad r_L = \frac{\hbar}{m\gamma c} \quad (10)$$

in the time direction, where $E = \overline{m\gamma c^2}$ is the total relativistic particle energy.

The momentum and energy in equations (9) and (10) are derived from nothing more than the vanishing of the Lorentz transformation of (2), whose results can be taken a step further:

$$\begin{aligned} E &= \frac{e_*^2}{r_L} = \frac{e_*^2 \gamma}{r_c} = mc^2 \gamma \\ &= mc^2 \left(1 + \frac{\beta^2}{1 - \beta^2} \right)^{1/2} \\ &= (m^2 c^4 + c^2 p^2)^{1/2} \end{aligned} \quad (11)$$

showing that this well known equation has its source in the two-term particle/PV coupling force.

2 Conclusions and comments

The vast accumulation of electron diffraction data leaves no doubt that the electron and proton possess a wave nature. If the corresponding waves are roughly expressed in terms of planewaves, then it is reasonable to assign $2\pi r_d$ and $2\pi r_L$ as the wavelengths in the space and time directions respectively. As a first approximation then, the electron and proton de Broglie waves are planewaves propagating within the PV continuum.

The Synge primitive (or planewave) quantization of spacetime [4, p.106] is an independent calculation that parallels the ideas of the previous paragraph. That quantization divides the space and time axes of the Minkowski spacetime diagram into equal segments, where the space and time segments are r_d and r_L respectively (Synge actually multiplies these two segments by 2π which defines a phase space). The particle/PV coupling of the previous section provides the physical explanation for that quantization in terms of the coupling force (1).

Although the implied mathematics of the two previous paragraphs involves planewaves (which are global), the PV wave phenomenon must be a local property associated with the particle/PV interaction in the neighborhood of the particle cores ($-e_*, m_e$) and (e_*, m_p), with characteristic (radian) frequencies defined by

$$\omega_c = \frac{e_*^2/r_c}{\hbar} = \frac{c}{r_c} \quad (12)$$

with

$$\omega_L = \frac{e_*^2/r_L}{\hbar} = \gamma \omega_c \quad \text{and} \quad \omega_d = \frac{e_*^2/r_d}{\hbar} = \beta \gamma \omega_c \quad (13)$$

for each particle. Then (11) yields

$$\omega_L^2 = \omega_c^2 + \omega_d^2. \quad (14)$$

The preceding results offer a simple explanation for the double-slit thought experiment [5, p.85]. Consider a collimated beam of monoenergetic electrons that is directed at

an opaque wall containing two narrow, parallel, and closely spaced slits A and B, with a detection screen at some distance beyond the slits. Being a particle (although with a wave-like nature), the electron cannot go through both slits at the same time. Now consider the two experiments: (1) with slit A open and slit B closed; and (2) with both slits A and B open. Assume that the slits are narrower than one de Broglie wavelength ($2\pi r_d$) and that their separation distance is several wavelengths.

If the electrons are particle-like with no wave-like qualities, the screen would show a bell-shaped excitation curve in case (1) and two superimposed bell-shaped curves in case (2). But for case (2), however, the *overwhelming* diffraction evidence demands a well defined oscillatory excitation curve on the screen — because the particle exhibits a definite wave-particle nature. Since the electron must go through A or B, but not both, this result is difficult to understand [5, p.85] with present-day physics. But if the free-space particle is accompanied by a PV de Broglie wave, the diffraction of that wave through A and B, and its interaction with the particle core, easily explains the oscillatory curve on the detection screen.

Submitted on March 21, 2015 / Accepted on March 27, 2015

References

1. Daywitt W.C. The Strong and Weak Forces and their Relationship to the Dirac Particles and the Vacuum State. *Progress in Physics*, 2014, v. 11, 18. See also www.planckvacuum.com.
2. Daywitt W.C. Why the Proton is Smaller and Heavier than the Electron. *Progress in Physics*, 2014, v. 10, 175.
3. Jackson J.D. Classical Electrodynamics. John Wiley & Sons, Inc., 1st ed., 2nd printing, NY, 1962.
4. Synge J.L. Geometrical Mechanics and de Broglie Waves. Cambridge University Press, 1954.
5. Leighton R.B. Principles of Modern Physics. McGraw-Hill Book Co., New York, Toronto, London, 1959.

Progress in Physics is an American scientific journal on advanced studies in physics, registered with the Library of Congress (DC, USA): ISSN 1555-5534 (print version) and ISSN 1555-5615 (online version). The journal is peer reviewed and listed in the abstracting and indexing coverage of: Mathematical Reviews of the AMS (USA), DOAJ of Lund University (Sweden), Zentralblatt MATH (Germany), Scientific Commons of the University of St.Gallen (Switzerland), Open-J-Gate (India), Referential Journal of VINITI (Russia), etc. **Progress in Physics** is an open-access journal published and distributed in accordance with the Budapest Open Initiative: this means that the electronic copies of both full-size version of the journal and the individual papers published therein will always be accessed for reading, download, and copying for any user free of charge. The journal is issued quarterly (four volumes per year).

Electronic version of this journal: <http://www.ptep-online.com>

Advisory Board of Founders:

Dmitri Rabounski, Editor-in-Chief
Florentin Smarandache, Assoc. Editor
Larissa Borissova, Assoc. Editor

Editorial Board:

Pierre Millette
Andreas Ries
Gunn Quznetsov
Felix Scholkmann
Ebenezer Chifu

Postal address:

Department of Mathematics and Science, University of New Mexico,
705 Gurley Avenue, Gallup, NM 87301, USA
